PROCESSING AND CHARACTERIZATION OF FIBER REINFORCED POLYMER NANOCOMPOSITES AND THEIR DEGRADATION UNDER HYGROTHERMAL LOADING

A thesis submitted in partial fulfillment

of the requirement for the award of the degree of

DOCTOR OF PHILOSOPHY

Submitted by

Bikramjit Sharma

(Registration No. - 950908014)

Under the supervision of

Dr. Rahul Chhibber

Assistant Professor

Department of Mechanical Engineering

Indian Institute of Technology, Jodhpur

Dr. Rajeev Mehta

Professor

Department of Chemical Engineering

Thapar Institute of Engineering and Technology, Patiala

THAPAR INSTITUTE
OF ENGINEERING & TECHNOLOGY
(Deemed to be University)

Department of Mechanical Engineering

Thapar Institute of Engineering and Technology, Patiala- 147004, India

SEPTEMBER 2018

CERTIFICATE

I, **Bikramjit Sharma** hereby certify that the work presented in this thesis report entitled "**Processing and characterization of fiber reinforced polymer nanocomposites and their degradation under hygrothermal loading**" in partial fulfillment of requirement for the award of degree of **DOCTOR OF PHILOSOPHY**, submitted in the Department of Mechanical Engineering, Thapar Institute of Engineering and Technology, Patiala is an authentic record of my research work carried out under the supervision of **Dr. Rahul Chhibber** (Assistant Professor, Department of Mechanical Engineering, Indian Institute of Technology, Jodhpur) and **Dr. Rajeev Mehta** (Professor, Department of Chemical Engineering, Thapar Institute of Engineering and Technology, Patiala). The results embodied in the thesis have not been submitted in part or full to any other University or Institute for the award of any other degree.

Bikramjit Sharma

(Bikramjit Sharma)

Registration No.: 950908014 Dated: 25 September 2018

It is certified that the above statement made by the student is correct to the best of our knowledge and belief.

Rahul Chhibber

Dr. Rahul Chhibber
Assistant Professor
Department of Mechanical Engineering
Indian Institute of Technology, Jodhpur

Rajeev Mehta

Dr. Rajeev Mehta
Professor
Department of Chemical Engineering
Thapar Institute of Engineering and Technology, Patiala

ACKNOWLEDGEMENT

First and foremost, I would like to thank the almighty whose countless blessings have made me who I am today. He enabled me with philosophy, perception, and motivation to present this work, after handling the tough times with empathy, professionally and clarity. During this thesis, many personnel directly or indirectly contributed to making this doctoral dissertation possible, and I will always remain deeply indebted to them.

Firstly, from the core of my heart, I would like to express special thanks to my esteemed supervisors, Dr. Rajeev Mehta and Dr. Rahul Chhibber for encouraging my research and for allowing me to grow as a research scientist. Their consistent support, dynamic supervision, valuable and innovative suggestions have enlightened my knowledge and skills in the area of nanocomposites. Both of them have been tremendous mentors now and forever.

Besides my supervisors, I wish to express humble and special thanks to Dr. Ajay Batish and Dr. S.K. Mohapatra for providing me the opportunity and necessary facilities in the department along with their encouragement and constant moral support to accomplish this task. I would like to acknowledge the valuable suggestions of the members of the Doctoral Committee, Dr. O.P. Pandey, Dr. V.P Agrawal and Dr. Deepak Jain for their insightful comments and questions, during my presentations. Special thanks go to Dr. O.P. Pandey, Dean of Research and Sponsored Projects for providing the possible research facilities. I am also thankful to Dr. Devender Kumar, Dr. Kishore Khanna, Dr. J.S. Saini and Dr. Tarun Nanda for their motivational and true advice. I would appreciate the wholehearted cooperation and valuable help rendered by teaching and non-teaching staff of the Department of Mechanical Engineering, Thapar Institute of Engineering and Technology.

I thank my fellow researchers Dr. Shilpa Narang, Dr. Mohit Garg with whom I have spent these years of research and enjoyed many interactive sessions. I am also thankful to all the laboratory staff members, who maintained all the machines and equipment so efficiently, which helped me in performing experiments accurately.

The financial assistance rendered by Naval Research Board, DRDO, India for setup of lab equipment, carrying out experiments and characterization of materials is gratefully acknowledged. The financial support acted as a catalyst and helped me in achieving tremendous results in my research.

A special thanks are also due to my family and words cannot express how grateful I am to my parents for all their sacrifice that they had made on my behalf and who have always been my strongest support and my source of motivation during moments of despair and discouragement. I would like to thank my brother for providing support and refreshing me during the hardships to strive towards the goal. I would like to thank the better-half, my wife, Priya Sharma, who has been a constant source of strength and inspiration. This thesis would not have been possible without her unconditional and unending love, support and cooperation as a friend and wife.

I want to thank my relatives and friends who have supported me by any means over the past years in my pursuit of completing my Doctoral degree.

I extend my special thanks to all who kept me well-balanced and have tried to make this challenging work a pleasant journey.

Patiala

25 September 2018 (Bikramjit Sharma)

ABSTRACT

Studies on the effect of different processing parameters (premixing parameters, curing time and curing temperature, post-curing temperature, resin to hardener mix ratio) on mechanical properties of fiber reinforced epoxy-clay nanocomposites containing 2 phr of Cloisite® 15A have been carried out. Further, Cloisite® 15A has been modified via a new silanization route with different quantities (0.1, 0.5, 2, 4 and 6 times the weight of clay (X)) of two different silane coupling agents viz. 3-aminopropyltriethoxysilane (APTES) and 3-glycidyloxypropyltrimethoxysilane (GPTMS). The silylated clay minerals have been characterized using Fourier transform infrared (FTIR) spectroscopy, Small angle X-ray scattering (SAXS) and Thermogravimetric analysis (TGA) to confirm the successful grafting of silanes on clay minerals. A detailed study has been done with regard to the effect of silanization of clay minerals on properties of glass fiber epoxy-clay nanocomposites as a function of two important parameters: chemical structure of silane and concentration of silane coupling agent used in grafting reaction.

The silane modified clays have been dispersed in epoxy resin by using high shear homogenization and sonication. The fiber reinforced epoxy-clay nanocomposites were manufactured using vacuum assisted wet layup or vacuum assisted resin infusion molding. An optimum quantity of silane for successful modification of large surface area of clay mineral layers and curing schedule of fiber reinforced epoxy-clay nanocomposites were also arrived at. The fiber reinforced epoxy-clay nanocomposites containing silane modified clay minerals have been characterized using Small angle X-ray Scattering (SAXS), Transmission electron spectroscopy (TEM) and Differential scanning calorimetry (DSC). The results indicate that the silane treatment of Cloisite® 15A aided exfoliation of clay mineral layers as evidenced by SAXS and TEM, promoted interfacial adhesion as suggested by the significant increase in mechanical properties. The incorporation of silane treated clay minerals led to an increase in tensile modulus, tensile strength, flexural modulus and flexural strength by 30%, 37%, 139% and 146%, respectively in nanocomposites containing clay minerals modified using 4X aminopropyltriethoxysilane. The fracture surfaces were also examined by Scanning electron microscopy (SEM), which revealed a considerable difference in failure modes of fiber reinforced epoxy nanocomposites containing Cloisite® 15A and those containing silane modified clay minerals.

The behavior of these novel fiber reinforced nanocomposites under different hygrothermal aging conditions had also been studied in detail. The amount of silane used for functionalization of clay minerals and polarity of silane groups influenced the long-term durability of fiber reinforced epoxy-clay nanocomposites in seawater. The incorporation of clay minerals in epoxy hindered the degradation of fiber reinforced nanocomposites, and those containing silylated clay minerals modified using a small amount of silane coupling agents (0.1X, 0.5X) exhibited better retention of tensile and flexural strength after exposure to seawater. The polarity of the organic moieties and morphology of clay minerals in epoxy significantly influenced the durability of nanocomposites in seawater.

LIST OF PUBLICATIONS

The results incorporated in this thesis are fully documented. Following publications in peer-reviewed SCI journals have come out of the work carried out.

International SCI Journals

Published

1. Effect of surface treatment of nanoclay on the mechanical properties of epoxy/glass fiber/clay nanocomposites; **Bikramjit Sharma**, Rahul Chhibber & Rajeev Mehta; Composite Interfaces, 23(7), 623-640(2016), IF = 1.046.
2. Curing studies and mechanical properties of glass fiber reinforced composites based on silanized clay minerals; **Bikramjit Sharma**, Rahul Chhibber and Rajeev Mehta; Applied Clay Science, 138, 89-99 (2017), IF = 3.101.
3. Effect of mixing parameters, post-curing and stoichiometry on mechanical properties of fiber reinforced epoxy-clay nanocomposites; **Bikramjit Sharma**, Rahul Chhibber and Rajeev Mehta; SAGE Part L Journal of Materials Design and Application 0(0) 0, 1–12. (2018), doi:10.1177/1464420717752023, IF = 2.322
4. Seawater ageing of glass fiber reinforced epoxy nanocomposites based on silylated clays; **Bikramjit Sharma**, Rahul Chhibber and Rajeev Mehta; Polymer Degradation and Stability 147, 103-114(2018), IF = 3.386.

ABBREVIATIONS USED

APDMES	3-aminopropyldimethylethoxysilane
APTES	3-aminoproyltriethoxysilane
ASTM	American society for testing of materials
CTE	Coefficient of thermal expansion
DGEBA	Diglycidyl ether of bisphenol-A
DMA	Dynamic Mechanical Analysis
DSC	Differential scanning calorimetry
E-CR	Chemically resistant E-glass
EDS	Energy dispersive spectroscopy
FTIR	Fourier transform infrared
GFRP	Glass fiber reinforced polymer/plastic
GPa	Gigapascals
GPTMS	3- glycidyloxypropyltrimethoxysilane
ILSS	Interlaminar shear strength
MMT	Montmorillonite
MPa	Megapascals
MWCNT	Multiwalled carbon nanotube
OMMT	Organically modified MMT
RH	Relative humidity
rpm	Revolutions per minute
SAXS	Small angle X-ray scattering
SCA	Silane coupling agents
SEM	Scanning electron microscopy
T_g	Glass transition temperature
$T_{g\infty}$	Glass transition temperature of the fully cured epoxy
TEM	Transmission electron microscopy
TGA	Thermogravimetric analysis
UTM	Universal testing machine
VARIM	Vacuum assisted resin infusion molding
VARTM	Vacuum assisted resin transfer molding
XRD	X-ray diffraction

NOMENCLATURE

GFRC	Glass fiber reinforced composite
C15GFRC	Glass fiber reinforced epoxy nanocomposite containing Cloisite® 15A
C15 AGFRC	Glass fiber reinforced epoxy nanocomposite containing APTES-treated glass fibers and Cloisite® 15A
C15 GGFRC	Glass fiber reinforced epoxy nanocomposite containing GPTMS-treated glass fibers and Cloisite® 15A
AC15 AGFRC	Glass fiber reinforced epoxy nanocomposite containing APTES-treated glass fibers and APTES-treated Cloisite® 15A
GC15 AGFRC	Glass fiber reinforced epoxy nanocomposite containing GPTMS-treated glass fibers and APTES-treated Cloisite® 15A
AC15 GGFRC	Glass fiber reinforced epoxy nanocomposite containing APTES-treated glass fibers and GPTMS-treated Cloisite® 15A
GC15 GGFRC	Glass fiber reinforced epoxy nanocomposite containing GPTMS-treated glass fibers and GPTMS-treated Cloisite® 15A
APS C15(x)	Cloisite® 15A surface treated with APTES. The quantity of silane coupling agent used has been mentioned in parentheses.
GPS C15(x)	Cloisite® 15A surface treated with GPTMS. The quantity of silane coupling agent used has been mentioned in parentheses.
AC15(x)GFRC	Glass fiber reinforced epoxy-clay nanocomposites incorporating Cloisite® 15A modified using different quantities of APTES.
GC15(x)GFRC	Glass fiber reinforced epoxy-clay nanocomposites incorporating Cloisite®15A modified using different quantities of GPTMS

TABLE OF CONTENTS

LIST OF FIGURES

LIST OF TABLES

Chapter 1 Introduction

Glass fiber reinforced polymer composites provide the opportunity to yield significant benefits to a variety of modern products. The application of fiber reinforced composites in the field of aerospace, automotive, construction and marine, sporting goods and wind turbines has increased significantly. Fiber reinforced composites have high specific strength, specific stiffness, high endurance strength, durability, light-weight, corrosion resistance, and ability to be customized to meet requirements of a specific application. Glass fiber reinforced epoxy composites have been widely used for marine applications for a very long time (Graham-Jones and Summerscales, 2015a; Mouritz et al., 2001; Moy, 2013). The selection of materials in above applications is dependent on the performance requirements (mechanical strength, stiffness, durability, wear resistance, weight, etc.), possible modes of failure, service conditions (temperature, humidity, and corrosion resistance), manufacturing method and cost of making the final product.

The mechanical properties of a fiber reinforced composite depend on some factors, e.g., shape, size and volume fraction of reinforcement, choice of polymers (epoxy, polyester, vinyl ester), the orientation of fibers in preform and lay-up, the presence of air voids, manufacturing methods, and the direction of measurement. The glass fiber reinforcements are commercially available in many forms like long longitudinal, woven mat, chopped fiber and chopped mat. Both unidirectional and woven cloth made of continuous glass fibers have high aspect ratios and are preferred over other forms when the strength of the composite is a prime requirement. E-glass fibers are more suitable for naval composites than other fiber types, because of low cost and higher ultimate strains. The conventional E- glass fibers contain boron which makes fibers sensitive to stress corrosion under long-term exposure to water and tensile stresses. The stress corrosion causes premature failure due to the development of cracks on the fiber surface. For this reason, E-CR glass fibers (Li et al., 2014; Stickel and Nagarajan, 2012), e.g. Advantex® and Hi-Pertex®, which are both boron free, as well as corrosion resistant, are preferred in marine applications. Epoxy based thermosetting polymer resins are used for producing high strength composites because of characteristics like compatibility with most of the fibers and good wetting due to low viscosity, high mechanical properties, excellent chemical and corrosion resistance, low volatility and low shrinkage during curing.

The fiber-matrix interfacial interactions play an essential role in the integrity and properties of the composites. In fiber reinforced composites, an optimal bond will efficiently transfer the

load to the strong fibers and provide high strength to composite. A popular method to improve adhesion between glass fibers and the polymer matrix is to perform silane treatment of glass fibers, which improves the mechanical performance and durability of composites. The organic modification of nanofillers using silane coupling agents has also shown potential benefits similar to those observed by silanization of glass fibers. The modification of clay minerals using organofunctional silanes has attracted interest of many researchers because grafting of silane molecules on clay mineral surfaces improve their dispersibility (Chen et al., 2005a, 2005b; De Maria et al., 2011; Ha et al., 2008; He et al., 2013; Park et al., 2009; Qian et al., 2009), wettability (Ianchis et al., 2011; Park et al., 2009), interfacial adhesion (Ha et al., 2007; Kráčalík et al., 2007; Park et al., 2009), and promotes exfoliation (Chen and Yoon, 2005a; Ha et al., 2007; Ha and Rhee, 2008; Sharma et al., 2016; Silva et al., 2011; Wang et al., 2006b). The exfoliated morphology leads to improvements in mechanical properties on addition of a small amount of clay mineral in polymer matrix (Chen and Yoon, 2005b; Ha et al., 2010, 2008, 2007; Ha and Rhee, 2008; Huskić et al., 2013; Ianchis et al., 2015; Piscitelli et al., 2012; Wang et al., 2006b) because of improved reinforcement effect of clay mineral. The selection of silane coupling agents for a particular application depends on the polymer resin to be bonded, thermal stability of silane, and reactivity with water because functional groups in silane can be hydrophilic or hydrophobic.

Fiber reinforced polymer composites can be manufactured using a wide variety of methods like hand lay-up, spray lay-up, resin infusion methods, compression molding, injection molding, filament winding, pultrusion, etc. (Wang et al., 2011). At present, Vacuum assisted resin infusion molding (VARIM) has been widely used to manufacture high-performance polymer composites in aerospace, automotive, and construction industries. The VARIM process has some unique requirements, e.g. the resin should have low viscosity and sufficient gel time to facilitate complete infusion and infiltration in fiber preforms. The advantages of VARIM include high fiber content and fewer voids in composite, safety because of the enclosure of resin and high level of dimension tolerance and repeatability.

A key factor driving the increased applications of fiber reinforced composites is continuous advancements in this area. This includes discoveries of new high-performance polymer resins, improved fiber reinforcements, improved manufacturing processes, and incorporation of nano and micro-scale reinforcements. The fiber reinforced polymer nanocomposites combine the advantages of both the fibers and nanofillers resulting in superior properties.

1.1 Fiber reinforced polymer nanocomposites

The growing demand for high-performance fiber reinforced composites led to the emergence of the hybrid materials incorporating nanofillers. The real starting point is generally considered to be the research pioneered by (Kojima et al., 1993) and (Okada and Usuki, 1995), from Toyota R&D on montmorillonite filled polyamide-6 nanocomposites. Subsequent developments further contributed to the surging interest in polymer nanocomposites and nanofillers such as nano-oxides, carbon nanotubes, carbon nanofibers, graphene and metal particles are currently being used as additives in polymers (Camargo et al., 2009; Marquis et al., 2011; Peponi et al., 2014; Šupová et al., 2011). The fiber reinforced polymer nanocomposites are three-phase hybrid composites in which the main reinforcing phase is continuous fibers, and the matrix itself is a composite too, incorporating nanometer size particles. The conventional fiber reinforced composites have good mechanical properties, but the properties obtained are highly anisotropic. A uniform dispersion of nanofillers cover a much greater area within the polymer matrix compared to conventional fibrous composites and hence provide significant property enhancement, even at a low filler loading. A broad spectrum of composite properties such as mechanical, electrical, magnetic, thermal, barrier, resistance to chemical attack, resistance to scratch and wear, and flame retardancy can be improved (Olad, 2011). However, the dispersion state, the quantity of nanofiller, and interfacial adhesion with polymers strongly influence the properties of these nanocomposites. Most of the polymers are incompatible with nanofillers and it is difficult to achieve uniform dispersion of nanofillers in the matrix. The agglomeration of nanoparticles during the preparation of nanocomposite and a lack of adhesion with the polymer can result in an early failure. Besides these, some other factors like volume fraction of reinforcement, choice of epoxy system, epoxy and hardener mix ratio, the orientation of fiber preform and lay-up, the presence of air voids, filtration of nanofillers in fiber preforms and curing schedule would influence the mechanical properties of fiber reinforced nanocomposites.

1.2 Clay minerals

Clay minerals are abundantly available in nature and found as fine-grained fractions in rocks, sediments, and soils. The clay minerals have attributes such as a layered structure with layers having a length in few microns and thickness in the nanometer range, ability to disperse in individual layers and hardens upon drying or firing (Bergaya and Lagaly, 2006). Clay minerals are classified according to their crystalline structure and interlayer ions.

1.2.1 Structure and characteristics of Montmorillonite

Montmorillonite (MMT) is a magnesium aluminum silicate, which belongs to the smectite group of clay minerals, having the general formula $(Na, Ca)_{0.33}$ $(Al, Mg)_2$ (Si_4O_{10}). Montmorillonite is most commonly used in nanocomposites because of its easy availability, high aspect ratios, high surface reactivity and well-known intercalation/exfoliation chemistry. Figure 1.1 shows the basic structure of 2:1 layered silicates (2:1phyllosilicates), without any substitution of atoms, which consists of an octahedral layer of alumina sandwiched between two tetrahedral layers of silica.

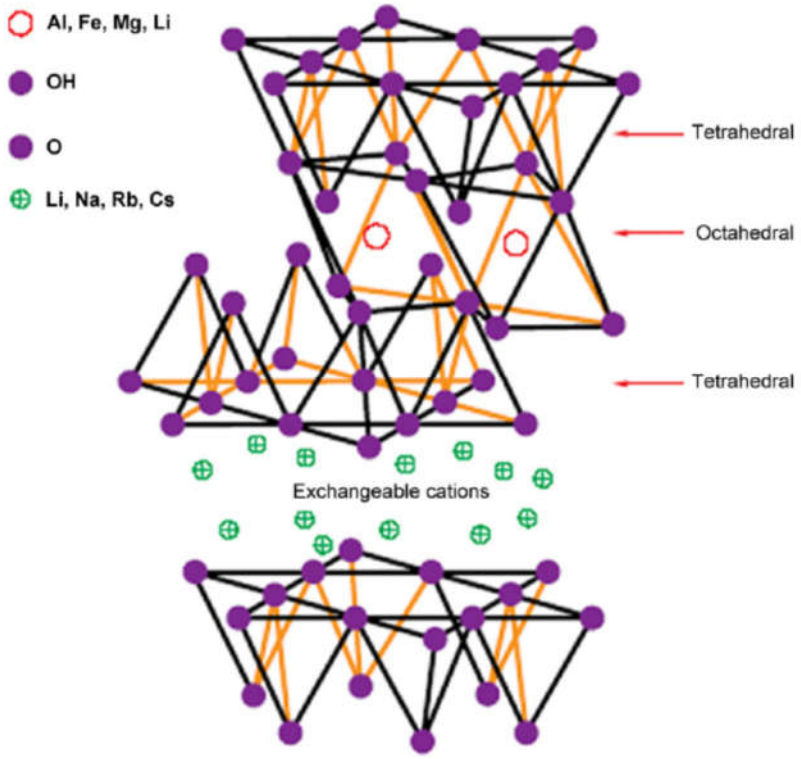

Figure 1.1 Structure of Montmorillonite layered silicate (Beyer, 2002; Pavlidou and Papaspyrides, 2008)

The structure of montmorillonite is formed by isomorphic substitution within the layers (replacement of Al^{3+} by Mg^{2+}). This replacement creates a negative charge on an overall crystal lattice, which is counterbalanced by cations such as sodium and calcium (Na^+ or Ca^{2+}) residing in the interlayers. But, these cations do not fit in the tetrahedral layers. Therefore the octahedral layers and the silica tetrahedral layers are bound together by relatively weak Vander-Waals forces. The interlayer space of MMT also holds – OH groups of the octahedral aluminum-hydroxyl sheets and the oxygen atoms of the tetrahedral silicate sheets. Obviously, in its pristine state, MMT is hydrophilic and will swell if water/ polar solvents enter the

interspaces. In this state, the clay minerals form agglomerates and would be unable to interact with a polymer, which will decrease the mechanical properties of the material. Also, the interlayer gap needs to be increased in MMT so that polymer chains can intercalate in between clay layers. Therefore, the clay minerals must be modified before these can be used to prepare nanocomposites. To make these compatible with polymers, the inorganic cations must be exchanged with organic cations by ion exchange reactions or adsorption of organic moieties on clay mineral layers (Kango et al., 2013; Kotal and Bhowmick, 2015; Varadwaj et al., 2016).

1.2.2 Silylation of clay minerals

The organic modification of clay minerals is done to achieve good dispersion of clay mineral layers into the polymer matrix, and to take advantage of its high aspect ratio and large surface area. The most popular compatiblizing agents used for clays are alkyl ammonium ions as they can be easily exchanged with the ions situated between the layers. The organic modification of clay minerals using onium ions by ion exchange methods only replaces the inorganic interlayer cations, increasing the d-spacing and compatibility with polymers. But clay remains hydrophilic after these modifications due to the presence of -OH groups located at the edges of silicate layers. The presence of hydroxyl groups can be utilized for organic modification of clay minerals by silylation. In the case of montmorillonite, a number of these may also exist in the interlayer space due to structural defects and irregularities. Silane coupling agents are silicon-containing species which can form linkages between organic and inorganic materials (Blum, 2016). The silane-grafting reaction or silylation of clay minerals would lead to strong covalent bonding of organic moieties, preventing their leaching in the solvents or resins during processing of nanocomposites (Figure 1.2). The functional groups at the other end of the silicon group make strong covalent bonds with a polymer or other silane molecules. Therefore a network will be formed between polymer, silane, and clay via covalent bonds. The strong adhesion can greatly improve the mechanical properties of resulting clay-based nanocomposites.

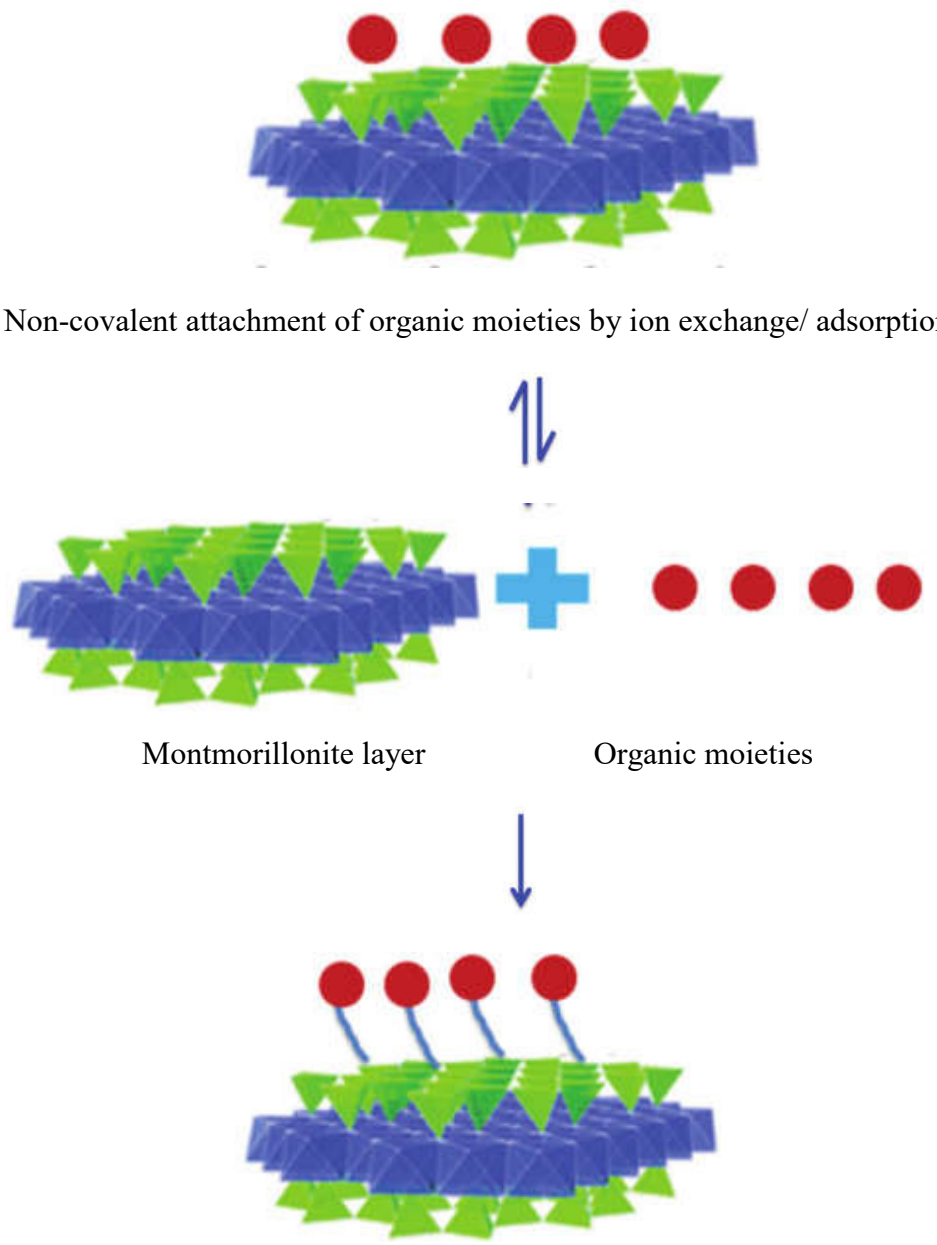

Figure 1.2 Schematic showing organic modification of clay minerals by ion exchange and silylation (Varadwaj et al., 2016)

1.2.3 Steps of silanization reactions

Silane coupling agents can form a durable bond between organic and inorganic materials. Silane coupling agents have the general structure R-SiX_3, where R is an organo-functional group and X is a hydrolyzable group typically alkoxy, acyloxy, or halogen (Figure 1.3). Epoxycyclohexyl, glycidoxy functional and amine functional silanes are widely used to pretreat the inorganic materials to make them compatible with the epoxy resins (Zabihi et al.,

2018). Initially, the silane monomers react in the presence of water (hydrolysis) to form reactive, hydrophilic, silanol groups Si–OH. Next, partial condensation occurs and oligomers are formed. During the condensation, silane molecules react with each other and then condense to form siloxane oligomers. The oligomers or monomers silanol are physically adsorbed to hydroxyl groups of the inorganic substrate by hydrogen bonds. Finally, under dehydration condensation reaction a robust covalent bond –Si–O–Si– between silanols and hydroxyl groups of the substrate are formed during a drying process.

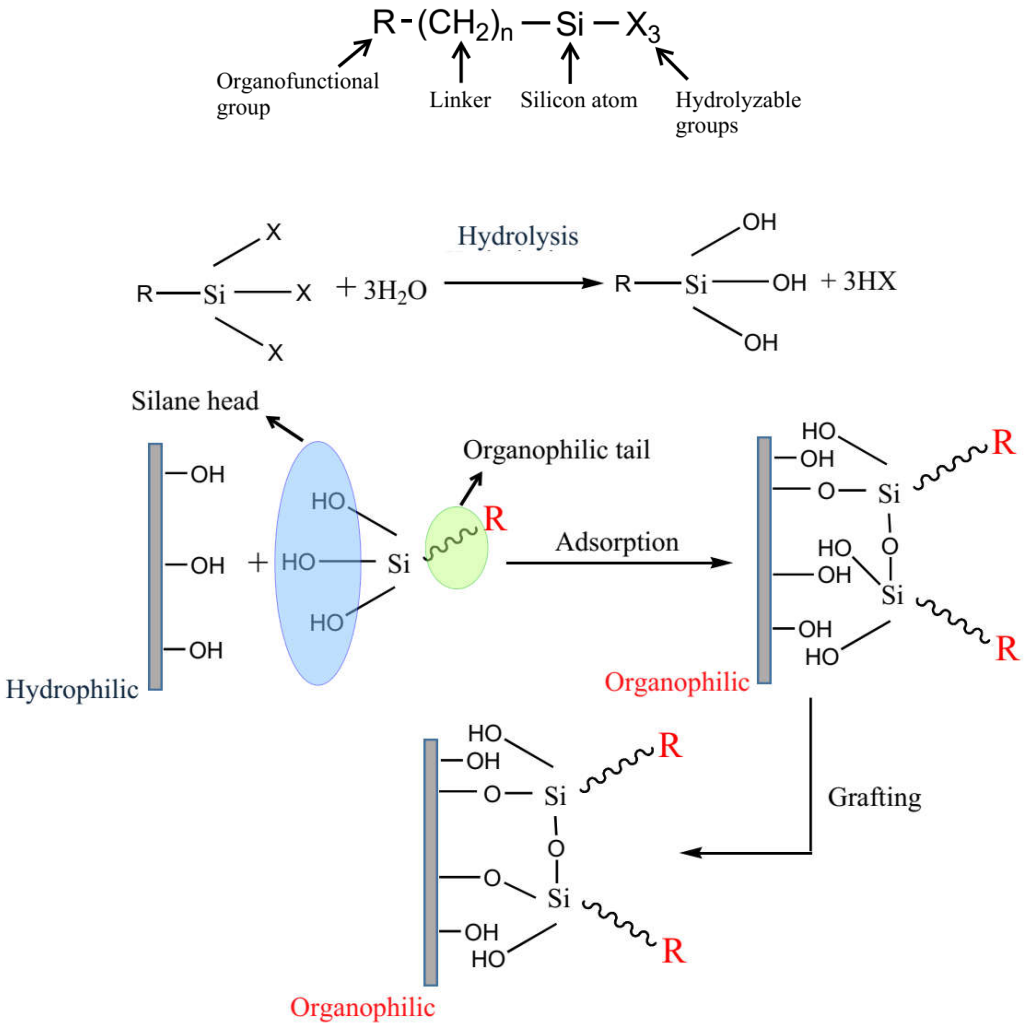

Figure 1.3 General structure of silane coupling agent and silane hydrolysis and grafting on an inorganic substrate

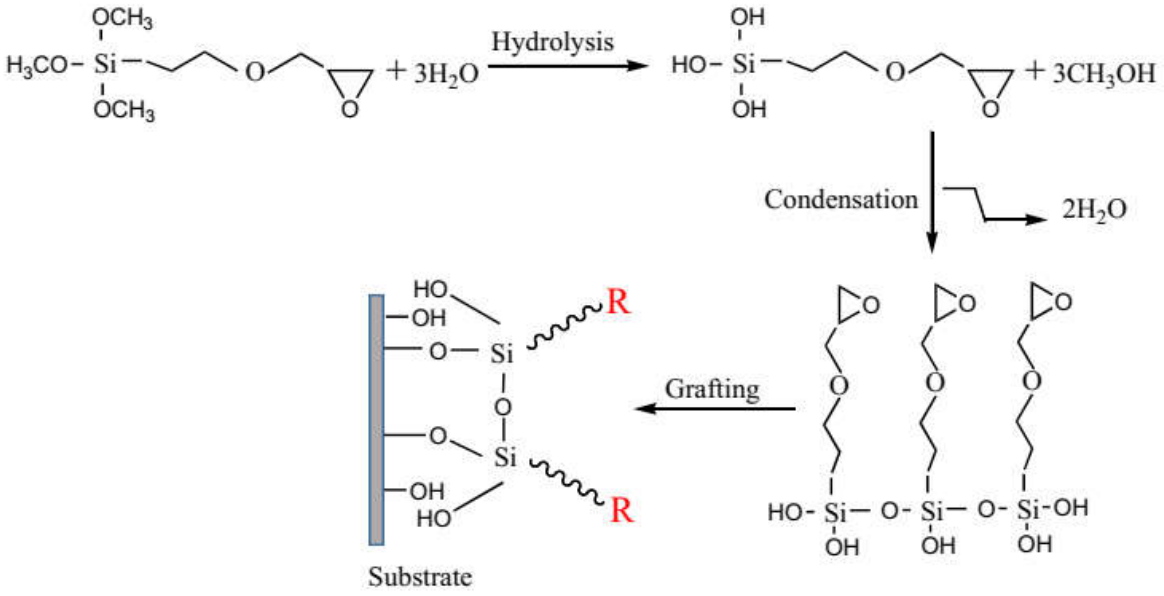

Figure 1.4 The hydrolysis and condensation reactions of glycidyloxypropyltrimethoxysilane

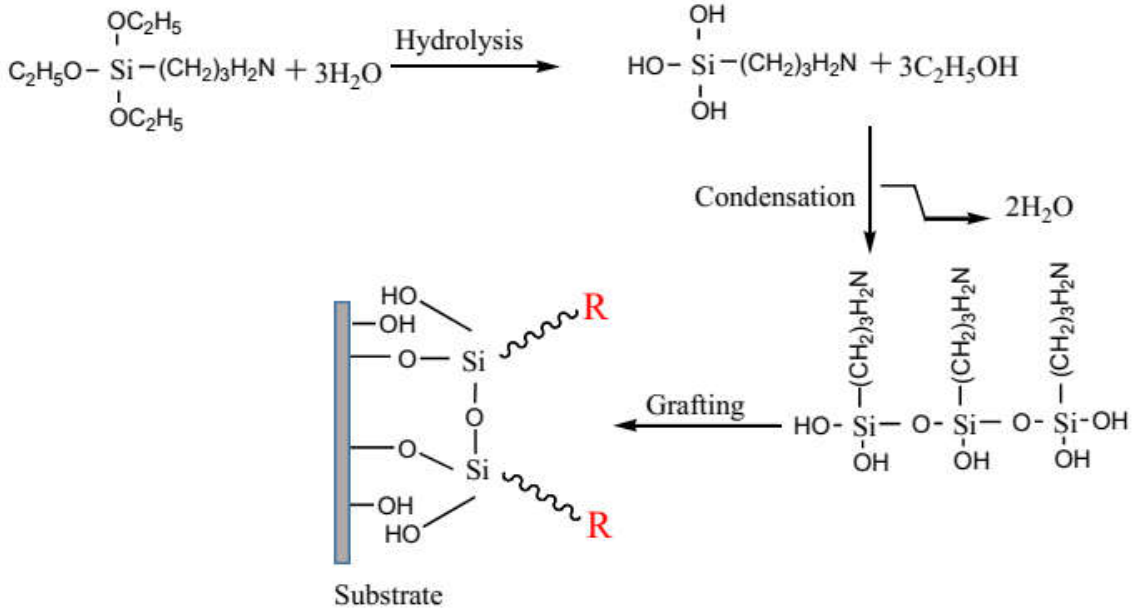

Figure 1.5 The hydrolysis and condensation reactions of aminopropyltriethoxysilane

Such successful silylation of clay minerals surfaces, glass fibers surfaces has been reported in present work. Considerable attention has been paid to the kind of silanes as well as solvents, the quantities of silanes and, nano-dispersion of clay mineral layers in hydrolyzed silanes. The silane coupling agents (3-aminopropyltriethoxysilane (APTES), 3-glycidyloxypropyltrimethoxysilane (GPTMS)) were hydrolyzed in a solvent to form silanol. To understand how a chemical reaction between silane coupling agents and the inorganic

substrate, a schematic representation of possible chemical reactions are shown in Figures 1.4 and 1.5. The silanization of the clay minerals can take place at three places: the interlayer space, external surface and at the edges because of the presence of hydroxyl groups as shown in Figure 1.6. The interlayer and edges grafting can increase the distance between the clay minerals layers. For the external surface, the silylation does not affect the interlayer spacing of the clay. In the case of montmorillonite clays, silane can readily intercalate into the interlayer space. Hence, all external surfaces, internal surfaces and broken edges are ready to be silylated (He et al., 2013; Herrera et al., 2004; Qian et al., 2009; Varadwaj et al., 2016). The silanization reaction can also take place onto organoclays to improve their compatibility with the epoxy matrix (Chen and Yoon, 2005b; Chen et al., 2005a; Huskić et al., 2013; Ianchis et al., 2015; Kráčalík et al., 2007; Piscitelli et al., 2012; Qian et al., 2009; Shanmugharaj and Ryu, 2012). The organoclays surface modified using silanes are referred to as twice-functionalized organoclays.

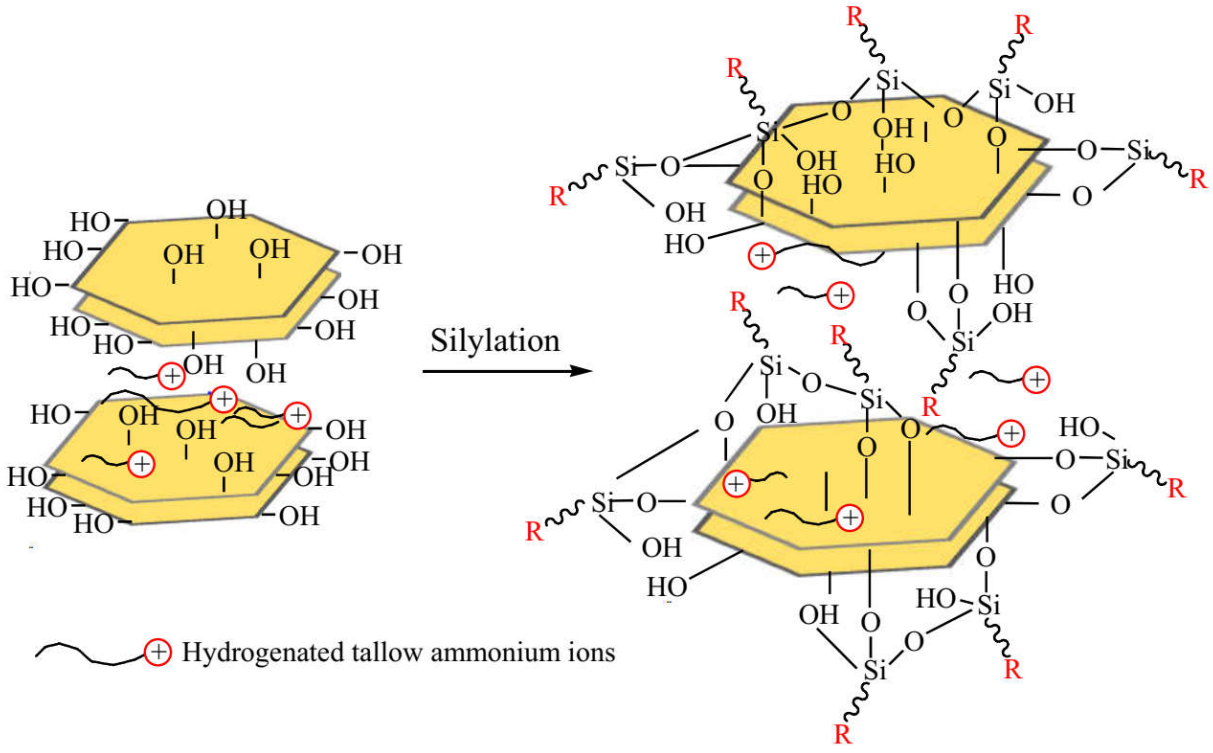

Figure 1.6 The silylation of organoclays

Infrared spectroscopy (IR), Fourier transform infrared spectroscopy (FTIR), Nuclear magnetic resonance (NMR) spectroscopy, X-ray photoelectron spectroscopy (XPS), X-ray diffraction (XRD), Thermogravimetric analysis (TGA) and contact angle measurements are used to verify grafting of silanes on clay minerals.

1.2.4 Silylated clay minerals based polymer nanocomposites

The silanes interact with pristine as well as organically modified montmorillonite (MMT and OMMT) because of the presence of –OH groups at broken edges, in interlayer spaces and at the external surface of clay mineral layers (Herrera et al., 2004; Zhang et al., 2006). Based on our knowledge, the silane grafting reaction is dependent on the nature of clay minerals (Daitx et al., 2015; He et al., 2005; Romanzini et al., 2015b, 2015a; Wan et al., 2008; Wang et al., 2005), the number of reactive sites available at broken edges, interspace or external surface of clay mineral (Herrera et al., 2004; Varadwaj et al., 2016; Zhang et al., 2006), the grafting temperature (Piscitelli et al., 2010; Yang et al., 2012), the chain length of silane moieties (He et al., 2013; Ianchis et al., 2012; Piscitelli et al., 2010), quantity of silane (Huskić et al., 2013; Piscitelli et al., 2010), solvent and method used for silanization of clay minerals (Bertuoli et al., 2014; Shanmugharaj et al., 2006; Shen et al., 2007; Su et al., 2013; Yang et al., 2012). The functionalization of clay minerals with SCAs can be confirmed by Infrared spectroscopy (IR), Fourier transform infrared spectroscopy (FTIR), Nuclear magnetic resonance (NMR) spectroscopy, X-ray photoelectron spectroscopy (XPS), X-ray diffraction (XRD) techniques. A quantitative measure of the amount of silane grafted on clay minerals is comparing the percent mass loss of silylated clay minerals with that of non-silane treated clay in Thermogravimetric analysis (TGA).

Shanmugharaj et al., (2006) studied the influence of different solvents on the grafting of aminopropyltriethoxy silane on MMT. Each silane was hydrolyzed in different solvents and clay was dipped and mixed in it by stirring. It was reported that the average d_{001}-spacing of silane modified clays increased in those cases when solvent had higher or lower surface energy than that of MMT, but the grafted amount of aminosilanes on clay reduced with the use of high surface energy solvents. Su et al., (2013) concluded that nonpolar solvents facilitate the interlayer grafting reaction which increases the interlayer spacing of MMT. In the case of polar-protic solvents, the decreased hydrolysis extent and the hydrogen bonding led to a small grafting of silane and a low degree of condensation among silane molecules. Su et al., (2012) reported simultaneous condensation of silane oligomers in between adjacent clay layers. The silylation of MMT was carried out using APTES. The silane molecules intercalated into MMT interlayer space, and the condensation of silane in between two adjacent clay layers led to an increase in the interlayer height of MMT. Further, a new surfactant was introduced, which showed the possibility of carrying some target matters in the expanded interspace of silylated clay minerals.

To prepare reinforced thermoplastics, Chen and Yoon, (2005b), modified an OMMT, Cloisite® 25A with glycidoxypropyltrimethoxysilane that improved the dispersion of silylated OMMT in poly (L-lactide) and poly[(butylenes succinate)-co-(butylene adipate)] nanocomposites. The tensile modulus and tensile strength of nanocomposites increased with an increase in clay minerals concentration. In a similar study, Chen and Yoon, (2005a) studied the effect of silane modification of three types of organically modified clays: Cloisite® 15A, Cloisite® 20A and Cloisite® 30B on properties of poly(L-lactide) clay nanocomposites. It is interesting to note that an exfoliated morphology was obtained only in nanocomposites containing silylated clay minerals. Higher grafting of silane on clay minerals resulted in better dispersion and higher degree of intercalation in poly(L-lactide) polymer. Wan et al., (2008) synthesized Polybutylene terephthalate (PBT)-clay nanocomposites based on silylated clay minerals. A MMT Cloisite® Na^+ and an OMMT Cloisite® 30B were silanized using APTES. The organic moieties of APTES were able to intercalate in interspace of clay minerals as evident from an increase in d_{001} space of silylated clays. PBT- silylated Cloisite® 30B had an intercalated structure and silylated clay minerals were observed to exist as swollen elliptical particles in PBT. The degree of crystallinity increased significantly in exfoliated Cloisite® 30B -PBT nanocomposites.

Kim et al., (2010) studied the effect of silylation of Cloisite® 25A OMMT on properties of Nylon 6-clay nanocomposites. Cloisite® 25A OMMT was modified using three different silane coupling agents, i.e., 3-aminopropyltriethoxysilane, 3-glycidoxypropyltrimethoxysilane, and 3-isocyanatepropyltriethoxysilane. The tensile modulus, tensile strength, and elongation of break of nanocomposites incorporating silylated Cloisite® 25A improved significantly than nanocomposites containing Cloisite® 25A. The highest improvements were attained in nanocomposites containing Cloisite® 25A modified with 3-glycidoxypropyltrimethoxysilane. This was mainly attributed to a possible reaction between silane groups with the hydroxyl and carboxyl groups of the polymer chain end. De Maria et al., (2011) carried out silylation of Dellite HPS, an MMT and Dellite 72T, an OMMT. The poly(methyl methacrylate) (PMMA)-clay nanocomposites were synthesized using the silylated clays. The clay minerals had an exfoliated morphology in nanocomposites at 1 wt% and 3 wt%. The glass transition temperature (T_g) of PMMA-clay nanocomposites increased as a result of silylation of clay minerals. The silylation of clay minerals improved thermal stability and hydrophobicity of clay minerals

Daitx et al., (2015) modified two different clays, i.e. Cloisite® Na^+ MMT and Halloysite using aminopropyltriethoxysilane to study the effect of silylation of clay minerals on properties of

PHBV nanocomposites. The silylation of MMT promoted homogeneous dispersion that led to an increase in the elongation at break. The tensile and fracture strength did not improve significantly. The silylation of halloysite clay did not influence the properties of PHBV nanocomposites. This was attributed to a limited scope of grafting of silane coupling agents on halloysite.

There are also a few reports involving thermosets, Ha et al., (2008, 2007), Ha and Rhee, (2008) carried out silylation of MMT with 3-aminopropyltriethoxysilane by dispersing MMT in the aqueous silane solution. The tensile modulus and tensile strength, wear resistance and fracture toughness of the nanocomposites increased in comparison to unmodified epoxy-clay nanocomposites and neat epoxy specimen. These improvements had been attributed to uniform dispersion of silane modified clays in epoxy and better adhesion of clays with epoxy. Park et al., (2009) modified MMT using three silane coupling agents: aminopropyltriethoxysilane, glycidoxypropylmethoxysilane, and methacyloxypropyltrimethoxysilane. The silylation of MMT led to enhancement of the specific component and dispersive components of surface free energy. A significant increase in critical stress intensity factor as well as interlaminar shear strength was observed in silylated clay –nanocomposites.

Wang et al., (2006b) observed that stiffness as well as toughness of the epoxy-clay nanocomposites improved on incorporation of clay minerals treated with 3-aminopropyltrimethoxysilane. Silylated clay minerals had exfoliated even when a small quantity of silane was used. Piscitelli et al., (2010) modified sodium montmorillonite (Na-MMT) using 3-aminopropyltriethoxysilane, N-2-aminoethyl-3-aminopropyltrimethoxysilane and 3-[2-(2-aminoethylamino) ethylamino]-propyl-trimethoxy silane, dissolved in glycerol. The processing involved two different temperatures: 80°C and 130°C, continuous stirring for 3h under nitrogen and use of two different silane concentrations. The amount of silane grafted and the d_{001} spacing of clay minerals increased with an increase in both the silane concentration in the solvent and reaction temperature. In a similar study, Piscitelli et al., (2012b) observed that epoxy-clay nanocomposites containing MMT treated with 3-aminopropyltriethoxysilane and 3-trimethoxysilylpropylethylenediamine exhibited a significant increase in tensile strength, elongation at break and toughness in comparison to pristine MMT composites.

Ianchis et al., (2012) functionalized Cloisite® 30B with four different alkoxysilanes. The effect of chain length of organofunctional groups on the degree of functionalization of clay mineral and properties of clay-polystyrene nanocomposites was studied. The grafting of silanes decreased with an increase in chain length, but as expected, the hydrophobicity of Cloisite®

30B increased. The glass transition temperature (T_g) of clay-polystyrene nanocomposites increased by the modification of Cloisite® 30B with different silane coupling agents. Huskić et al., (2013) carried out the silylation of montmorillonite (MMT) with different amount of silanes for different reaction periods. Small angle X-ray scattering (SAXS) indicated an increase in d_{001} spacing of MMT with an increase in the concentration of silane. Also, the epoxy-clay nanocomposites containing silylated MMT had slightly higher glass transition temperature (T_g) and increased elastic modulus in comparison with the nanocomposites containing other commercial OMMT epoxy nanocomposites/ neat epoxy.

Ryu et al., (2016) performed silylation of MMT using different concentrations of aminopropyltriethoxysilane (APTES). XRD, FTIR, and Differential Thermogravimetric analysis (DTG) were used to verify grafting of organic moieties. The interlayer spacing of MMT increased with an increase in the concentration of APTES during the silylation. DTG results showed that the grafting yield (a measure of silane grafted on MMT) was almost constant for a higher concentrations of silanes. The corresponding epoxy-clay nanocomposites based on silylated clays had an intercalated structure. The incorporation of silylated MMT at different clay content i.e. 2, 6 and 10 wt% resulted in significant increase in tensile modulus, tensile strength, and fracture toughness. The water uptake of epoxy was also reduced with an incorporation of silylated MMT.

Shen et al., (2007) carried out silanization of Ca MMT with two different SCAs viz. 3-aminopropyltriethoxysilane (APTES) and trimethylchlorosilane (TMCS) via two different grafting reactions. The silylated clay minerals were characterized using FTIR, XRD, and TGA. In the first grafting reaction the MMT was dispersed in a silane-water/ethanol mixture. In the second reaction, MMT was exposed to saturated vapor from refluxing silane for 6h. The results indicated a more significant amount of silanes intercalated in interlayer space of MMT using second grafting reaction. This had been attributed to the availability of more non-condensed silane molecules during silylation. The grafting of silanes was also significantly influenced by the size of organic moieties.

Bruce et al., (2014) carried out silylation of MMT using three different silane coupling agents, i.e. 3-aminopropyldimethylethoxysilane (APDMES), 3-aminopropyltriethoxysilane (APTES) and n-propyldimethylmethoxysilane (PDMMS). In the case of APDMES, grafting reaction was carried out using different concentrations of silane, whereas the concentration of APTES and APDMES was fixed. The effect of a change in concentration of APDMES on silylation of MMT was evident from a larger increase in interlayer height and higher weight loss as

compared to other silanes. TGA curves also revealed that the APTES and APDMES were grafted on MMT in the same amount, whereas PDMMS was barely grafted. The addition of silylated clays caused a stoichiometric imbalance between epoxy and amine groups. Therefore the thermal/mechanical properties of nanocomposites incorporating MMT modified using different concentrations of APDMES were different. Overall, an improvement in mechanical as well as thermal properties was achieved with incorporation of silylated MMTs.

Silva et al., (2011) prepared epoxy-clay nanocomposites based on two different clay minerals, a MMT, modified using N-(2-aminoethyl)-3-aminopropyltrimethoxysilane and the other, a commercially available OMMT, Cloisite® 30B. The silylated MMT was characterized by FTIR, XRD, NMR, and TGA to confirm grafting of silanes. Further, epoxy-clay nanocomposites were synthesized using different concentrations of silylated MMT, i.e. 0.5, 1, 2.5, 5 wt%. A better dispersion state and absence of diffraction peak in SAXS patterns of nanocomposites containing silylated MMT led to higher improvements in tensile modulus, tensile strength, and toughness of nanocomposites than those of Cloisite® 30B based nanocomposites.

Bertuoli et al., (2014) silanized Cloisite® Na MMT using 3-aminopropyltriethoxysilane dissolved in various solvents, i.e. ethylene glycol, tetrahydrofuran and distilled water-ethanol solution at two different temperatures 50°C and 80°C. The silylated clays were characterized using FTIR, XRD, and TGA. The XRD results indicate that APTES was able to intercalate in interlayer space. TGA indicated that the highest amount of silane was grafted on MMT dispersed in hydroalcoholic media (water-ethanol solution). The amount of grafted silane on MMT dispersed in ethylene glycol and tetrahydrofuran was very low in comparison to those in MMT dispersed in water and MMT dispersed in hydroalcoholic media.

M. and Ivanković, (2013) carried out silylation of a Na MMT, Nanofil 757 using different concentrations of 3-aminopropyltriethoxysilane and different grafting reaction times. The amount of grafted silane increased with an increase in the concentration of APTES, which was evident from an increase in interlayer spacing of Nanofil 757. The NMR spectroscopy confirmed grafting of silane in the interlayer space because of condensation of silane molecules with interlayer silanol groups. The nanocomposites incorporating silylated MMT had higher storage modulus and glass transition temperature (T_g) as compared to nanocomposites incorporating OMMTs Nanofil 2 and Nanofil 8.

Choi et al., (2009) studied the mechanical properties of epoxy-clay nanocomposites containing three different clay minerals added at different concentrations (2, 6, 10 wt%). Cloisite® Na^+, Cloisite Na^+ modified with 3-aminopropyltriethoxysilane, and Cloisite® 15A OMMT based nanocomposites were prepared. The highest increase in elongation at break of nanocomposites was observed in nanocomposites containing 6 wt%, silylated Na^+ MMT. This composition exhibited the highest toughness also. The clay minerals had an intercalated morphology in the nanocomposites incorporating 6 wt% clay.

Romanzini et al., (2015a) synthesized nanocomposites based on an unsaturated resin and Cloisite® 30B OMMT, Cloisite® 15A OMMT and Cloisite® Na modified with two different silane coupling agents viz. vinyltriethoxysilane and γ-methacryloxypropyltrimethoxysilane. The nanocomposites clay minerals containing onium ions, i.e. Cloisite® 15A and Cloisite® 30B exhibited an exfoliated clay morphology which was confirmed by TEM and decreased enthalpy (DSC experiments). The flexural strength and impact strength of these nanocomposites were higher than nanocomposites with silylated clay minerals. However silylated clay minerals based nanocomposites had higher flexural modulus and higher thermal deflection temperature due to improved clay minerals-matrix interactions.

Ianchis et al., (2015) synthesized epoxy-clay nanocomposites containing Cloisite® 93A OMMT modified with three different alkoxysilanes (phenyldimethylethoxysilane, octyldimethylmethoxysilane and octadecyldimethylmethoxysilane). The silane molecules were able to intercalate in clay interspace and increase the d_{001} spacing of OMMT. The highest increase was obtained in the case wherein silane with longest hydrocarbon chain was used. The epoxy-silylated clay nanocomposites had an intercalated morphology. The nanocomposites containing clay minerals modified with octyldimethylmethoxysilane and octadecyldimethylmethoxysilane showed a significant increase in glass transition temperature (T_g) and storage modulus of nanocomposites.

Not much literature is available on fiber reinforced epoxy composites containing silyated clay minerals. Hamidah et al., (2010) observed an increase in the flexural modulus and flexural strength of the glass fiber reinforced epoxy-clay nanocomposites containing Nanomer® 1.30E treated with aminopropyltrimethoxysilane.

The literature review on nanocomposites based on silylated clay minerals has been presented in Table 1.1 in chronological order.

Table 1.1 Selected studies on silylated clay minerals-polymer nanocomposites

S. No	Material System	Synthesis Technique	Key Results	Reference
1.	Epoxy-clay nanocomposites containing Nanomer® PGW MMT modified with aminotriethoxysilane	Mixing of clay minerals (1, 2, 3 wt%) using high shear homogenizer Solution processing	High exfoliation of clay mineral layers led to improvements in storage modulus, tensile modulus and tensile strength of nanocomposites based on silylated clay.	Wang et al., (2006b)
2.	Epoxy-clay nanocomposites containing Cloisite® Na^+ MMT modified with aminotriethoxysilane	Silylated MMT in different concentrations, i.e. 2, 4, 6 and 10 wt% was mixed in epoxy resin by stirring. *In-situ* polymerization	The tensile modulus and tensile strength of epoxy-clay nanocomposites increased with increase in the concentration of silylated MMT. The clay minerals had an exfoliated morphology in nanocomposites	Ha et al., (2007)
3.	Epoxy-clay nanocomposites containing Cloisite® Na^+ MMT modified with aminotriethoxysilane	Silylated MMT in different concentrations, i.e. 2, 4, 6 and 10 wt% was mixed in epoxy resin by stirring. *In-situ* polymerization	Silylated clay minerals had an intercalated morphology in an epoxy matrix. Silylation of clay minerals led to a uniform dispersion of mineral layers in epoxy. The fracture toughness decreased with the incorporation of silylated clay minerals because of embrittlement of matrix, increase in air voids and debonding of MMT from the epoxy matrix.	Ha et al., (2008)
4.	Polybutylene terephthalate(PBT)- clay nanocomposites based on Cloisite® 30B / Cloisite® Na^+ modified with 3-aminopropyltrieth oxysilane	Melt-compounding	Silylation increased interlayer height of MMT and OMMT. PBT-Cloisite® 30B had an exfoliated structure. The PBT-silylated Cloisite® 30 B showed slight intercalation forming aggregates. The degree of crystallinity of PBT increased with the incorporation of Cloisite® 30B	Wan et al., (2008)

S. No	Material System	Synthesis Technique	Key Results	Reference
5.	Epoxy-clay nanocomposites incorporating Cloisite® Na^+ MMT modified with 3-aminopropyltrieth oxysilane and Cloisite® 15A OMMT	Solution processing. Acetone was used to facilitate mixing. Clay minerals added at different concentrations (2, 6, 10 wt%)	The nanocomposites containing silylated MMT exhibited the highest elongation at break and fracture toughness. The nanocomposites based on 6 wt% clay minerals had an intercalated morphology, and it showed highest improvements in properties as compared to other compositions.	Choi et al., (2009)
6.	Epoxy-clay nanocomposites containing Cloisite® Na^+ MMT modified with aminotriethoxysil ane, glycidoxypropyl methoxysilane, and methacyloxyprop yltrimethoxysilan e	Mixing of silylated MMT by stirring followed by ultrasonication *In-situ* polymerization	The treatment of clay with silane coupling agents promoted dispersion of clay mineral layers in epoxy. The critical stress intensity factor (K_{IC}) and interlaminar shear stress (ILSS) values for all of treated MMT/epoxy composites increased significantly because of improved adhesion between clay mineral layers and epoxy. The nanocomposites containing clay minerals treated with aminopropyltriethoxysilane showed the highest improvement in properties.	Park et al., (2009)
7.	Epoxy-clay nanocomposites containing Cloisite® Na^+ MMT modified with aminotriethoxysil ane	*In-situ* polymerization	Epoxy-silylated MMT nanocomposites exhibited 82% higher fracture toughness as compared to epoxy-pristine MMT nanocomposites. The epoxy-silylated MMT nanocomposites also showed higher tensile modulus and tensile strength at different temperatures, i.e. -30°C, 25°C and 40°C, which had been attributed to a good dispersion and improved adhesion between MMT and epoxy.	Ha et al., (2010)
8.	Nylon 6-clay nanocomposites based on silylated Cloisite® 25A	Melt-mixing with twin screw extruder	The tensile modulus, tensile strength, elongation at break of Nylon 6-silylated Cloisite® 25A nanocomposites increased	Kim et al., (2010)

S. No	Material System	Synthesis Technique	Key Results	Reference
	modified with 3-aminopropyltriethoxysilane, 3-glycidoxypropyltrimethoxysilane, and 3-isocyanate propyltriethoxysilane		significantly regardless of the type of silane coupling agent because silylated clay minerals had and exfoliated morphology.	
9.	Glass fiber reinforced epoxy-clay nanocomposites based on Nanomer® 1.30E OMMT modified with aminotriethoxysilane	Mixing of clay minerals using mechanical stirrer Hand lay-up method	The flexural properties of glass fiber reinforced epoxy-clay nanocomposites increased with incorporation of silylated clay minerals. The silylated clay minerals were also observed to be attached to glass fibers and this improved the fiber-matrix adhesion at interfaces.	Hamidah et al., (2010)
10.	Poly(methyl methacrylate) (PMMA)- clay nanocomposites based on Dellite HPS MMT and Dellite 72T OMMT modified with chloro-dimethyl-octadecylsilane	Nanocomposites were prepared using different concentrations of silylated clays (1, 3, 5 wt%) *in situ*-intercalative polymerization	Silylation of MMT and OMMT increased the thermal stability of nanocomposites. Exfoliated morphology was observed in nanocomposites containing 1 wt% and 3 wt% clay minerals.	De Maria et al., (2011)
11.	Epoxy-clay nanocomposites based on MMT/ Cloisite® 30B OMMT modified with 3-aminopropyltriethoxysilane	Epoxy resin was preheated to 50°C, epoxy-clay resin mixing using high shear homogenizer *In-situ* polymerization	A better dispersion and absence of diffraction peak in SAXS patterns of epoxy-clay nanocomposites led to higher improvements in tensile modulus, tensile strength, and toughness of nanocomposites based on silylated clays. The nanocomposites based on Cloisite® 30B had an intercalated morphology.	Silva et al., (2011)
12.	Epoxy-clay nanocomposites incorporating MMT modified	Mixing of clay minerals using two	Higher (T_g) and improved tensile modulus of epoxy-silylated clay nanocomposites as compared to epoxy-pristine	Piscitelli et al., (2012a)

S. No	Material System	Synthesis Technique	Key Results	Reference
	with 3-aminopropyltrieth oxysilane and N-(2-aminoethyl)-3-aminopropyltrime thoxysilane	different methods. (a) sonication (b) sonication with ball-milling *In-situ* polymerization	MMT or epoxy pronounced better interfacial interactions of silylated clay minerals. A combination of sonication and ball-milling, used to shear clay minerals yielded superior dispersion and corresponding improved mechanical properties of nanocomposites containing 3 wt% clay minerals.	
13.	Epoxy-clay nanocomposites containing silylated Nanofil 757® MMT, Nanofil 2® and Nanofil 8® OMMT	Different amounts (1, 3, 5 mass%) of silylated MMT/ OMMT *In-situ* polymerization	The silane molecules were able to intercalate in interlayer space of MMT. The amount of grafted silane increased with an increase in the concentration of silane in grafting reaction. Epoxy-clay nanocomposites containing silylated MMT exhibited improved thermomechanical properties.	M. and Ivanković, (2013)
14.	Epoxy-clay nanocomposites incorporating MMT modified with three different SCA's i.e. 3-aminopropyldime thylethoxysilane (APDMES), 3-aminopropyltrieth oxysilane (APTES), n-propyldimethylm ethoxysilane (PDMMS)	Mixing of MMT by sonication for 30 min. *In-situ* polymerization	The interlayer space of MMT increased with an increase in the concentration of APDMES used during grafting reaction. The grafting of APTES also increased the interspacing of MMT, but in the case of PDMMS, a decrease was observed. The silylated clay nanocomposites had intercalated structure. The size of organic moieties did not significantly influence the amount of grafted silane. The mechanical and thermal properties of silylated-clay nanocomposites had been significantly impacted by the concentration of silane used during grafting reaction.	Bruce et al., (2014)

S. No	Material System	Synthesis Technique	Key Results	Reference
15.	Nanocomposites based on an unsaturated resin and Cloisite® 30B OMMT, Cloisite® 15A OMMT and Cloisite® Na modified with compatible silanes, vinyltriethoxysilane (CVTES) and γ-methacryloxypropyltrimethoxysilane (CMPS)	Mixing of clay minerals using mechanical stirring and ultrasonication Resin transfer molding into a mold	The nanocomposites with onium ion modified clay minerals, i.e. Cloisite® 15A®, and Cloisite® 30B exhibited exfoliated morphology and superior dispersion as compared to silylated Cloisite® Na^+ clay minerals. However, silylated clay minerals based nanocomposites showed higher flexural modulus and higher thermal deflection temperature due to improved clay minerals-matrix interactions.	Romanzini et al., (2015a)
16.	Epoxy-clay nanocomposites containing Cloisite® 93A OMMT modified with three different silanes (phenyl dimethylethoxysilane, octyl dimethylmethoxy silane and octadecyldimethylmethoxysilane)	Mixing of clay minerals using 3-roll mill *In-situ* polymerization	The silylated clay minerals were more compatible with epoxy because of their enhanced hydrophobic behavior. The clay minerals had an intercalated structure in epoxy matrix. The improved adhesion and intercalation of clay minerals brought improvements in thermo-mechanical properties of nanocomposites.	Ianchis et al., (2015)
17.	Epoxy-clay nanocomposites containing MMT modified with aminopropyltrieth oxysilane	Epoxy resin and pristine and silylated MMT mixed in a solvent using a high-speed mechanical stirrer Solution blending and cured in Teflon plates under vacuum	Interlayer space of MMT increased after silanization. The epoxy-clay nanocomposites based on silylated MMT had formed intercalated structure. In contrast to pristine MMT-epoxy nanocomposites, the tensile strength, fracture toughness of silylated MMT-epoxy nanocomposites increased with an increase in clay content.	Ryu et al., (2016)

1.3 Fiber reinforced epoxy-clay nanocomposites

The fiber reinforced epoxy nanocomposites based on clay minerals have attracted great attention in today's materials research because clay minerals have a high modulus (176 GPa), high in-plane strength, high aspect ratio (more than 1000), a high surface area (more than 750 m^2/g), low cost, abundance in nature, and are benign to the environment (Pavlidou and Papaspyrides, 2008; Saba et al., 2016). These properties make clay minerals a preferred material for the design of hybrid composites. The improvements in performance of glass / carbon / plant -fibers- epoxy composites with an addition of clay minerals have been reported by many researchers (Alamri et al., 2012; Njuguna et al., 2007; Raji et al., 2016; Venkatram et al., 2016; Verma, 2016). The improvements in various properties viz. compressive strength (Subramaniyan and Sun, 2006), flexural modulus and flexural strength, durability, wear resistance (Daud et al., 2009; Firdosh et al., 2015; Guermazi et al., 2013; Iqbal et al., 2009; Khan et al., 2011; Rafiq et al., 2017; Senthil Kumar et al., 2015; Sharma et al., 2012; Tsai et al., 2006), tensile modulus and tensile strength (Kanny and Mohan, 2014; Khan et al., 2010), Interlaminar shear strength (Quaresimin and Varley, 2008), impact properties (Iqbal et al., 2009; Khan et al., 2010; Mohan et al., 2015; Rafiq et al., 2017), improved fatigue life (Helmy and Hoa, 2014; Withers et al., 2015), flame retardancy and improved thermal stability (Beyer, 2002; Lin et al., 2006; Mohan et al., 2015; Zhou et al., 2012) are of interest. These distinguishing characteristics make the fiber reinforced epoxy-clay nanocomposites more and more important in the modern polymer industry.

The preparation scheme of fiber reinforced epoxy-clay nanocomposites has been shown in Figure 1.7. The synthesis of fiber reinforced epoxy-clay nanocomposites is carried out in two steps. In the first step the clay minerals are dispersed in epoxy resin. The clay minerals layers try to retain the original parallel packing due to electrostatic attraction and are difficult to disperse in the polymer resin. Therefore, clay minerals layers are dispersed in polymer resin by application of high shear forces, e.g. mechanical mixing, high shear homogenization, ultrasonic mixing mechanical mixing followed by ultrasonication. Often, degassing of the mixture is performed to avoid entrapment of air. The second step is mixing of hardener in resin-clay mixture and impregnation of the mixture in fibers preforms to manufacture three-phase hybrid nanocomposite, in which the main reinforcing phase is continuous fibers as shown in Figure 1.8.

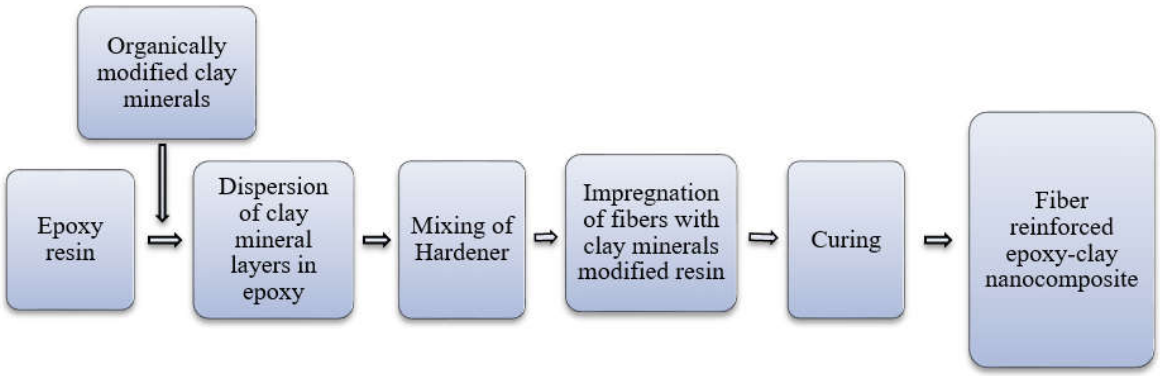

Figure 1.7 Preparation scheme for fiber reinforced epoxy-clay nanocomposites

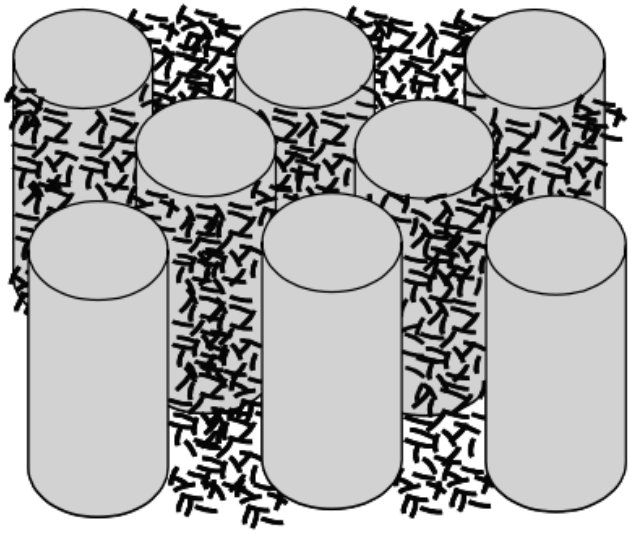

Figure 1.8 Clay minerals reinforcement of matrix in a fiber reinforced composite (Vlasveld et al., 2005)

In the past, the fiber reinforced polymer-clay nanocomposites had been predominantly synthesized using hand lay-up method, compression molding, pre-pregging and resin infusion methods (Chowdhury et al., 2006; Dean et al., 2006; Gabr et al., 2015; Gurusideswar and Velmurugan, 2014; Mohan et al., 2015; Njuguna et al., 2007; Nuhiji et al., 2016; Withers et al., 2015; Zhou et al., 2012).

Three different types of structures are formed depending on the chemistry and processing conditions. Small angle X-ray scattering (SAXS) and Transmission electron microscopy (TEM) are generally used to investigate the morphology of nanocomposites. A schematic illustration of three possible structures, with corresponding SAXS and TEM results, is shown in Figure 1.9. When the polymer is unable to penetrate between the clay mineral layers, a phase separated (immiscible) composite is obtained. In this case, there is no change in interlayer

space of clay minerals and the X-ray scan of nanocomposites would essentially look the same as is in the organoclay powder. If the polymer enters the interlayer space and increases d-spacing as indicated by change in SAXS patterns, an intercalated nanocomposite is obtained. In this case, the diffraction peak gets shifted to lower 2θ values, indicating an increase in d_{001} spacing. If the clay mineral layers are completely and uniformly dispersed in a random direction, an exfoliated or delaminated nanocomposite is obtained.

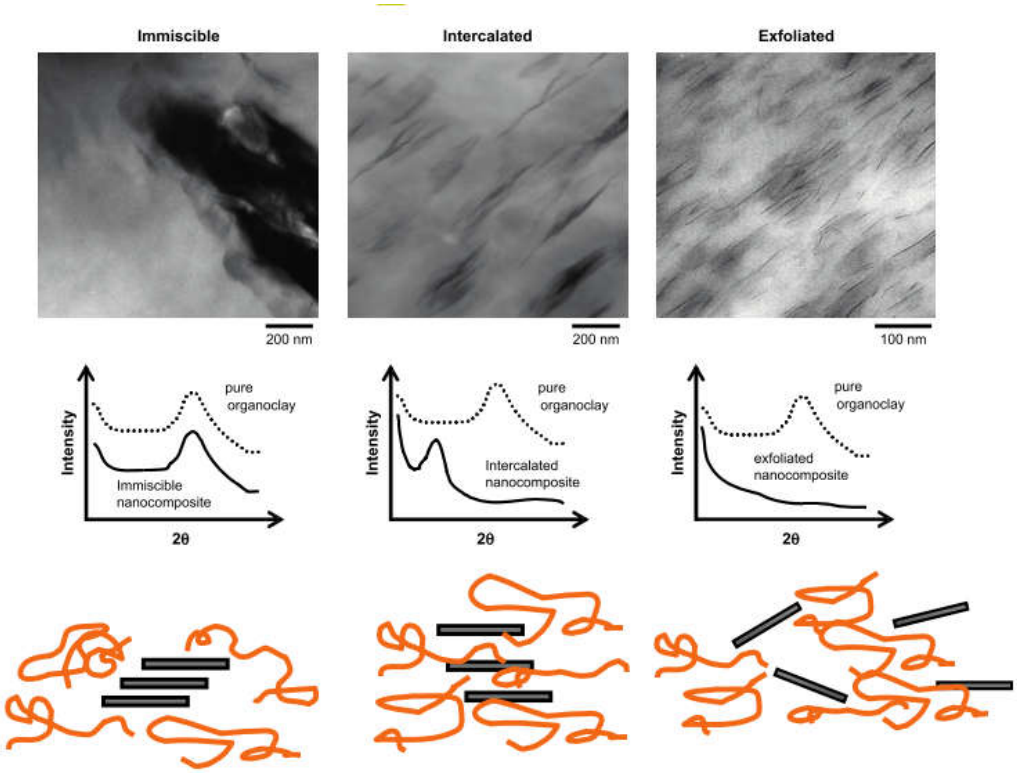

Figure 1.9 Illustration of different structures with corresponding XRD and TEM results(Paul and Robeson, 2008)

In a fully exfoliated morphology, no diffraction peak is expected since the regular stacking of clay layers does not exist or the layers move to a considerable distance apart, which would not be detected by SAXS. TEM results confirm the formation of exfoliated morphology.

Intercalation / exfoliation of clay mineral layers is one of the primary requirements to achieve better mechanical properties of polymer-clay nanocomposites. A uniform dispersion and exfoliation of clay minerals generate a large surface area for interaction with the matrix. However, the dispersion is dependent on the type of clay mineral, polymer and the processing technique (Albdiry et al., 2012; Paul and Robeson, 2008).

1.3.1 Fiber reinforced polymer clay nanocomposites: synthesis, properties, and applications

A number of articles have been recently published on synthesis, characterization, and applications of r fiber reinforced as well as clay minerals reinforced polymer composites (Albdiry et al., 2012; Azeez et al., 2013; Paluvai et al., 2014; Pavlidou and Papaspyrides, 2008; Sathishkumar, T.P. Satheeshkumar and Naveen, 2014). However, in this section, the review of literature is limited to processing and characterization of fiber reinforced polymer-clay nanocomposites.

In fiber reinforced polymer-clay nanocomposites, homogeneous dispersion of clay mineral layers, the volume fraction of reinforcements, the orientation of fibers and lay-up, interfacial adhesion between the reinforcements and matrix and complete crosslinking of resin and hardener are crucial aspects for improved performance over conventional fiber reinforced composites. Lin et al. (2006) had reported the effect of different processing methods on the dispersion of commercially available organically modified montmorillonite Cloisite® 15A in the matrix of glass fiber reinforced epoxy composites. The dispersion state of clay mineral layers and mechanical properties of fiber reinforced epoxy-clay nanocomposites was influenced by the (i) orientation of fibers relative to the direction of impregnation of resin (ii) dispersion of clay minerals in different regions in a laminate (iii) quantity of clay minerals in the matrix. The flexural modulus and thermal decomposition temperature of nanocomposites increased with an increase in the concentration of clay minerals. Subramaniyan and Sun (2006) manufactured composites using vacuum assisted wet lay-up method to avoid filtration of clay minerals and observed an increase in elastic modulus of fiber reinforced epoxy composites with incorporation of organoclay at 3% and 5% by weight. Interestingly, highest improvement in elastic modulus was observed in laminates cured at room temperature and post-cured at elevated temperature. The compressive strength of laminates was influenced by volume fraction and orientation of glass fibers in composites. Some other recent studies undertaken on correlate processing variables to mechanical properties have been discussed below.

Nuhiji et al. (2016, 2013) concluded that a rapid heating rate during curing lowered the viscosity of nanofiller–epoxy resin mixture and facilitated the penetration of polymer chains in clay interlayer space as well as promote adhesion between epoxy and fibers. The use of Quickstep™ process during curing of laminates significantly reduced the agglomeration of clay minerals in fiber preforms and imparted better mechanical properties to fiber reinforced composites (Davies et al., 2007; Zhang and Fox, 2005). Quickstep™ process is a novel

manufacturing process developed by Quickstep Technologies Pvt. Ltd., Perth, Australia which facilitates dispersion of clay minerals in fiber preform layers by reducing the viscosity of epoxy resin-clay mixture through the application of rapid heating rates and mechanical vibrations. Mohan et al. (2015) carried out a systematic study about the effect of quantity of clay minerals, fiber orientation and fiber volume fraction on tensile modulus and ballistic limit during projectile impact. The increase in tensile modulus of nanocomposites was more significant with low quantities of clay minerals because of exfoliation of clay mineral layers. The damping behavior and ballistic limit improved with an increase in the amount of clay in fiber reinforced epoxy composites with different fiber orientations and volume fractions. Quaresimin and Varley (2008) had reported improvement in matrix-dominated properties of carbon fiber reinforced composites with the addition of nanofillers in epoxy. The compressive strength, interlaminar shear strength, and impact strength significantly increased which had been attributed to a delayed opening as well as the growth of cracks in the nano-modified matrix.

Zhou et al., (2012) studied the effect of incorporation of different quantities of clay minerals on thermal and mechanical properties of epoxy-clay nanocomposites. Furthermore, carbon fiber reinforced epoxy-clay nanocomposites were synthesized with 2 wt% clay minerals. The tensile properties, flexural properties and fatigue life of carbon fiber reinforced epoxy-clay nanocomposite increased significantly as compared to carbon fiber reinforced neat epoxy composites. Khan et al., (2010) observed that the tensile modulus, tensile strength, and elongation at failure of carbon fiber reinforced composites increased with incorporation of organoclay at different concentrations. The inclusion of organoclay was found to delay the delamination damage growth in laminates and improve fatigue life for a given cyclic load level. In a similar work, Withers et al., (2015) observed improvement in tensile properties and operational life under vibro-creep-fatigue loadings at 60°C of fiber reinforced composites incorporating clay minerals, which had been attributed to strong adhesion between glass fibers and clay-epoxy matrix. Helmy and Hoa, (2014) carried out static strength and fatigue tests on glass fiber epoxy-clay tapered beam specimens with different lay-ups of glass fibers. The tensile fatigue life of composites improved significantly with the addition of clay minerals due to a decreased crack growth rate over the whole fatigue life except in the early stages of loading.

Some other studies describe the effect of clays minerals with different origins, charge exchange capacities and organic modification, epoxies, the volume fraction of clay minerals, process conditions and morphology of clay minerals in the nanocomposite, etc., which are of importance. Timmerman et al., (2002) synthesized carbon fiber reinforced epoxy-clay

nanocomposites incorporating Cloisite® 25A and alumina particles to study the effect of nanoparticle reinforcement on the response of carbon fiber reinforced composite to cryogenic cycling. Cloisite® 25 A was incorporated into epoxy resin at different concentrations viz. 2, 5, 8 parts per hundred resin (phr) whereas a fixed concentration, i.e. 5 phr of alumina particles was used. An increase in interlaminar shear strength had been observed with incorporation of Cloisite® 25A at 2 and 5 phr. The flexural strength increased with an addition of alumina particles also.

Haque et al. (2003) attained significant improvements in mechanical and thermal properties of conventional glass fiber reinforced composites with incorporation of small amounts of Montmorillonite (MMT) I.28 E. The Thermogravimetric analysis (TGA) of composites revealed that the decomposition rate decreased with incorporation of MMT in epoxy matrix. The Dynamic mechanical analysis (DMA) indicated an increase in glass transition temperature (T_g) with an increase in clay loadings up to 2%. Also, both the interlaminar shear strength and flexural strength of S2-glass epoxy-clay nanocomposites increased by 44% and 24% respectively, with an addition of 1% MMT. But at higher clay concentrations a decrease was observed in all properties.

Avila et al. (2006) performed low-velocity impact tests on glass fiber reinforced epoxy-clay nanocomposites. Nanomer® I.30 E OMMT in different quantities (1, 2, 5 and 10 wt%) were dispersed in epoxy using direct mixing method. XRD patterns indicated an intercalated morphology of nanocomposites. The delamination resistance as well as damping resistance increased with the incorporation of OMMT.

Chowdhury et al., (2006) investigated (i). effect of the addition of nanoclay in different weight percentage and (ii). effect of post-curing on flexural and thermal properties of woven carbon fiber reinforced epoxy matrix composites. Nanomer® I.28E® OMMT in different concentrations, i.e. 1, 2 and 3 wt% were dispersed in epoxy using sonication route. Vacuum assisted resin infusion molding process was used to prepare the carbon fiber reinforced composites. The post-curing of some specimens was done at 100°C for 5 h in a convection oven. The flexural strength and flexural modulus of all specimen increased with 2 wt% OMMT concentration. The highest improvement in flexural strength was 14% that in thermally post-cured samples. However, the modulus of samples cured at room temperature and post-cured at elevated temperature remained almost the same. The DMA results indicated that the storage modulus and loss modulus improved with an addition of 2 wt% OMMT, and then it decreased

at 3 wt% concentration. The scanning electron micrographs of failure surface showed that there was good bonding between fiber and matrix in 2 wt% samples.

Hamidi et al., (2008) investigated the morphology, void content and spatial void distribution in resin transfer molded glass fiber reinforced epoxy-clay nanocomposites. The composite disks containing E-glass fibers, 13.6% (by volume) and different concentrations of Cloisite® 25A OMMT, e.g. 2, 5, 10 wt% were synthesized. The microscopic image analysis of the specimen was carried out at different cross-sections of composites in five different radial directions. The overall void content was observed to increase to 5.1%, and 8.3% in composites containing 5 wt% and 10 wt% OMMT, respectively as compared to fiber reinforced neat epoxy composite. But the presence of OMMT in resin reduced the voids located within the fiber preform by at least 60%.

Xu and Hoa, (2008) investigated the effect of incorporation of clay minerals on the flexural strength and fracture toughness of carbon fiber reinforced epoxy-clay nanocomposites. 2, 4 and 6 phr of Nanomer® I.30E OMMT had been dispersed in epoxy resin. The clay minerals were mixed in the epoxy resin at 80°C using a mechanical stirrer, and the mixture was diluted with 11 parts (50%) of acetone. This mixture was passed through a high pressure mixing machine to prepare a paste. The fiber reinforced epoxy-clay nanocomposites had been manufactured through a hot melt layup and autoclave process. The mode I interlaminar fracture toughness of fiber reinforced composite increased by 53% and 85% with incorporation of 2 and 4 phr OMMT, respectively. At 2 phr, the flexural strength also increased by 38%, but at 6 phr a decrease was observed.

Kornmann et al., (2005) used a hand lay-up method in combination of vacuum bagging to synthesize glass fiber reinforced epoxy-clay nanocomposites. The laminates were placed in a vacuum bag and kept in a hydraulic press under a pressure of 2 bar. Then post-curing was done by removing the vacuum bag and heating the specimens at 140°C for 10h. The flexural modulus and flexural strength increased by 6% and 27%, respectively with incorporation of OMMT. The water uptake was similar for both the materials in the early stages of the experiment, but at 50 °C, it was much high in nanocomposite than in neat epoxy composite.

Dorigato et al., (2012) investigated the fiber-matrix interfacial shear strength of E-glass polymer matrix composites by the single-fiber micro debonding method. The interlaminar shear strength increased by 30%, which had been attributed to stronger fiber-matrix interface

due to the presence of OMMT. Also, the wettability of fibers with polymer increased due to the incorporation of OMMT.

Zulfli and Chow, (2012) prepared glass fiber reinforced epoxy nanocomposites, containing different concentrations of OMMT by hand lay-up technique. The flexural modulus, flexural strength, impact strength and fracture toughness were highest in nanocomposites containing 4 wt% OMMT. The thermal stability of glass fiber reinforced composites was greatly enhanced at this concentration, which was attributed to exfoliation of OMMT mineral layers.

Zhou et al., (2008) synthesized carbon fiber reinforced nanocomposites based on two nano-modified matrices: Cloisite® 10A OMMT- epoxy and Cloisite® Na^+ MMT-phenol. It is interesting to note that SAXS patterns indicated formation of an intercalated structure if OMMT was first mixed in epoxy resin by sonication method. An exfoliated structure in the case if OMMT had been mixed with the hardener first, and then epoxy resin was mixed This had been attributed to smaller size and more flexible molecules of the hardener, which could quickly enter the interspace and separate the clay mineral layers. Also, the tensile strength of intercalated nanocomposites was low as compared to fiber reinforced neat epoxy composites. The exfoliated nanocomposites exhibited an enhanced tensile strength and tensile modulus. The tensile properties of composites in the rubbery state were improved with an addition of OMMT. The flexural properties and glass transition temperature (T_g) of carbon fiber reinforced epoxy/phenol-clay nanocomposites increased with an increase in volume fraction of clay minerals.

Zhou et al., (2012) synthesized epoxy-clay nanocomposites with different quantities (1, 2, 3 and 4 wt%) of clay minerals. The nanocomposites were characterized using dynamic mechanical analysis, thermogravimetric analysis, and flexural property measurements. The composition with 2 wt% clay minerals improved flexural and thermal properties. Further, carbon fiber reinforced nanocomposite incorporating 2 wt% clay minerals showed significant improvements in tensile properties, flexural properties and fatigue performance as compared to fiber reinforced neat epoxy composites.

Bozkurt et al., (2007) carried out organic modification of Na^+ MMT using Hexadecyltrimethylammonium chloride salt by an ion exchange method, and synthesized glass fiber reinforced epoxy-clay nanocomposites with different concentrations (1, 3, 6, 10 wt%) of Na^+ MMT and OMMT. The flexural properties, storage and loss modulus, fire retardancy increased with the incorporation of clay minerals, however at 10 wt% the mechanical, glass transition temperature

(T_g) and flammability of nanocomposites significantly decreased. The glass transition temperature (T_g) improved with the incorporation of OMMT. An incorporation of clay minerals did not significantly influence the tensile properties.

Gurusideswar and Velmurugan, (2014) studied the stress-strain response of epoxy, glass fiber reinforced epoxy composites and glass fiber reinforced epoxy-clay nanocomposites at different strain rates, viz. 0.5, 5, 50 and 500 mm/min. An incorporation of clay minerals in epoxy increased the tensile modulus, but a decrease in tensile strength was observed. The glass fiber reinforced epoxy nanocomposites containing 1.5% clay minerals exhibited a small increase in tensile modulus and tensile strength. At higher concentrations, i.e. 3% and 5%, agglomeration of clay mineral layers led to a decrease in tensile properties.

Dean et al., (2006) synthesized three-phase hybrid nanocomposites with carbon fibers, epoxy modified with different quantities of clay minerals (2, 4, 6 wt%). Exfoliated morphology had been obtained in nanocomposites containing 2 wt% Cloisite® 30B OMMT. The gelation time was calculated from DMA scans at two different cure temperatures. It was concluded that a change in process temperature significantly influences gelation time. The highest improvement was achieved in matrix-dominated properties, i.e. flexural modulus and flexural strength.

Kanny and Mohan, (2014) investigated the effect of a change in concentration of Cloisite® 30B on flow rate and viscosity of epoxy-clay resin mixture, the compressibility of laminate, the extent of curing, tensile stress-strain behavior, and the storage modulus of E-glass fiber reinforced epoxy-clay nanocomposites. The clay content was 1, 2, 3, 4 and 5 wt%. The flow rate and compressibility decreased with an increase in clay minerals content, because of an increase in viscosity of clay – epoxy resin mixture. The tensile modulus, tensile strength, storage modulus, glass transition temperature (T_g) of fiber reinforced clay nanocomposite increased due to increase in clay concentration up to 3 wt% but then decreased at higher clay concentrations.

Rafiq et al., (2017) synthesized hybrid materials with E-CR glass fiber mat, epoxy and two different concentrations of Nanomer® I.30 OMMT (1.5 wt% and 3 wt%). The damage resistance of the laminates under low-velocity impact increased with incorporation of OMMT. The nanocomposite containing 1.5 wt% OMMT showed the highest impact strength as compared to other composition.

Khan et al., (2011) investigated the effect of clay minerals concentration on impact and quasi-static response of epoxy-clay nanocomposites and corresponding carbon fiber reinforced

epoxy-clay nanocomposites. The clay concentrations was 1, 3 and 5 wt%. The flexural modulus, flexural strength, and impact toughness of both epoxy-clay nanocomposites and fiber reinforced epoxy-clay nanocomposites were highest at 3 wt% concentration, and then a decrease in these properties was observed at 5 wt%. The quasi-static fracture toughness was highest in compositions incorporating 5 wt% clay minerals.

Tsai et al., (2006) synthesized epoxy-clay nanocomposites and glass fiber reinforced epoxy-clay nanocomposites to study the effect of clay minerals concentrations (2.5, 5, 7.5 wt %) on static strengths of nanocomposites. The tensile strength of epoxy-clay increased with increase in the concentration of clay minerals, but the strain to failure decreased. The compressive strength of fiber reinforced epoxy-clay nanocomposites was highest in a composition incorporating 5 wt% clay minerals.

A summary of the literature on fiber reinforced clay-polymer nanocomposites in chronological order has been listed in Table 1.2.

Table 1.2 Summary of a literature review on fiber reinforced clay-polymer nanocomposites

S. No.	Material System	Synthesis Technique	Key Results	Reference
1.	Carbon fiber reinforced epoxy nanocomposites (modified with CLOISITE 25 A® OMMT or alumina particles)	Mechanical stirring to mix nanofillers in epoxy. Hot melt impregnation to manufacture prepregs.	Interlaminar shear strength increased with the addition of clay/alumina particles and was highest in laminates containing alumina. Transverse flexural strength and flexural modulus decreased with the addition of nanoclay, an increase in flexural strength and a slight decrease in modulus observed in laminates containing alumina. Increase in transverse coefficient of thermal expansion at low clay loadings. Addition of alumina particles showed little effect on CTE.	Timmerman et al., (2002)
2.	Epoxy-clay and glass fiber reinforced	Mechanical mixing and ultrasonication to mix MMT (1, 2, 5, 10 wt%) in epoxy resin.	At higher clay loadings (5 and 10 wt%), more clay mineral aggregates formed. Glass transition temperature (T_g), Interlaminar shear strength, flexural strength and flexural	Haque et al., (2003)

S. No.	Material System	Synthesis Technique	Key Results	Reference
	epoxy-clay nanocomposite (Nanomer® 1.28 E)	VARIM	modulus of glass fiber reinforced nanocomposite increased at low clay loading (1%), whereas a decrease in these properties had been observed at higher clay loadings.	
3.	Glass fiber reinforced epoxy-clay nanocomposites	Hand layup/vacuum bagging method.	Improvement in flexural and barrier properties by addition of clay minerals.	Kornmann et al., (2005)
4.	Glass fiber reinforced epoxy-clay nanocomposite. (Nanomer® I.30 E)	Direct mixing method. Vacuum assisted wet layup.	The addition of clay minerals reduced delamination, increased rebound during impact testing.	Avila et al., (2006)
5.	Woven carbon fiber reinforced epoxy nanocomposites containing Nanomer® I.28E OMMT	Mixing of OMMT (1, 2, 3 wt %) in epoxy resin using sonication. VARIM.	An increase in flexural properties and storage modulus and loss modulus with the incorporation of OMMT up to 2 wt%. Values decreased at higher concentrations of OMMT. Post-cured samples showed better properties than room temperature cured samples.	Chowdhury et al., (2006)
6.	Carbon fiber reinforced epoxy nanocomposites containing Cloisite® 30B OMMT	Mechanical stirring of epoxy and clay resin mixture Vacuum assisted resin infusion molding	With every 2 wt% increase in the concentration of clay minerals, the viscosity of epoxy-clay resin mixture increased 10 times. Exfoliated morphology was achieved only in nanocomposites incorporating 2 wt% clay minerals. The highest improvements in flexural properties attained in these nanocomposites. Incorporation of clay minerals did not enhance interlaminar shear strength and fracture toughness of fiber reinforced composites.	Dean et al., (2006)
7.	Glass fiber reinforced epoxy-clay nanocomposites	Mixing of clay in epoxy resin by direct mixing, solution mixing,	Ultrasonic dispersion provided the best results in terms of dispersion of clay mineral layers.	Lin et al., (2006)

S. No.	Material System	Synthesis Technique	Key Results	Reference
	containing Cloisite® 15A OMMT	and ultrasonic dispersion methods. VARTM.	Longitudinal flexural modulus and glass transition temperature (T_g) of fiber reinforced nanocomposite increased, but a decrease in flexural strength observed at high clay loadings (5 wt%).	
8.	Nanomer® I.30E OMMT epoxy nanocomposites and corresponding glass fiber reinforced nanocomposites	Vacuum assisted hand lay-up	The strength of epoxy improved with an addition of clay minerals, but strain to failure of specimens decreased. The fiber reinforced epoxy-clay nanocomposites exhibited improved compressive strength.	Tsai et al., (2006)
9.	E-glass fibers and epoxy modified with Na^+ MMT/ OMMT	Mechanical stirring and ultrasonication of epoxy-clay resin mixture Hand lay-up method	The d_{001} spacing of MMT increased after organic modification. The void content in the composite increased with an increase in the concentration of clay minerals. The tensile and flexural properties of both MMT and OMMT nanocomposites were same at 1 wt% clay concentration. The nanocomposites incorporating 6 wt% OMMT exhibited the highest improvements in flexural strength, storage modulus, loss modulus, glass transition temperature (T_g), but the tensile strength was unaffected. The fire retardancy of composites increased significantly with incorporation MMT/OMMT	Bozkurt et al., (2007)
10.	E-glass fiber reinforced epoxy-clay Nanocomposites .	Mechanical stirring and sonication.	Overall void content increased with an increase in clay content. Reduction in voids located within the fiber performs.	Hamidi et al., (2008)
11.	Carbon fiber reinforced epoxy nanocomposite containing different	Shear mixing Attrition milling process. Hand layup.	Increase in ILSS, $G_{IIC,}$ and impact absorption capability with the addition of Cloisite 30B® and VGCF modifiers.	Quaresimin and Varley, (2008)

S. No.	Material System	Synthesis Technique	Key Results	Reference
	Nanofillers: Cloisite® 30B, Pyrograf®-III (VGCF)		A decrease in mode I crack opening behavior with the addition of nanofillers.	
12.	Carbon fiber reinforced epoxy nanocomposites containing Nanomer® I.30E OMMT	Mechanical stirring and high-pressure mixing method Hot melt lay-up Autoclave	The fracture toughness of fiber reinforced composites increased with the incorporation of clay minerals at 2 phr and 4 phr.	Xu and Hoa, (2008)
13.	Carbon fiber/ Cloisite® 15A OMMT-epoxy nanocomposites Carbon fiber/ Cloisite® Na^+ MMT- phenol nanocomposites	Mixing of clay minerals in epoxy resin/ hardener using sonication for 30 min. *In-situ* polymerization Hand-layup and Compression molding	Exfoliation of OMMT in epoxy nanocomposites ocuured if clay was mixed with the hardener. An intercalated structure had formed if clay was mixed with epoxy resin. Superior tensile properties of epoxy-OMMT carbon fiber reinforced composites in comparison with carbon fiber neat epoxy nanocomposites in the rubbery state. Flexural and glass transition temperature (T_g) increased with the incorporation of clay minerals in epoxy/ phenol nanocomposites	Zhou et al., (2008)
14.	Epoxy nanocomposites and carbon fiber reinforced epoxy nanocomposites with Nanomer® I.30P OMMT	Shear mixing sonication in a bath sonicator Hand lay-up, cured using a vacuum hot press	The nanocomposites had been prepared with 1, 3, 5 wt% OMMT. The flexural modulus, flexural strength and impact toughness of both epoxy nanocomposites and carbon fiber reinforced nanocomposites were highest in a composition containing 3 wt% clay minerals, and then a decrease in these properties was observed at 5 wt%. The quasi-static fracture toughness was highest at 5 wt%	Khan et al., (2011)
15.	E-glass fiber/matrix, OMMT	Hand lay-up technique	An introduction of OMMT led to the formation of a stronger fiber-matrix interface, which increased the interfacial shear strength by 30%.	Dorigato et al., (2012)

S. No.	Material System	Synthesis Technique	Key Results	Reference
16.	Glass fiber reinforced epoxy composites, containing various concentrations of OMMT	Hand lay-up technique	A balance of flexural modulus, flexural strength, and impact strength and fracture toughness was achieved only at 4 wt% OMMT loadings.	Zulfli and Chow, (2012)
17.	Epoxy-MMT nanocomposites Carbon fiber reinforced MMT epoxy nanocomposites	Mixing of clay minerals in epoxy resin by sonication Vacuum assisted resin transfer molding in preparing carbon fiber reinforced epoxy-clay nanocomposites	Epoxy-clay nanocomposite incorporating 2 wt% clay minerals had the highest storage modulus and flexural strength. The carbon fiber reinforced epoxy-clay nanocomposite with 2 wt% MMT showed improvements in tensile strength, flexural strength and crack propagation resistance in tension-tension fatigue tests.	Zhou et al., (2012)
18.	Glass fiber reinforced epoxy nanocomposite incorporating Garamite 1958® OMMT	Preheating of epoxy to reduce the viscosity. Mechanical stirring of the epoxy-clay resin mixture Hand lay-up method	The stress-strain behavior was approximately linear up to the maximum stress point and was sensitive to strain rates. The highest modulus and tensile strength observed at highest strain rate, 500 mm/min. The presence of clay minerals at low concentration increased both the tensile modulus and tensile strength of glass fiber reinforced composites.	Gurusides war and Velmurug an, (2014)
19.	S-glass fiber reinforced epoxy nanocomposites containing Nanomer® I.30E OMMT	Manual mixing and high shear homogenization Hand lay-up and autoclave	A small increase in tensile strength of glass fiber reinforced epoxy composite with the addition of OMMT. The strain to failure decreased. The fiber orientation and presence of clay had a significant effect on fatigue life of composite. The presence of OMMT effectively suppressed the crack propagation.	Helmy and Hoa, (2014)

S. No.	Material System	Synthesis Technique	Key Results	Reference
20.	Silane treated E-glass fiber reinforced epoxy nanocomposites based on Cloisite® 30B OMMT	Mechanical stirring of epoxy-clay resin mixture Vacuum assisted resin infusion molding	The flow rate of epoxy-clay resin mixture and compressibility of laminate decreased due to increase in viscosity of the mixture. The exfoliation of clay minerals observed in nanocomposites containing up to 3 wt% clay minerals. The improvements in tensile properties, storage modulus, and glass transition were highest in nanocomposites containing 3 wt% clay minerals. The properties of nanocomposites decreased with a further increase in clay content.	Kanny and Mohan, (2014)
21.	Silane treated E-glass fiber reinforced epoxy nanocomposites based on Cloisite® 30B OMMT	Stirring of epoxy-clay resin mixture maintained at 70 °C Vacuum assisted resin infusion molding	Exfoliated structures were obtained at 1 wt% and 2 wt% clay minerals concentrations whereas at higher concentrations (3, 4, 5 wt%) intercalated structures were formed. The Young's modulus and ballistic limit of nanocomposites increased with an increase in clay minerals concentration. The improvements in damping characteristics and crack resistance attained in nanocomposites with 2 to 3 wt% clay minerals	Mohan et al., (2015)
22.	Glass fiber reinforced epoxy-clay nanocomposites based on Cloisite® 30B	Preheating of epoxy resin. Mixing of clay minerals using a magnetic stirrer Hand lay-up	The fiber reinforced epoxy-clay nanocomposites showed improved tensile properties and operational life under Vibro-creep-fatigue loadings at 60 °C.	Withers et al., (2015)
23.	E-CR glass fiber reinforced epoxy nanocomposites with Nanomer® I.30 OMMT	High shear mixing Hand lay-up and hot pressing method	Exfoliated structures obtained at two different clay mineral loadings (1.5 wt% and 3 wt%). The nanocomposite containing 1.5 wt% clay minerals showed better impact resistance in comparison with other compositions.	Rafiq et al., (2017)

The following studies explain the importance of mixing parameters, e.g. speed of stirrer/ homogenizer, amplitude, and duration of ultrasonication, the temperature during premixing, degassing the solution after sonication/ homogenization and curing schedule in development of nanocomposites by *in-situ* polymerization method.

Borsig et al., (2007) investigated the influence of organically modified montmorillonite on crystallization and melting behavior of syndiotactic propylene –clay nanocomposites. One of the important findings was that montmorillonite mineral layers could act as obstacles to lower the rate of crystallization, but at the same time provide more nucleating sites for crystallization to occur. Dean et al., (2007) prepared nanocomposites containing 1, 2.5 and 5-wt% clay minerals by three different methods: two solvent based dispersion methods (bath sonication and ultrasonic probe sonication) and a non-solvent high-speed shear mixing method. SEM and TEM were used to investigate the morphology of nanocomposites. Ultrasonication (combined with a solvent), brought superior nanoscale dispersion and resulted in an increase in fracture toughness, strength, and strain to failure of nanocomposites.

Ingram et al., (2007) investigated different factors, e.g. use of sonication, choice of curing agent, the effect of the moisture content of the clay and cure temperature influencing the degree of intercalation of OMMT. Higher cure temperatures and higher levels of clay moisture increased the extent of exfoliation. Chow and Yap, (2008) used response surface methodology to investigate the effect of process variables on the flexural properties of 4 wt% OMMT and epoxy nanocomposites. The speed of the mechanical stirrer, post-curing time and post-curing temperature were able to influence the flexural modulus and flexural strength.

Kaushik et al., (2009) observed that the tensile and flexural properties of nanocomposites were mainly dependent on the dispersion state of nanofiller. The graphite flakes in different quantities (2, 4, 6, 8, 10 wt%) were mixed in unsaturated polyester resin and nanocomposites were prepared. The tensile modulus, flexural modulus, and flexural strength increased steadily with incorporation of graphite up to 10 wt%, which had been attributed to a uniform dispersion and good interfacial adhesion between graphite flakes and polyester.

Ngo et al., (2009) studied the effect of temperature, duration and speed of pre-mixing on the dispersion of OMMT in epoxy resin. The XRD and TEM results indicated that the clay mineral particles were broken down into smaller and smaller sized layers with an increase in pre-mixing temperature and pre-mixing speed. During premixing step, these parameters did not show a significant effect on intercalation/exfoliation of OMMT but improved the dispersion of clay

minerals by breaking large particles into smaller aggregates. Also, speed was seen to be more influential than the temperature in terms of clay minerals dispersion.

Ngo et al., (2012) studied the effect of incorporation of Cloisite® 30B on the mechanical properties of epoxy nanocomposites. Nanocomposites were prepared by premixing the nanoclay in epoxy under different temperatures and using different mixing devices: a mechanical stirrer, a microfluidizer, and a homogenizer. The tensile modulus increased almost linearly with an increase in both clay loading and the quality of dispersion. It was observed that incorporation of Cloisite® 30B did not significantly affect the glass transition temperature (T_g) of the epoxy. The storage modulus of epoxy nanocomposites increased with a homogeneous dispersion of clay in epoxy.

Bakar et al., (2013) investigated the effect of sonication amplitude and mixing time on the mechanical and thermal properties of epoxy-clay nanocomposites. The impact strength of nanocomposites increased with an increase in the amplitude of sonication at short mixing times but affected the impact strength if sonicated for longer mixing times. The effect of mixing time was more pronounced than the sonication amplitude regarding deflections produced under loads applied at high temperature.

Banerjee et al., (2013) studied the dispersion of clay minerals in polypropylene-clay nanocomposites. The lower content of compatibilizer promoted good dispersion and intercalation of polymer chains into clay interspaces. The higher percentage of grafted maleic anhydride onto the compatibilizer led to a decrease in mechanical properties of nanocomposites. The concentration of clay also influenced the dispersion of clay minerals in polypropylene. A reduction of mechanical properties at high clay minerals concentrations had been attributed to increased clay agglomeration.

Zunjarrao et al., (2006) observed high shear mixing method enabled better dispersion of clay minerals in comparison to ultrasonication method when the volume fraction of clay minerals varied from 0.5 to 6%. The flexural modulus increased with an increase in clay volume fraction but the fracture toughness increased with clay minerals loadings up to 2% and then decreased. The experimental results of the flexural modulus for nanocomposites were closer to theoretical predictions for the volume fraction of clay up to 2 %.

The compatibility of organic modifier with the polymer matrix is also an essential factor for synthesis of intercalated/ exfoliated nanocomposites. The structure of nanocomposites and its properties are influenced by organic modifier used in the modification of clay minerals

(Kornmann et al., 2001; Le Pluart et al., 2005). In a recent work, Singla et al., (2014) studied the role of the organic modifier of montmorillonite in the synthesis of Poly (lactic acid)/clay nanocomposites synthesized through microwave-assisted in situ ring opening polymerization. The organic modifiers in Cloisite® 15A and Cloisite® 30B promoted exfoliation of clay mineral layers as well as participated in the polymerization of lactide. Velmurugan and Mohan, (2004) observed no change in d_{001} spacing of Na^+ bentonite even if high shear mixing method was employed to disperse clay at different concentration in epoxy matrix. In contrast, Garamite 1958 OMMT, when mixed in a matrix using high shear method showed a small change in d_{001} spacing. Also, the elastic modulus, storage modulus and thermal stability of epoxy-clay nanocomposites containing Garamite were greater in comparison to Na^+ bentonite epoxy composite and pure epoxy.

Chen and Tolle, (2004) synthesized fully exfoliated epoxy-clay nanocomposites by dispersing OMMT in a solution of epoxy resin and acetone by high shear mixing and ultrasonication. The clay mineral layers were homogeneously and randomly distributed in the matrix. Lam et al., (2005) studied the effect of sonication time on the exfoliation of clay mineral particles and micro-hardness of epoxy-clay nanocomposites. The XRD results indicated little change in d_{001} spacing of clay minerals. However, the particle size, observed by scanning electron microscopy (SEM) was influenced by different ultrasonication times. The micro-hardness of the epoxy-clay nanocomposites was a maximum (12 Hv) at 10 min of ultrasonication time and decreased with further increase in ultrasonication time. Yuhana et al., (2012) carried out experiments to determine the effect of ultrasonication time on properties of epoxy-clay nanocomposites. The mixing step involved mechanical stirring followed by ultrasonication for either 1h or 3h. The highest d_{001} spacing of nanoclay had been achieved with 1h of ultrasonication. It had been concluded that an extended ultrasonication did not improve the thermal stability of nanocomposites.

1.4 Environmental degradation of polymeric composites

The fiber reinforced epoxy composites have been the mainstay of high-performance structural materials for aerospace, defence, marine, automotive, civil infrastructure, sporting goods, etc. The downside of polymeric composites is their inherent sensitivity to environmental factors such as temperature, exposure to liquids, gases, electrical fields and radiation. It is well known that polymer composites undergo swelling on the absorption of fluids and expansion strains, residual stresses are generated. The combination of mechanical loads and hygrothermal loads can cause irreversible changes in chemical, physical and mechanical properties and reduce the

useful life of the composites. Additional, residual stresses are generated due to the mismatch in moisture induced volumetric expansion between the matrix and the fibers. Also, in the matrix, water acts as a plasticizer increases free volume and lowers the glass transition temperature. The water that is absorbed by polymer matrix ends up reaching to fiber-matrix interface and has a detrimental effect on the chemical bonds between fiber and matrix thereby limiting the useful life of glass fiber reinforced composites. Extensive data are available for a multitude of polymers and polymeric composites on exposure to fluids (Maxwell et al., 2005; Weitsman and Elahi, 2000). Therefore, modifying the matrix material with nanofillers to increase the service life of composites in adverse environmental conditions is a research area of great interest. In the quest to realize the potential of nanofillers in imparting improved barrier properties to fiber reinforced polymer composites, extensive studies have been presented.

1.4.1 Hygrothermal studies on fiber reinforced epoxy-clay nanocomposites

There are many applications in which fiber reinforced composites are exposed to the moist environment and high temperatures. The main downside of polymeric composites is the loss of inherent mechanical properties caused by degradation of matrix due to swelling, embrittlement, plasticization and chemical hydrolysis (Garg et al., 2016; Mourad et al., 2010; Ray, 2006; Ray and Rathore, 2014; Thomason and Ali, 2009; Wang et al., 2015). Recent reviews of the marine applications of fiber reinforced composites have included use for naval ships and submarines, propellers, offshore energy, and underwater repair of steel pipelines (Graham-Jones and Summerscales, 2015a; Mouritz et al., 2001; Santhosh et al., 2011; Summerscales, 2015). The water that is absorbed by polymer matrix ends up reaching to fiber-matrix interface. It has a detrimental effect on the chemical bonds between fiber and matrix thereby limiting the useful life of glass fibers reinforced composites. Therefore, modifying the matrix material with nanofillers to increase the service life of composites in marine conditions is a research area of great interest. In the field of nanocomposites, some studies are available which advocate excellent moisture barrier capacity of clay minerals (Abacha et al., 2007; Kim et al., 2005; Mittal et al., 2015; Saharudin et al., 2016; Tan and Thomas, 2016). The improvement in barrier properties of composites is achieved if the clay mineral layers are dispersed uniformly in the polymeric matrix, has an intercalated or exfoliated morphology and forms strong interfacial bonds with matrix (Alamri and Low, 2012; Kim et al., 2005; Liu et al., 2005a; Tan and Thomas, 2016; Zainuddin et al., 2009). Clay minerals have also gained popularity in marine antifouling coatings as well as antimicrobial films (Armstrong et al., 2012; de Azeredo, 2012; Dong et al., 2015).

Kim et al., (2005a) studied moisture absorption and thermo-mechanical properties of epoxy modified with three different types of organoclays: a quaternary alkylamine modified montmorillonite (KH-MT®), a quaternary ammonium modified montmorillonite (Cloisite® 20A) and octadecylamine modified montmorillonite (I30P®). The nanocomposites were hygrothermally treated in an environmental chamber at 85°C for 25 days. The rate of diffusion of moisture into nanocomposites containing I30P and Cloisite® 20A OMMT was slower than those based on KH-MT. The moisture diffusivity of nanocomposites was observed to decrease with increasing clay content (3% and 5%). Moisture diffusivity decreased by 36% and 39% and 19% with 5 wt% clay content of I30P, Cloisite® 20A, and KH-MT respectively as compared to neat epoxy resin. The glass transition temperature (T_g) of both epoxy and nanocomposite decreased linearly with the increase in moisture content.

Kornmann et al., (2005) used a hand lay-up method in combination with vacuum bagging and hot processing technique to manufacture glass fiber reinforced epoxy-clay nanocomposites. The flexural modulus and strength of epoxy increased by 6% and 27%, respectively with incorporation of OMMT. The presence of glass fibers inhibited water uptake in epoxy. The water uptake curves were similar at 23 °C, but at 50°C water uptake was much higher in fiber reinforced epoxy-clay nanocomposites than in glass fiber reinforced neat epoxy composite.

Wang et al., (2006a) studied the effect of hydrothermal environment on thermal and mechanical properties of neat epoxy and epoxy-clay nanocomposite. The epoxy nanocomposites were prepared using a "slurry compounding approach." Moisture absorption experiments showed less moisture uptake by neat epoxy in comparison to nanocomposite. Moisture absorption did not significantly influence the values of fracture toughness and tensile modulus. The tensile strength of neat epoxy was found to be constant, whereas that of epoxy-clay nanocomposite decreased after moisture absorption.

Chow, (2007) carried water absorption tests on glass fiber reinforced epoxy nanocomposite containing Nanomer® I.30E OMMT. The glass transition temperature (T_g) of epoxy increased with the incorporation of OMMT. The specimens were first dried at 80°C in a vacuum oven and then immersed in water stored at 30 °C. The water absorption of epoxy decreased with the incorporation of both glass fibers and OMMT.

Zainuddin et al., (2009) conducted accelerated ageing experiments to study the long-term durability of nanophase epoxy. Neat epoxy/ epoxy-clay nanocomposite samples were exposed to four different environment conditions: cold and dry, cold and wet, high temperature and dry,

high temperature and wet. The conditioning of all the sets was carried out for 15, 45 and 90 days. An increase in weight was observed in all the samples with time due to absorption of moisture. For samples subjected to hot-wet conditions at 80 °C, the weight gain was 3.12% and 2.1% in neat and modified epoxy samples, respectively after 90 days. The degradation in flexural strength and flexural modulus was higher in samples under hot-wet conditions for 90 days than room temperature samples. The nanocomposites containing 2% clay minerals showed an increase in strength and modulus after hygrothermal ageing. The scanning electron micrographs revealed relatively less number of cracks and better interfacial bonding in nanocomposites in comparison with neat counterparts, similarly conditioned.

Zainuddin et al., (2010) investigated the durability of neat /nanophase glass fiber reinforced composites subjected to different temperature and moisture conditions. Vacuum assisted resin infusion molding method was used to fabricate the glass fiber reinforced epoxy-clay nanocomposites. The 2 wt% GFRP composites exhibited the highest flexural modulus and significant enhancements in properties as compared to other samples. The samples were conditioned under four different environment conditions: cold and dry, cold and wet, high temperature and dry, high temperature and wet. The conditioning of all the sets was carried out for 15, 45 and 90 days. After 90 days, the moisture the weight gain due to moisture absorption were 4.25% in neat epoxy, 3.85% in nanocomposite containing 1wt% I.28E and 3.06% in nanocomposites containing 2 wt% I.28E thus confirming an increase in the barrier to liquids with the incorporation of clay minerals. Under all conditions, though the flexural properties were found to degrade with time.

Sharma et al., (2012) performed fiber reinforced epoxy-clay nanocomposites containing different concentrations (1, 3, 5 wt%) of Cloisite® 30B. The tensile strength increased with the incorporation of OMMT up to 3 wt%, but it decreased at 5 wt%. The flexural strength and hardness increased linearly with the addition of OMMT up to 5 wt%. Durability studies conducted on nanocomposites in water and alkaline medium for one month showed degradation in mechanical properties of all specimens. The decrease in tensile and flexural strength was less in the sample with clay modified epoxy matrix as compared to the sample with the neat epoxy matrix. The water barrier properties of epoxy improved by the addition of both glass fiber and nanoclay, which had been attributed to the increase in the tortuosity path for water penetration.

Manfredi et al., (2008) synthesized fiber reinforced epoxy-clay nanocomposites based on two different OMMTs: Cloisite® 10A and Cloisite® 30B. The flexural modulus, flexural strength,

interlaminar shear strength and impact strength of fiber reinforced composites increased with incorporation of OMMT in epoxy. The moisture uptake curves showed a two-stage diffusion of water in composite immersed in distilled water at 80°C. The nanocomposites had a higher rate of moisture diffusion and additionally the decrease in the mechanical properties was also higher in fiber reinforced composites containing OMMTs.

Al-Qadhi et al., (2013) investigated the effect of different loading (1, 2, 3.5, 5, 10 wt%) of Nanomer® I.30E OMMT on mechanical, thermal and water uptake properties of epoxy. The tensile modulus increased with incorporation of OMMT and was highest in nanocomposites containing 10 wt% OMMT. But, the tensile strength and water uptake did not improve at higher OMMT loading, and this had been attributed to increased microvoids and aggregates. The glass transition temperature (T_g) decreased monotonously with an increase in OMMT loading.

Hossain et al., (2014) carried out low-velocity impact tests on carbon fiber reinforced epoxy-clay nanocomposites based on I-28E OMMT after immersion in seawater. The nanocomposites containing OMMT exhibited superior water barrier properties as compared to fiber reinforced neat epoxy composites. The impact strength, toughness, and energy absorbed by fiber reinforced neat epoxy nanocomposites decreased significantly due to softening of matrix and weakening of bonds between fibers and epoxy. The presence of clay minerals in the epoxy matrix reduced the development of delamination by arresting the crack propagation path. Therefore, the fiber reinforced epoxy-clay nanocomposites showed better performance as compared to neat epoxy-based composites.

Firdosh et al., (2015) investigated the hygrothermal behavior of glass fiber reinforced nanocomposites containing different concentrations of Cloisite® 15A, i.e. 2, 3, 4, 5 wt% exposed to different temperatures 30°C, 50°C, 60°C at 95% RH. The presence of Cloisite® 15A decreased the moisture diffusion and degradation of composites, and the nanocomposites containing 4 wt% clay minerals exhibited the highest retention of tensile strength after hygrothermal ageing. A decrease in mechanical properties observed with an increase in temperature.

Mittal et al., (2015) synthesized glass fiber reinforced clay-vinyl ester nanocomposites based on MMT modified with 3-aminopropyltriethoxysilane. The silylated MMT was characterized using XRD and FTIR. The successful grafting of silane was evident from increased d_{001} spacing and the characteristic bands of silanes in FTIR spectra. The XRD results of

nanocomposites revealed that extent of intercalation increased after silane modification of MMT. The silylated MMT nanocomposites exhibited better tensile properties and flexural properties in dry/ wet conditions as compared to epoxy-MMT nanocomposites.

The selected studies on water uptake and hygrothermal loading of clay minerals based nanocomposites have been given in Table 1.3.

Table 1.3 Selected studies on water uptake and hygrothermal loading of nanocomposites incorporating clay minerals

S. No.	Material System	Process conditions	Key Results	Reference
1.	Epoxy modified with three different types of OMMT i.e. KH-MT, Cloisite® 20A, and Nanomer® I.30P	Ultrasonication of resin and clay mixture. *In-situ* polymerization and curing under vacuum Samples exposed to 85°C and 85% relative humidity.	Better moisture barrier properties of Cloisite® 20A and Nanomer® I.30 based nanocomposite than KH-MT based nanocomposites. Increase in glass transition temperature (T_g) of epoxy with the presence of nanofillers. T_g decreased after exposure to hygrothermal conditions	Kim et al., (2005a)
2.	Epoxy-clay nanocomposites and corresponding glass fiber reinforced epoxy-clay nanocomposites containing MMT modified using octadecylamine salt	In-situ polymerization and Vacuum assisted hand lay-up method. Immersion in distilled water at two different temperatures, i.e. 23°C and 50°C	An Improvement in flexural properties of epoxy with addition of OMMT. The water uptake increased with an increase in temperature. The glass fiber reinforced neat epoxy composites exhibited the lowest water uptake. Incorporation of clay minerals increased the water uptake in samples exposed to 50 °C	Kornmann et al., (2005)
3.	Neat epoxy and pristine clay modified epoxy nanocomposite.	Slurry compounding approach. Samples immersed in deionized water at 60 °C	Higher moisture absorption by nanocomposite. The tensile strength of nanocomposites decreased significantly after hygrothermal ageing.	Wang et al., (2006a)

S. No.	Material System	Process conditions	Key Results	Reference
4.	Neat epoxy, epoxy- OMMT/ glass fiber reinforced nanocomposites based on Nanomer® I.30E	Direct mixing of 3 wt% OMMT Hand lay-up for preparing laminates. Samples immersed in water at 30 °C	Glass transition temperature (T_g) increased with an addition of clay minerals. Moisture barrier properties of glass fiber reinforced epoxy composites and glass fiber reinforced epoxy nanocomposites were better than neat epoxy	Chow, (2007)
5.	Glass fiber reinforced epoxy-clay nanocomposites containing two different OMMTs i.e. Cloisite® 10A and Cloisite® 30B	Mixing of clay minerals (3 wt% and 5 wt% of Cloisite® 10A, 3 wt% of Cloisite® 30B) using a mechanical stirrer Fiber reinforced composites prepared using pultrusion Samples immersed in distilled water at 80 °C	Clay minerals had an intercalated structure in the epoxy matrix. The nanocomposites containing Cloisite® 10A had a higher flexural modulus, flexural strength, interlaminar shear strength. A higher moisture absorption rate observed in nanocomposites containing 3 wt% Cloisite® 10A.	Manfredi et al., (2008)
6.	Epoxy nanocomposites containing Nanomer® I.28E OMMT	Mechanical mixing *In-situ* polymerization	Under accelerated ageing conditions: A decreased equilibrium weight gain in nanophase samples over neat samples. Degradation in strength and modulus of all conditioned samples. Samples with low clay loadings had better flexural properties. Less number of cracks and better interfacial bonding in nanophase specimens	Zainuddin et al., (2009)
7.	E-Glass neat epoxy / epoxy modified with Nanomer® I.28E OMMT. (1-2 wt%)	Mechanical mixing. VARIM.	When subjected to accelerated conditioning: The barrier to liquids increased with incorporation of clay minerals in epoxy. Flexural tests performed showed that GFRP containing 2 wt% clay had the highest	Zainuddin et al., (2010)

S. No.	Material System	Process conditions	Key Results	Reference
			modulus and strength. The properties degraded with an increase in exposure time.	
8.	E-glass fiber reinforced epoxy-clay nanocomposites based on Cloisite® 30B OMMT (1, 3 and 5 wt% of resin)	Mechanical mixing, ultrasonication Hand lay-up method	An addition of OMMT up to 3 wt% increased tensile strength and micro-hardness but a decrease at 5 wt%. The flexural strength increased significantly with clay loading and the highest value was observed in specimens incorporating 5 wt% clay. The resistance to degradation increased by the addition of both glass fiber and nanoclay.	Sharma et al., (2012)
9.	Epoxy-clay nanocomposites containing different concentrations (1, 2, 3.5, 5,10 wt%) of Nanomer® I.30E OMMT	High shear mixing of OMMT in epoxy resin *In-situ* polymerization	Exfoliated and disordered intercalated structures formed. Tensile modulus increased monotonously with an increase in OMMT concentration. The tensile strength of nanocomposites increased up to 3.5 wt% loading and then decreased. The rate of diffusion and equilibrium moisture content decreased in nanocomposites containing small quantities of OMMT, but it increased at 10 wt% clay loadings.	Al-Qadhi et al., (2013)
10.	Carbon fiber reinforced epoxy-clay nanocomposites based on I-28E OMMT	Mixing of 2 wt% OMMT in epoxy resin using a magnetic stirrer Vacuum assisted resin transfer molding Exposure to seawater at room temperature	The fiber reinforced epoxy-clay nanocomposites exhibited lower moisture absorption and higher retention of strength. The total absorbed as well as delamination energy decreased significantly after exposure to seawater.	Hossain et al., (2014)
11.	Glass fiber reinforced clay-vinyl ester nanocomposites containing	Ultrasound probe sonication and twin screw extruder for mixing of different concentrations, i.e. 2, 3, 4, 5 wt% of	Intercalated structures formed. The glass fiber reinforced nanocomposites exhibited lower diffusion of moisture and higher retention of strength as compared to	Firdosh et al., (2015)

S. No.	Material System	Process conditions	Key Results	Reference
	Cloisite® 15A OMMT	Cloisite 15A®-vinyl ester Hand lay-up, hot pressing for curing Exposed to 30,50, 60°C at 95% Relative Humidity (RH)	neat vinyl ester based composites.	
12.	Glass fiber reinforced clay-vinyl ester nanocomposites based on MMT modified with 3-aminopropyltriethoxysilane	Hand lay-up and hot press Immersion in seawater at room temperature for 65 days	The silylated MMT was characterized using XRD, FTIR, and TGA. The successful grafting of silane was evident from increased d_{001} spacing and FTIR characteristic bands of APTES. The silylation promoted intercalation of MMT in the vinly ester matrix. The silylated MMT-vinyl ester nanocomposites exhibited better tensile properties and flexural properties in dry/ wet conditions as compared to untreated MMT vinyl ester nanocomposites.	Mittal et al., (2015)
13.	Epoxy-clay nanocomposites based on MMT modified with 3-aminopropyltriethoxysilane	Epoxy resin and pristine/silylated MMT mixed in acetone using a high-speed mechanical stirrer Solution blending and cured in Teflon plates under vacuum	The water uptake decreased significantly with incorporation of MMT. The equilibrium water uptake in epoxy-silylated MMT nanocomposites was slightly less than epoxy-MMT nanocomposites.	Ryu et al., (2016)

1.5 Gaps in the literature

The hybrid fiber reinforced polymer clay nanocomposites are advanced materials which offer superior performance as compared to the conventional fiber reinforced composites. While the synthesis and morphology of these nanocomposites have been studied extensively, there are

few aspects which have received considerably less attention. The gaps found in the literature are as follows

1. The uniform dispersion, intercalation/exfoliation and compatibility between clay minerals and polymer are the key factors in the synthesis of a nanocomposite. There are some critical parameters which influence the mechanical properties of hybrid fiber reinforced clay-polymer nanocomposites e.g. curing schedule, epoxy resin and hardener mix ratio, and post-curing schedule have been studied rarely.
2. Surface modification of clay minerals using silane coupling agents has offered a unique level of mechanical property enhancements in polymer clay nanocomposites. Very few investigations on the effects of incorporation of silylated clay minerals on properties of hybrid fiber reinforced polymer-clay nanocomposites are available. The effect of a change in process parameters viz. choice of solvent, method of grafting silanes, the amount of silane, grafting temperature, etc. on mechanical properties of fiber reinforced epoxy-clay nanocomposites containing silylated clay minerals had not been studied.
3. Only a few studies have been carried out to investigate the effect of incorporation of silylated clay minerals on mechanical properties and durability of hybrid fiber reinforced epoxy-clay nanocomposites under marine / hygrothermal conditions. The performance of these novel nanocomposites incorporating silylated clay minerals exposed to seawater vis-à-vis the amount of grafted silane on clay minerals had not been studied.

1.6 Objectives of thesis

From the identified gaps in the literature review, the following objectives have been framed for Processing and characterization of fiber reinforced polymer nanocomposites and their degradation under hygrothermal loading.

1. Synthesis and characterization of nanoclay filled fiber reinforced polymer (FRP) composites.
2. Study on the effect of hygrothermal loading conditions on properties of nanoclay filled fiber reinforced polymers.

The main objectives of this research were to synthesize and characterize glass fiber reinforced epoxy nanocomposites based on silylated clay minerals, and to improve the hygrothermal

resistance of conventional glass fiber reinforced epoxy composites. The clay minerals layers once exfoliated, can be homogeneously dispersed in the matrix and significant improvements in material properties can be obtained. Cloisite® 15A organoclay was chosen due to its good compatibility with epoxy. Cloisite® 15A has high surface modifier concentration (125 meq/100 g clay) and large interlayer distance (31.5 °A), which favours the penetration of the polymer precursors between clay mineral layers and therefore the formation of an exfoliated nanocomposite (Nazir et al., 2016; Sinha Ray, 2013). These characteristics make Cloisite® 15A suitable for silylation reaction. The silane coupling agents can form an interpenetrating network between clay minerals and epoxy, which would lead to strong clay mineral-polymer interfacial interactions and a substantial increase in mechanical properties of nanocomposites. This is so because the mechanical properties of clays are very high as compared to the epoxy matrix. The scope of this investigation covers different methods of silylation of clay minerals, amount of grafted silanes vis- a- vis quantity of silane coupling agents used during grafting reaction and characterization of silylated clay minerals. The novelty of the present work lies not only in the new combination of material components, but also in the way these silylation processing has been done. Specifically, silylation process involved nano-dispersion of clay minerals in hydrolyzed silanes. This in turn enabled use of very high concentration of silanes, which significantly increased grafting of silanes on clay minerals. It should also be mentioned that processing of these highly loaded silynated clays – epoxy mixture was quite tricky because of the very high viscosity of these systems. Furthermore, the research has been carried out with a goal to study the effect of process parameters and incorporation of silylated clay minerals on morphology, mechanical properties and seawater durability of fiber reinforced epoxy-clay nanocomposites. The hygrothermal studies have been undertaken to characterize the moisture diffusion, damage resistance and tensile and flexural behavior of these novel glass fiber reinforced epoxy-silylated clay nanocomposites.

1.7 Outline of thesis

The present study sheds light on a newly developed approach to surface modification of clay minerals, which gave promising results and a unique level of mechanical properties enhancement of glass fiber reinforced epoxy composites. This thesis embodies the subject matter resulting out of this study and has been organized in seven chapters. The outline of the chapters is briefly described as follows.

Chapter 1: This chapter begins with a general introduction of fiber reinforced polymer composites, methods to manufacture and applications in automotive, structural and other fields.

Another section has been dedicated to clay minerals, need of organic modification of clay minerals, the importance of surface modification by grafted silanes and steps of silylation reactions. The fiber reinforced epoxy-clay nanocomposites have been discussed in the context of synthesis and morphology. The effect of hygrothermal loadings on polymer composites is presented. A comprehensive review of the literature on three major aspects of this thesis: (i) silylation of clay minerals, (ii) factors influencing properties of fiber reinforced epoxy-clay nanocomposites, (iii) hygrothermal studies of fiber reinforced epoxy-clay nanocomposites have been given. In the end, the scope of this work has been presented.

Chapter 2: This chapter lists all the materials used for the fabrication of fiber reinforced epoxy-clay nanocomposites. Also, details regarding the silylation of clay minerals, characterization of silylated clay minerals and their corresponding nanocomposites have been presented using a schematic diagram.

Chapter 3: It describes the methodology adopted to (i) obtain a uniform dispersion of a commercially available organically modified montmorillonite, Cloisite® 15A in epoxy resin (ii) synthesize fiber reinforced epoxy-clay nanocomposites using vacuum assisted wet lay-up method. The dispersion state of the clay minerals and mechanical properties of fiber reinforced epoxy-clay nanocomposites have been investigated with respect to change in process conditions which include the temperature of resin-clay mixture, the speed of homogenization and ultrasonic probe amplitude during premixing of clay minerals in epoxy resin. The extent of curing of the matrix and mechanical properties of nanocomposites resulting from a change in epoxy/amine stoichiometry has also been addressed. Also, the effect of post-curing at different temperatures on the mechanical properties of fiber reinforced epoxy-clay nanocomposites has been reported.

Chapter 4: In this chapter, the effect of surface modification of Cloisite® 15A using different amounts of two silane coupling agents (3-aminopropyltriethoxysilane, 3-glycidyloxypropyltrimethoxysilane) on mechanical properties of fiber reinforced epoxy-clay nanocomposites has been reported. A new method of silane treatment of clay minerals has been reported wherein the clay minerals are nano-dispersed in hydrolyzed silanes. Fourier transform infrared spectroscopy (FTIR) has been used to verify grafting of silanes on clay minerals. Further, the silylated clay minerals have been dispersed in an epoxy resin and glass fiber reinforced epoxy-clay composites have been manufactured. These nanocomposites have been characterized using Small angle X-ray scattering (SAXS), Transmission electron microscopy (TEM), tensile and flexural properties measurements and Differential scanning

calorimetry (DSC). A detailed study has been done about the effect of silanization of clay minerals on properties of glass fiber epoxy-clay nanocomposites as a function of two important parameters: chemical structure of silane and concentration of silane coupling agents in solvents, and an optimized silane concentration has been arrived at.

Chapter 5: Firstly, a modification in the method of silylation of clay minerals discussed in the previous chapter has been reported which enabled the use of very high concentration of silane coupling agents and increased grafting amount of silanes on Cloisite® 15A. The ratio of the weight of the silane coupling agent to that of the weight of clay mineral (X) is varied from 0.1 to 6. Small angle X-ray scattering and Thermogravimetric analysis have been carried out on silylated clay minerals to quantify the grafting of silanes as a function of the ratio of the weight of silane agent to that of the clay mineral. Also, curing studies were carried out on fiber reinforced epoxy nanocomposites containing Cloisite® 15A at different cure temperatures, i.e., 70°C, 80°C, 85°C, 95°C and for two different curing time periods, e.g., 7h and 10h. Significant improvements in mechanical properties of fiber reinforced nanocomposites have been obtained with the incorporation of clay minerals silylated using a high concentration of silanes in a solvent and chosen curing schedule. An attempt has been made to correlate the results with the morphology of nanocomposites by Transmission electron microscopy and that of fractured surfaces by Scanning electron microscopy.

Chapter 6: In this chapter, the performance of fiber reinforced epoxy-silylated clay nanocomposites exposed to seawater vis-à-vis the amount of silane-grafted on clay minerals has been discussed. The durability studies on fiber reinforced epoxy nanocomposites containing clay minerals treated using different amounts of two silane coupling agents (3-Aminopropyltriethoxysilane, 3-Glycidyloxypropyltrimethoxysilane) have been carried out in simulated seawater, at two different temperatures i.e. 25°C and 55°C. The weight gain resulting from moisture absorption and the physical and chemical changes in nanocomposites with seawater ageing have been reported. The exfoliation and strong adhesion between epoxy and clay mineral layers promoted by silylation of clay minerals suppressed degradation of fiber reinforced epoxy nanocomposites subjected to marine conditions.

Chapter 7: it discusses the summary and significant findings of the experimental work of this thesis along with the scope for possible extension of the present work.

Chapter 2 Materials and Methods

2.1 Introduction

Polymer nanocomposites are synthesized using methods such as *in-situ* polymerization, melt blending, and solution processing methods (Azeez et al., 2013; Pavlidou and Papaspyrides, 2008; Sinha Ray and Okamoto, 2003; Thelakkadan et al., 2013). *In-situ* polymerization method has gained popularity because of its simplicity and suitability for mass production. The first step of *in-situ* polymerization is dispersing the nanofiller in the resin precursor. This is done by mechanical mixing (Kim et al., 2005; Lam et al., 2005a; Qi et al., 2006), ultrasonic mixing (Ho et al., 2006; Yasmin et al., 2006), mechanical mixing followed by ultrasonication (Wang et al., 2006a; Yang et al., 2007), shear mixing (Kim et al., 2008; Woo et al., 2007; Zainuddin et al., 2010) or slurry compounding approach (Alamri and Low, 2012). Preparation conditions like organic modification, temperature, and choice of solvents strongly influence dispersion of clay mineral layers. The second step is the initiation of the polymerization reaction by the addition of hardeners. To gain a fundamental understanding and optimize the processing variables, many researchers have explored epoxy systems, curing agents, organic modifiers, processing conditions, curing conditions: temperature and time, viscosity and the functionality of resin.

During the preliminary work, the effect of change of added ingredients, stoichiometry, mixing conditions and post-curing schedule on mechanical properties of fiber reinforced epoxy-clay nanocomposites has been studied. The clay minerals have been dispersed in epoxy resin by homogenization and ultrasonication. The fiber reinforced epoxy-clay nanocomposites have been manufactured using vacuum assisted wet lay-up method.

A newly developed method of silane treatment of clay minerals has been employed wherein the clay minerals are nano-dispersed in hydrolyzed silanes. Also, the silylation of clay minerals has been carried out using different amounts of two different silane coupling agents 3-aminopropyltriethoxysilane (APTES) and 3-glycidyloxypropyltrimethoxysilane (GPTMS). The hygrothermal studies have been carried out in simulated seawater maintained at two different temperatures, i.e. 25°C and 55°C. The samples were taken out of the water bath periodically, and tensile and flexural tests were carried out. The physical and chemical changes in composites due to absorption of seawater have also been studied using Scanning electron microscopy (SEM) and Fourier transform infrared spectroscopy (FTIR), respectively.

2.2 Materials

2.2.1 Glass fibers

The woven roving glass fiber mat WR 360 100 CM TL, made from Advantex® glass fibers was purchased from Owens Corning, India. The balanced woven construction of WR 360 provides bi-directional (0°/90°) reinforcement, excellent dimensional stability, consistent glass loading and is suitable for particularly large parts such as boat hulls, storage vessels, etc. WR 360 has a sizing which makes it compatible with epoxy. Advantex® glass fibers combine the electrical and mechanical properties of traditional E-glass with the acid corrosion resistance of CR glass. Advantex® meets the requirements of both E and CR glass stated in ISO 2078 and ASTM D578-98 (Corning, 2006).

2.2.2 Epoxy system

The epoxy system consisted of the liquid diglycidyl ether of bisphenol -A (DGEBA) and an amine hardener. Dow Chemicals International Limited, India supplied the Airstone® epoxy system (Airstone® 780E resin and Airstone® 786H hardener). The epoxide equivalent weight of the resin was 172 g/eq, and the amine content in hardener was 9.5 meq/g. The stoichiometric mixture (100:31 parts by weight) of Airstone® 780E with 786H hardener had a low viscosity (100 mPas) at 40°C, which should promote uniform dispersion of clay minerals in epoxy and also good wetting of glass fibers. Airstone epoxy system is suitable for the production of large fiber reinforced parts that require long infusion time and used in the manufacture of structural composites for diverse applications including construction, marine, and infrastructure.

2.2.3 Cloisite® 15A

A commercially available organically modified clay mineral, Cloisite® 15A (Montmorillonite treated with dimethyl dehydrogenated tallow quaternary ammonium salt) has been purchased from Nanoshel limited, India. Cloisite® 15A has a cation exchange capacity of 125 meq/100g (Nazir et al., 2016).

2.2.4 Silane coupling agents

The silane coupling agents: 3-Aminopropyltriethoxysilane (APTES; purity >98%) and 3-Glycidyloxypropyltrimethoxysilane (GPTMS; purity > 97%) have been purchased from Tokyo chemicals industry, Japan. The chemical structures of silane coupling agents are shown in Figure 2.1. The solvents used for hydrolysis of silane coupling agents (SCAs) were acetone (purity = 99%) or a mixture of ethanol (purity = 99.9%) and distilled water. Acetone and ethanol were purchased from Loba Chemie Pvt. Ltd., India.

Figure 2.1 Chemical structure of (a) 3-Aminopropyltriethoxysilane, (b) 3-Glycidyloxypropyl - trimethoxysilane

2.3 Methodology

2.3.1 Silane treatment of glass fibers

The glass fibers have been treated with either of the two silane coupling agents: 3-glycidyloxypropyltrimethoxysilane and 3-aminopropyltriethoxysilane. Each of the silanes was hydrolyzed in a solvent to form silanol which would react with glass fibers. Acetone was the solvent for 3- aminopropyltriethoxysilane and, a 95% ethanol with 5% distilled water solution used as a solvent for 3-glycidyloxypropyltrimethoxysilane. The hydrolysates were prepared as a 0.4 % solution, and pH was maintained between 4 - 4.5. The hydrolysis time was 5 min. Glass fiber mat was then immersed in a silane solution for 1 min, and then rinsed with the solvent to remove unreacted silane monomers or oligomers. The glass fiber mat was squeezed and dried at room temperature for 24 h. The fibers were heat-treated for 5 min at 110ºC before use.

2.3.2 Silane treatment of clay minerals

The silane treatment was performed using the following two methods

Method 1

Each silane coupling agent was hydrolyzed in a solvent to form silanol as described in the previous section. Then Cloisite® 15A was put into the hydrolyzed silane solution and dispersed into the solution by ultrasonic mixing and homogenizing. The amount of silane required was calculated using the formula

$$\text{Silane (g)} = \frac{\text{filler weight (g)} \times \text{filler specific area } (\frac{m^2}{g})}{\text{wetting specific area of silane } (\frac{m^2}{g})} \quad (2.1)$$

The external specific surface area for montmorillonite clay is 40 m^2/g, the wetting specific area of APTES is 353 m^2/g and for GPTMS, it is 330 m^2/g (Plueddemann, 1982; Polymer, INC.,

2011; Shokoohi et al., 2008). The silylated clay minerals were extracted by vacuum filtration and dried at 110 ºC for 1 h. The clay minerals were stored in a vacuum desiccator.

Method 2

The amount of the silane coupling agents (SCAs) used was 0.1X, 0.5X, 2X, 4X and 6X with respect to the weight of clay mineral (X). Each SCA was mixed with a solvent and hydrolysis was carried out. The hydrolysis of aminopropyltriethoxysilane was done in acetone, and glycidyloxypropyltrimethoxysilane was hydrolyzed in a solution containing 95% ethanol and 5% distilled water (Choi et al., 2009; Ha and Rhee, 2008; He et al., 2005; Zhang et al., 2006). Further, the Cloisite® 15A was nano-dispersed in silane solution by using a high shear homogenizer operated at 12,000 rpm and ultrasonic mixing using a probe sonicator. The solvent was then removed using a Heidolph rotary evaporator. The modified clay minerals were washed twice with the solvent to remove soluble homo condensates (Chen et al., 2005a, 2005b; Huskić et al., 2013; Ianchis et al., 2015, 2011; Zhang et al., 2006).

2.3.3 Dispersion of clay minerals in epoxy resin

2 parts per hundred resin (2 phr) of clay mineral was added to DGEBA resin and mixed for 5 min using a glass rod, followed by high shear homogenization (Ultra-Turrax® T25, IKA Inc.) for 3 min and sonication using a probe sonicator operated for 5 min. Subsequently, homogenization and sonication steps were repeated and the mixture was degassed under vacuum. The Qsonica Q800 probe sonicator was operated on pulse mode, 80-s on/ 30-s off with shutdown temperature of 40 °C.

2.3.4 Manufacturing of fiber reinforced epoxy-clay nanocomposites

A predetermined amount of curing agent was added and mixed with DGEBA resin containing clay minerals by mechanical stirring (2 min at 500 rpm) at 25 °C. The mixture was placed in a vacuum desiccator for 30 min for degassing. Vacuum assisted wet lay-up method (Subramaniyan and Sun, 2006) and vacuum assisted resin infusion method were used for manufacturing fiber reinforced epoxy-clay nanocomposites.

2.3.5 Hygrothermal studies

To adequately assess the durability of fiber reinforced epoxy-clay nanocomposites, tensile and flexural tests were carried out on specimens after exposure to seawater after 30, 60 and 120 days. The specimens were cut and prepared as per ASTM D 3037/3039 and ASTM D790 standards. Application of two coats of epoxy sealed the open sides and edges, to inhibit absorption of water by capillary action. All the specimens were heated in a convection oven at

85°C for 7 h after application of epoxy barrier coating. The specimens were immersed in simulated seawater maintained at different temperatures: 25°C ± 1°C and 55°C ± 1°C inside stainless steel baths (Daihan WiseBath®). The simulated seawater was prepared as per ASTM D1141 and the concentrations of different salts added are given in Table 2.1. The pH of the simulated seawater was maintained in the range 8.0-8.2.

Table 2.1 Concentration of salts in simulated seawater

Element	Concentration (g/L)
NaCl	24.530
$MgCl_2$	5.200
Na_2SO_4	4.090
$CaCl_2$	1.160
KCl	0.695
$NaHCO_3$	0.201
KBr	0.101
H_3BO_3	0.027
$SrCl_2$	0.025
NaF	0.003

The gravimetric measurements were performed on Mettler Toledo XS104 having a measurement precision of 0.1 mg. The samples were taken out of seawater, wiped with a cloth and dried for 5-7 min under ambient conditions, weighed and replaced in the bath after the measurements. The water uptake in samples was measured using the formula

$$M(\%) = \frac{M_t - M_0}{M_0} \times 100 \quad (2.2)$$

Where M_t is the weight at time t and M_0 is the initial sample weight.

2.4 Characterization

2.4.1 Small angle X-ray scattering (SAXS)

Small angle X-ray scattering measurements on clay mineral samples were carried out on PANalytical XPERT Pro diffractometer. The samples were scanned in transmission mode using a CuKα radiation ($\lambda = 0.154$ nm) within the range of $2\theta = 1°$ to 15°. The step scan size and time were 0.0200° and 2 s respectively.

2.4.2 Fourier transform infrared spectroscopy(FTIR)

FTIR spectroscopy of silane modified clays was performed on a Bruker FTIR Spectrometer in the range 4000 cm^{-1} to 450 cm^{-1} at a resolution of 4 cm^{-1}. The samples were ground and mixed with KBr powder and pressed into discs for FTIR characterization.

2.4.3 Thermogravimetric analysis (TGA)

Thermogravimetric analysis of clay minerals was carried out in a Shimadzu TGA 50 thermogravimetric analyzer. The clay minerals were heated to 800°C at a rate of 10°C /min under a nitrogen environment, and the weight loss was measured. Before testing, samples were stored in microcentrifuge tubes, and placed in a vacuum desiccator containing silica gel, to avoid absorption of moisture from the atmosphere. Thermogravimetric analysis of fiber reinforced epoxy-clay samples was also carried out using Mettler Toledo TGA/SDTA 851. The samples were heated to 700°C at a rate of 10°C /min under nitrogen atmosphere.

2.4.4 Tensile and flexural tests

The specimens were cut and tested as per the ASTM standards D3037/3039 for tensile test and D790 for 3-point bending test. The tensile test specimens were cut in size 250 mm × 25 mm × 0.64-0.66 mm (length × width × thickness). The specimen size for bending test was 50 mm × 13 mm × 0.64-0.66 mm. Four specimens of each material composition were tested on a Zwick/ Roell Universal Testing Machine (UTM). The crosshead speed for tensile testing was 2 mm/min, and for flexural testing, the rate of crosshead movement (R) was calculated using the following formula

$$R = \frac{ZL^2}{6d} \qquad (2.3)$$

where

L= support span, mm; d= depth of beam, mm

Z= the rate of straining of the outer fiber, mm/min. The value of Z was taken as 0.01

2.4.5 Differential scanning calorimetry (DSC)

The calorimetric measurements were performed on a Perkin-Elmer DSC 4000 standard single furnace differential scanning calorimeter. The samples were heated under a nitrogen flow (200 ml/min) from room temperature to 300°C at a heating rate of 10°C / min. The samples were cooled to -4°C keeping the cooling rate the same as heating rate, i.e. 10°C / min. The heating and cooling cycles were repeated twice.

2.4.6 Transmission electron microscopy (TEM)

TEM was carried out using TECNAI G^2 20 transmission electron microscope at an accelerating voltage of 100 kV. Fine particles were deposited on a TEM copper grid for examination.

2.4.7 Scanning electron microscopy (SEM)

The fractured surfaces of glass fiber reinforced epoxy-clay nanocomposites were observed with JEOL, JSM-6510LV scanning electron microscope. The fractured surfaces were sputter coated with gold prior to SEM to avoid electric charging of specimens during the examination.

A schematic sequence of synthesis and testing of fiber reinforced epoxy-clay nanocomposites and fiber reinforced epoxy nanocomposites based on silylated clay minerals are presented in Figures 2.2 and 2.3, respectively. The effect of different parameters on the mechanical properties of fiber reinforced epoxy nanocomposites is discussed in the following chapter.

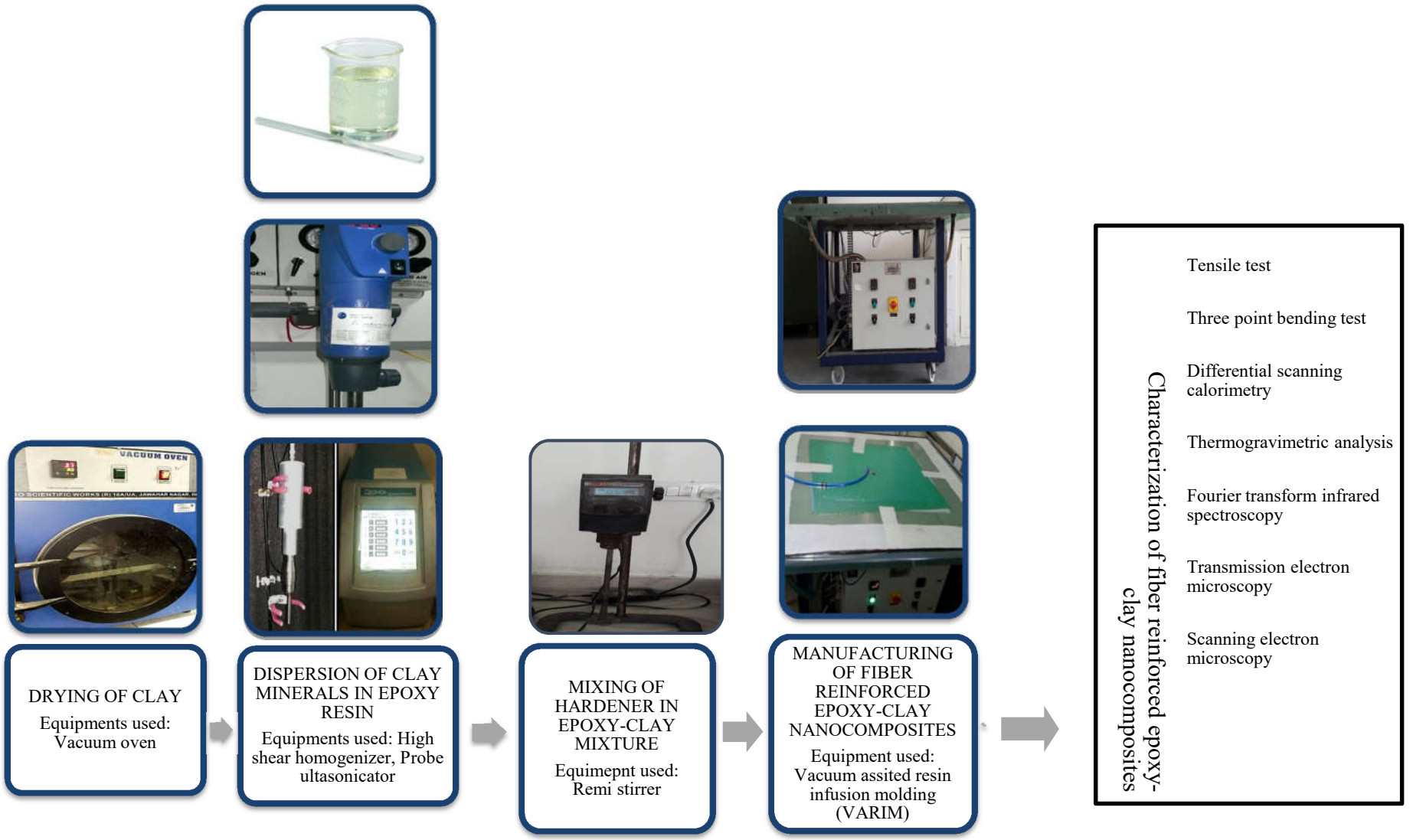

Figure 2.2 Schematic sequence of steps in synthesis of fiber reinforced epoxy-clay nanocomposites

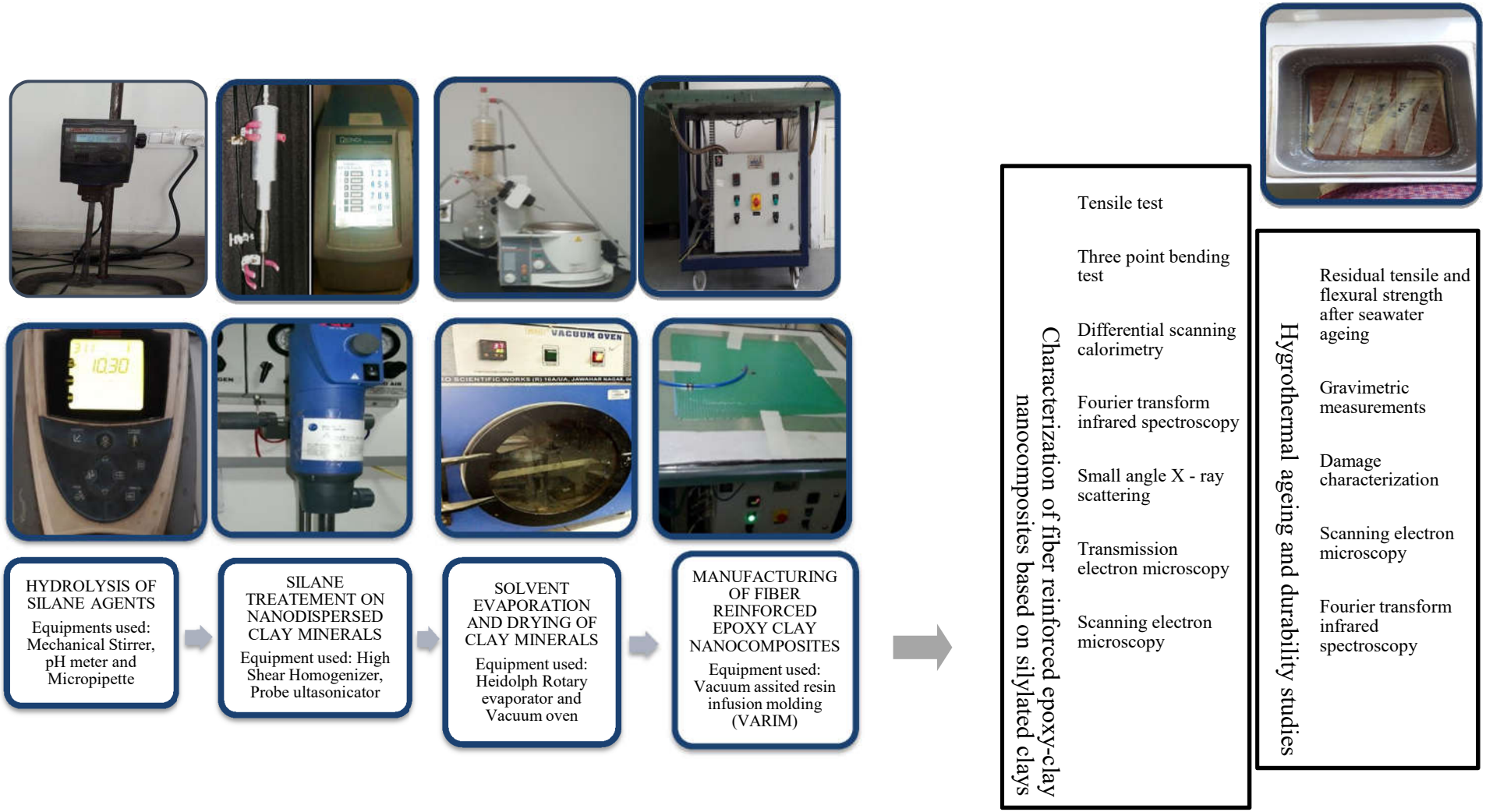

Figure 2.3 Schematic sequence of steps in synthesis and testing of fiber reinforced epoxy nanocomposites containing silylated clay minerals

Chapter 3 Fiber reinforced epoxy-clay nanocomposites

3.1 Introduction

In fiber reinforced epoxy-clay nanocomposites, homogeneous dispersion of clay mineral layers, interfacial adhesion between the reinforcement and matrix and complete crosslinking of resin and hardener are crucial aspects for improved performance over conventional fiber reinforced composites. Besides these, some other factors like volume fraction of reinforcement, choice of epoxy system, resin and hardener mix ratio, the orientation of fiber preform and lay-up, the presence of air voids, filtration of clay minerals in fiber weave and curing schedule would influence the mechanical properties of the composites. One of the objectives of this study was to synthesize intercalated/exfoliated nanocomposites and explore and select processing parameters, i.e. the temperature of epoxy resin and speed of impeller during homogenization, ultrasonic probe amplitude, the post-cure temperature to improve mechanical properties of fiber reinforced epoxy-clay nanocomposites. The extent of curing of the matrix and mechanical properties of nanocomposites resulting from a change in epoxy/amine ratio stoichiometry have also been investigated.

3.2 Materials

The E-CR glass woven roving, WR 360 made of Advantex® glass fibers was purchased from Owens Corning, India. A commercially available organically modified montmorillonite, Cloisite® 15A was purchased from Nanoshel limited, India. The epoxy system consisted of the liquid diglycidyl ether of bisphenol-A (DGEBA) and an amine hardener. Dow chemicals international limited, India supplied the 'Airstone' epoxy (Airstone® 780E resin and Airstone® 786H hardener).

3.3 Methodology

3.3.1 Dispersion of Cloisite® 15A in epoxy resin

2 parts per hundred resin (phr) of Cloisite® 15A was added to DGEBA resin and was dispersed by stirring for 5 min using a glass rod, followed by high shear homogenization (Ultra-Turrax® T25, IKA Inc.) for 3 min and sonication using a probe sonicator operated for 5 min. The Qsonica Q800 sonicator was operated on pulse mode, 80-s on/ 30-s off with shutdown temperature of 40 °C. Subsequently, homogenization and sonication steps were repeated and the mixture was degassed under vacuum. The mixing of clay minerals in epoxy was carried out using three different processing conditions (PC1, PC2, and PC3) as shown in Table 3.1.

The selection of process conditions was based on equipment capabilities and a review of the literature. From the literature on epoxy-clay nanocomposites (Azeez et al., 2013; Dean et al., 2007; Ngo et al., 2009; Pavlidou and Papaspyrides, 2008; Thelakkadan et al., 2013; Zunjarrao et al., 2006) and the preliminary studies performed earlier, it was established that temperature, the speed of mixing and ultrasound amplitude are critical process parameters which influence the clay minerals morphology and hence the mechanical properties of nanocomposites.

Table 3.1 Processing conditions for fiber reinforced epoxy-clay nanocomposites

Process conditions	High shear homogenization		Ultrasonic probe amplitude, %	Whether post-cured/ Temperature (°C)	Resin: hardener ratio
Code	Speed, rpm	Temperature during mixing, °C			
PC1	10000	40	40	No	100:31
PC2	20000	80	80	No	100:31
PC3	20000	25	80	No	100:31
PC4	20000	25	80	Yes / 100	100:31
PC5	20000	25	80	Yes / 130	100:31
PC6	20000	25	80	Yes / 150	100:31
PC7	20000	25	80	No	100:29.5
PC8	20000	25	80	No	100:28

3.3.2 Manufacturing of fiber reinforced epoxy-clay nanocomposites

A predetermined amount of curing agent was added and mixed in DGEBA resin containing clay minerals by mechanical stirring (2 min at 500 rpm) at 25 °C. The mixture was placed in a vacuum desiccator for 30 min for degassing. Vacuum assisted wet lay-up method (Subramaniyan and Sun, 2006) was used for manufacturing fiber reinforced epoxy-clay nanocomposites. A dry fiber preform mat was placed on mold surface, and the modified epoxy resin was poured on it. The resin was then dispersed uniformly on glass fiber mat using a hand

scraper. Subsequently, another fiber layer was placed, and the resin-clay mixture was again applied consistently to wet and cover the fibers. Finally, vacuum bagging was performed and the air was evacuated by a vacuum pump. The vacuum was maintained until gelation of epoxy. The fiber reinforced nanocomposites were cured as per the recommendation by the manufacturer, i.e. heating the laminate for 7 h at a temperature of 70 ºC, on the mould. To generate the baseline data, fiber reinforced neat epoxy composites without clay were also manufactured using the same curing schedule. Some laminates were also post-cured at three different temperatures viz. 100, 130 and 150°C for 3 h.

3.3.3 Testing of materials

The tensile and flexural tests were conducted on specimens cut from laminates using a Zwick/ Roell universal testing machine. The values reported are an average of tests done on four specimens. The tensile test specimens were tested as per ASTM 3037/3039 standard. Three-point bending test was performed as per ASTM D790 standard. The tensile test specimens were cut in size 250 mm × 25 mm × 0.64-0.66 mm (length × width × thickness). The specimen size for bending test was 50 mm × 13 mm × 0.64-0.66 mm. The crosshead speed in the tensile test was kept at 2 mm/min. The interlaminar shear strength (ILSS) was calculated by the following formula:

$$\text{ILSS}=\frac{0.75 \times \text{P}}{\text{b}\times\text{h}} \qquad (3.1)$$

Where P is the failure load, b and h are the specimen width and thickness, respectively. The calorimetric measurements were performed in Perkin Elmer DSC 4000 (standard) by heating the samples to 300°C from room temperature at a heating rate of 10°C/min under nitrogen flow. The samples were cooled down to -4°C at a cooling rate equal to heating rate. The heating and cooling cycles were repeated twice. The glass transition temperature (T_g) was calculated as the mid-point value of glass transition range. Thermogravimetric analysis (TGA) was carried out using Mettler Toledo TGA/SDTA 851. The sample was heated to 700°C at a rate of 10°C /min under nitrogen atmosphere.

3.4 Results and Discussion

A uniform dispersion of clay minerals in the polymer matrix is dependent on many factors such as clay mineral modifier, concentration of clay minerals, the mixing conditions (type of mixing, temperature, and mixing duration) and choice of epoxy (Albdiry et al., 2012; Azeez et al., 2013; Bakar et al., 2014; Camargo et al., 2009; Liu et al., 2005b; Pavlidou and Papaspyrides, 2008).

The mechanical properties of nanocomposites prepared at different processing conditions have been tabulated in Table 3.2. The processing conditions have a substantial effect on tensile and flexural properties of glass fiber reinforced composites. The following subsections provide details to illustrate and discuss the effect of different process conditions and compositions.

Table 3.2 Tensile and flexural properties of glass fiber reinforced epoxy composites

Material code	Tensile modulus, GPa	Tensile strength, MPa	Elongation at break, %	Flexural modulus, GPa	Flexural strength, MPa	Interlaminar shear strength, MPa
GFRC	8.3 ± 0.16	313 ± 12	4.2 ± 0.3	10.2 ± 0.17	235 ± 18	2.9 ± 0.17
C15GFRC(PC1)	7.2 ± 0.22	256 ± 22	3.9± 0.22	12.5 ± 0.61	304 ± 22	3.9 ± 0.32
C15GFRC(PC2)	8.7 ± 0.15	368 ± 18	5.7 ± 0.13	15.3 ± 1.4	363 ± 20	4.6 ± 0.27
C15GFRC(PC3)	9.2 ± 0.65	348 ± 7	5.6 ± 0.15	12.3 ± 1.05	262 ± 6	3.8 ± 0.27
C15GFRC(PC4)	9.4 ± 0.01	378 ± 11	4.5 ± 0.14	13.8 ± 0.05	271 ± 19	2.8 ± 0.21
C15GFRC(PC5)	8.4 ± 0.21	326 ± 12	4.7 ± 0.3	11.3 ± 0.70	229 ± 18	3.3 ± 0.44
C15GFRC(PC6)	7.6 ± 0.09	270 ± 8	4.2 ± 0.3	11.4 ± 0.90	210 ± 25	3.5 ± 0.13
C15GFRC(PC7)	7 ± 0.13	279 ± 23	4.4 ± 0.3	10.3 ± 0.35	178 ± 7	2.9 ± 0.12
C15GFRC(PC8)	7.8 ± 0.53	279 ± 10	4.5± 0.5	9.6 ± 0.94	177 ± 21	2.8 ± 0.34

3.4.1 Effect of speed and temperature during mixing, and ultrasonic probe amplitude

In the case of C15GFRC(PC1) (GFRC containing 2 phr of Cloisite® 15A), both tensile modulus and tensile strength decreased by 13% and 18% respectively, as compared to GFRC without organoclay (Figure 3.1(a)). This can be attributed to agglomeration of clay minerals in epoxy matrix. In general, the clay mineral layers do not readily disperse in monomers due to the interactions of the silicate layers. The agglomerated clay particles reduce the tensile properties because of stress concentration effect, the lower aspect ratio of clay particles and reduced clay minerals/polymer surface interactions. Gurusideswar and Velmurugan (2014), Kornmann et al. (2005), Quaresimin and Varley (2008), Zerda and Lesser (2001) had also reported a decrease in tensile strength of glass fiber reinforced epoxy composites after addition of organically

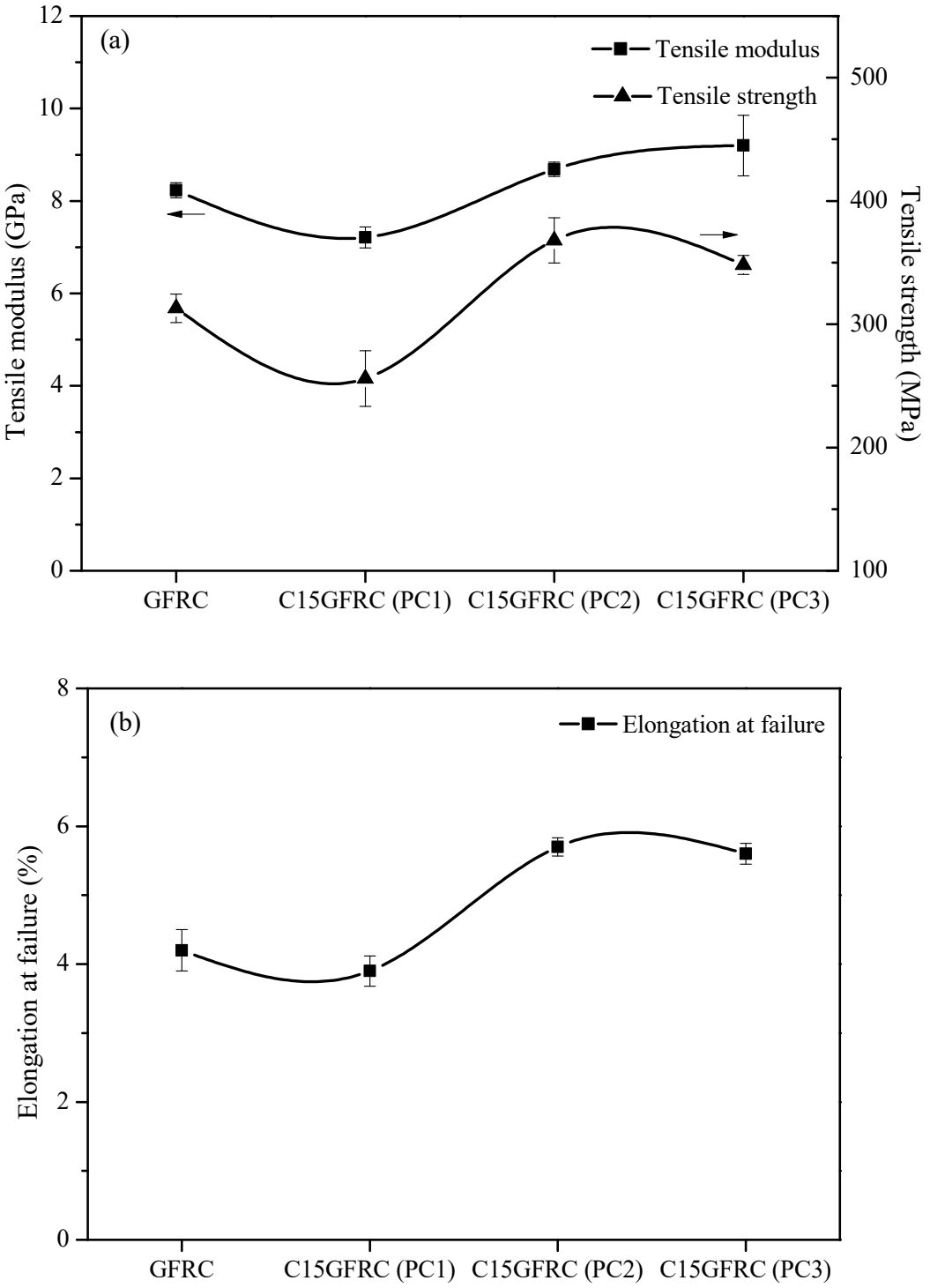

Figure 3.1 (a) Tensile modulus and tensile strength (b) elongation at failure of GFRC, C15GFRC(PC1), C15GFRC(PC2) and C15GFRC(PC3)

modified clay minerals in epoxy matrix. The percent elongation at failure did not change significantly because of dominating role of glass fibers on tensile properties of composite (Figure 3.1(b)). In a fiber reinforced nanocomposite, manufactured using vacuum assisted method, the volume fraction of glass fibers is high (V_f = 50 - 55%), and fibers dominate the tensile properties. The clay mineral layers must be uniformly dispersed and exfoliated in the matrix to realize the full potential of nano-reinforcement. The modification of clay minerals with organic modifiers, use of high shear forces to delaminate clay minerals, the low viscosity of resin at a higher temperature, longer gelation time promote homogeneous dispersion during synthesis of nanocomposites by *in-situ* polymerization. The effect of mixing parameters on properties of epoxy-clay nanocomposites has been reported by many researchers (Agubra et al., 2013; Bakar et al., 2014; Ngo et al., 2009; Zunjarrao et al., 2006). Much better dispersion of clay using process conditions as in PC2 (speed of impeller = 20000 rpm, the temperature during mixing = 80°C and ultrasonic probe amplitude = 80%) manifests in an increase in tensile modulus, tensile strength, and elongation at break. The tensile strength and elongation at break of C15GFRC (PC2) increased by 43% and 46%, respectively in comparison to C15GFRC (PC1) as a result of an increase in speed of homogenization, premixing temperature, and ultrasonic probe amplitude.

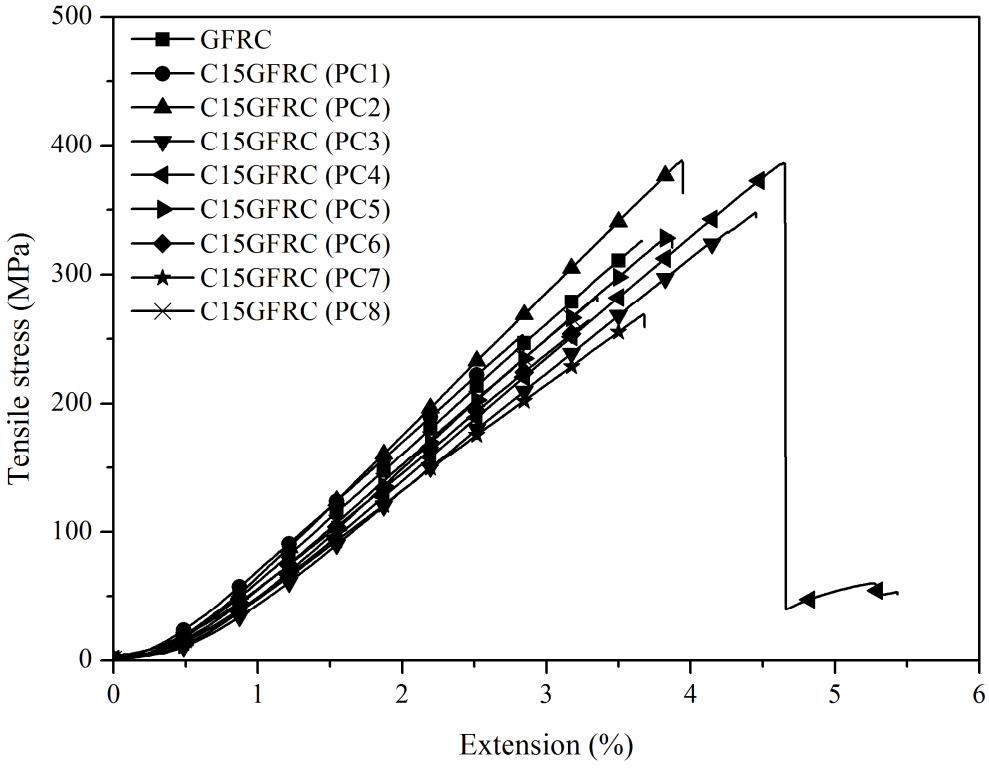

Figure 3.2 Tensile stress vs percent extension of fiber reinforced composites

High temperature during premixing of clay reduces the viscosity of the epoxy resin and makes possible the diffusion of monomer molecules in interlayer spaces of clay minerals and promotes better dispersion of clay minerals in matrix (Albdiry et al., 2012; Khan et al., 2010; Mohan et al., 2015; Ngo et al., 2007, 2009; Nuhiji et al., 2016). The representative tensile stress vs. percent elongation curves of all nanocomposites are shown in Figure 3.2. The representative values are a subset of values listed in Table 3.2. The increase in percent elongation at break and tensile strength can be attributed to a fine dispersion of clay minerals and adequate bonding between clay mineral layers and matrix of fiber reinforced composites. It would be pertinent to mention that the use of high temperature during premixing would limit the applicability of this method for mass production of large fiber reinforced epoxy parts because of difficulties in uniform heating and long times required to heat and cool large quantities of resin. Therefore, process conditions PC3 were of importance wherein the temperature of the resin during premixing, the speed of mixing and ultrasonic amplitude were 25 °C, 20000 rpm, and 80%, respectively. The tensile modulus and tensile strength of C15GFRC (PC3) were 9.2 GPa and 348 MPa, respectively showing an increase of 10% in tensile modulus and 11% in tensile strength over GFRC.

The error bars in Figure 3.1 (a) denote the standard deviation of four measurements and it can be concluded that within the limits of reproducibility the tensile modulus, tensile strength and percent elongation at break of C15GFRC (PC3) were equal to corresponding values obtained for C15GFRC (PC2). The flexural measurements elucidate the effect of clay minerals on the matrix-dominated properties of the fiber reinforced composites (Quaresimin and Varley, 2008; Vlasveld et al., 2007). The flexural modulus and strength of GFRC were 10.2 GPa and 235 MPa, respectively. The incorporation of clay minerals in epoxy increased both flexural modulus and flexural strength of fiber reinforced composites by 20% and 11.5%, respectively in the case of C15GFRC(PC3) as shown in Figure 3.3. The higher modulus of composites containing clay is a result of matrix stiffening because of its adhesion to the high modulus ceramic clay mineral layers. The flexural strength as shown in Figure 3.3(b), on the other hand, was limited by failure due to compression. The increase in tensile and flexural strength of composites on modification of matrix using clay minerals has also been reported by other researchers (Daud et al., 2009; Kumar et al., 2010; Vlasveld et al., 2007; Withers et al., 2015).

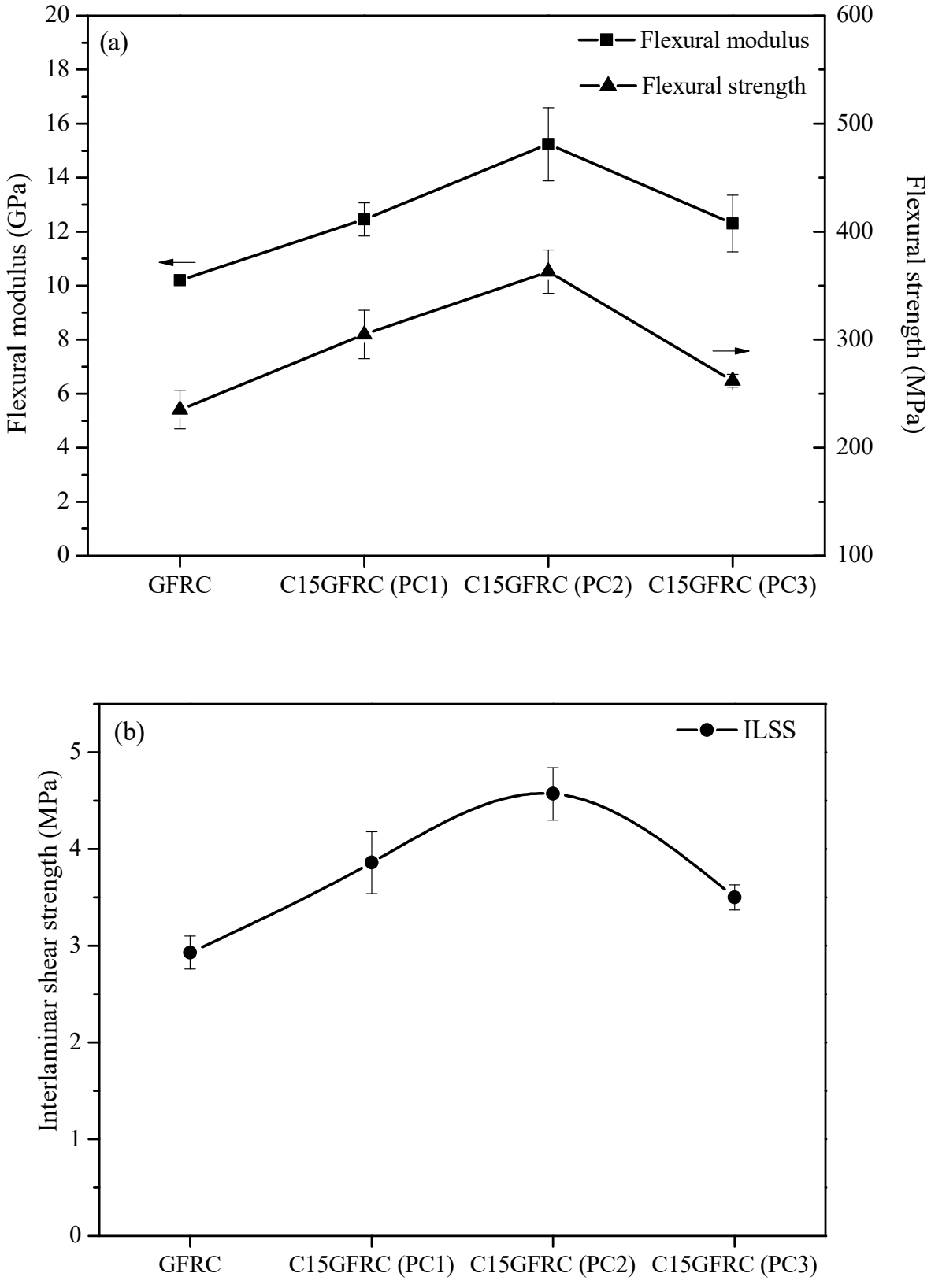

Figure 3.3 (a) Flexural modulus and flexural strength (b) Interlaminar shear strength of GFRC, C15GFRC(PC1), C15GFRC(PC2) and C15GFRC(PC3)

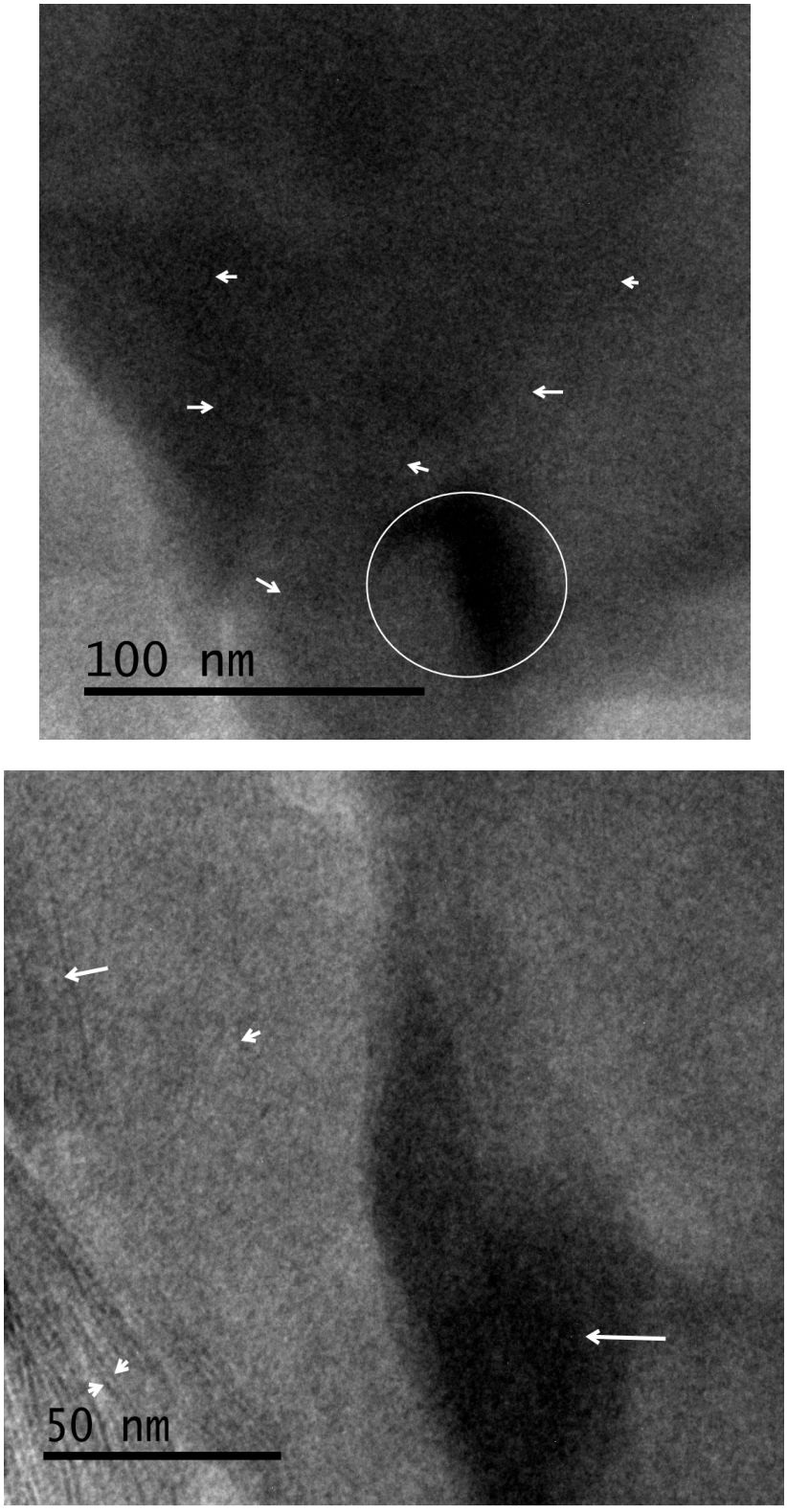

Figure 3.4 Transmission electron micrographs of C15GFRC(PC3) at different magnifications

The interlaminar shear strength of the composite increased with the incorporation of clay minerals in an epoxy matrix. The clay mineral in C15GFRC(PC3) had intercalated morphology as observed using Transmission electron microscopy. The clay mineral layers were seen to be randomly oriented and uniformly dispersed throughout the matrix but a fully exfoliated structure was not observed (Figure 3.4(a)). The clay mineral aggregates in which clay layers were seen to be regularly stacked (Figure 3.4(b)). Small angle X-ray scattering (Figure 3.5) revealed the changes in the interlayer spacing of Cloisite® 15A in fiber reinforced epoxy-clay nanocomposites. The characteristic peak of Cloisite® 15A at 2θ = 2.41° corresponding to d-spacing, d_{001}, of 3.65 nm was shifted to lower angle indicating an increase in d_{001} spacing of Cloisite® 15A in epoxy. Two diffraction peaks at values 2θ = 1.22° and 2θ =1.49° corresponding to d-spacing of 7.23 nm and 5.91 nm respectively, were observed.

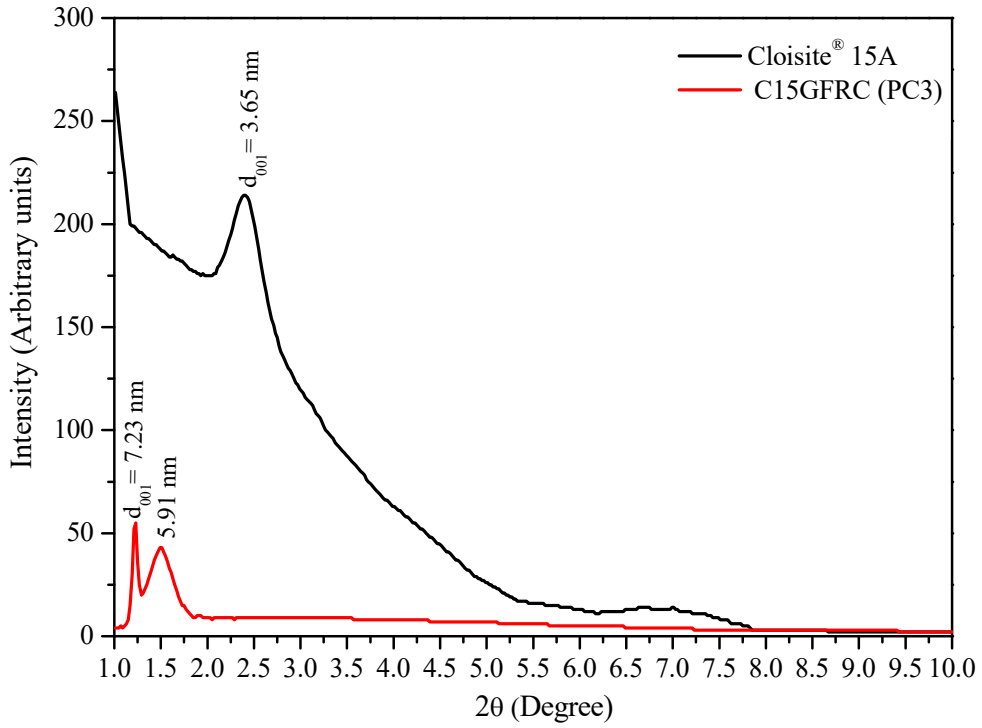

Figure 3.5 Small angle X-ray scattering of Cloisite® 15A and C15GFRC (PC3)

3.4.2 Effect of post-curing on mechanical properties of composites

The laminates synthesized using process condition PC3 were post-cured at different temperatures viz. 100 °C, 130°C and 150°C in an oven and these have been denoted as C15GFRC (PC4), C15GFRC (PC5) and C15GFRC (PC6), respectively. The temperature and schedule of post-curing can be optimized to enhance the mechanical properties of composites. The post-curing of thermosets at temperatures slightly below the glass transition temperature, T_g, for long periods of time (also called annealing), increases mass density of polymer and this

phenomenon is known as physical ageing. The physical ageing has a significant effect on the mechanical response of epoxies and their composites (Odegard and Bandyopadhyay, 2011). The increase in T_g, modulus and strength and a decrease in free volume is linked with the physical ageing of epoxy (Carbas et al., 2013; Chowdhury et al., 2006; Hiremath et al., 2014; Kumar et al., 2015).

In the present work, post-curing of laminates was performed at temperatures above the glass transition temperature of the fully cured network, $T_{g\infty}$ ($T_{g\infty} > T_g$) to study the effect of post-cure temperature on mechanical properties. To get values of $T_{g\infty}$, a DSC was done wherein the nanocomposite samples were subjected to 3 cycles of heating and cooling. The glass transition temperature of epoxy increased on the incorporation of organically modified clay minerals due to clay - polymer interactions, which restrict the mobility of chains. The DSC thermograms of GFRC and C15GFRC (PC3) are shown in Figures 3.6 (a) and 3.6(b). The DSC curves for 2nd and 3rd heating scans were identical. The glass transition temperature (T_g) of GFRC (as cured) was 60°C as obtained from the first heating scan, whereas the glass transition temperature (ultimate) was 66°C, from 2nd and 3rd heating scans. In the case of C15GFRC, the glass transition temperature (as cured) was 77°C and the glass transition temperature obtained from the second heating scan was 87 °C. In the third heating scan, although T_g increased from 87 to 90°C no residual curing exotherm was observed. The effect of incorporation of clay minerals was evident as the enthalpy relaxation peak (Morancho and Salla, 1999) had significantly diminished and the glass transition temperatures had increased by approximately 17 °C. This would also impart better thermal stability to C15GFRC as compared to GFRC. The T_g (ultimate) of composites obtained from second/third heating scan can be considered as $T_{g\infty}$, the temperature of the fully cured network obtained using DSC.

PC4, PC5, and PC6 correspond to process conditions, wherein the fiber reinforced epoxy-clay nanocomposites were initially prepared and cured as in PC3 and then post-cured at 100, 130 and 150 °C, respectively for a 3 h as shown in Figure 3.7. The test conditions for determination of tensile and flexural properties remained unchanged. The tensile modulus and tensile strength of C15GFRC(PC4) were 9.4 GPa and 378 MPa, respectively compared to 9.2 GPa and 348 MPa for C15GFRC(PC3) as shown in Figure 3.8. Though the modulus remained unchanged, a small increase in the tensile strength was observed with post-curing the nanocomposite at 100°C for 3 h. A slight decrease in percent elongation at break was observed and this is a result of embrittlement of epoxy at elevated temperature. The flexural modulus and flexural strength were not significantly influenced by post-curing at 100°C for 3 h.

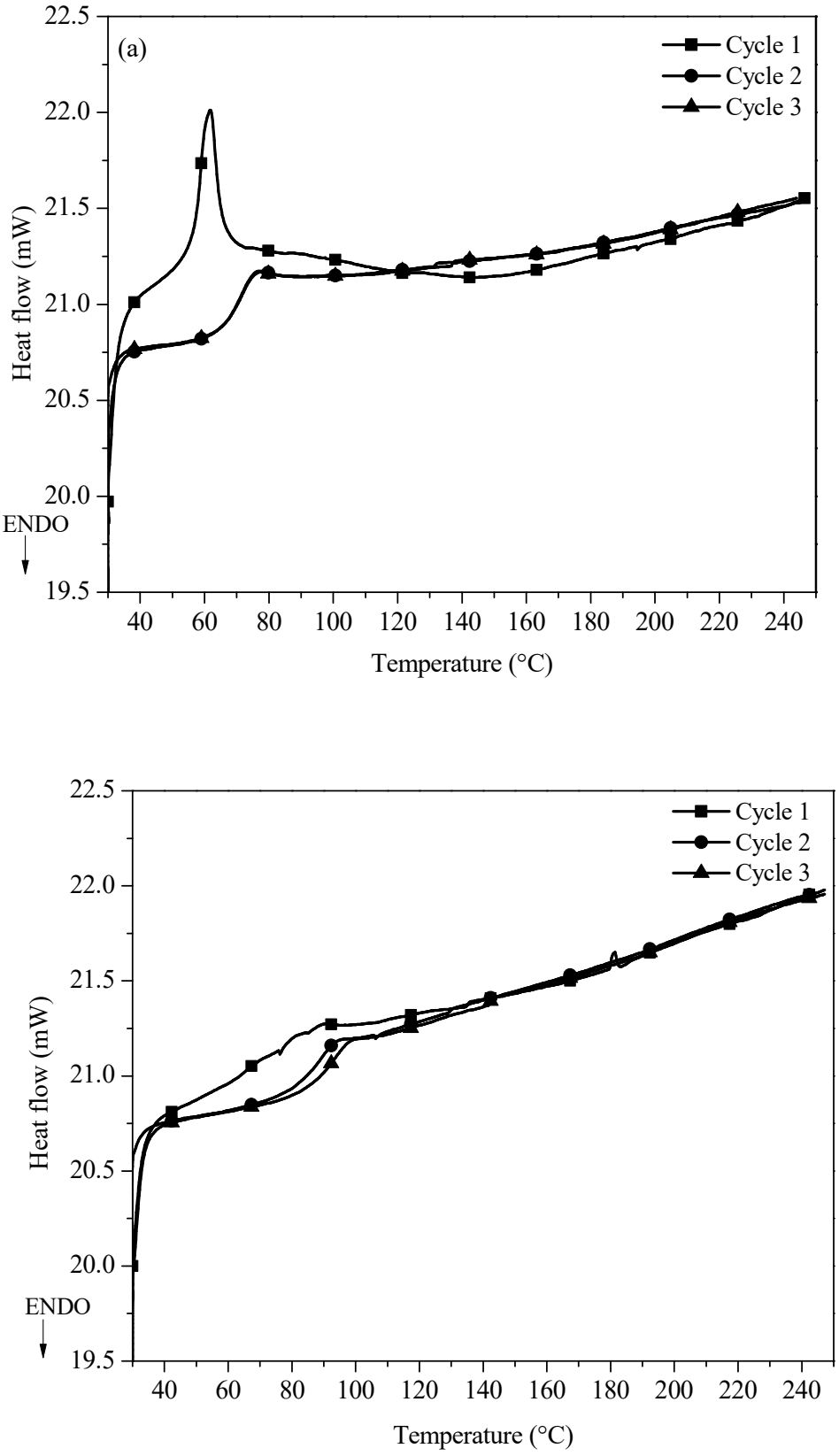

Figure 3.6 DSC thermograms of (a) GFRC and (b) C15GFRC(PC3)

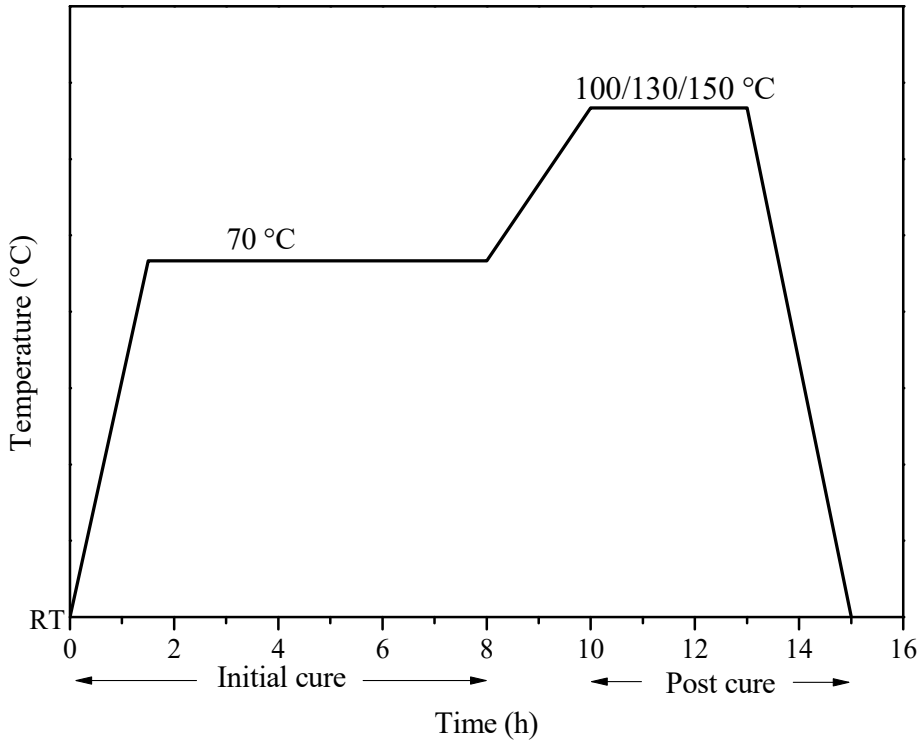

Figure 3.7 Cure schedule of C15GFRC(PC4), C15GFRC(PC5) and C15GFRC(PC6)

The tensile modulus, tensile strength and percent elongation at break decreased significantly after post-curing at a higher temperature as shown in Figure 3.8. The warpage of fiber reinforced epoxy-clay nanocomposites after post-curing at higher temperature was clearly evident. Similar results have been reported in a recent study by Carbas et al. (2013), a decrease in tensile modulus and tensile strength of two different epoxies post-cured above glass transition temperature of the fully cured network ($T_{g\infty}$) determined using DSC, was reported. It was further stated that the thermal degradation or oxidative cross-linking was the reason for the decrease in tensile modulus and strength. In C15GFRC (PC5) and C15GFRC (PC6), the tensile strength and flexural strength were severely affected by an increase in post- cure temperature as shown in Figures 3.8 and 3.9.

There could be three possible reasons for the deterioration in mechanical properties of samples post-cured at 130°C and 150°C.

(a) The first possible reason may be due to boiling of free or bound water / low molecular weight impurities present in the composites leading to the generation of voids and internal stresses.

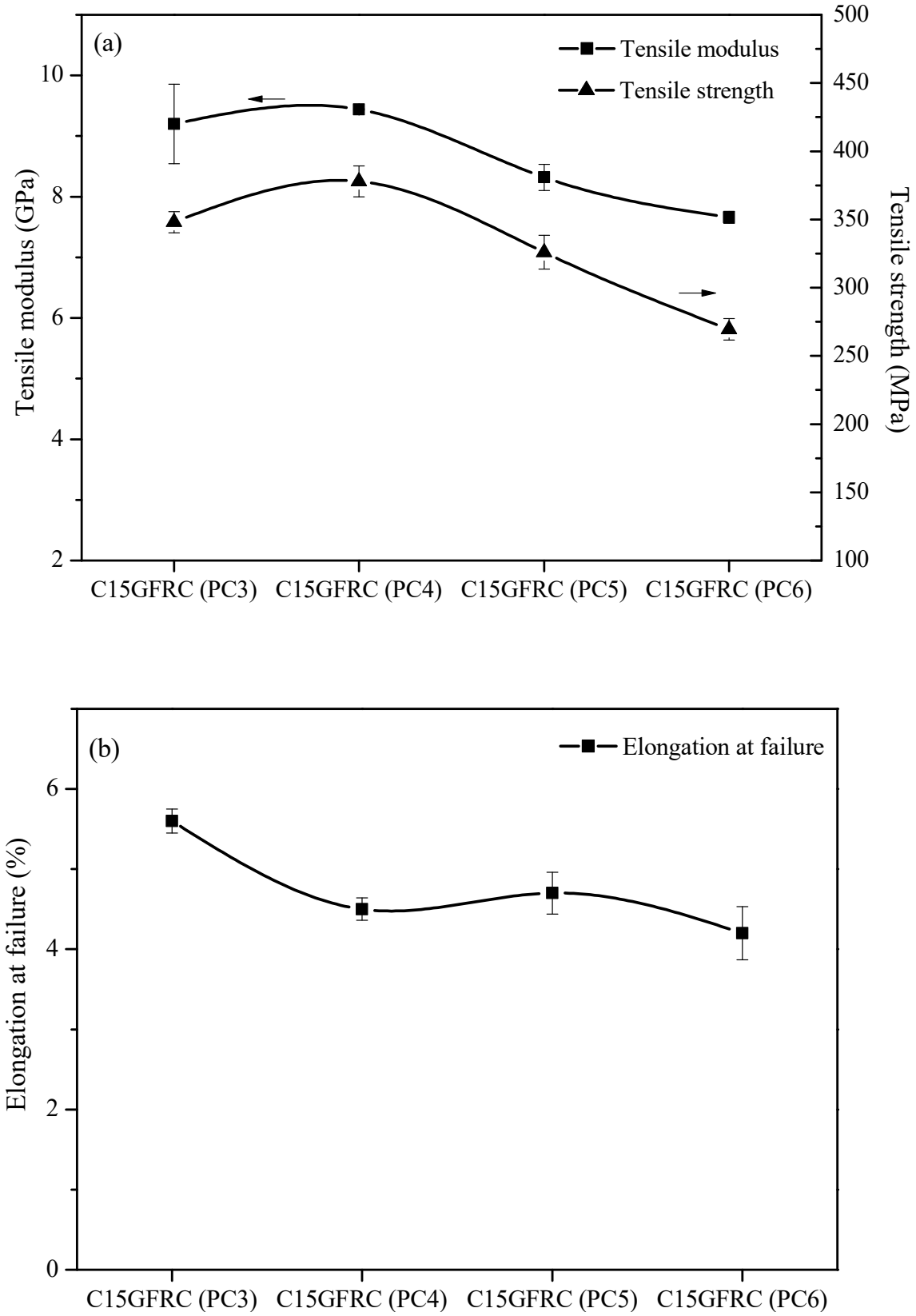

Figure 3.8 (a) Tensile modulus and tensile strength (b) elongation at failure of C15GFRC (PC3), C15GFRC(PC4), C15GFRC(PC5) and C15GFRC(PC6)

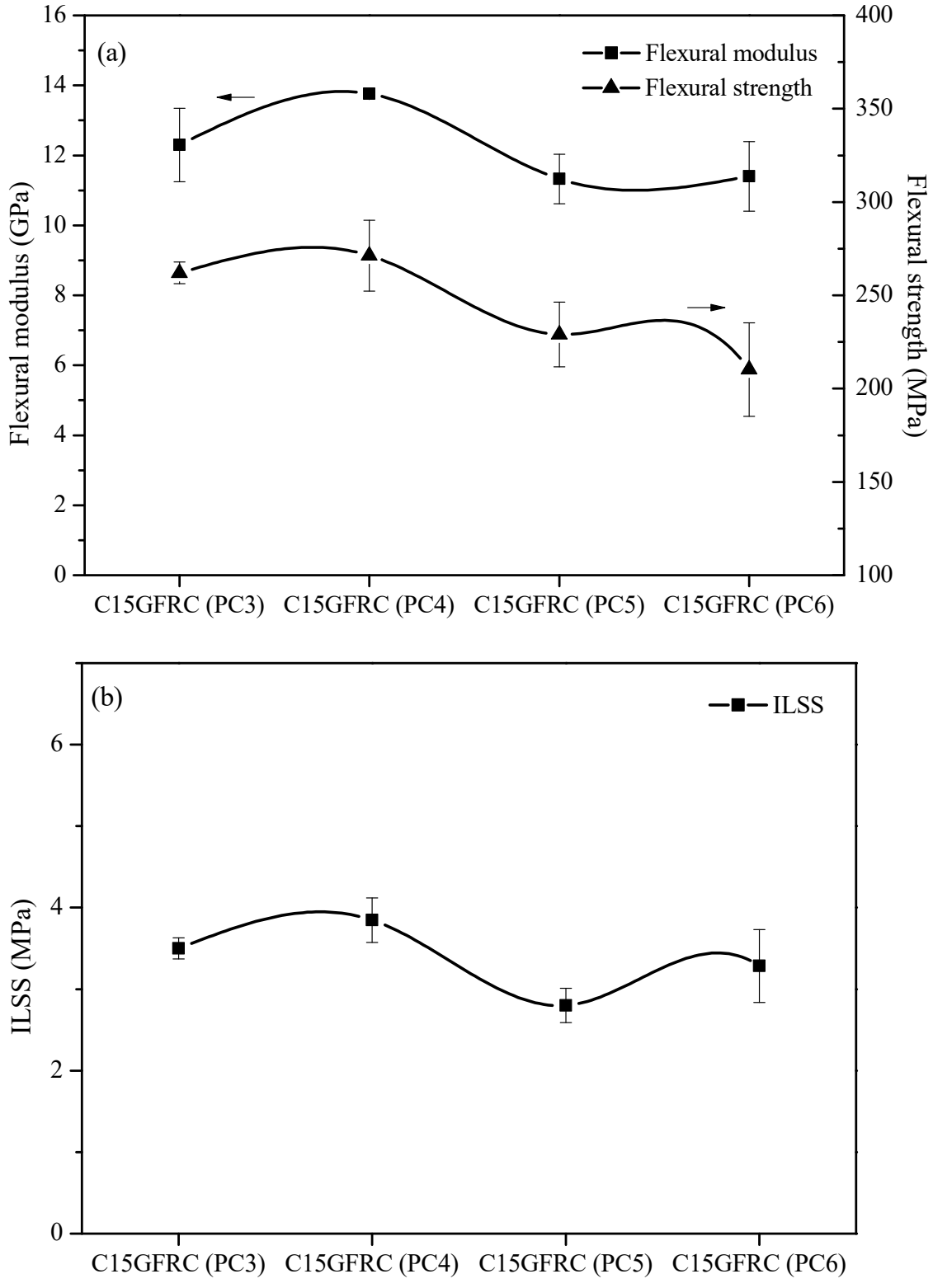

Figure 3.9 (a) Flexural modulus and flexural strength (b) Interlaminar shear strength of C15GFRC(PC3), C15GFRC(PC4), C15GFRC(PC5) and C15GFRC(PC6)

(b). Defects due to residual stresses in composites

The second possible reason may be that in fiber reinforced polymer composites significant residual stresses are set-up during polymerization and thermal cooling. The residual stresses exist in continuous fiber laminates immediately after polymerization because of restricted volume changes (contraction of the polymer is restricted by surrounding continuous fiber/ nano-reinforcements) of the polymer matrix that occur during the polymerization process. The cooling of cured composites result in thermal cooling stresses at (a) fiber-matrix interfaces (b) each ply of a laminate due to a mismatch between shrinkage of constituents, constraints from other laminas and a gradient in cooling rates of different plies in thick laminates (Drzal, 1990; Safarabadi and Shokrieh, 2014; Zhao et al., 2006). The thermal cooling stresses increase as the difference between cure/post-cure temperature and room temperature increases. These stresses may lead to fiber-matrix debonding, matrix cracking, warpage, and delamination of laminas which have an adverse effect on the mechanical behavior of composites (Safarabadi and Shokrieh, 2014; Zhang et al., 2004). Therefore, post-curing laminates at temperatures much above $T_{g\infty}$ would result in localization of stresses around the curing induced defects and affect the load carrying capacity of composites.

(c) The possibility of degradation of organic modifier in Cloisite® 15A.

According to Park and Jana (2004), the cure temperature of epoxy-clay nanocomposites should be lower than the thermal dissociation temperature of the ammonium ions present in organically modified clays. Also in the same study, the epoxy-clay nanocomposites cured at 180°C a limited exfoliation of clay and plasticization of the matrix was observed. This was attributed to the stoichiometric imbalance caused due to excess of primary amines produced as a result of thermal dissociation of ammonium ions and ammonium chloride salts. The TGA curve of Cloisite® 15A is shown in Figure 3.10. The initial loss in the temperature range from 30°C to 200°C represents the elimination of adsorbed water. The onset of degradation of organic modifier was at 230 °C. The maximum weight loss occurred between the temperature range of 272°C to 410°C, which can be attributed to the loss of water present in interlayer space of clay mineral, alkanes, alkenes, CHO's and COOH's (Cervantes-Uc et al., 2007; Edwards et al., 2005).

In the present study though the post-curing of samples was done at 100°C, 130°C and 150°C for 3h and the post-cure temperature was low as compared to the fast heating rate in TGA. Therefore, the possibility for degradation of organic modifier even at 130°C and 150°C can be ruled out.

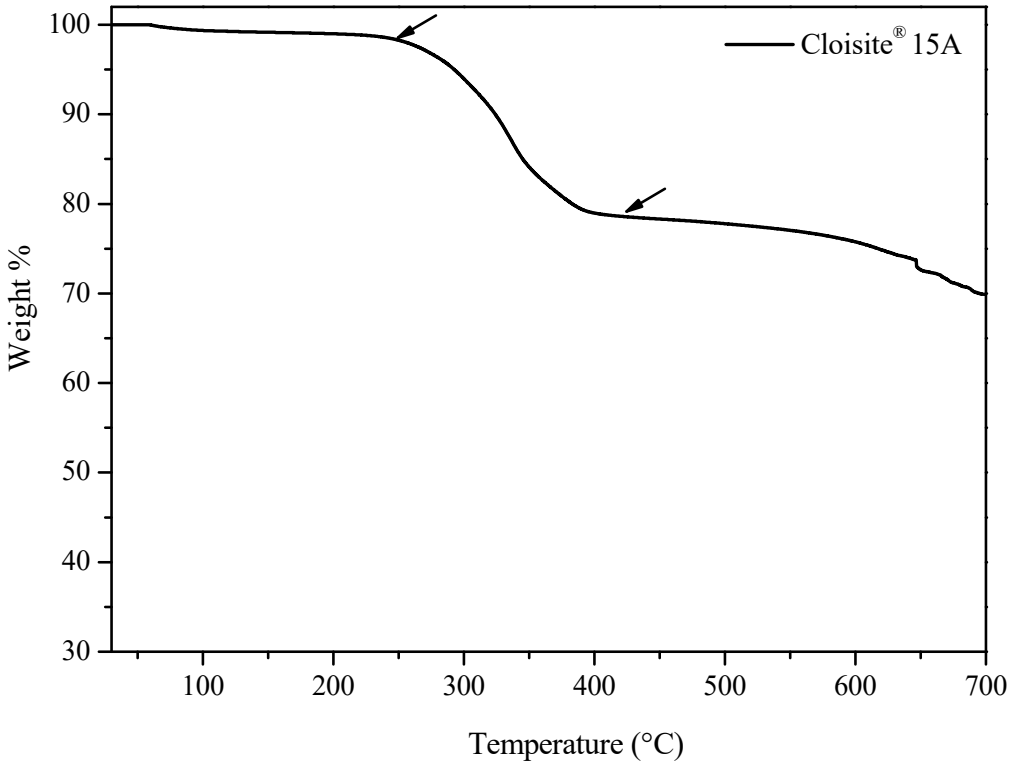

Figure 3.10 TGA curve of Cloisite® 15A

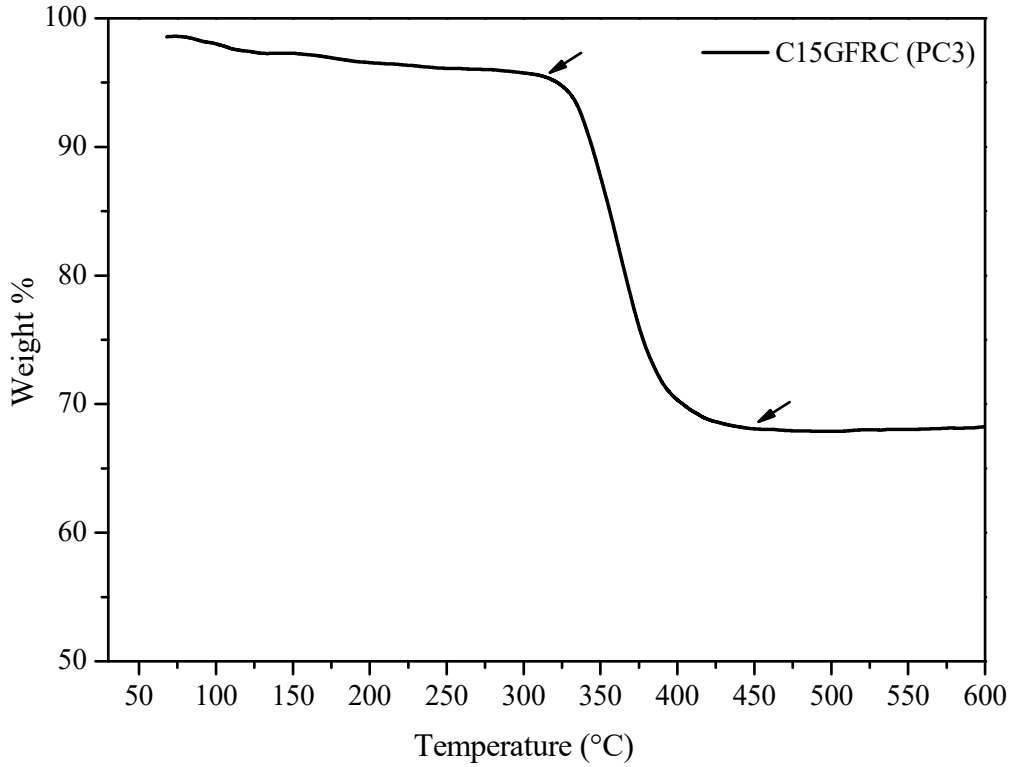

Figure 3.11 TGA curve of C15GFRC(PC 3)

Another possible reason may be related to thermal degradation of epoxy and glass fibers. However this was ruled out by conducting a TGA on one composite sample (C15GFRC(PC3)). The thermal stability of C15GFRC (PC3) was studied in terms of percentage weight loss as a function of temperature in a nitrogen atmosphere. The thermal degradation of epoxy-clay nanocomposite was a single stage process which occurred due to degradation of crosslinks. As shown in Figure 3.11, the onset degradation temperature of the epoxy matrix was 312°C and the loss of weight continued up to 450°C. The temperature range during that degradation of epoxy occurred was far above than the temperature at which post-curing was carried out.

In the present study, cooling after post-curing at 100,130 and 150°C was done by stopping the heat flow to composite and letting it cool to room temperature gradually. It should be mentioned that flow rate of cooling is also expected to significantly influence the resolution of thermal stresses because of more relaxation time available to polymer chains. This would limit the drop in properties on high-temperature post-curing.

3.4.3 Effect of stoichiometric ratio of resin and hardener on mechanical properties

Similar to cure schedule, the stoichiometric balance between epoxy and amine groups has a significant impact on the mechanical behavior of epoxy and its nanocomposites. Most studies reported in literature deal with resin and hardener mixed in stoichiometric proportions. The effect of non-stoichiometric ratio with an excess of hardener or resin on the mechanical behavior of fiber reinforced epoxy-clay nanocomposites has not been studied in detail. The choice of epoxy and hardener ratio is certainly the most critical issue in tailoring polymer composites because many properties, e.g. tensile strength, tensile modulus, hardness and glass transition temperature (T_g) of fiber reinforced composites depend on cross-link density of cured matrix (Goodman and Hanna, 2014; Minty et al., 2016; Ratna, 2009). An excess of unreacted amine groups would cause plasticization of the epoxy matrix. Secondly, the fiber reinforced composite exposed to moisture and seawater would be more susceptible to degradation due to chemical hydrolysis because of the high reactivity of polar amine groups with water (García del Cid et al., 2012; Grave et al., 1998; Palmese and McCullough, 1992).

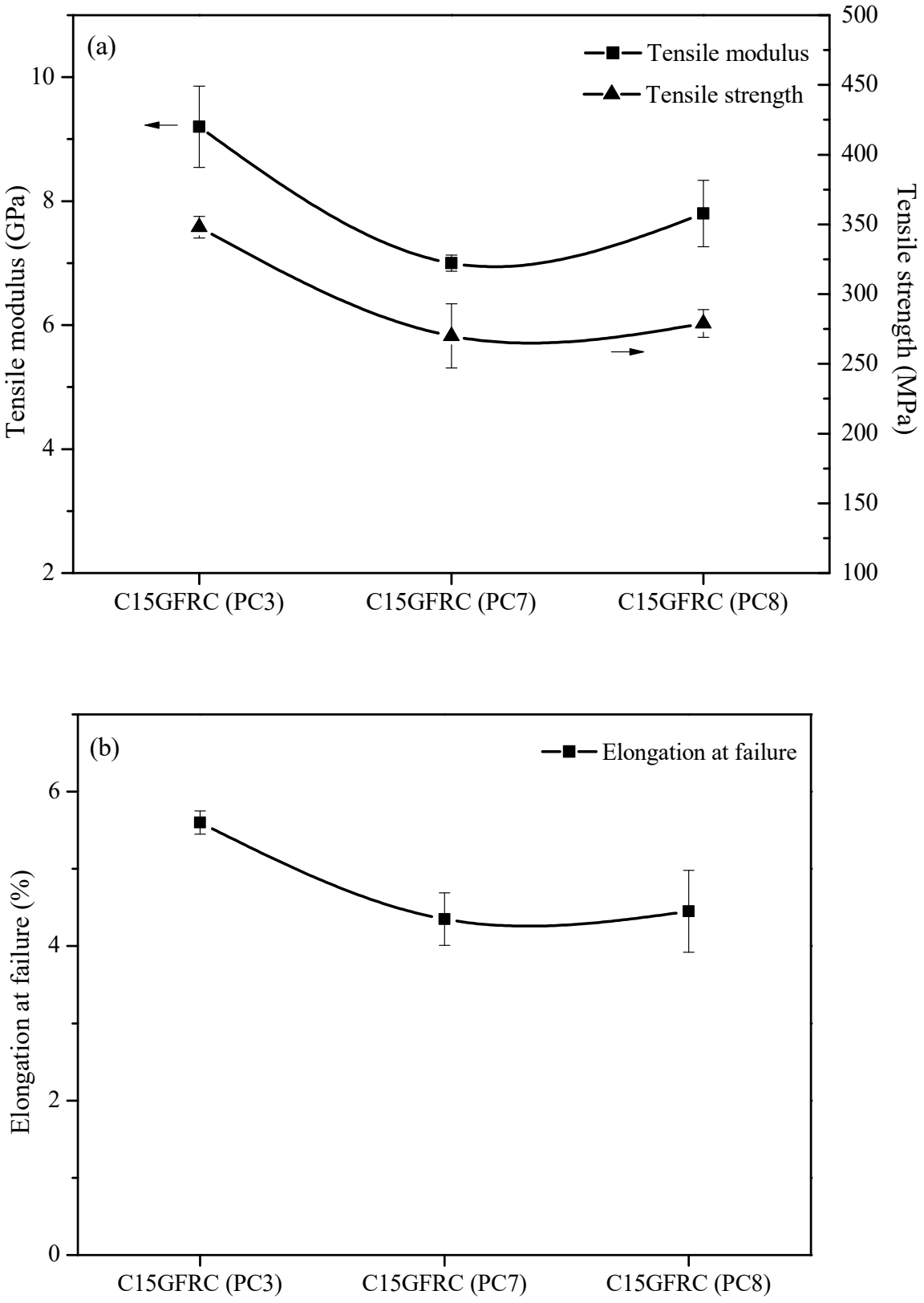

Figure 3.12 (a) Tensile modulus and tensile strength (b) elongation at failure of C15GFRC (PC3), C15GFRC(PC7), and C15GFRC(PC8)

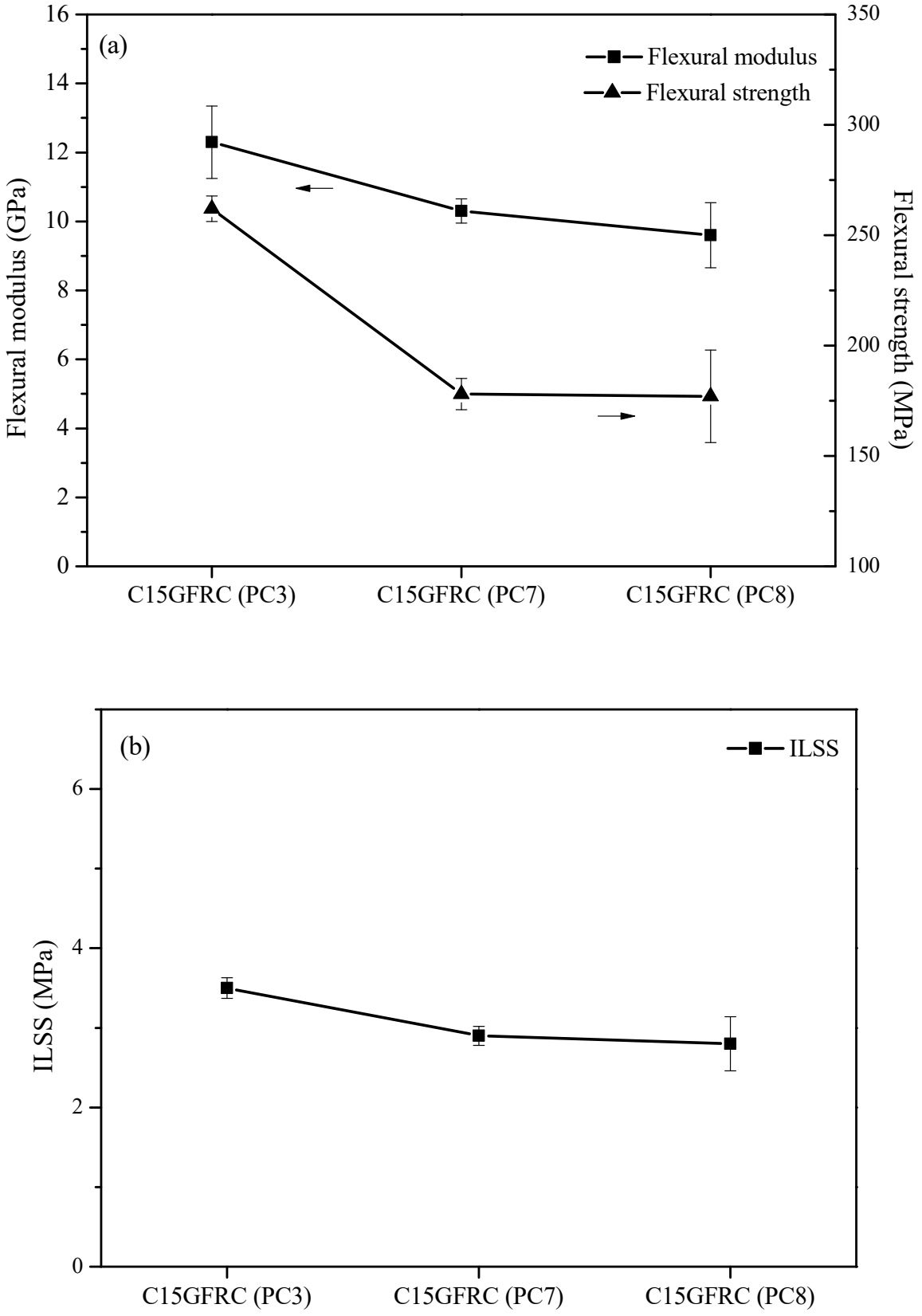

Figure 3.13 (a) Flexural modulus and flexural strength (b) interlaminar shear strength of C15GFRC (PC3), C15GFRC(PC7), and C15GFRC(PC8)

The tensile modulus, tensile strength, flexural modulus and flexural strength of fiber reinforced epoxy-clay nanocomposites were significantly affected with a decrease in the quantity of hardener as compared to C15GFRC(PC3) (PC3 corresponds to process conditions in which epoxy and hardener were mixed in a stoichiometric proportion) as shown in Figures 3.12 and 3.13. PC7 and PC8 refer to those compositions and conditions in which non-stoichiometric proportions were used and the quantity of hardener was decreased by 5% and 10%, respectively. C15GFRC (PC7) exhibited a decrease of 23%, 20%, 16 % and 32% in tensile modulus, tensile strength, flexural modulus and flexural strength, respectively. However, the difference in mechanical properties of C15GFRC(PC7) and C15GFRC(PC8) was not significant. The interlaminar shear strength of fiber reinforced epoxy-clay nanocomposites decreased also, as shown in Figure 3.13(b). C15GFRC (PC7) and C15GFRC (PC8) exhibited lowest mechanical properties as compared to all other fiber reinforced composites manufactured using different process conditions (PC1, PC2, PC3, PC4, PC5 or PC6). Thus, the incomplete curing reaction of epoxy due to a shortage of amino groups resulted in a marked decrease in mechanical properties of C15GFRC (PC7) and C15GFRC (PC8). It is also expected that the hygrothermal properties of PC7 and PC8 would also be much lower due to reason discussed above.

Fourier transform infrared (FTIR) spectroscopy is a very useful tool for characterization of organic compounds in epoxies. FTIR spectra analysis was used to investigate the relative changes in the intensity of bands associated with the monomer/polymer after curing reaction. The absorption peaks observed in FTIR spectra of DGEBA at 3056 cm^{-1}, 1247 cm^{-1}, 915 $cm^{-1,}$ 830 cm^{-1} denote epoxy groups. The detailed peak assignments of the main absorption bands for the (bisphenol-A-(epichlorhydrin) epoxy with 1, 4-Bis (2, 3 epoxypropoxy) butane and butanedioldiglycidyl ether groups) are given in Table 3.3. The FTIR spectra of GFRC, C15GFRC(PC3) and C15GFRC(PC7) are also shown in Figure 3.14. The peak at 915 cm^{-1} had disappeared after curing of nanocomposites due to ring-opening polymerization. The intensity of remaining epoxy characteristic peaks decreased due to the reaction of epoxide rings to form ether linkages during the curing process. The relative intensities of peaks attributed to symmetric stretching of the epoxy ring at 1247 cm^{-1} for GFRC, C15GFRC(PC3) and C15GFRC (PC7) are shown in inset 1, reflect that more unreacted epoxy groups were present in C15GFRC(PC7) as compared to GFRC and C15GFRC(PC3). One more band, which has been used by many other researchers (Cholake et al., 2014; Coates, 2000; Poisson et al., 1996) to study epoxy curing kinetics was observed at 3056 cm^{-1} (inset 2). This band was more

prominent in C15GFRC (PC7) indicating that in C15GFRC(PC7) the curing reaction was not complete due to the scarcity of amino groups and resulted in a decrease in the mechanical properties of fiber reinforced epoxy-clay nanocomposite.

Table 3.3 Tentative assignments of FTIR peaks in DGEBA (Cholake et al., 2014; Coates et al., 2000)

Group frequency, wave number (cm^{-1})	Tentative assignment
3056	Symmetric stretching of C-H of the oxirane ring
2966-2873	Stretching C–H of CH_2 and CH aromatic and aliphatic
1608	C=C stretching of aromatic ring
1509	C– C stretching of aromatic ring
1456	Bending of CH_2 and CH_3
1247	Symmetric stretching of epoxy ring
1184	C– O aromatic ring stretching
1107	Aromatic stretching
1036	C– O – C stretching of ether group
915	C– O stretching of oxirane group
830	C– O – C stretching of oxirane group
760	CH_2 rocking

In contrast to these results, few studies have reported that use of non-stoichiometric ratios with an excess of epoxy groups favored exfoliation of clay minerals in the matrix (Chin et al., 2001; Lan et al., 1996). Chin et al., 2001 observed that the interlayer spacing of MMT increased extensively when the resin to hardener ratio was well below the stoichiometric amount (as earlier reported by Lan et al., 1996). The nanocomposites with DGEBA cured with stoichiometrically equivalent amount had an intercalated morphology, whereas a decrease in concentration of curing agent below the stoichiometric amount aided exfoliation. It was concluded that the higher concentration of curing agents limited exfoliation because of higher

rates of extragallery crosslinking with a decreased diffusion of polymer chains in intragallery regions.

García del Cid et al. (2012) studied the influence of non-stoichiometric DGEBA- hardener ratio on curing and thermo-mechanical properties of epoxy-clay nanocomposites. The increase in d-spacing of clay in nanocomposites was found to be influenced by the structure of organic modifier in clays but was independent of the stoichiometry of epoxy. It was reported that the incorporation of clay minerals and excess hardener also increased the extent of curing of epoxy. However, the glass transition temperature (T_g) and elastic storage modulus of nanocomposites were highest at stoichiometry less than 1. Recent studies by Gao et al. (2016) and Gude et al. (2012) on epoxy-hardener stoichiometry concluded that the reinforcement effect of amine functionalized multi-walled carbon nanotubes on thermomechanical properties was more significant in compositions with less cross-linked networks i.e. epoxide rich compositions. Clearly, more detailed studies on the contribution of non-stoichiometric epoxy hardener ratio on mechanical properties of fiber composites are required because of the influence of many factors like nature and interactions of surface modifier, fiber/ nanofiller volume fraction, dispersion of nanofillers, type of hardener and curing conditions.

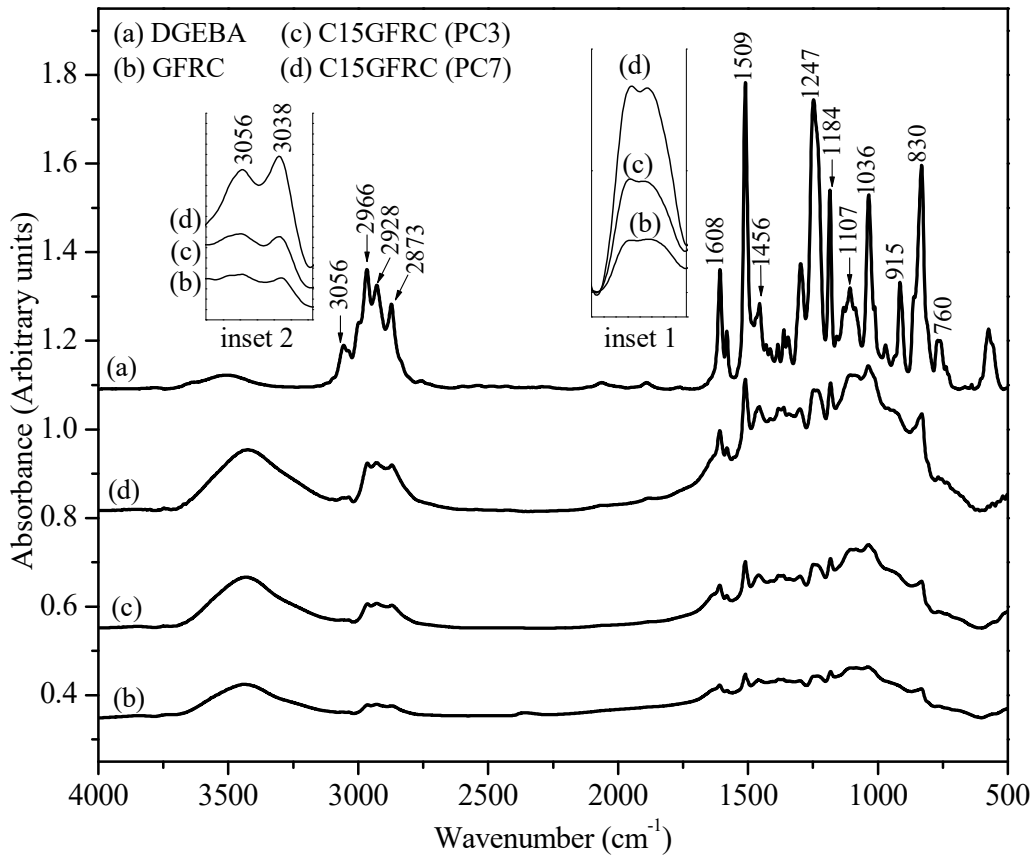

Figure 3.14 FTIR spectra of DGEBA and fiber reinforced epoxy-clay nanocomposites

3.5 Closing remarks

The exploratory studies on the effect of different processing parameters (premixing parameters, post-curing temperature, resin to hardener mix ratio) on the mechanical properties of fiber reinforced epoxy-clay nanocomposites containing 2 phr (parts per hundred resin) of a commercially available organically modified montmorillonite clay, Cloisite® 15A had been carried out. This study highlights three main outcomes

(i) Effect of speed and temperature during mixing, and ultrasonic probe amplitude

The improvement in tensile modulus and tensile strength, flexural modulus and flexural strength of glass fiber reinforced composites incorporating clay minerals were dependent on dispersion state of clay minerals in epoxy. The mixing of Cloisite® 15A in epoxy resin performed using low speed of homogenization (10000 rpm), epoxy and clay mixture temperature (40°C), and low ultrasonication amplitude (40%) led to a decrease in tensile modulus and tensile strength by 13% and 18%, respectively as compared to neat epoxy-glass fiber reinforced nanocomposites. To get good mechanical properties, the speed of homogenization, and temperature of epoxy and clay mixture during mixing and ultrasonic amplitude were increased. The tensile strength, flexural modulus, flexural strength and interlaminar shear strength of nanocomposites increased by 17.5%, 50%, 54.5% and 58.5%, respectively when the mixing temperature of epoxy and clay mixture was 80 °C, the speed of homogenization (20000 rpm) and ultrasonic probe amplitude (80%). The elevated temperature during premixing can pose difficulty in mass production of large fiber reinforced parts. Therefore, it was decided to continue working with speed of homogenization, ultrasonic probe amplitude but the epoxy-clay mixture temperature during mixing at 25 °C. The fiber reinforced epoxy-clay nanocomposites exhibited 12% increase in tensile strength, 20% increase in flexural modulus and 12% increase in flexural strength as compared to neat epoxy-glass fiber reinforced composites. The small angle X-ray scattering (SAXS) and transmission electron microscopy (TEM) observations revealed that intercalated nanocomposites were formed.

(ii) Post-curing effect

Post-curing of fiber reinforced epoxy-clay nanocomposites at 100°C showed no significant change in mechanical properties in comparison to samples which were not post-cured. The mechanical properties of fiber reinforced epoxy-clay nanocomposites reduced after post-cure at higher temperatures, i.e. 130°C and 150°C, and this can be attributed to generation of voids and internal stresses due to

1 boiling of free or bound water and low molecular weight impurities present in the nanocomposites
2 residual stresses due to thermal cooling.

The degradation of epoxy and organic modifier in Cloisite 15A® at 150°C can be ruled out. The TGA of Cloisite®15A and fiber reinforced epoxy-clay nanocomposites were also carried out to support these conclusions. Also, the glass transition temperature of the fully cured epoxy ($T_{g\infty}$) obtained from DSC was 90 °C. Therefore, the post-cure temperature exceeding the glass transition temperature of fully cured epoxy by a good margin has a detrimental effect on the mechanical properties of fiber reinforced composites.

(iii) Effect of change in resin to hardener ratio

The non-stoichiometric ratio of epoxy resin and hardener resulted in a decrease in both the extent of cure of epoxy and mechanical properties of fiber reinforced epoxy-clay nanocomposites. The nanocomposites with non-stoichiometric ratios of epoxy and hardener were not fully cured as evident from FTIR analysis of nanocomposites. This led to a significant decrease in mechanical properties of fiber reinforced nanocomposites.

The next step was to study surface treatment of clay minerals using silane coupling agents. The following chapter discusses the functionalization of clay and its adhesion with the epoxy matrix.

Chapter 4 Effect of surface treatment of glass fibers and clay minerals

4.1 Introduction

Silane coupling agents are widely used to enhance adhesion between glass fibers and epoxy matrix and shield against the deleterious effects of diffusion of water on mechanical properties of composites. The mechanical properties of composites increase significantly if the silane coupling agent interacts with the reinforcement as well as the polymer matrix (Blum, 2016; Shokoohi et al., 2008; Xie et al., 2010). Silylation of clay minerals promote exfoliation of clay minerals which results in improvements in mechanical properties of polymer composites (Chen and Yoon, 2005b; Ha et al., 2010, 2008, 2007; Ha and Rhee, 2008; Huskić et al., 2013; Ianchis et al., 2015; Piscitelli et al., 2012; Wang et al., 2006b). Thus, it is desirable that the surface area per unit mass of the filler (clay minerals) which can be silyated should be maximized. In the studies reported in the literature on silylated clay polymer nanocomposites, clay minerals had not been dispersed at the nanoscale, only in few studies, clay had been intercalated to some extent (Sharma et al., 2017). Thus, if the clay can be exfoliated or nano-dispersed before silanization, interesting results can be expected.

In this chapter, a new method of silane treatment has been reported wherein the clay minerals were nano-dispersed in hydrolyzed silanes. The silylated clay minerals were then dispersed in epoxy resin, and glass fiber reinforced epoxy-clay laminates were manufactured using vacuum assisted wet-layup method. The fiber reinforced epoxy nanocomposites containing silylated clay minerals have been characterized using Small angle X-ray scattering (SAXS), Transmission electron microscopy (TEM) and Differential scanning calorimetry (DSC). Additionally, the effect of silane treatment of glass fibers on the tensile and flexural properties of glass fiber reinforced epoxy-clay nanocomposites was also studied.

4.2 Materials and Methods

4.2.1 Silane treatment of the inorganic phase

Each of the silane coupling agents (3-aminopropyltriethoxysilane (APTES), 3-glycidyloxypropyltrimethoxysilane (GPTMS)) was hydrolyzed in a solvent to form silanol. The silane treatment of glass fibers was then carried out as discussed in section 2.3.1. The silane treatment of clay minerals was performed using the following two methods:

Method 1

5g of Cloisite® 15A was put into the hydrolyzed silane solution and dispersed into the solution by ultrasonic mixing and homogenizing as discussed in section 2.3.2. The amount of silane required was calculated using an empirical formula. The silylated clay minerals were extracted by vacuum filtration and dried at 110 ºC for 1 h. The clay minerals were then stored in a vacuum desiccator.

Method 2

5g of Cloisite® 15A was immersed in a dilute solution containing different quantities of silanes. The amount of silane coupling agents (SCAs) used was 0.1X, 0.5X, 2X, and 4X, where X is the weight of clay mineral. Further, the Cloisite® 15A was nano-dispersed in silane solution by using a high shear homogenizer operated at 12,000 rpm for 3 min and ultrasonic mixing using a probe sonicator operated at an amplitude of 80% for 10 min. The solvent was then removed using a Heidolph rotary evaporator. The modified clay minerals were washed twice with the solvent used for hydrolysis to remove soluble homo condensates. Clay minerals were further dried in a vacuum oven at 60°C for 48 h. Clay minerals were ground using a pestle mortar and then heat treated for 15 min at 120 ºC before use. Figure 4.1 shows the Cloisite® 15A modified with silane coupling agent: APTES or GPTMS and the amount of silane is mentioned in parentheses. The clay minerals were observed to be coated with 0.1X silane solutions. Whereas at higher quantities of silane coupling agents, i.e. 4X, the clay minerals had clustered in a complex manner and were hard from outside and sticky from inside. It was not possible to grind it into very fine powder and thus the silylated clay minerals, APS C15(4) and GPS C15(4) were dispersed into epoxy by grinding to the smallest possible size.

4.2.2 Dispersing clay minerals in epoxy

2 phr of clay minerals were added to the epoxy resin and was mixed using a glass rod for 5 min. A high shear homogenizer operated at 20000 rpm was then used for breaking agglomerates of clay minerals into small sizes and mixing it uniformly in epoxy resin. The ultrasonic mixing was performed for 5 min, using an ultrasonic probe operating at an amplitude of 80%. The homogenization and ultrasonic mixing were repeated before the mixture was placed in a vacuum desiccator for degassing for 1h.

Figure 4.1 Clay minerals after silane treatment as a function of concentration of silanes in solution

4.2.3 Manufacturing fiber reinforced epoxy-clay nanocomposites

The epoxy resin and hardener were mixed in a stoichiometric ratio of 100: 31. After mixing, the epoxy resin containing clay minerals was poured onto fiber mats ensuring that it wets the fibers. The laminate was then sealed using a vacuum bag and vacuum was applied to create pressure on the laminate. A vacuum of about 1 MPa was maintained for 180 min till the gelation of epoxy. Curing was performed as per the schedule specified by the manufacturer, i.e. heating the laminate for 7 h at a temperature of 70 ºC, on the mould. The mould temperature was controlled by a proportional–integral–derivative controller and all the nanocomposites were cured using the same curing schedule. The fiber reinforced laminate was cut using a high-speed cutter to prepare the specimen for tensile and bending tests.

4.3 Results and Discussions

4.3.1 Effect of silane treatment of glass fibers and clay minerals

The tensile and flexural properties of composites incorporating silylated Cloisite® 15A and glass fibers woven roving surface treated with different silane coupling agents are shown in Figures 4.2 and 4.3. The tensile modulus and tensile strength of glass fiber reinforced epoxy-clay nanocomposites denoted by C15GFRC were comparable with both APTES treated glass fiber epoxy-clay nanocomposite, C15 AGFRC, and GPTMS treated glass fiber epoxy-clay nanocomposites, C15 GGFRC. The tensile stress vs. elongation curve of the representative specimens is shown in Figure 4.6. The flexural modulus and flexural strength of C15 AGFRC improved significantly by 38% and 76%, respectively in comparison to C15GFRC (Figure 4.3). The tensile and flexural properties of fiber reinforced epoxy-clay nanocomposites containing silane treated glass fibers and silane treated Cloisite® 15A are shown in Table 4.1

Table 4.1 Tensile of flexural properties of nanocomposites incorporating silane treated glass fibers and clay minerals

Material code	Tensile modulus, GPa	Tensile strength, MPa	Elongation at break, %	Flexural modulus, GPa	Flexural strength, MPa
GFRC	8.3 ± 0.16	313 ± 12	4.2 ± 0.3	10.2 ± 0.17	235 ± 18
C15GFRC(PC3)	9.2 ± 0.65	348 ± 7	5.6 ± 0.15	12.3 ± 1.05	262 ± 6
C15 AGFRC	8.5 ± 0.15	369 ± 21	4.7 ± 0.15	17.0 ± 0.8	461 ± 13
C15 GGFRC	8.2 ± 0.15	329 ± 20	4.6 ± 0.28	14.6 ± 0.9	422 ± 32
AC15 AGFRC	7.8 ± 0.1	374 ± 45	5.5 ± 0.64	18.7 ± 0.9	386 ± 33
GC15 AGFRC	8.3 ± 0.1	356 ± 38	4.8 ± 0.4	17.0 ± 1.0	502 ± 37
AC15 GGFRC	6.9 ± 0.2	288 ± 5	4.5 ± 0.25	14.0 ± 0.4	325 ± 18
GC15 GGFRC	8.0 ± 0.2	290 ± 31	4.1 ± 0.44	15.5 ± 1.0	443 ± 22

In the case of C15 GGFRC, incorporating glass fibers surface modified using GPTMS, the flexural modulus and flexural strength increased by 18% and 61%, respectively. The increase in flexural properties can be attributed to improved adhesion between glass fibers and epoxy matrix and has been reported by other researchers also for glass fiber reinforced-

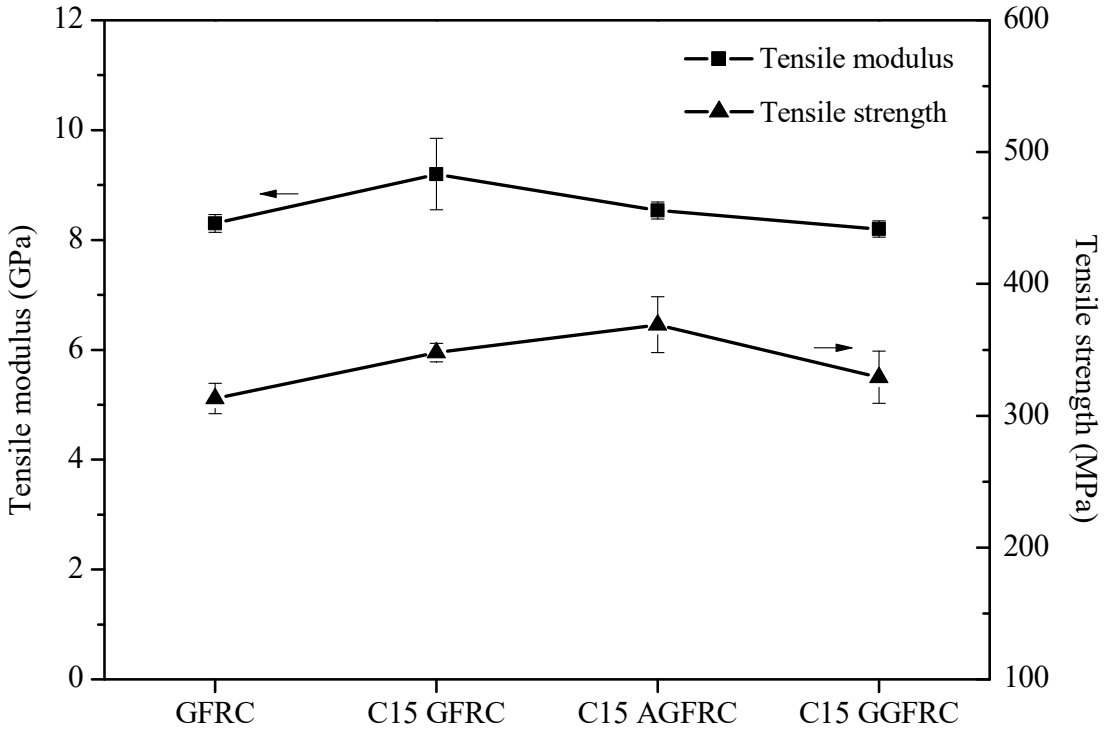

Figure 4.2 Tensile properties of neat epoxy - glass fiber reinforced composites and Cloisite® 15A modified epoxy - glass fiber reinforced composites

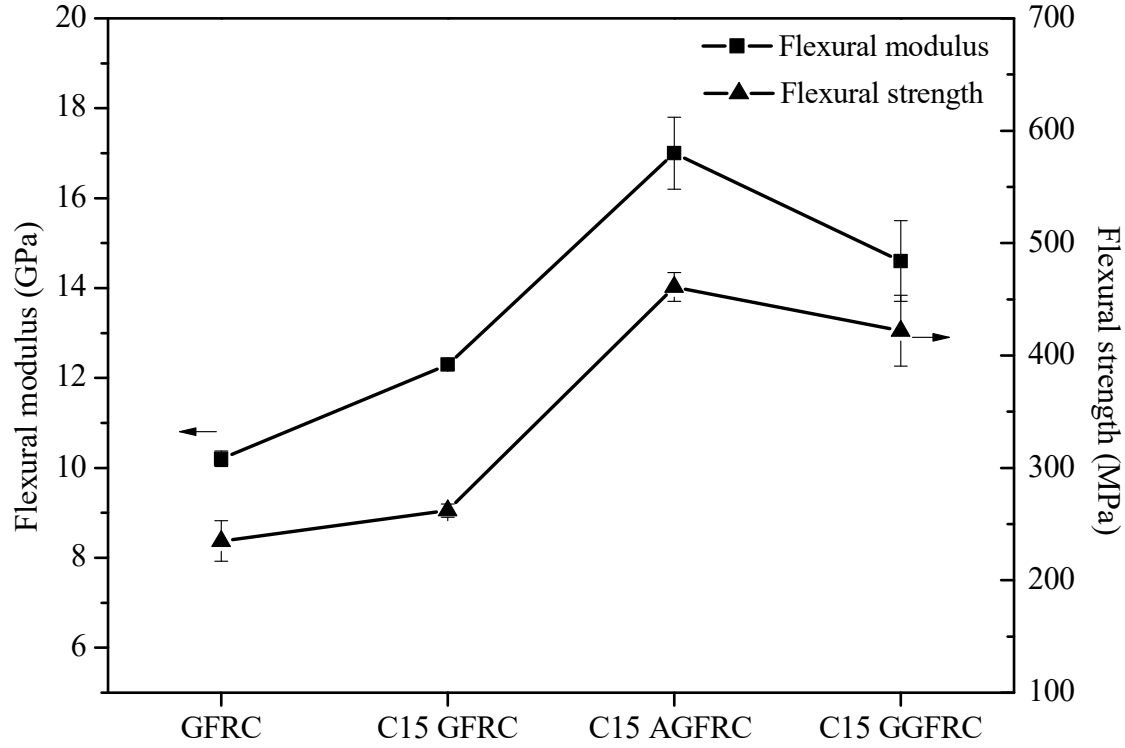

Figure 4.3 Flexural properties of neat epoxy - glass fiber reinforced composites and Cloisite® 15A modified epoxy - glass fiber reinforced composites

polymer composites (Iglesias et al., 2002; Park and Jang, 2004; Sever et al., 2008; Shokoohi et al., 2008; Xie et al., 2010). Surprisingly, the incorporation of silylated clay minerals did not show improvements in tensile and flexural properties of silane treated glass fiber composites as compared to silane treated glass fiber-untreated Cloisite® 15A based nanocomposites. Referring to Figure 4.4 (a), the tensile modulus and tensile strength of Cloisite® 15A based nanocomposite, C15AGFRC (APTES treated glass fiber epoxy-clay nanocomposite) were 8.5 GPa and 369 MPa, respectively. In the case of GPTMS treated glass fiber epoxy-clay nanocomposites (C15 GGFRC), the tensile modulus and tensile strength were 8.2 GPa and 329 MPa, respectively. The tensile modulus and tensile strength of APTES treated clay minerals in GPTMS treated glass fiber composites (AC15 GGFRC) were approximately same within the reproducibility limits for comparisons, as shown in Figure 4.4(b). The tensile properties of composites incorporating GPTMS treated clay minerals the (GC15 GGFRC) were also approximately same as C15 GGFRC. The flexural modulus of Cloisite® 15A based nanocomposites with APTES treated glass fibers and GPTMS treated glass fibers were 17 GPa and 14.64 GPa, respectively. The flexural modulus values remained unchanged on the incorporation of silane treated clay minerals. The flexural strength of Cloisite® 15A based nanocomposites with APTES treated glass fibers and GPTMS treated glass fibers were 462 MPa and 422 MPa, respectively. An incorporation of APTES treated clay minerals in both the APTES treated glass fiber composites and GPTMS treated glass fiber composites led to a decrease in flexural strength (16% in case of AC15 AGFRC and 22% in case of AC15 GGFRC) of composites as shown in Figures 4.5(a) and 4.5(b). The tensile and flexural properties of treated glass fiber reinforced composites decreased with the incorporation of silylated clay minerals. There can be two possible reasons: the insufficient amount of silane and clustering of clay minerals after silylation. A successful hydrophobic silane coating must eliminate hydroxyl groups available on montmorillonite to make it hydrophobic. The factors which contribute to the ability of silane to form a hydrophobic coating are its functional groups, the extent of surface coverage, the residual unreacted groups and the distribution of silane on the surface (Arkles et al., 2009; Ishida, 1984; Kim and Mai, 1998). Therefore, the amount of silane grafted on the clay minerals would influence the morphology of clay minerals in nanocomposites. The resulting nanocomposite will exhibit higher mechanical properties because of intercalation/exfoliation of clay minerals in the polymer matrix. Chen and Yoon, 2005 had studied the effect of silane modification of three

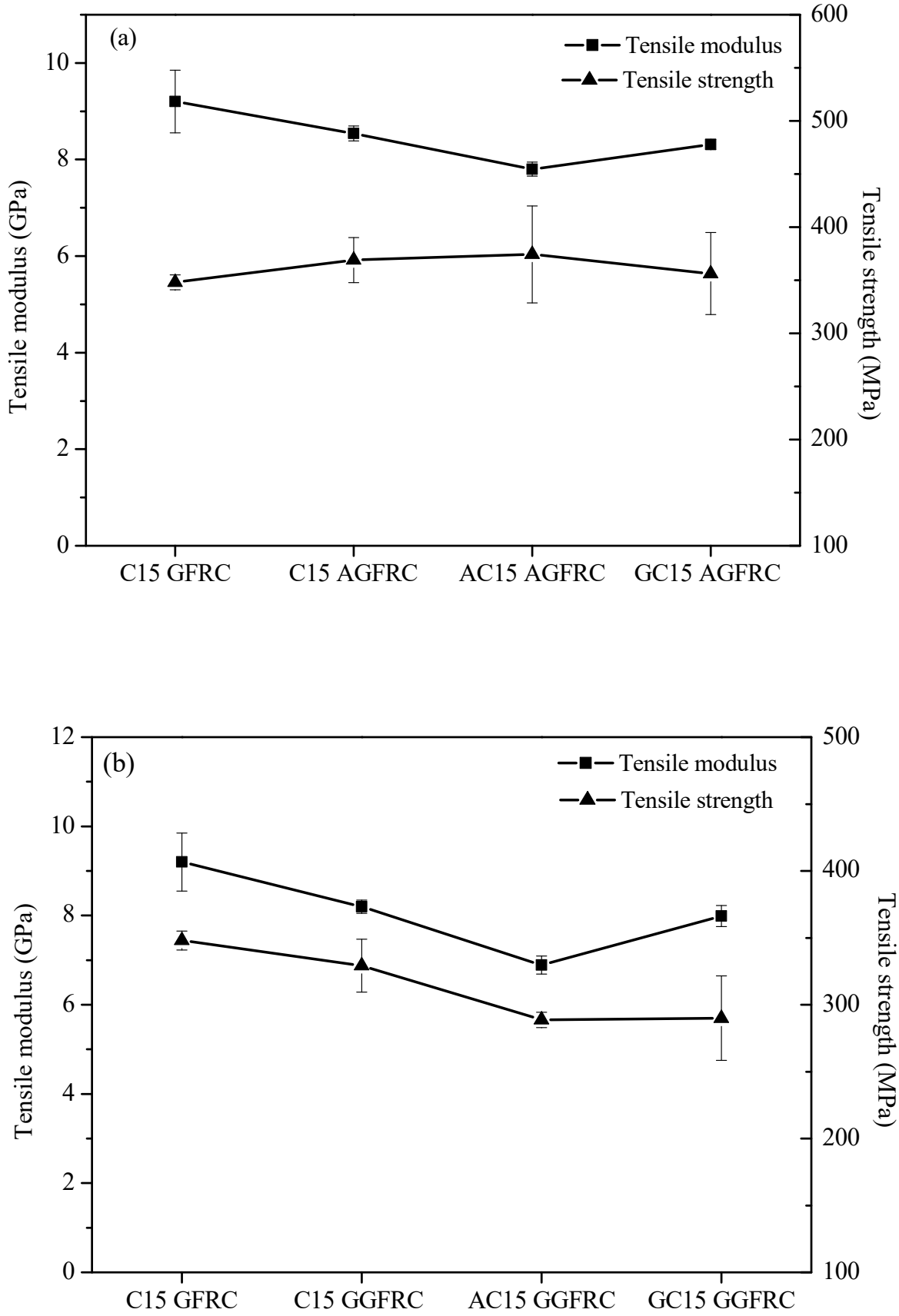

Figure 4.4 Tensile properties of silane treated glass fiber reinforced composites incorporating (a) APTES treated clay minerals and (b) GPTMS treated clay minerals

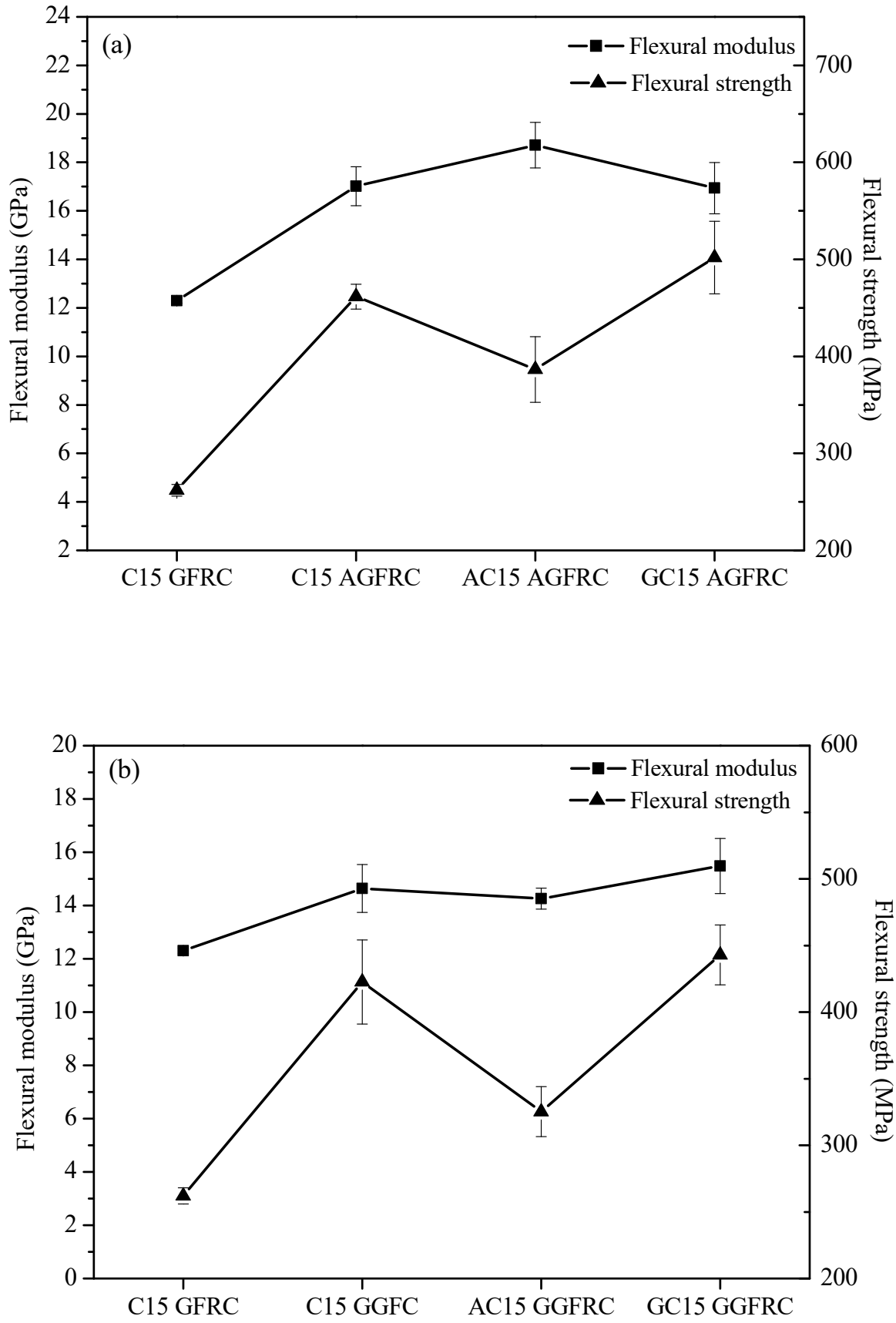

Figure 4.5 Flexural properties of silane treated glass fiber reinforced composites incorporating (a) APTES treated clay minerals and (b) GPTMS treated clay minerals

types of organically modified clays: Cloisite® 15A, Cloisite® 20A and Cloisite® 30B on properties of poly(L-lactide) clay nanocomposites. It is interesting to note that an exfoliated morphology was obtained only in nanocomposites containing silane treated clay minerals. Higher grafting of silane on clays resulted in better dispersion and a higher degree of exfoliation of the clays in poly(L-lactide) matrix.

The silylated clay minerals after drying had formed small clusters. In the case of fiber reinforced nanocomposites based on APTES treated clay minerals, a decrease in mechanical properties can be attributed to visibly poor dispersion of clay minerals. Therefore, the silylated clay minerals should be crushed to a fine powder before mixing in epoxy resin. Thus, further experiments were conducted to investigate the morphology, extent of curing and morphology of fiber reinforced epoxy nanocomposites containing Cloisite® 15A surface modified using different amounts of silane coupling agents, e.g. 0.1X, 0.5X, 2X and 4X. The silylation was carried out using Method 2 described in section 4.2.1 in this report.

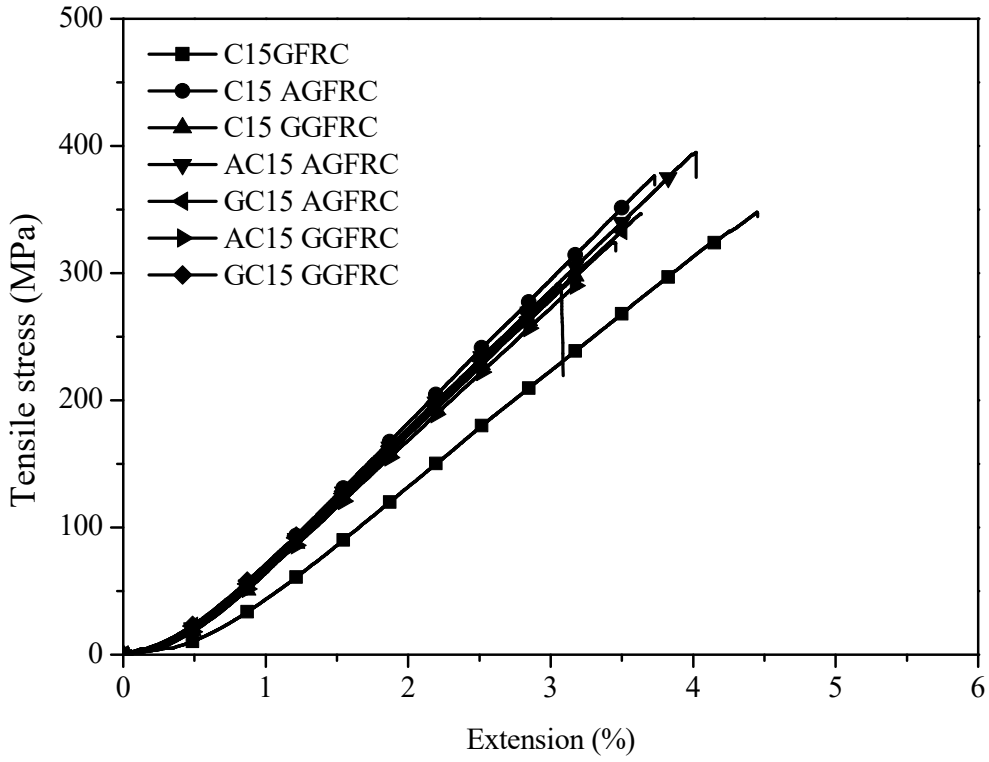

Figure 4.6 Tensile stress vs elongation curves for representative composites

4.3.2 Silane treatment of clay minerals using different quantities of silane coupling agents

4.3.2.1 Characterization of clay minerals

FTIR spectroscopy was used to verify the grafting of silanes on clay minerals. FTIR spectroscopy has been widely used to investigate the adsorption of silanes on silicates. Figure

4.7 shows the FTIR spectra of Cloisite® 15A, 3-glycidyloxypropyltrimethoxysilane treated Cloisite® 15A and 3-aminopropyltriethoxysilane treated Cloisite® 15A at different concentrations (given in parentheses).

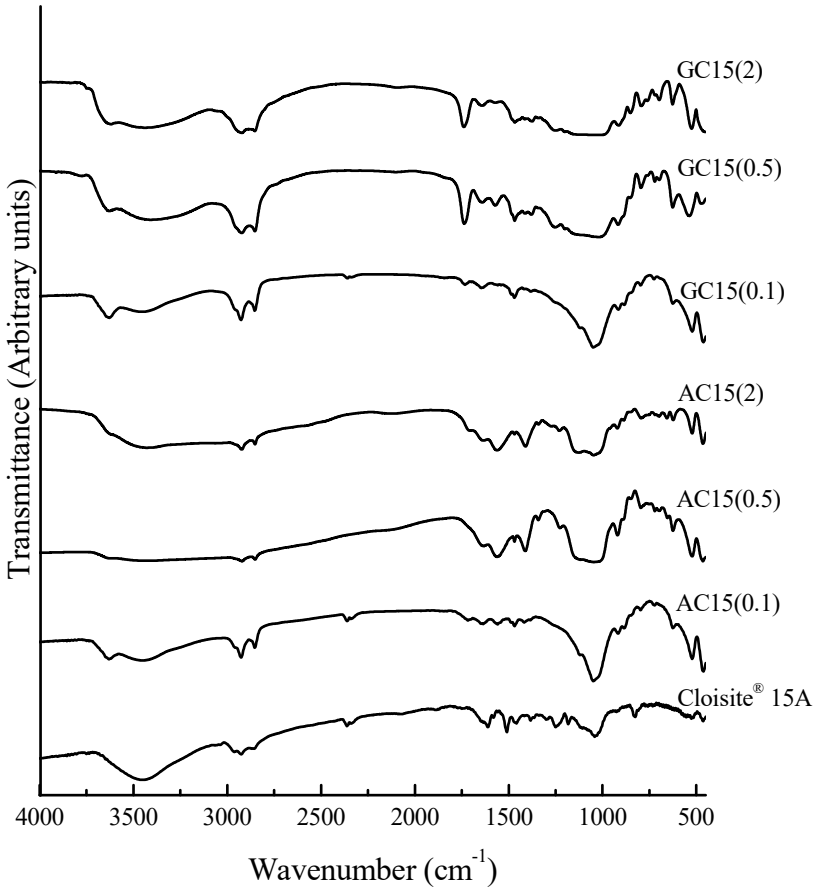

Figure 4.7 FTIR spectra of Cloisite® 15A and silane modified Cloisite® 15A

The assignment of peaks was done taking a cue from the literature. In FTIR spectra of Cloisite® 15A, the band at 3460 cm^{-1} was assigned to a hydroxyl group and H- bonded OH stretch. The bands located at 2930 cm^{-1} and 2842 cm^{-1} were due to the –CH asymmetric and symmetric stretching of $–CH_2$ groups from the chemical structure of surfactant. The surface modification of organoclay was evident from the appearance of a very strong band at 1047 cm^{-1} which was assigned to the Si–O –Si stretch in silane modified clays. The peak at 3638 cm^{-1} was assigned to Si-OH hydroxyl stretching in clays modified using 0.1X silane. Also, bands at 2930 cm^{-1} and 2850 cm^{-1} in modified clays had become more pronounced after modification of clay mineral surface with silane coupling agents. When the concentration of silane was increased, two effects were observed (i) The band at 1047 cm^{-1} became broader and more complex which indicated that Si-O-Si chains have become longer or branched, and (ii) The decrease in peak

intensity at 3638 cm^{-1}, which could be attributed to the hydrogen bonding interaction between the hydrolyzed silanes and –OH groups available in clay. This peak had reached an asymptotic value of intensity in the case of APTES treated clay minerals with 0.5X and 2X silane concentration indicating utilization of all –OH available on clay mineral surface.

4.3.2.2 Mechanical properties of fiber reinforced composites incorporating silylated clay minerals

The results obtained for fiber reinforced epoxy-clay nanocomposites are summarized in this section. The terminology used for these nanocomposites is indicated on the X-axis, and it consists of the symbol of clay mineral/ silylated clay mineral followed by the concentration of silane in parentheses and an abbreviation GFRC. The tensile modulus and tensile strength of C15GFRC were 9.2 GPa and 349 MPa respectively. The tensile modulus and tensile strength (Figure 4.8) decreased when silylated clay minerals AC15(0.1), GC15(0.1), AC15(0.5), GC15(0.5), AC15(4), GC15 (4) were used in glass fiber reinforced epoxy composites. But there were exceptions also, with the addition of AC15(2) and GC15(2) the tensile modulus has increased marginally but the tensile strength had increased by 11% and 8.5%, respectively. This increase can be explained by the morphology of nanocomposites, improved adhesion between the silane treated clay and epoxy, and curing reaction. The AC15(2)GFRC and GC15(2)GFRC samples had exfoliated morphology, in which clay mineral layers were randomly oriented and separated and thus an enormously large surface area was available for polymer/filler interaction. This increased the effectiveness of stress transfer between clay minerals and epoxy matrix.

Secondly, the functional groups available in silanes can potentially interact with inorganic clay minerals and epoxy resin individually thus forming a network between clay, silane, and epoxy, which improves the adhesion between clay minerals and epoxy matrix. The third reason for an increase in properties was related to increase of the extent of curing and the crosslinking density of epoxy. This increased the mechanical properties of nanocomposites. Figure 4.9 shows the stress vs. percent elongation curves of nanocomposites, high values of percentage elongation before failure were observed for AC15(2)GFRC and GC15(2)GFRC, whereas all other nanocomposites broke in a brittle fashion like AC15(0.5)GFRC and GC15(0.5)GFRC. This is clear evidence of improved adhesion between clay minerals and epoxy in AC15(2)GFRC and GC15(2)GFRC compositions. The flexural test results were in line with these findings and both flexural modulus and flexural strength improved with an addition of clay minerals treated with 2X silane as shown in Figure 4.10. The decrease in tensile modulus,

tensile strength, flexural modulus and flexural strength of AC15(0.1)GFRC, GC15(0.1)GFRC, AC15(0.5)GFRC, GC15(0.5)GFRC may be due to insufficient concentration of silanes, which could not cover the enormously large surface area (m^2/g) produced by nanodispersion of clay minerals in hydrolyzed silanes or incomplete curing of epoxy. Vennerberg et al., 2014 have also reported a decrease in tensile modulus and tensile strength of multiwalled carbon nanotubes (MWCNT) epoxy nanocomposites when silane functionalization of MWCNT was carried out with 0.1 wt%, 0.5 wt% and 1 wt% concentration of silanes.

In the case of AC15(4)GFRC, GC15(4)GFRC visually poor dispersion of silylated clay minerals in epoxy resin was observed, because of sedimentation of clay during processing that led to reduced strength of composites. But, treatment of clay minerals with a high concentration of silanes in solution, did not improve the mechanical properties of nanocomposites. The flexural strength and flexural modulus of nanocomposites incorporating 4 wt% of silane concentration were lowest in comparison to other compositions. The possible reason for this may be a high agglomeration of clay minerals in epoxy. To investigate the silylation effect on the mechanical properties of nanocomposites, the morphology (TEM), the degree of clay dispersion (SAXS) and thermal behavior (DSC) were studied.

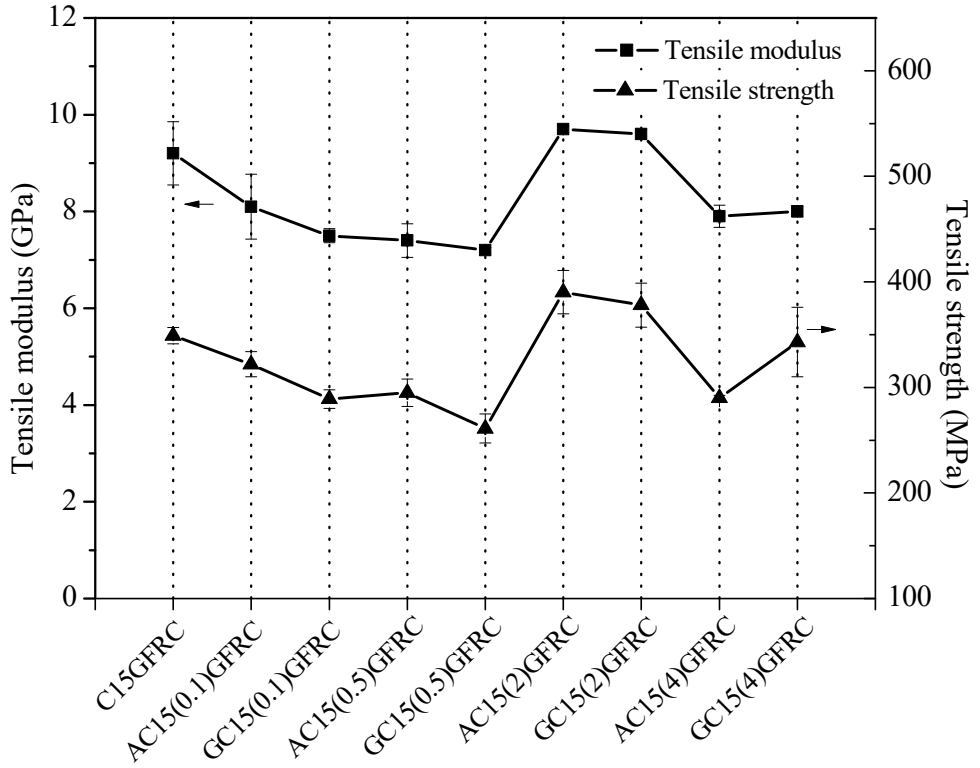

Figure 4.8 Effect of clay modification on tensile properties

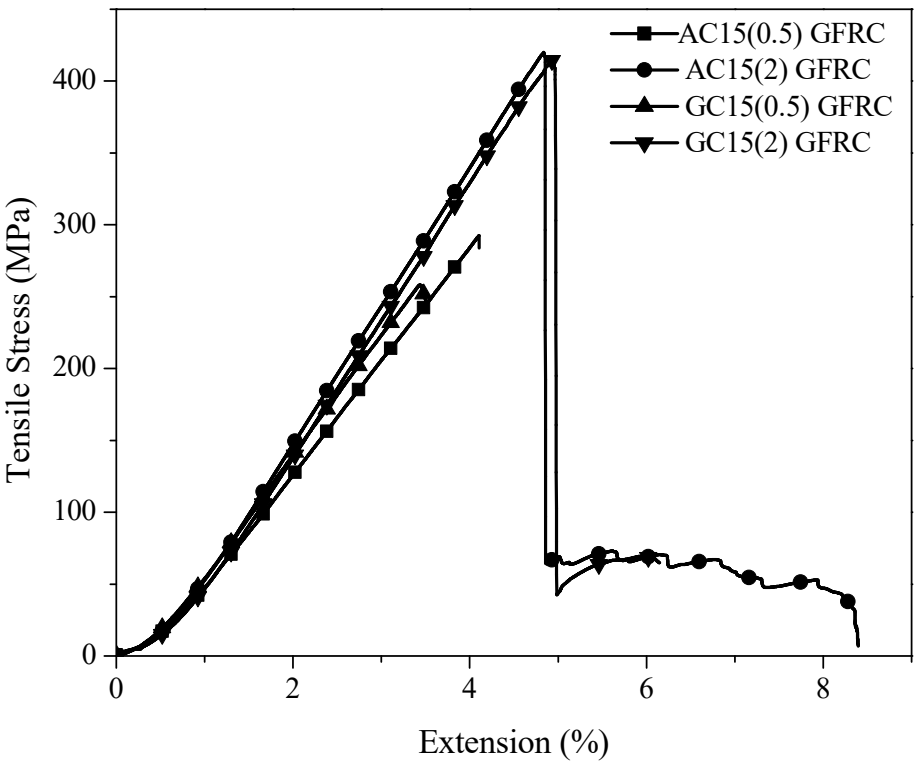

Figure 4.9 Percentage elongation before failure for nanocomposites

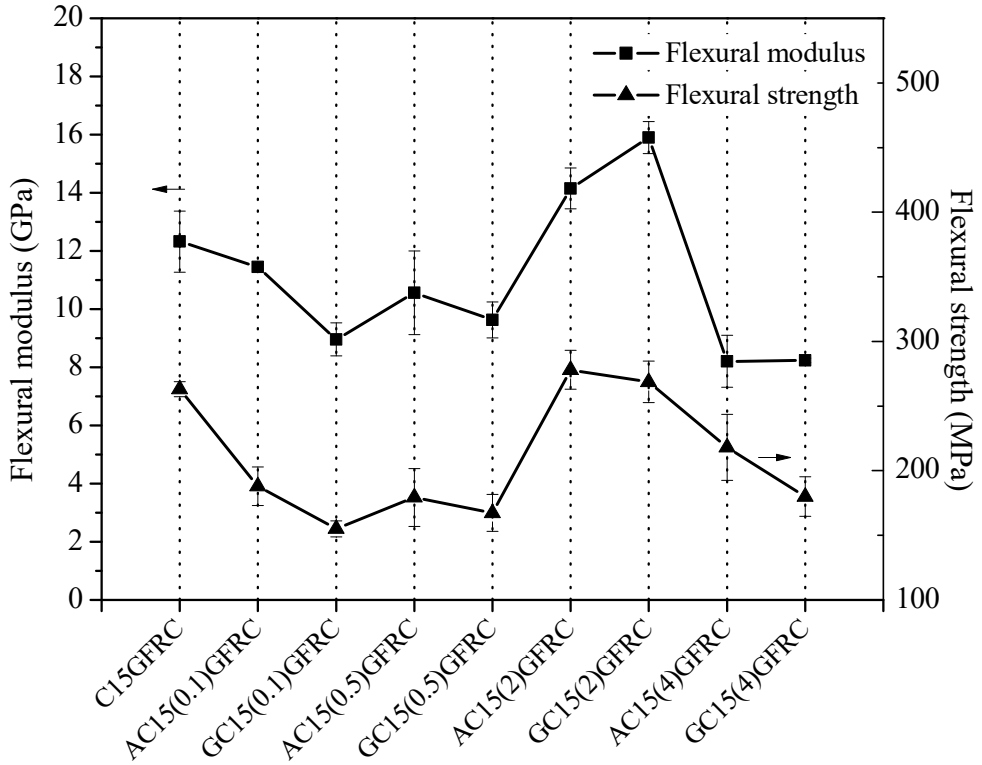

Figure 4.10 Effect of clay modification on flexural properties

4.3.2.3 Morphology of glass fiber reinforced composites

Small angle X-ray spectra (Figure 4.11) revealed the changes in the interlayer spacing of Cloisite® 15A in fiber reinforced epoxy-clay nanocomposites. The characteristic peak of Cloisite® 15A at $2\theta = 2.41°$ corresponding to d-spacing, d_{001}, of 3.65 nm shifted to lower angles indicating an increase in d_{001} spacing of Cloisite® 15A in epoxy. Two diffraction peaks at values $2\theta = 1.22°$ and $2\theta = 1.49°$ corresponding to d-spacing of 7.23 nm and 5.91 nm respectively, were observed for nanocomposite containing unmodified clay, i.e. without silane treatment. It was significant that for all fiber reinforced epoxy nanocomposites which contain silane modified clays no peak was visible in this small-angle region, confirming that clay was exfoliated.

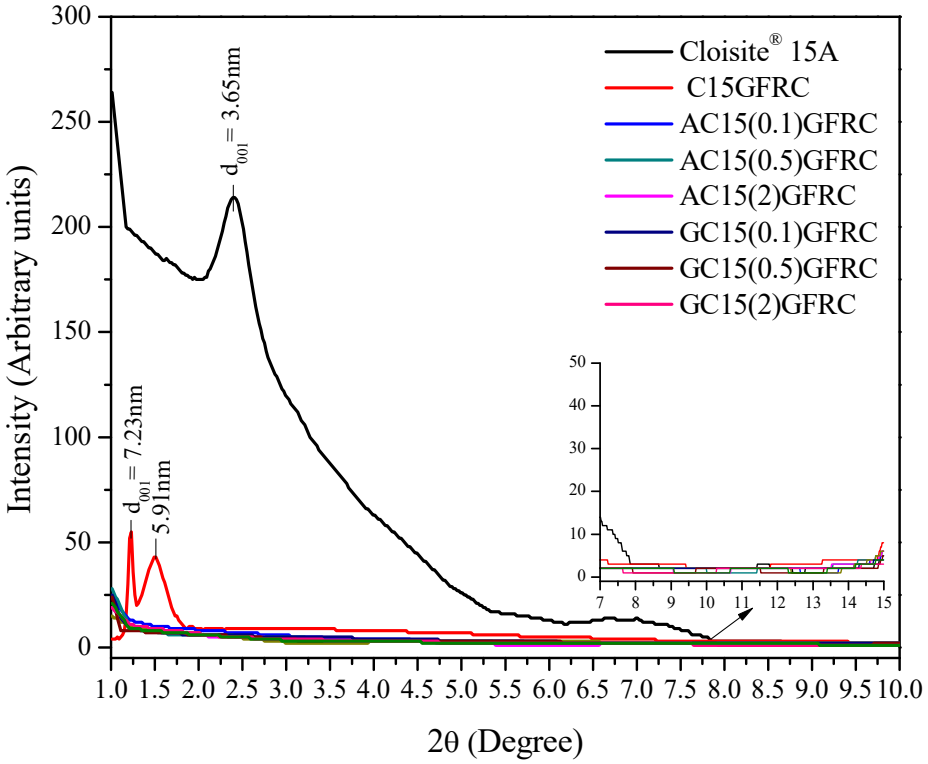

Figure 4.11 Small angle X-ray scattering of C15GFRC, AC15(0.1)GFRC, AC15(0.5)GFRC, AC15(2)GFRC and GC15 (0.1)GFRC, GC15(0.5)GFRC, GC15(2)GFRC

TEM of C15GFRC showed that the clay platelets had been sheared off during processing of nanocomposites. In some regions, clay layers were pushed to a basal distance of 8.81nm implying exfoliation, but largely an intercalated structure is seen as shown in Figure 4.12. The TEM of AC15 (2)GFRC and GC15(2)GFRC (Figure 4.13) confirms that the clay mineral layers were mainly exfoliated and the layers were scattered randomly. Exfoliation of clay is one of

the main requirements to achieve better mechanical properties of clay nanocomposites, and the same has been observed in the present study.

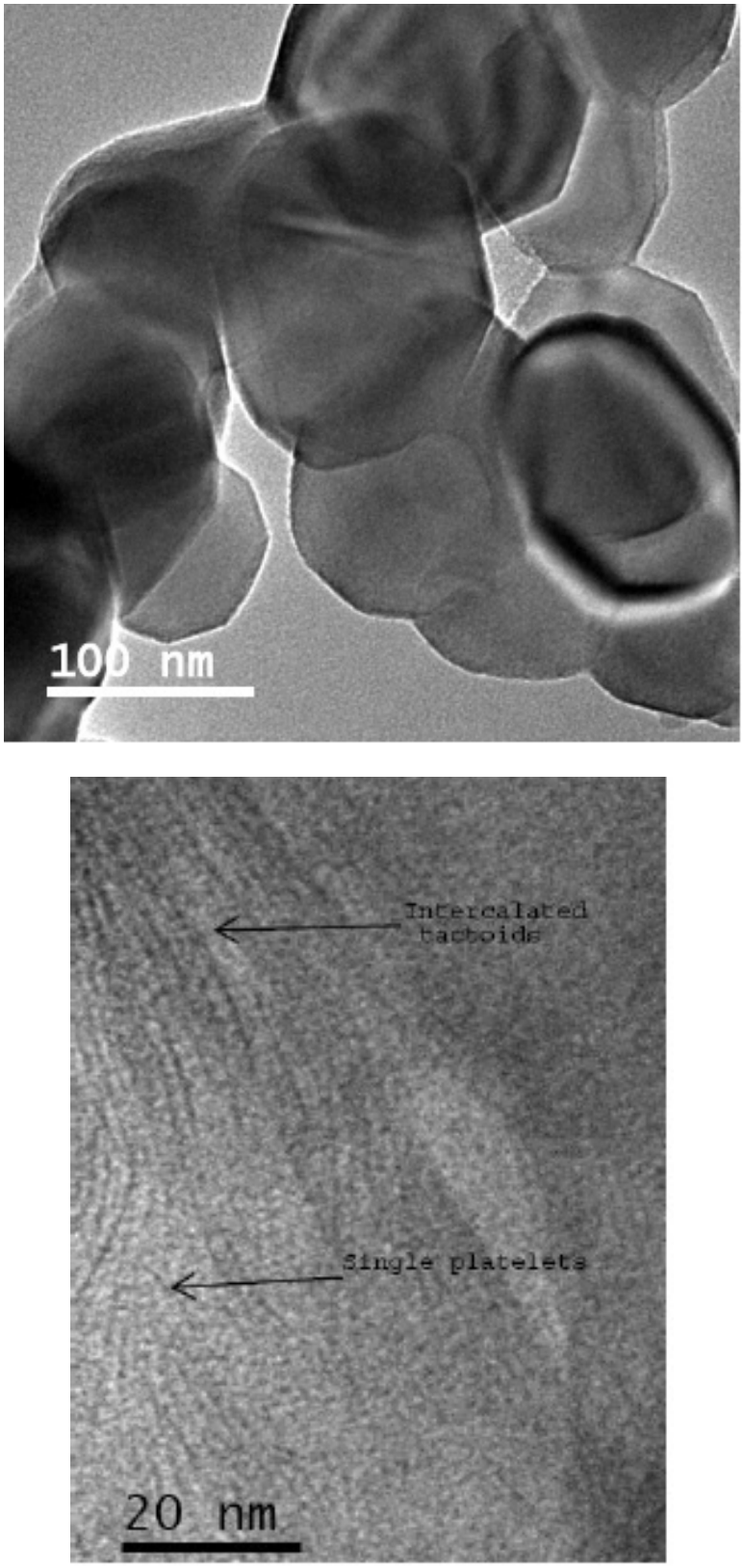

Figure 4. 12 Transmission electron micrographs of C15GFRC at different magnifications

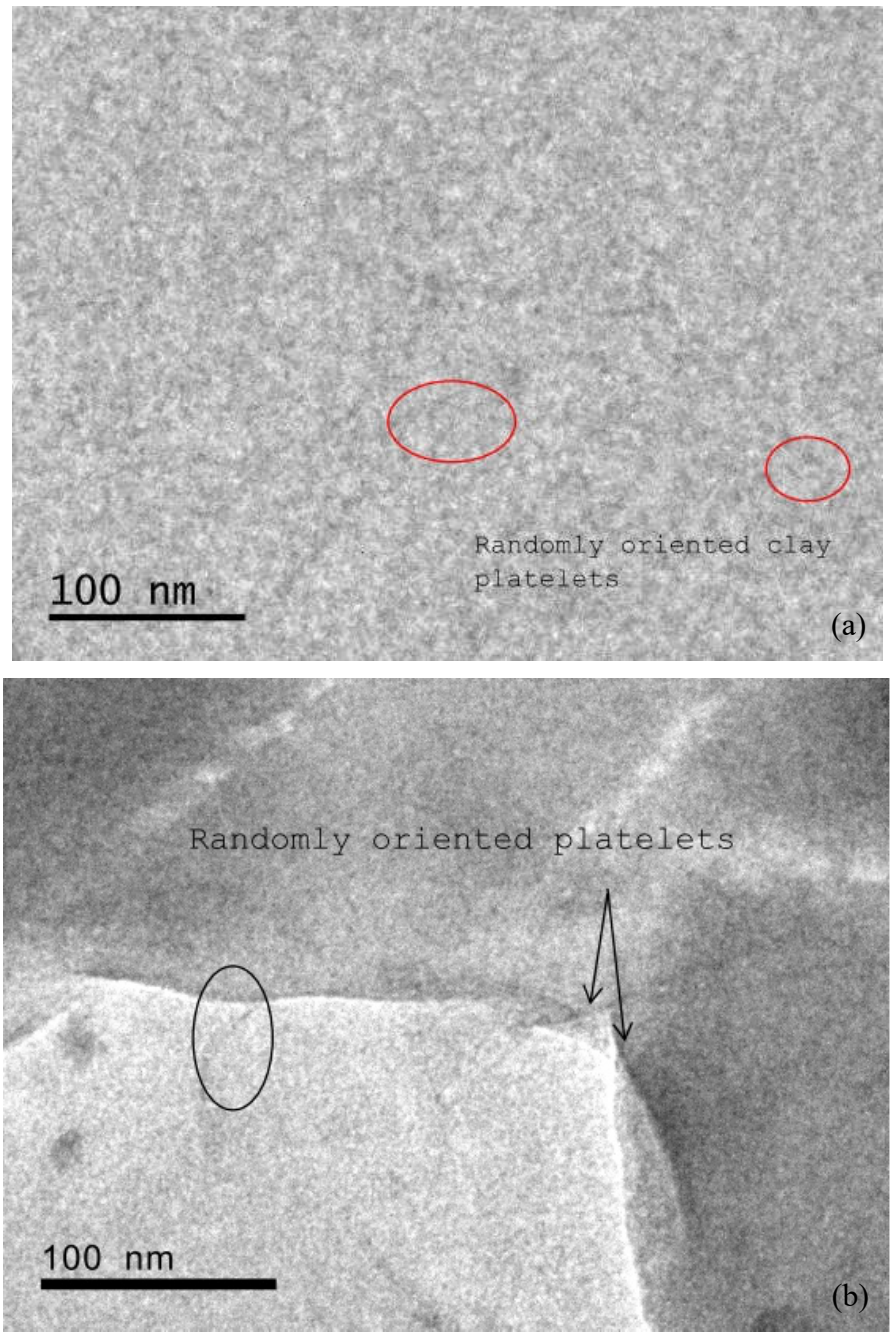

Figure 4.13 Transmission electron micrographs of (a) AC15(2)GFRC and (b) GC15(2)GFRC

4.3.2.4 Thermal transitions and curing

The DSC analysis revealed that the nanocomposites which showed a decrease in mechanical properties were under-cured. Some researchers (Lu and Nutt, 2003a, 2003b; Ngo et al., 2007) have annealed the samples before the heating cycle in DSC. This is done to remove the variations in thermal history of samples during curing and to cure the partially cured samples completely. In the present study, the samples were not preheated before DSC scans because the variations in thermal history of fiber reinforced epoxy-clay nanocomposites were not expected as the mould temperature was controlled by a proportional–integral–derivative controller and all the nanocomposites were cured using same curing schedule.

In DSC scans, each sample was heated to 300°C from room temperature under nitrogen flow in an aluminium pan. The samples were then cooled down to -4°C at a cooling rate of 10°C/min. The heating and cooling scans were repeated thrice. The DSC thermograms of 2nd and 3rd heat scans of C15GFRC were identical as can be seen in Figure 4.14. Although T_g had increased from 87 to 90°C, but there is no residual curing exotherm observed. Therefore only two scans were conducted on the remaining samples. The DSC curves of the first two heating scans are shown in Figures 4.15 and 4.16. The first heating scan gave important information about thermal properties of nanocomposites. The glass transition temperatures (T_g) of nanocomposites: AC15(2)GFRC, AC15(4)GFRC, GC15(2)GFRC and GC15(4)GFRC were higher than that of C15GFRC which indicate better curing. But other compositions had lower values of glass transition temperatures than that of C15GFRC indicating lower extent of cure as compared to C15GFRC. To investigate the enthalpy relaxation peak in DSC, many researchers (Hutchinson et al., 1996; Morancho and Salla, 1999; Ngo et al., 2007; Piscitelli et al., 2012) have performed different heating and cooling rate experiments. The enthalpy relaxation is the shaded region between the first and second DSC curves (Morancho and Salla, 1999) during heating scans as shown in Figure 4.17. The enthalpy relaxation was observed to be superimposed over the glass transition, but the change in slope was sufficient to represent glass transition The higher enthalpy relaxation to reach the equilibrium state exhibited by AC15(0.1)GFRC, AC15 (0.5)GFRC, GC15(0.1)GFRC and GC15(0.5)GFRC may be attributed to incomplete curing reactions (Hutchinson et al., 1996; Lu and Nutt, 2003a). During the second scan, the glass transition temperature of all the nanocomposites had shifted to a higher temperature. The changes in glass transition temperature are shown in Table 4.2.

Table 4.2 Glass transition temperatures (°C)

Composition	Heating cycle 1	Heating cycle 2
C15GFRC	77	87
AC15(0.1)GFRC	70	82
AC15(0.5)GFRC	69	83
AC15(2)GFRC	83	84
AC15(4)GFRC	83	86
GC15(0.1)GFRC	68	89
GC15(0.5)GFRC	69	82
GC15(2)GFRC	81	89
GC15(4)GFRC	90	90

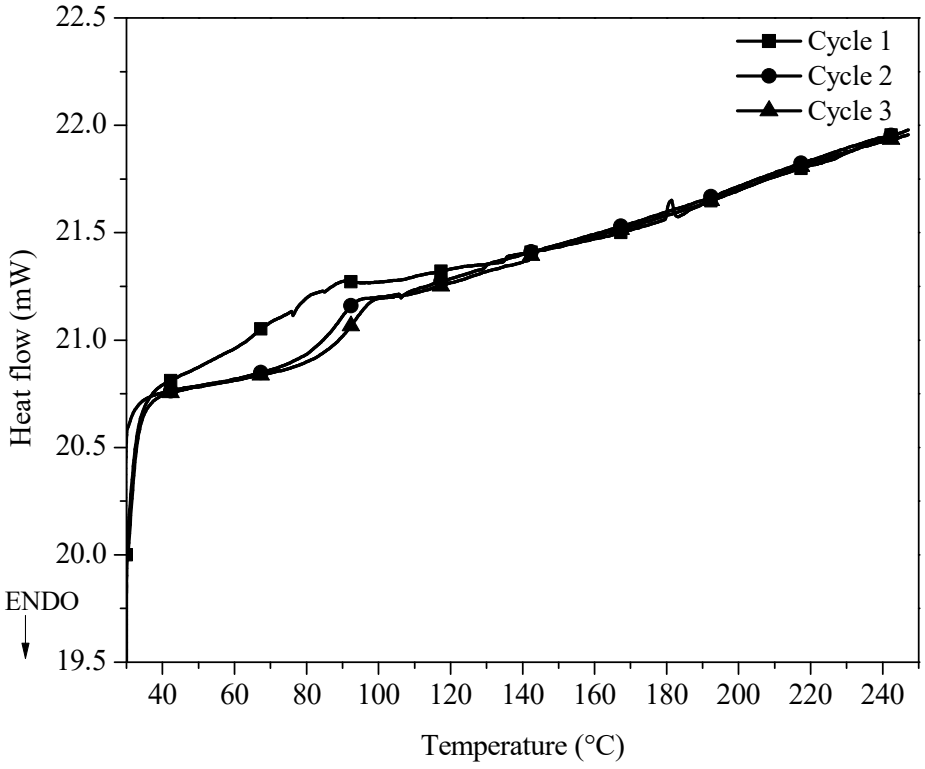

Figure 4.14 DSC curves of C15GFRC

The exotherm in the DSC (inset in Figure 4.18) gave information on the heat of cure of fiber reinforced epoxy-clay nanocomposites. The heat of curing becomes smaller as the resin becomes more cross-linked and it becomes undetectable if the resin is fully cured. The increased crosslinking density results in an increase in T_g and also the mechanical properties of epoxy composites. AC15(2)GFRC, AC15(4)GFRC, GC15(2)GFRC, GC15(4)GFRC, C15GFRC showed reduced heat of curing, which indicates increased cross-linking in an epoxy matrix. In a recent study, Shanmugharaj and Ryu, 2012 have reported a slight drop in peak exotherm in DSC, conducted at different heating rates, attributed to the increased degree of cure in nanocomposites containing silane modified clay in comparison to pristine epoxy-clay nanocomposites. Also, the exotherm profile and the heat of reaction were same irrespective of different heating rates.

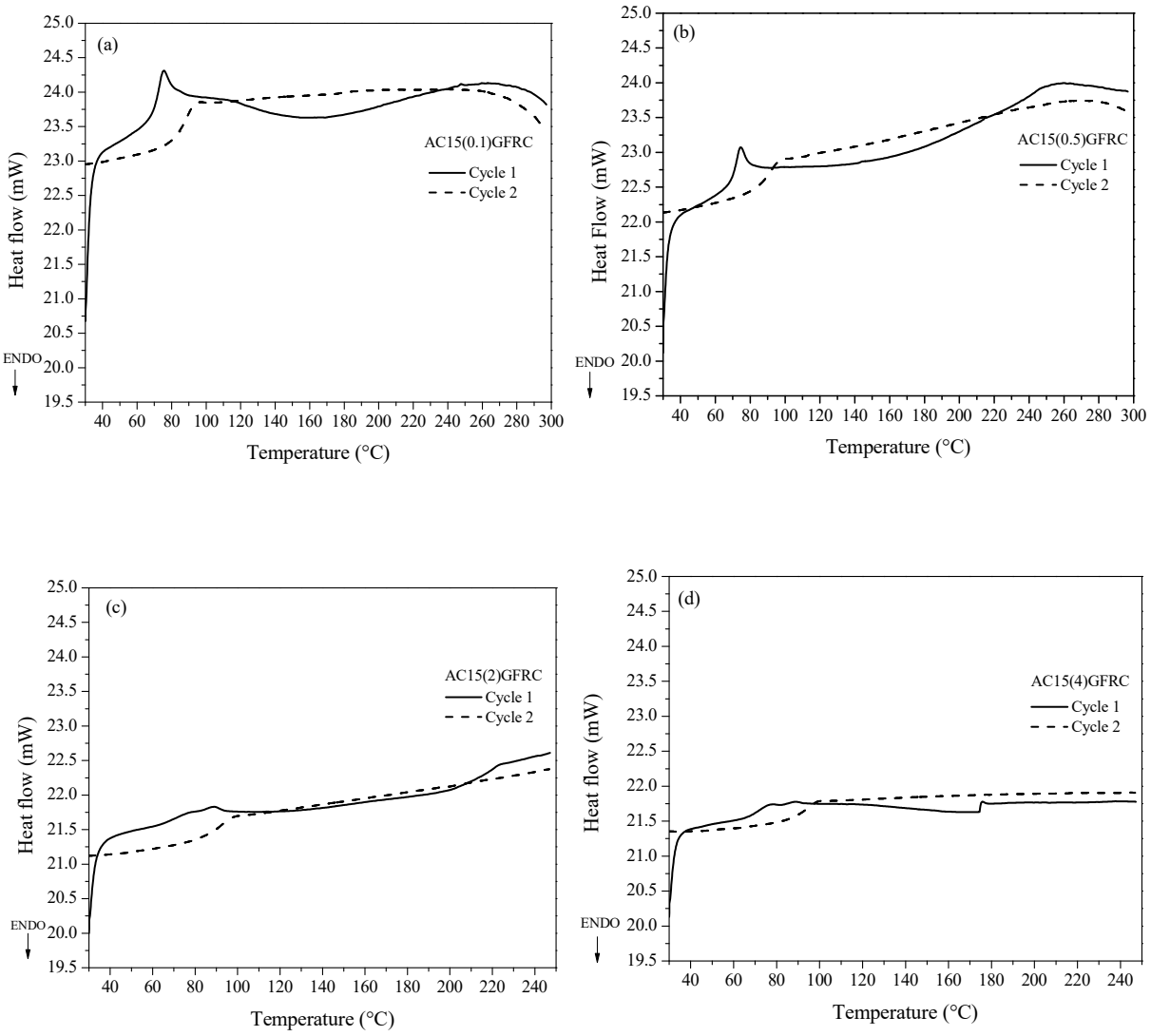

Figure 4.15 DSC traces of (a) AC15(0.1)GFRC, (b) AC15(0.5)GFRC, (c) AC15(2)GFRC, (d) AC15(4)GFRC

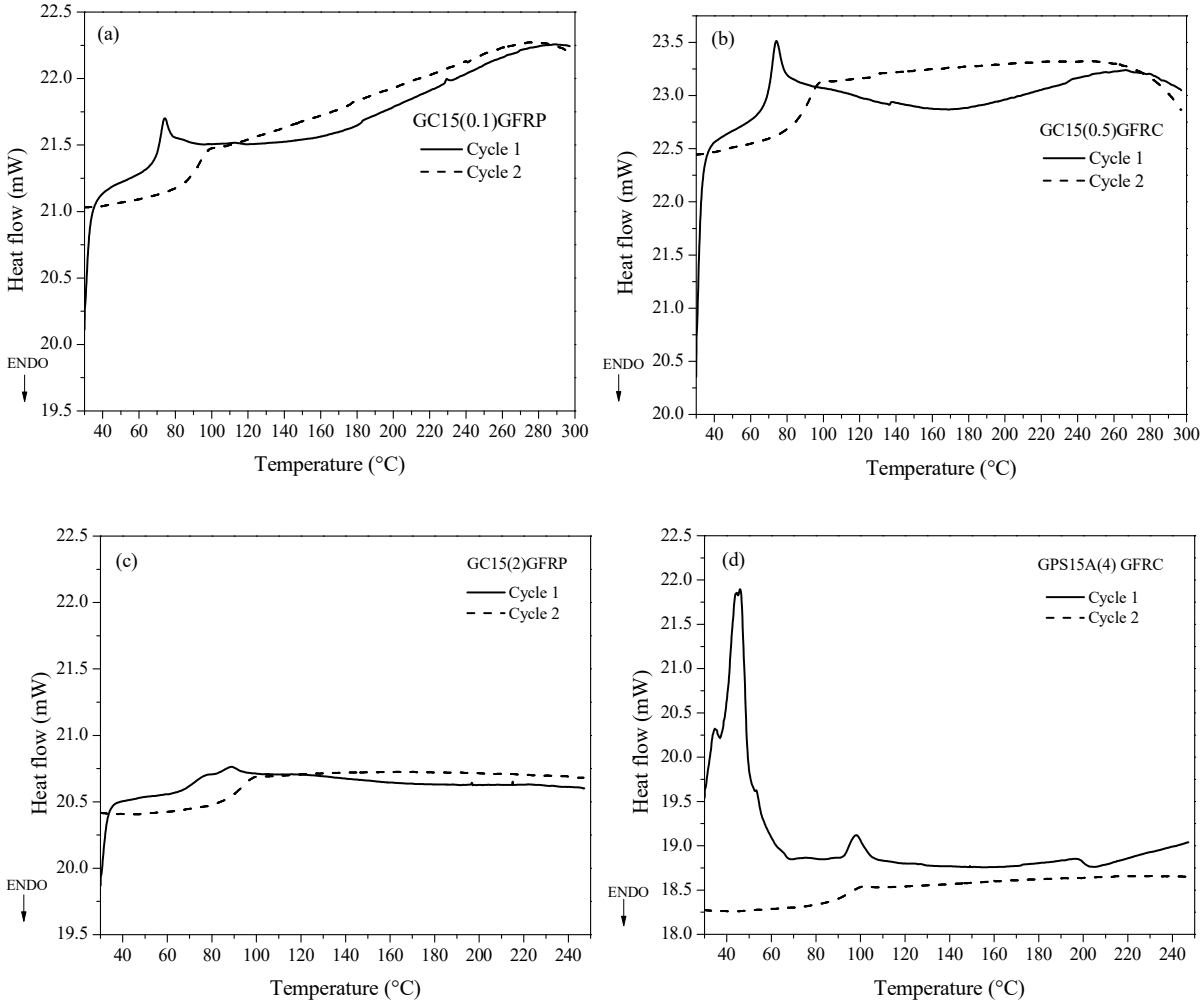

Figure 4.16 DSC traces of (a) GC15(0.1)GFRC, (b) GC15(0.5)GFRC, (c) GC15(2)GFRC, (d) GC15(4)GFRC

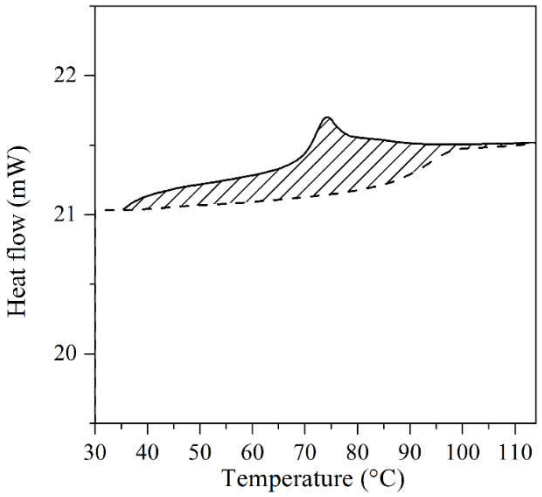

Figure 4.17 Enthalpy relaxation in GC15(0.1)GFRC

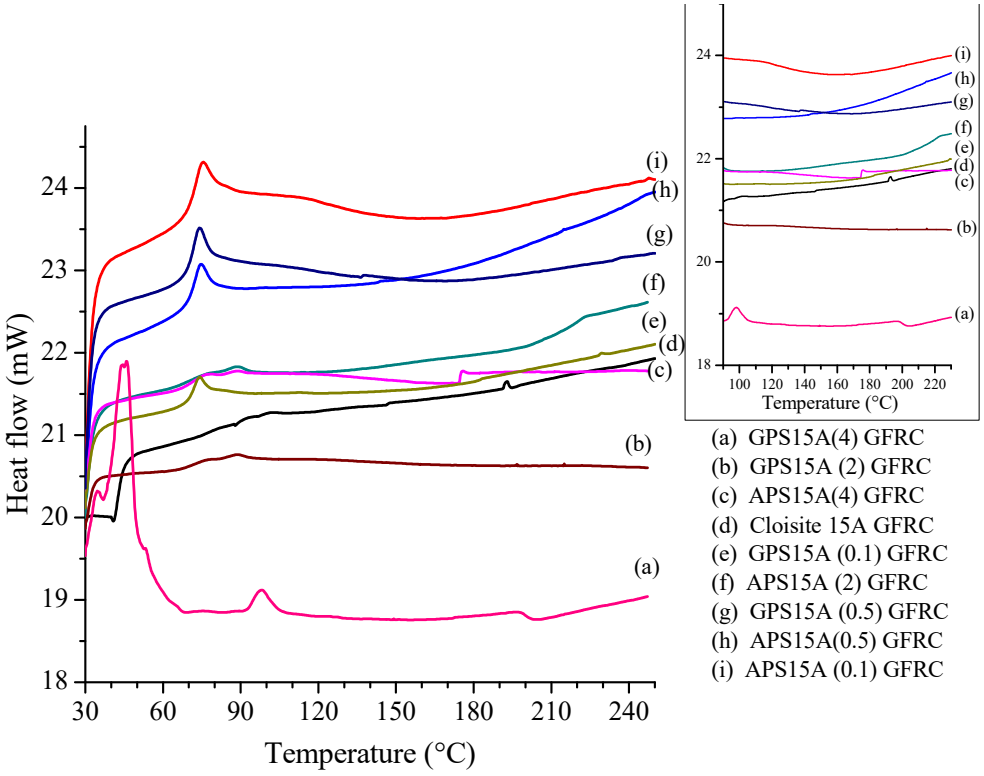

Figure 4.18 DSC traces of heating cycle 1

4.4 Closing remarks

The surface modification of inorganic reinforcement with silane coupling agents improved the adhesion of reinforcement with an epoxy matrix. The silane treatment of glass fibers with APTES/GPTMS significantly increased the flexural modulus (38% in the case of APTES treated glass fibers, and 18% in the case of GPTMS treated glass fibers) and the flexural strength (75% in the case of APTES treated glass fibers, and 61% in the case of GPTMS treated glass fibers) of three-phase hybrid nanocomposites. The tensile and flexural properties of silylated glass fiber reinforced composites decreased with incorporation of silylated clay minerals. The clay minerals were dried after silylation and had formed small crystals. The clay-clusters did not break properly during homogenization and ultrasonication and led to poor dispersion of clay minerals in the matrix.

Further experiments have been performed to elucidate the effect of silylation of clay minerals on the mechanical properties of glass fiber reinforced epoxy nanocomposites isolating the effects of silane treatment of glass fibers. The silylation of clay minerals has been performed using different quantities of silane coupling agents, and the silylated clay minerals were ground to avoid clustering of clay minerals. The grafting of silanes on Cloisite® 15A nanoclay has been confirmed by FTIR, which show bands related to Si-O bonding and presence of silanols.

The fiber reinforced composites incorporating silylated clay minerals gave some encouraging results and composition containing 2X silane treated clay minerals, AC15(2)GFRC showed improvements in tensile strength, flexural modulus, and elongation at break in comparison to compositions with 0.1X, 0.5X, 4X silane treated clay minerals. This can be attributed to exfoliation of clay mineral layers in the matrix as well as better curing of 2X silane treated nanoclay fiber reinforced nanocomposites as confirmed by TEM and DSC, respectively. The total absence of the characteristic clay peak ($2\theta = 2.41°$) in SAXS patterns, which is indicative of the absence of an ordered layer structure, confirmed that exfoliated nanocomposites had been formed.

Further studies have been carried out to (i) quantify the grafting of silanes on clay minerals, (ii) investigate the effect of curing schedule on mechanical properties of glass fiber reinforced epoxy-clay nanocomposites, (iii) modify silanization method to improve mechanical properties of glass fiber reinforced composites based on silylated clay minerals. These studies have been presented and discussed in the following chapter.

Chapter 5 Curing studies and mechanical properties of fiber reinforced epoxy-clay nanocomposites

5.1 Introduction

In this chapter, a modification in the method of silanization of clay minerals has been reported which enabled the use of very high concentration of silane coupling agents. As a result of this, 3-aminopropyltriethoxysilane silylated clay minerals had an exfoliated and encapsulating platelets morphology in nanocomposites. The ratio of the weight of silane coupling agent to that of the weight of clay minerals (X) was varied from 0.1 to 6. The mechanical properties of fiber reinforced epoxy-clay nanocomposites increased significantly with incorporation of silylated clay minerals and the optimum curing schedule. Small angle X- ray scattering and thermogravimetric analysis were carried out on silane modified clay minerals to quantify the grafting of silanes as a function of the ratio of the weight of silane agent to that of clay minerals. Also, curing studies were carried out on fiber reinforced epoxy nanocomposites containing Cloisite® 15A at different cure temperatures, e.g., 70°C, 80°C, 85°C, 95°C and for two different curing time periods, e.g. 7h and 10h. A qualitative study of fiber matrix interfaces aided by scanning electron microscopy has been presented.

5.2 Methodology

5.2.1 Silane functionalization of clay minerals

5g of Cloisite® 15A was immersed in a dilute solution containing different quantities of silanes viz. 0.1X, 0.5X, 2X, 4X and 6X with respect to the weight of clay mineral (X). Further, the Cloisite® 15A was nano-dispersed in silane solution by using a high shear homogenizer operated at 12,000 rpm for 3 min and ultrasonic mixing using a probe sonicator operated at an amplitude of 80% for 10 min. The solvent was then removed using a Heidolph rotary evaporator. The modified clay minerals were washed twice with the solvent used for hydrolysis to remove soluble homo condensates (Chen et al., 2005a, 2005b; Huskić et al., 2013; Ianchis et al., 2015, 2011; Zhang et al., 2006). Thin layers of silane modified clay minerals were laid in Petri plates to avoid large aggregations and then were dried in a vacuum oven at 60 ºC for 48 h. The dried clay minerals were ground in a pestle mortar to obtain a fine powder. Silylated clay minerals were heated for 15 min at 120 ºC before mixing in epoxy resin to remove residual solvent and moisture. To remove free water from the clay minerals, drying temperature was kept below the degradation temperature of quaternary ammonium modifier and organic moieties of silane coupling agents. The onset degradation temperature of the organic modifier

in Cloisite® 15A was 230°C as determined from TGA. The results of thermogravimetric analysis of Cloisite® 15A and silylated clay minerals are reported in section 5.3.1.1. Drying at 120°C was unlikely to cause the degradation of organic moieties as both APTES and GPTMS are gamma-substituted silane coupling agents and can withstand long-term continuous exposure to 160°C (Gelsest, 1967).

5.2.2 Fiber reinforced epoxy-clay nanocomposites

Clay minerals at 2 parts per hundred resin were added to Airstone® 780E resin and mixed for 5 min using a glass rod, a high-speed homogenizer operated at 20,000 rpm for 3 min and ultrasonic mixing using probe sonicator operated at an amplitude of 80% for 5 min. The homogenization and ultrasonication were repeated. A stoichiometric amount of Airstone® 786H hardener was added to the homogeneous mixture and degassing was done using a vacuum desiccator for 30 min. Finally, the epoxy was infused into the WR360 woven roving to manufacture high-quality two-ply laminate using vacuum assisted resin infusion method. Further, curing of the laminate was carried out on the heated mold.

5.2.3 Characterization of materials

Thermogravimetric analysis (TGA) of clay minerals was carried out using a Shimadzu TGA 50 thermogravimetric analyzer. The clay minerals were heated to 800°C at a rate of 10°C /min under a nitrogen environment and the weight loss was measured. Before testing, samples were stored in microcentrifuge tubes, and placed in a vacuum desiccator containing silica gel, to avoid absorption of moisture from atmospheric conditions. All Small angle X-ray scattering (SAXS) measurements on clay mineral samples were carried out on PANalytical XPERT Pro diffractometer.

Four specimens of each material were cut and tested as per the ASTM standards D3037/3039 for tensile test and D790 for 3 point bending test. Transmission electron microscopy (TEM) was carried out using TECNAI G^2 20 transmission electron microscope at an accelerating voltage of 100 kV. The calorimetric measurements were performed on a Perkin-Elmer DSC 4000 standard single furnace differential scanning calorimeter.

The terminology used for silane modified clay minerals consists of a prefix A (for APTES) or G (for GPTMS) followed by the concentration of silane in parentheses. A suffix GFRC is added to the symbol of silane modified clay minerals to denote nanocomposites containing silanized clay minerals.

5.3 Results and Discussion

5.3.1 Characterization of silane treated clay minerals

5.3.1.1 Thermogravimetric analysis

A quantitative investigation on grafting of silanes on clay minerals was conducted by thermogravimetric analysis of silane modified clay minerals. The TGA curves are shown in Figures. 5.1 and 5.2. The data obtained for Cloisite® 15A was in good agreement with results obtained by (Cervantes-Uc et al., 2007). The free water loss from Cloisite® 15A had occurred up to 110 °C. The onset of degradation of organic modifier was at 230 °C.

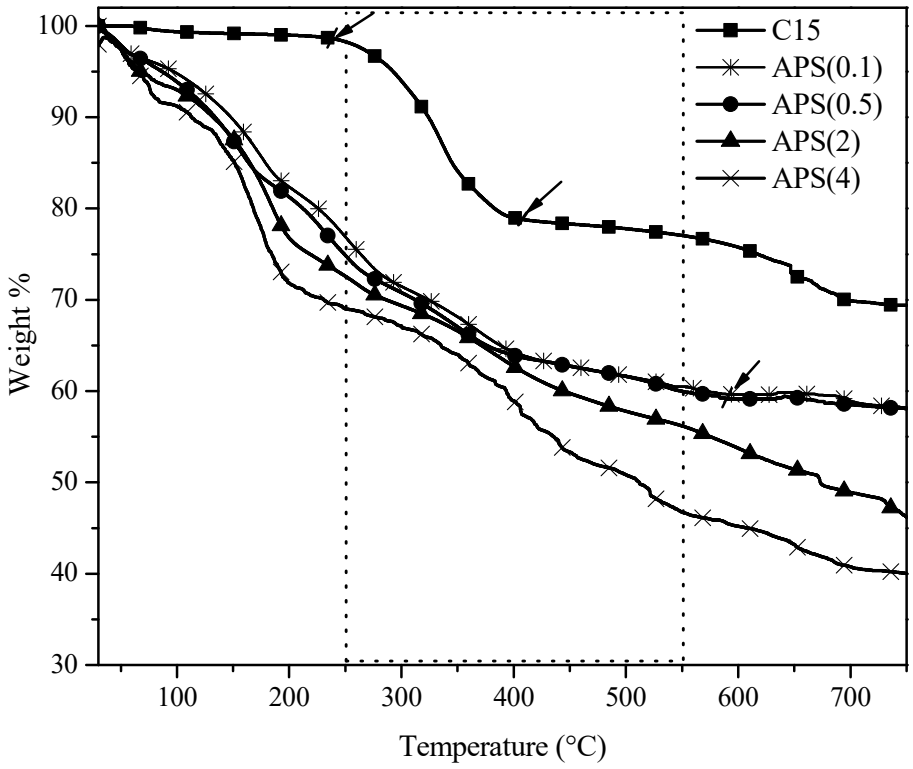

Figure 5.1 TGA curves of Cloisite® 15A and 3-aminoprpyltriethoxysilane treated Cloisite® 15A clay minerals

The maximum weight loss occurred between the temperature range of 272°C to 410°C, which can be attributed to the loss of water present in interlayer space of clay mineral, alkanes, alkenes, CHO's and COOH's (Cervantes-Uc et al., 2007; Edwards et al., 2005). For the silane modified clay minerals, the weight loss continued until 550 °C, which can be due to degradation of grafted silanes. From the literature on 3-aminopropyltriethoxysilanes grafted clay minerals, the initial loss in the temperature range from 30°C to 200°C in Figure 5.1 represents the elimination of adsorbed water. The weight loss in temperature range from 200 to 300°C can be attributed to loss of adsorbed silanes (hydrogen bonded with hydroxyl groups on broken

clay edges), whereas the mass loss in temperature range from 320 to 550°C can be attributed to degradation of intercalated and covalently bound silanes (Bertuoli et al., 2014; Shanmugharaj et al., 2006; Shen et al., 2007; Su et al., 2013). On the other side, the weight loss curves of clay minerals modified using glycidyloxypropyltrimethoxysilane (GPS(0.1), GPS(0.5), GPS(2), GPS(4), GPS(6)) shown in Figure 5.2 were quite close to the weight loss curve of Cloisite® 15A, in the temperature range from 100 to 200°C, but were differentiable above this temperature. The major weight loss in the temperature range from 250 to 550°C can be attributed to the loss of silane moieties due to degradation of epoxide ring and the ether linkage (Carli et al., 2014; Vejayakumaran et al., 2008)

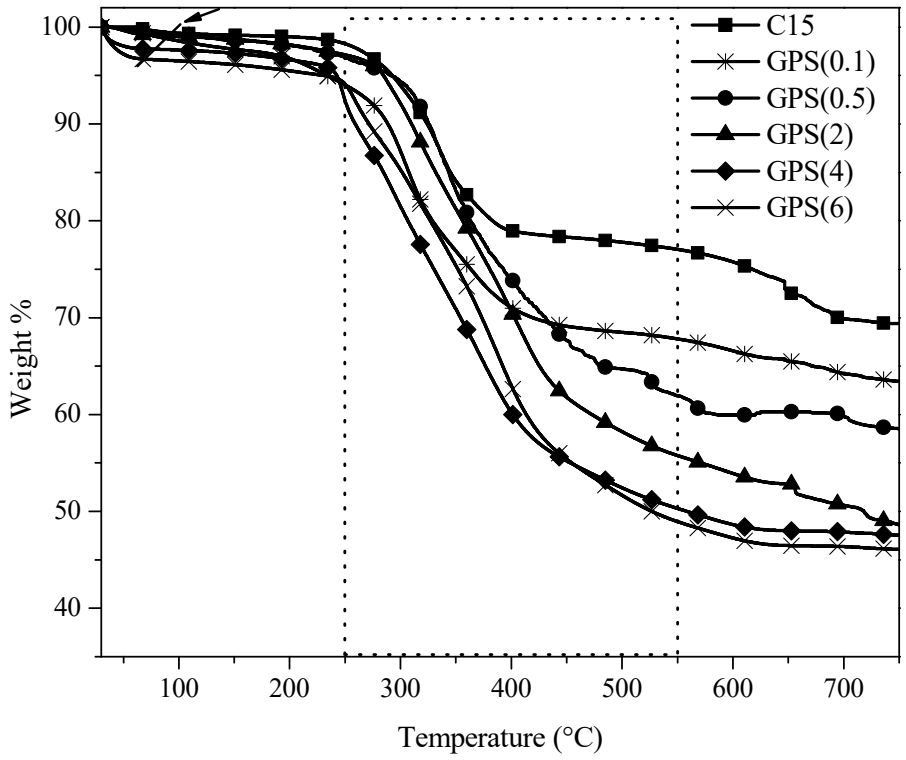

Figure 5.2 TGA curves of 3-glycidyloxypropyltrimethoxysilane treated Cloisite®15A clay minerals

The TGA results revealed that the increase in the quantity of silane used during processing of silylated clay minerals favored grafting of silanes on clay minerals. The degree of functionalization of silylated clay minerals could not be calculated from TGA results because of overlapping of decomposition steps which are characteristics to quaternary ammonium salts in Cloisite® 15A and grafted silanes. It was assumed that the amount of grafted silane is equal to the difference in weight loss between the silylated clay minerals and Cloisite® 15A.

The grafting ratio R_g was calculated using the following relationship (Guo et al., 2008; Morancho and Salla, 1999)

$$R_g = \left(\frac{W_1'}{W_1} - \frac{W_0'}{W_0}\right) \times 100\% \quad (5.1)$$

where W_1 = weight of silane modified clay mineral at 250°C

W_0 = weight of Cloisite® 15A at 250°C

W_1' = residual weight of silane modified clay mineral at 550°C

W_0' = residual weight of Cloisite® 15A at 550°C.

The region between 250°C - 550°C was considered for quantitative determination of grafted silanes (Ianchis et al., 2012; Shanmugharaj et al., 2006; Vejayakumaran et al., 2008; Xie et al., 2001). The weight loss in different clay minerals in the temperature range from 250°C to 550°C are shown in Table 5.1.

Table 5.1 Weight loss and grafting ratio

Clay mineral	Weight loss (%)	Grafting ratio (%)
Cloisite® 15A (C15)	20	-
APS(0.1)	26.33	5.48
APS(0.5)	25.44	4.59
APS(2)	26.47	5.62
APS(4)	32.15	11.3
GPS(0.1)	28.33	7.48
GPS(0.5)	36.65	15.80
GPS(2)	42.34	21.49
GPS(4)	46.44	25.59
GPS(6)	47.44	26.59

The results were reproducible in two independent experiments as shown in Figure 5.3. Considering an accuracy of ± 1% in the measuring range, in the case of 3-aminopropyltriethoxysilane grafted clay minerals, the grafting ratio (11.3 %) increased

significantly only with silanization carried out using silane amount equal to four times the weight of clay mineral. In the case of 3- glycidyloxypropyltrimethoxysilane grafted clay mineral, the grafting ratio increased proportionally with the increased amount of silane during processing, and highest grafting ratio (26.59 %) could be observed in GPS(6).

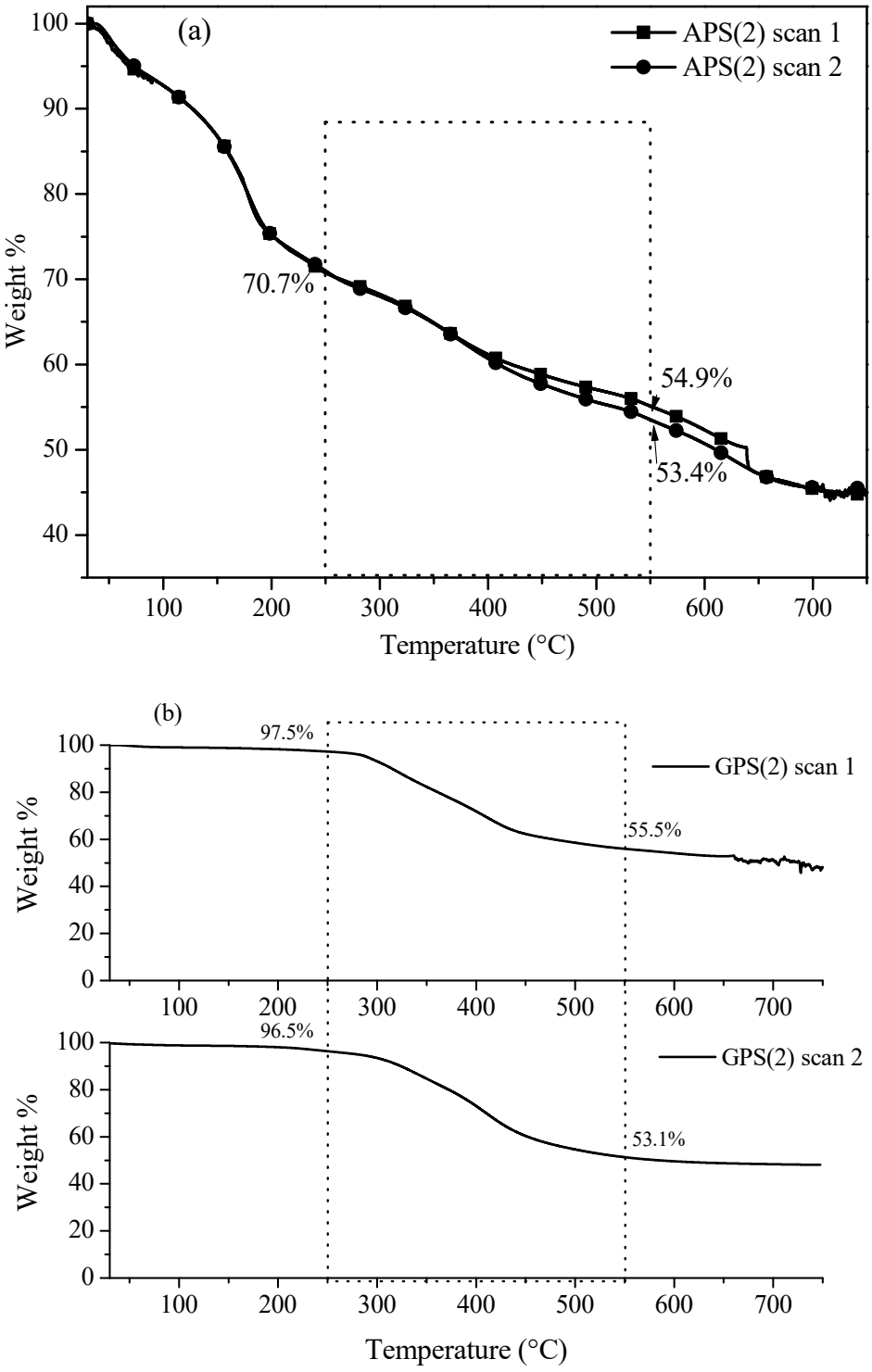

Figure 5.3 TGA curves of APS(2) and GPS(2) in two different experiments

5.3.1.2 Small angle X-ray scattering (SAXS)

High shear mixing followed by ultrasonication during silanization reaction would shear off the clay mineral layers and increase the grafting of silanes in clay mineral interlayers. This was confirmed by SAXS. The SAXS patterns of Cloisite® 15A and silylated clay minerals are shown in Figure 5.4. The characteristic peak of Cloisite® 15A at $2\theta = 2.71°$ corresponding to d_{001} spacing of 3.25 nm had broadened in the SAXS pattern of clay minerals modified using aminopropyltriethoxysilane. This confirms silylation of Cloisite® 15A essentially at the interlayer space. The silanization of the clay minerals can take place at three places: the interlayer space, external surface and at the edges. The interlayer and edges grafting can increase the distance between the clay minerals layers. For the external surface, silylation has no effect on interlayer spacing of clay. A summary of the relevant literature on the increase of d_{001}- spacing of different clays after silylation using APTES has been shown in Table 5.2. The previous studies had reported increase of d_{001}- spacing ranging between 2 °A to 8 °A. Exfoliation of clay minerals by silanization has not been reported earlier in the literature. The exfoliation of clay on silylation using APTES in this work is because of nano-dispersion of clay minerals in hydrolyzed silanes.

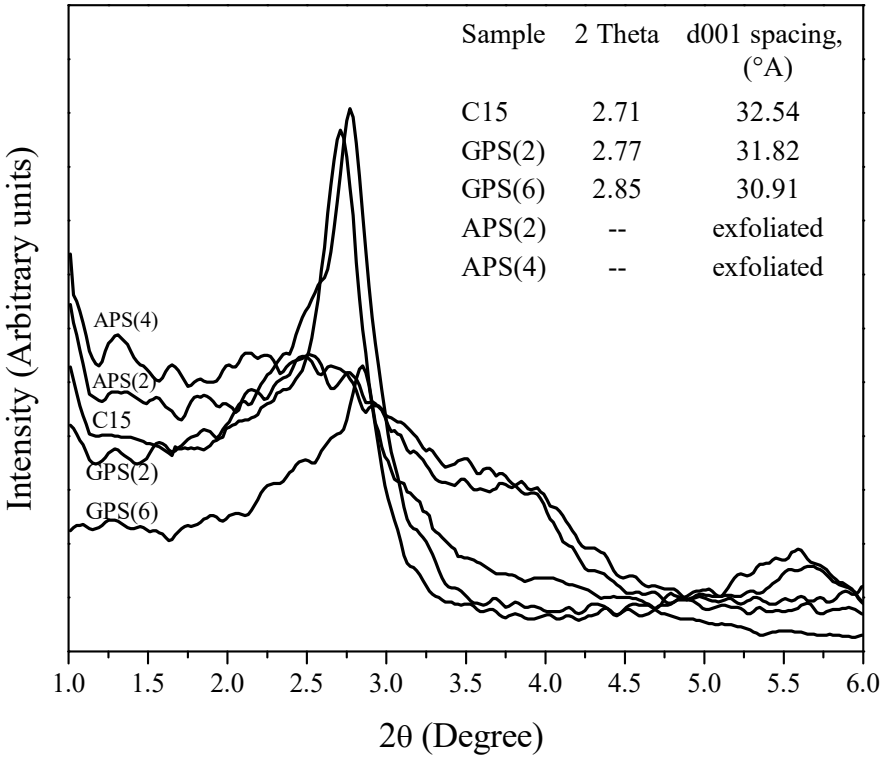

Figure 5.4 Small angle X-ray scattering patterns of Cloisite® 15A and silane modified clay minerals

The characteristic d_{001} peak of clay minerals modified using glycidyloxypropyltrimethoxysilane did not shift significantly and the corresponding d_{001} spacing of clay minerals are shown in Figure 5.4. A very small change in d_{001}-spacing of clays after silylation using 3-glycidyloxypropyltrimethoxysilane has also been reported by other researchers (Chen and Yoon, 2005a; Chen et al., 2005a; Xu et al., 2009) as shown in Table 5.2.

Table 5.2 Summary of relevant literature on change in d_{001} spacing after silanization

S. No	Silane coupling agents	Clay minerals	Mixing method	d_{001} spacing (°A)		Reference
				Before modification	After modification with SCA[a]	
1.	GPTMS	Cloisite® 25A	Refluxing the mixture at 72°C for 12h	18.46	18.62	Chen et al., (2005a)
2.	GPTMS	Cloisite® 15A	Refluxing the mixture at 72°C for 12h	31.8	31.5	Chen and Yoon, (2005a)
		Cloisite® 20A		24.5	23.8	
		Cloisite® 30B		18.1	18.3	
3.	APTES	Cloisite® Na	Stirring for 30 min	12.6	Not reported	(Shanmug haraj et al., 2006)
4.	APTES	Cloisite® Na	Stirring for 30 min	12.8	20.8	Ha et al., (2007)
5.	APTES	Cloisite® Na	Refluxing and constant stirring	10.1	14.1	Wan et al., (2008)
		Cloisite® 30B		18	19	
6.	GPTMS	Na-Mt	Agitation for at 8h at 80°C	11.6	12.5	Xu et al., (2009)
7.	APTES	Cloisite® Na	Mechanical stirring	12.8	20.8	Choi et al., (2009)
8.	APTES	Na Mt	stirred at 60°C for 30 min	11.7	16.6/ 21.8	Piscitelli et al., (2010)

9.	APTES	Ca Mt	Stirred at 60°C for 6h	14.8	18	Su et al., (2013)
10.	APTES	Cloisite® Na	Stirred for different time and at different temperatures	12.1	12.5/ 17.5/ 18.6/19.6/ 20.5	Bertuoli et al., (2014)
11.	APTES	Cloisite® Na	Stirring for 3h, centrifuged at 5000 rpm for 20 min	11.4	13.4	Bruce et al., (2014)
12.	APTES	Cloisite® Na	Stirring for 2h	11.9	13.7	(Daitx et al., 2015)
13.	APTES (4.4, mmol/g)	Na Mt	Stirring for 30 min and vacuum drying	12.6	21	(Ryu et al., 2016)
14.	APTES	Ca Mt	Stirring for 10h at 80°C, centrifuged	14.8	20.9	(Su et al., 2012)
15.	APTES	Ca Mt	(a) Stirring in silane-water/ethanol mixture (b) Exposed to saturated vapors of SCA's	12.6	19.5 Method (a) 19.8 Method (b)	(Shen et al., 2007)

[a] Silane coupling agent

5.3.2 Curing studies on fiber reinforced epoxy-clay nanocomposites

The curing studies were carried on fiber reinforced epoxy-clay nanocomposites containing Cloisite® 15A to determine a curing schedule, which optimized mechanical properties. DSC scans were also obtained to understand the effect of curing temperature and time on glass transition temperature (T_g) of nanocomposites. The nanocomposites were cured at different temperatures: 70°C, 80°C, 85°C and 95°C, and for two different cure time periods: 7 and 10h.

The effect of curing time and curing temperature on the tensile and flexural properties is shown in Figures 5.5 and 5.6. The tensile modulus increased for samples cured at temperatures up to 85°C and then it decreased by 20% for sample cured at 95°C. The tensile modulus increased with an increase in both time and temperature (70°C), but the effect of a change in curing time did not influence the tensile modulus values at other cure temperatures. The tensile strength also increased by 38% with an increase in cure temperature from 70°C to 85°C, but then it decreased slightly when the cure temperature was 95°C. Thus optimum tensile properties were obtained at 85°C/7h. No significant changes in flexural modulus were observed with changes in curing schedule. The flexural strength was highest in samples cured at 70°C and a small decrease was observed with an increase in curing temperature. The increase in the tensile modulus and tensile strength of fiber reinforced epoxy-clay nanocomposites with an increase in curing temperature of 70°C to 85°C may be attributed to increase in cross-link density of epoxy matrix. The increase in cross-link density results in improved tensile strength, modulus, hardness, and glass transition temperature (T_g) of thermoset (Goodman and Hanna, 2014), but at the same time makes the material brittle. The absence of residual cure peak in the DSC heating curve indicated that the nanocomposites were fully cured (Figure 5.7). The glass transition temperature (T_g) of nanocomposites are shown in Table 5.3. The T_g of nanocomposites increased with increase in curing temperature of 70°C to 80°C, but the change in T_g between 80°C to 85°C was very small.

T_g of nanocomposites obtained from the second heating scan was 87°C, which can be considered as $T_{g\infty}$, the temperature of the fully cured network obtained using DSC. Curing the resin above $T_{g\infty}$ causes the epoxy network to remain in the rubbery state after gelation and vitrification do not take place (de Paiva et al., 2008). Vitrification is liquid or rubber to glass transition during the polymerization of the epoxy resin. The decrease in mechanical properties at higher curing temperature at 95°C can, therefore, be explained using this perspective and similar results were reported by Carbas et al., (2014) and Mravljak and Šernek, (2011). At 85°C, the effect of curing time on tensile modulus, tensile strength, and flexural modulus was insignificant, but the flexural strength decreased slightly at longer curing time. Therefore keeping in mind the economy of the manufacturing process, the curing time for all nanocomposites was fixed as 7h.

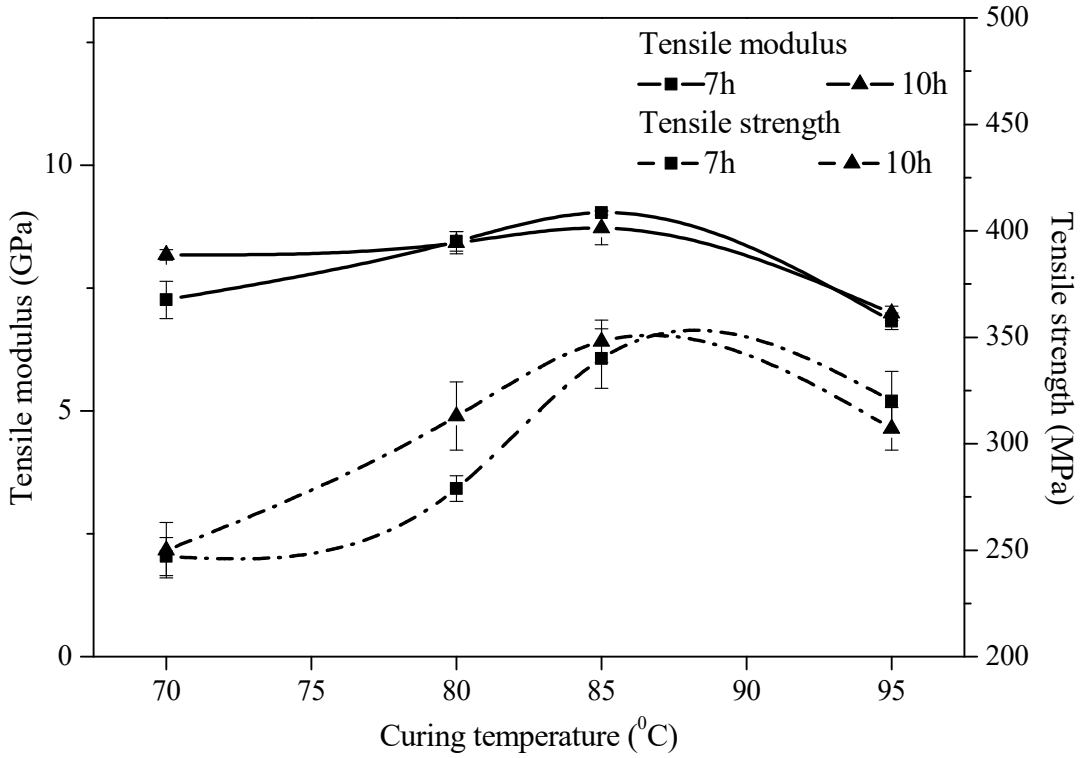

Figure 5.5 Effect of curing time and temperature on tensile properties

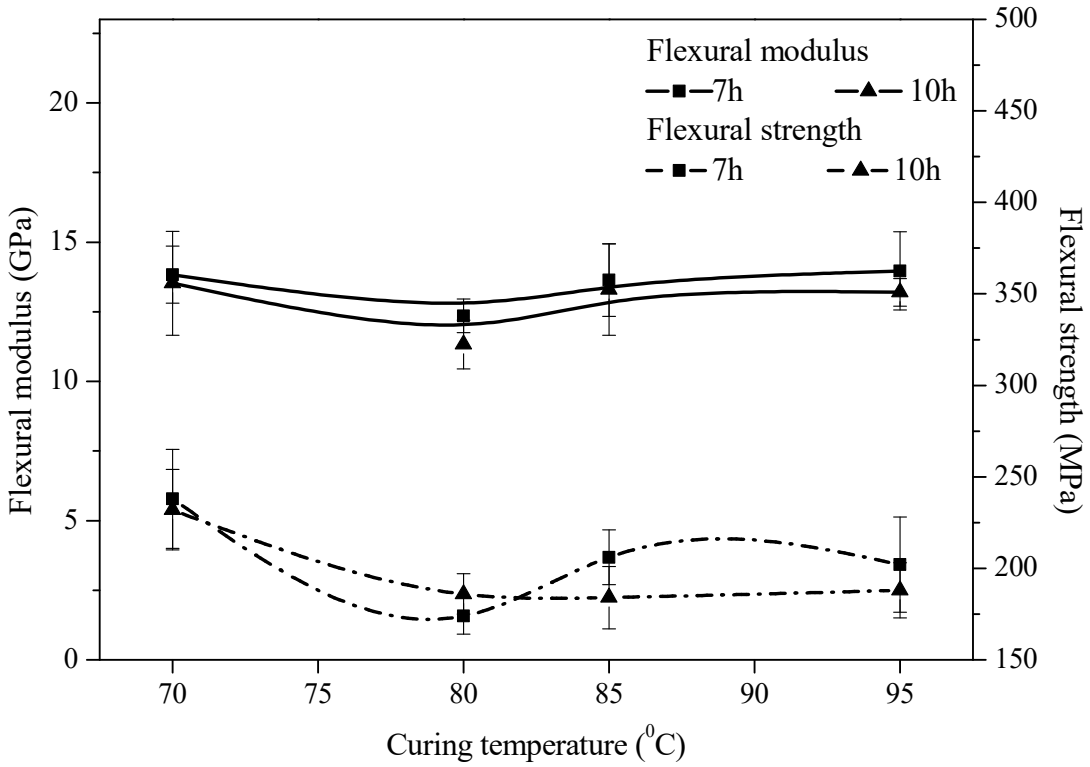

Figure 5.6 Effect of curing time and temperature on flexural properties

Table 5.3 Glass transition temperature of nanocomposites cured at different temperatures

Curing temperature (°C)	**Glass transition temperature (T_g), °C**	
	Heating scan 1	Heating scan 2
70	77	87
80	82	88
85	85	87

Table 5.4 Glass transition temperature of nanocomposites containing silane modified clay minerals

Composition	**Cured 7h/85°C**	
	Heating cycle 1	Heating cycle 2
AC15 (0.1)GFRC	90	91
AC15 (0.5)GFRC	92	92
AC15 (2)GFRC	88	89
AC15 (4)GFRC	86	92
GC15(0.1)GFRC	87	88
GC15(0.5)GFRC	85	89
GC15(2)GFRC	87	88
GC15(4)GFRC	86	90
GC15(6)GFRC	86	91

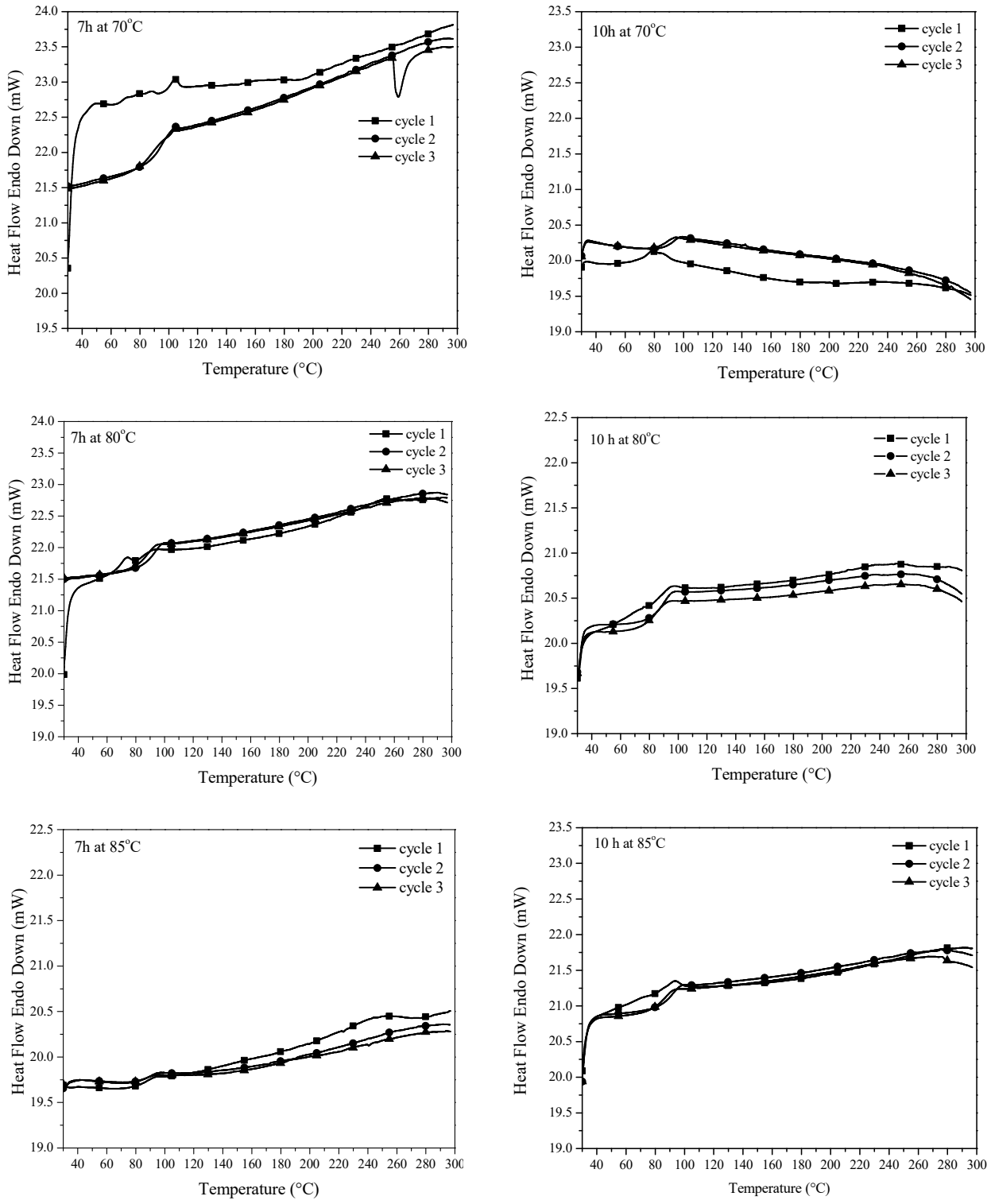

Figure 5.7 DSC curves of C15GFRC cured using different schedule

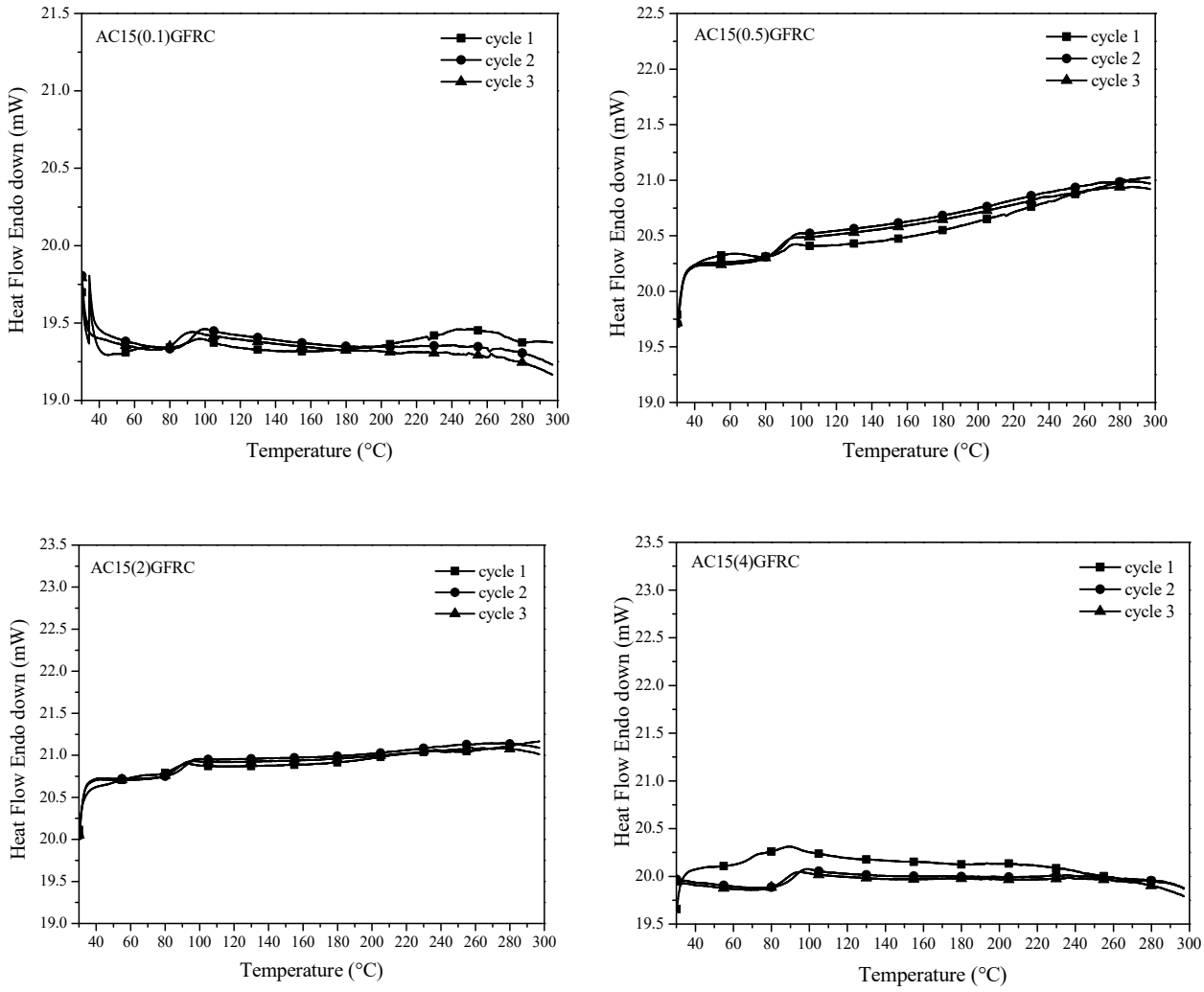

Figure 5.8 DSC curves of AC15GFRC cured using different schedule

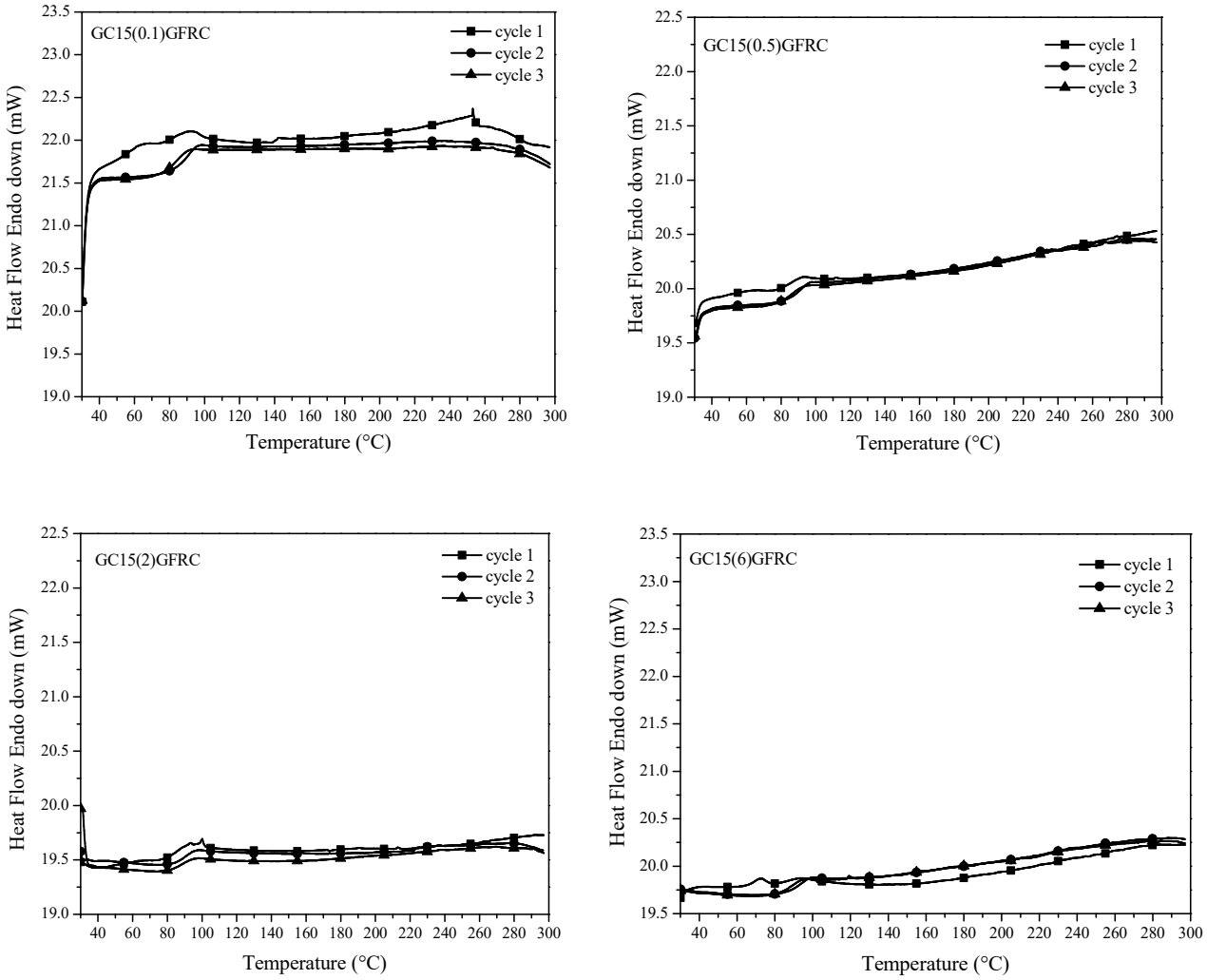

Figure 5.9 DSC curves of GC15GFRC cured using different schedule

The T_g of all nanocomposites (Table 5.4) remained almost the same during the second heating scan and there was no change in the curve representing a residual cure, which indicates that the epoxy was fully cured. The glass transition temperature was taken as mid-point value of the glass transition range. No significant changes in the T_g of nanocomposites containing silylated clay minerals were observed vis-a-vis concentration of grafted silanes. In our previous study (Chapter 4), the incorporation of silylated clay minerals in epoxy led to an increase in glass transition temperature (T_g) of fiber reinforced nanocomposites. A different cure temperature (85 °C) in the present study has resulted in almost a 10°C increase in the glass transition temperature of nanocomposites. The greater degree of curing of epoxy in the present study would lead to increase in the crosslink density of polymer chains, which would dominate the effect of organoclay - polymer interactions in restricting the mobility of chains (Becker et al., 2005, 2003; McIntyre et al., 2005). The DSC curves of all nanocomposites are shown in Figures 5.8 and 5.9.

5.3.3 Morphology of fiber reinforced epoxy nanocomposites based on silylated clay minerals

The morphology of the composite samples containing silylated clay minerals was studied by TEM. The terminology used for nanocomposites incorporating silane modified clay minerals consists of a prefix A (for APTES) or G (for GPTMS) followed by the concentration of silane in parentheses and the abbreviation GFRC. As shown in Figure 5.10, the fiber reinforced epoxy-clay nanocomposites containing Cloisite® 15A (C15GFRC) had intercalated morphology wherein the clay mineral layers were observed to be sheared off and limited delamination had occurred. The treatment of clay minerals with both silane coupling agents aided exfoliation and clay mineral layers were observed to be spatially disordered and oriented in different directions as shown in Figures 5.11 and 5.12.

In the case of AC15(4)GFRC, the majority of clay mineral layers were uniformly dispersed, exfoliated and interestingly, some encapsulated clay mineral particles were also observed (Figure 5.13). The clay mineral layers were seen to be located at the surface of the particle as well as encapsulated in epoxy, which is similar to structure observed by Voorn et al., (2006) and De Maria et al., (2011). A possible explanation of encapsulation of clay minerals is that the silanes do not always form a monolayer on the filler surface but can form polysiloxane layers. The structure of the polysiloxane layer is affected by several factors like processing conditions, solvent, concentration, and functionality of silanes, pH of the solution. The siloxane networks can form a rigid cage-like structure (Demjen et al., 1997; Iglesias et al., 2002; Xie et al., 2010) and clay mineral layers may be encapsulated in these networks. The other possibility is by joining of siloxane linkages (Traynor et al., 2015), the other ends of which are linked with clay mineral layers. The encapsulating clay minerals have better-reinforcing effect in comparison to other modified clay minerals due to improved adhesion with polymer matrix (Mballa et al., 2013; Mirzataheri et al., 2010; Rong et al., 2006; Xia et al., 2003).

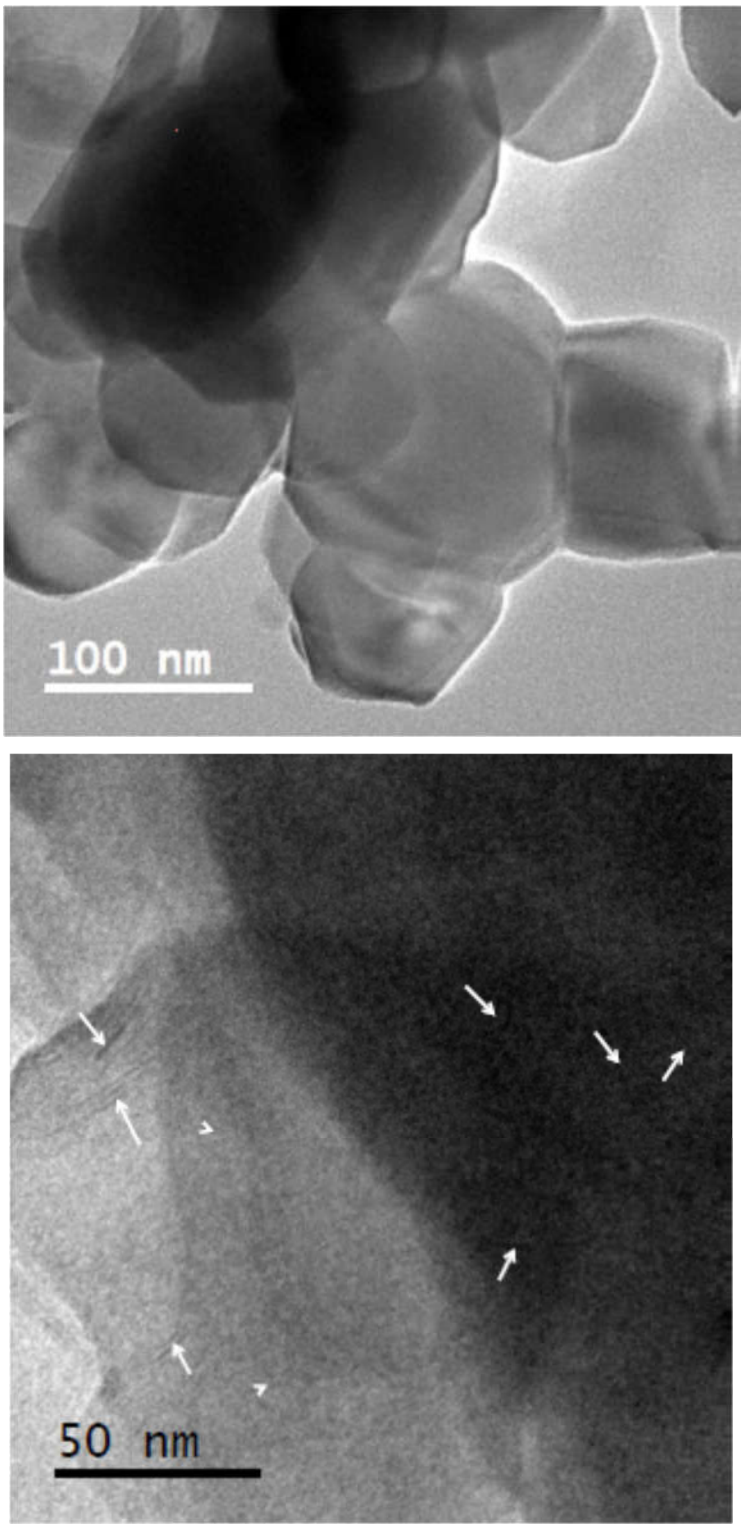

Figure 5.10 Transmission electron micrographs of C15GFRC at different magnifications

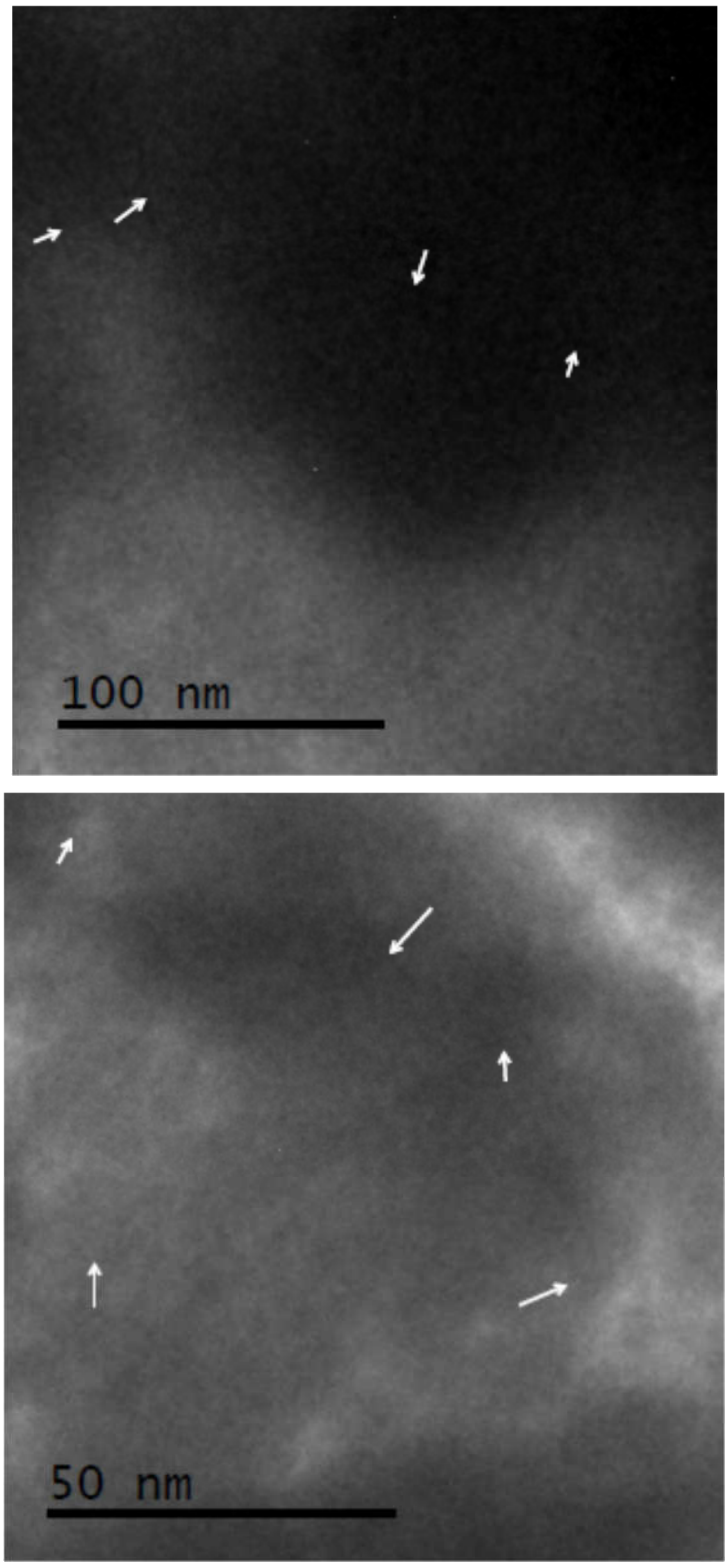

Figure 5.11 Transmission electron micrographs of AC15(2)GFRC at different magnifications

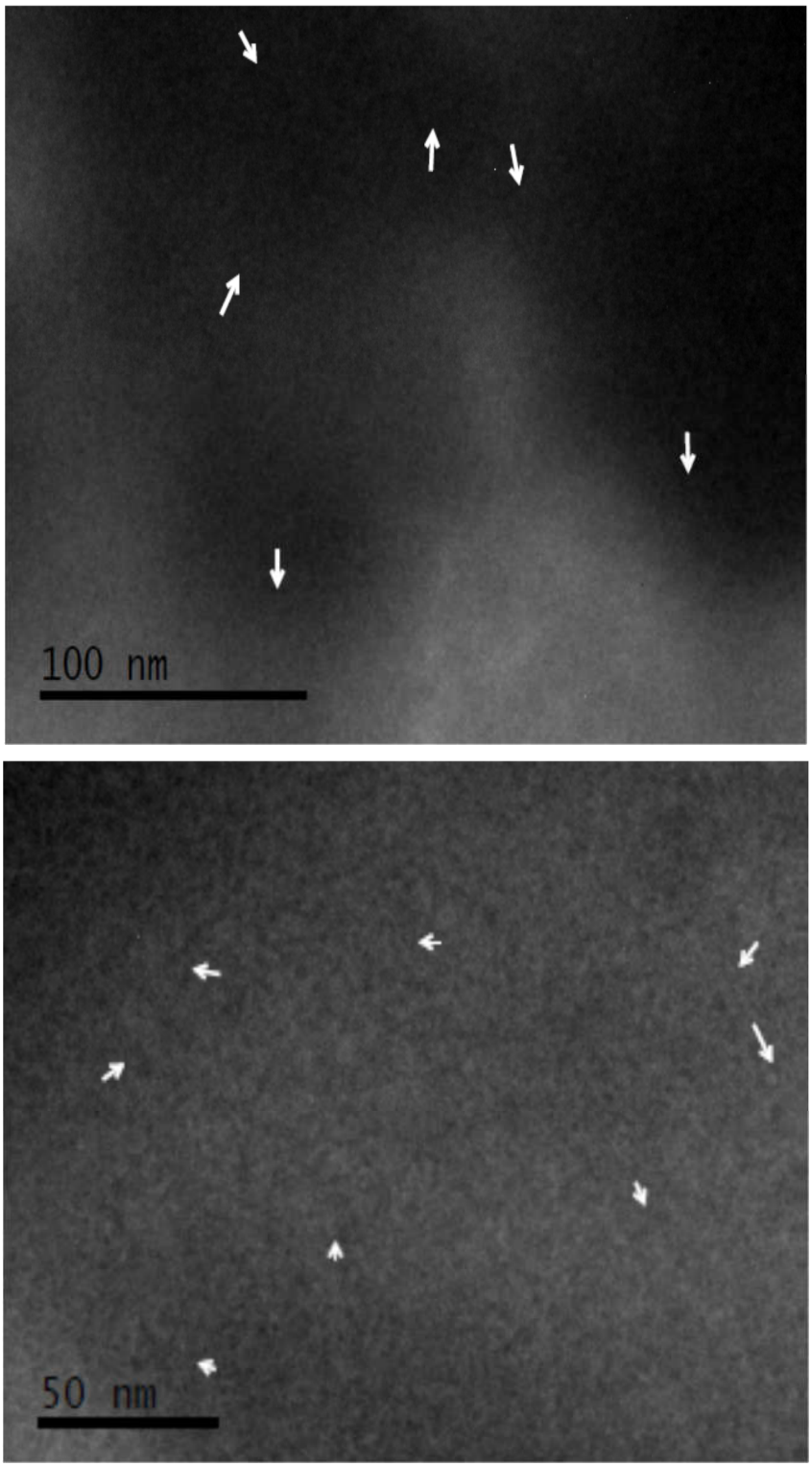

Figure 5.12 Transmission electron micrographs of GC15(2)GFRC at different magnifications

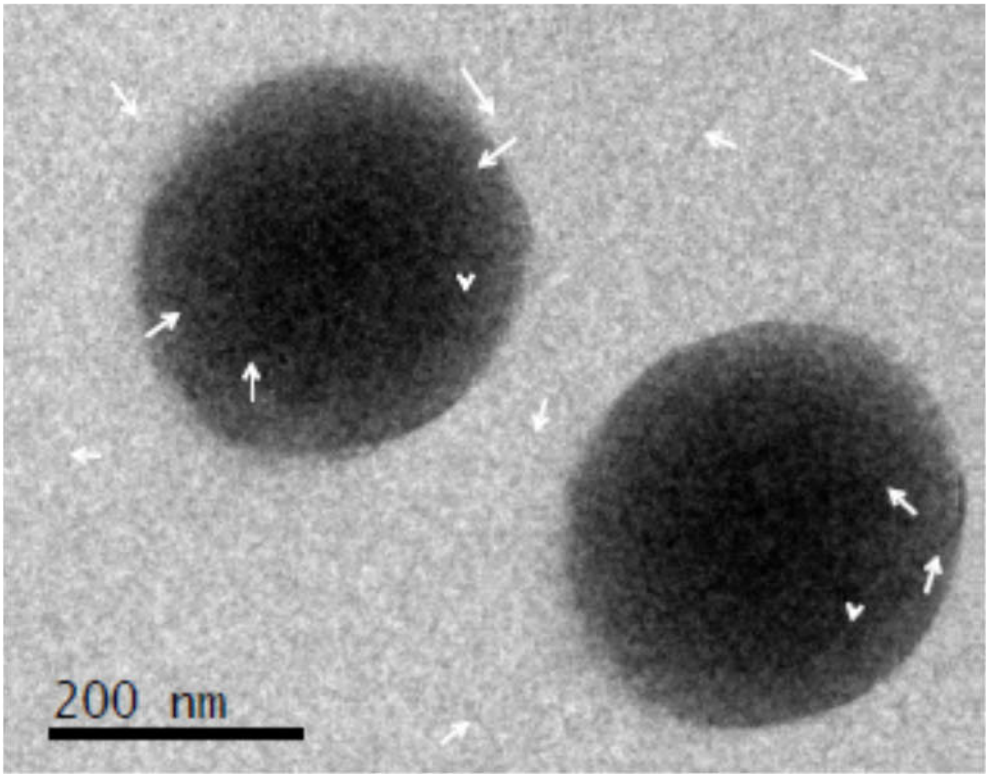

Figure 5.13 Transmission electron micrographs of AC15(4)GFRC

5.3.4 Effect of incorporation of silane modified clay minerals on mechanical properties

The results obtained for fiber reinforced silylated epoxy-clay nanocomposites have been summarized in this section. The tensile modulus and tensile strength of glass fiber reinforced neat epoxy composite (GFRC) were 7.9 GPa and 377 MPa, respectively (Figure 5.14). After incorporation of 2 phr of Cloisite® 15A, the tensile modulus increased but the tensile strength decreased in fiber reinforced epoxy nanocomposite containing Cloisite® 15A (C15GFRC). The tensile modulus increased because C15GFRC had an intercalated morphology. However, the tensile strength decreased because of poor stress transfer between the matrix and reinforcement. Kornmann et al., (2005) and Quaresimin and Varley, (2008) had also observed a decrease in the tensile strength of glass fiber reinforced epoxy laminates after addition of OMMT. The percent elongation before failure was not significantly affected by the addition of Cloisite® 15A in an epoxy matrix.

The incorporation of silane treated clay minerals led to improvements in tensile and flexural properties of nanocomposites. The SCAs used in the present study (amine functional silane and glycidyl functional silane) are widely known for improving the dispersibility of inorganic fillers and promoting interfacial adhesion with epoxy. The grafting of silanes on clay minerals

played an important role in improving the mechanical properties. An increase in tensile modulus, tensile strength, and flexural strength were observed on the incorporation of clay minerals treated with 0.1X silane treated clay minerals, e.g. AC15(0.1)GFRC and GC15(0.1)GFRC as compared to C15GFRC (Figure 5.14 and 5.15). Similar results were reported by Ha et al., (2007) and Ianchis et al., (2015) on the incorporation of silane treated clay minerals in epoxy-clay nanocomposites. Much larger enhancement in tensile modulus, tensile strength, flexural modulus and flexural strength were seen in AC15(4)GFRC, GC15(4)GFRC and GC15(6)GFRC. The glass fiber reinforced epoxy-clay nanocomposites containing clay minerals treated with APTES outperformed than treated with GPTMS and the highest improvements were observed in AC15(4) GFRC, in which tensile modulus, tensile strength, flexural modulus and flexural strength increased by 30%, 37%, 139% and 146%, respectively as compared to C15GFRC. This can be attributed to silane functionality (amino group) of the coupling agent. The results indicate that an increased grafting of silanes on clay minerals led to a significant increase in mechanical properties of fiber reinforced epoxy-clay nanocomposites. Similarly, in the case of fiber reinforced epoxy-clay nanocomposites containing clay minerals treated with GPTMS, the highest properties were observed for GC15(6)GFRC. It should be pointed out that it was not possible to obtain good homogeneous sheets for composition greater than 4X in APTES and 6X in GPTMS. This was because of the very high viscosity of epoxy-clay resin mixture containing clay minerals treated with an even higher concentration of silanes. The silane modification of clay minerals also brought significant change in the elongation at failure of nanocomposites tested under tensile load. The percent elongation values for all nanocomposites are shown in Figure 5.16. The percent elongation increased to a maximum value of 11.8 before failure, in nanocomposites containing clay minerals modified with APTES. The percent elongation before failure for APS15A(0.1)GFRC was much higher in comparison to GPS15A(0.1)GFRC. The improved interfacial adhesion between clay minerals and polymer matrix would have affected the strain at failure as shown in Figure 5.17.

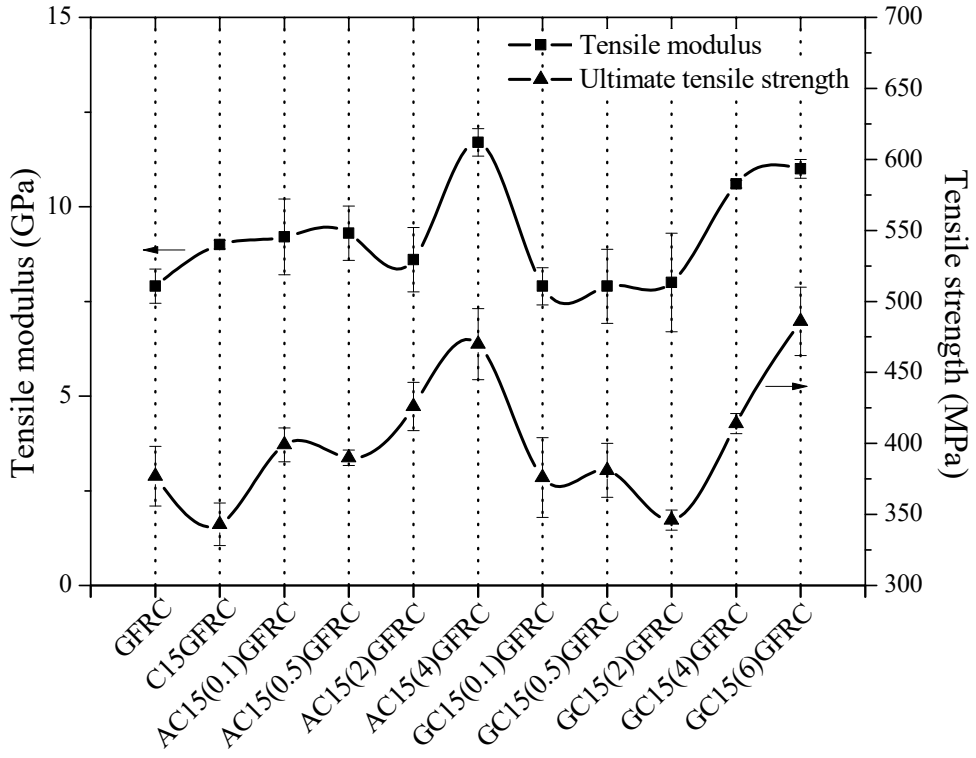

Figure 5.14 Tensile properties of fiber reinforced epoxy-clay nanocomposites

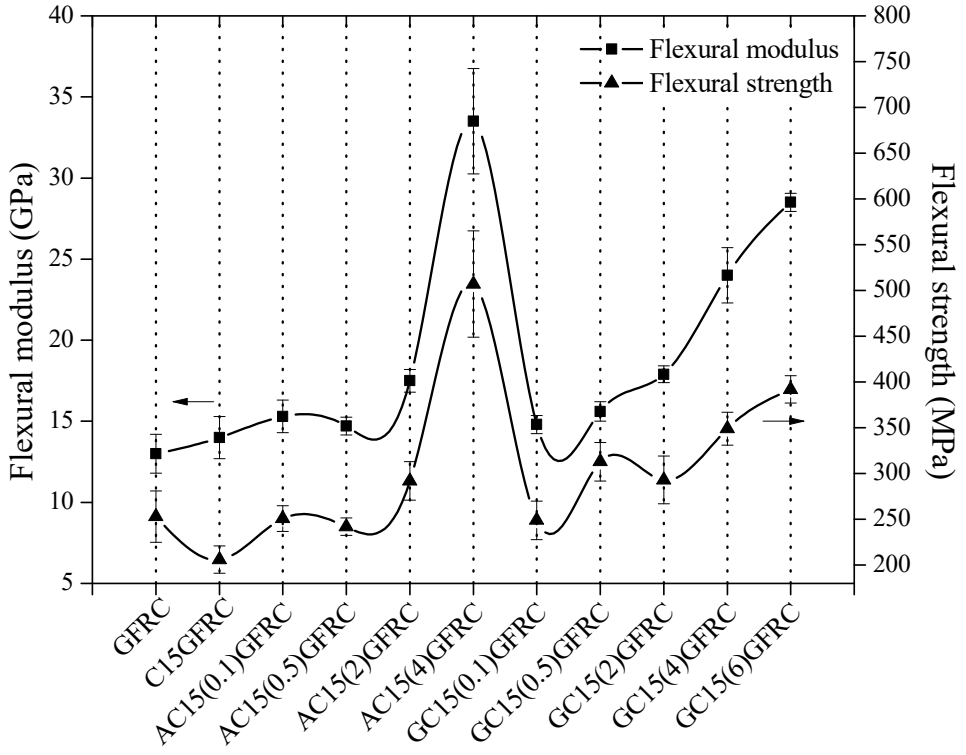

Figure 5.15 Flexural properties of fiber reinforced epoxy-clay nanocomposites

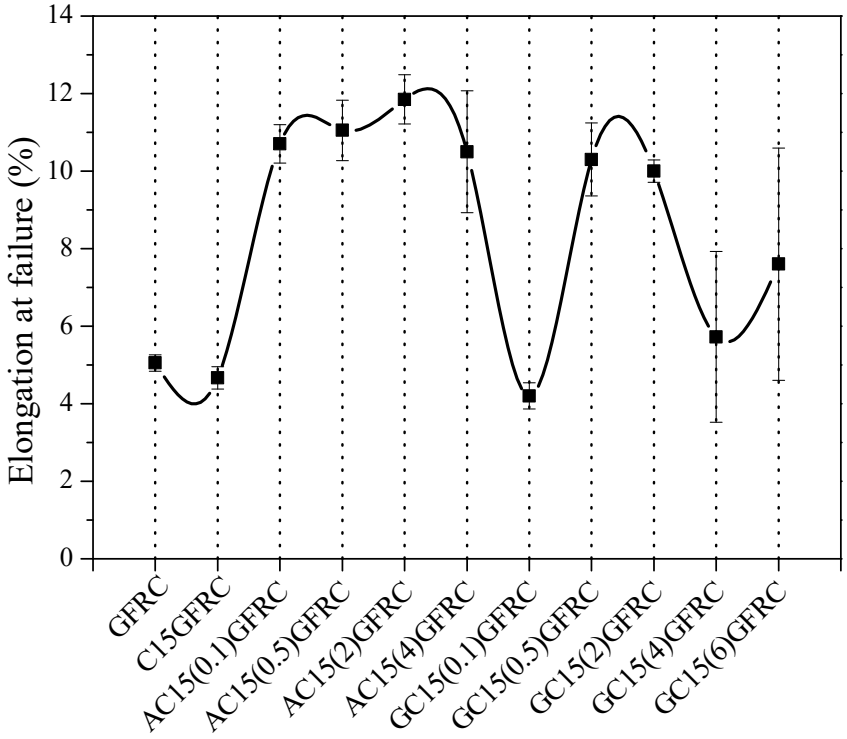

Figure 5.16 Percent elongation before failure in nanocomposites

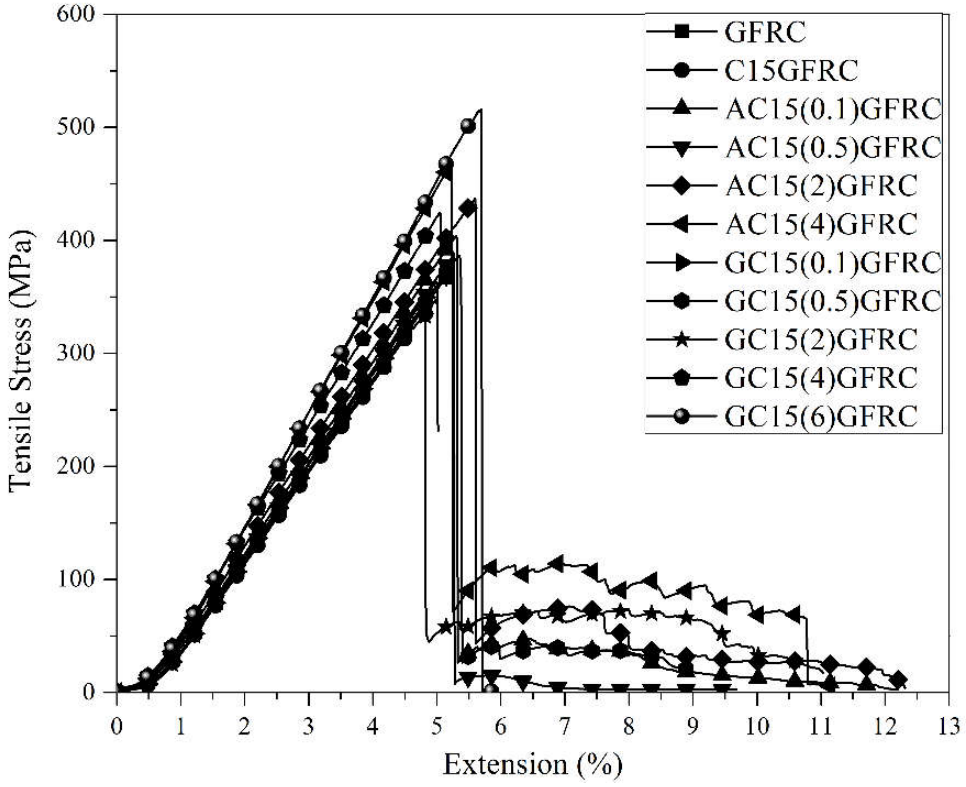

Figure 5.17 Stress vs extension curves of nanocomposites

5.3.5 Analysis of fractured surfaces

SEM was carried out on surfaces after removal of peel ply and fractured surfaces were studied. A peel ply or release cloth is a removable layer between the composite and vacuum bag which absorbs the excess of resin and was removed after curing of the composite. The peel ply created a textured surface on composites as shown in Figure 5.18(a).

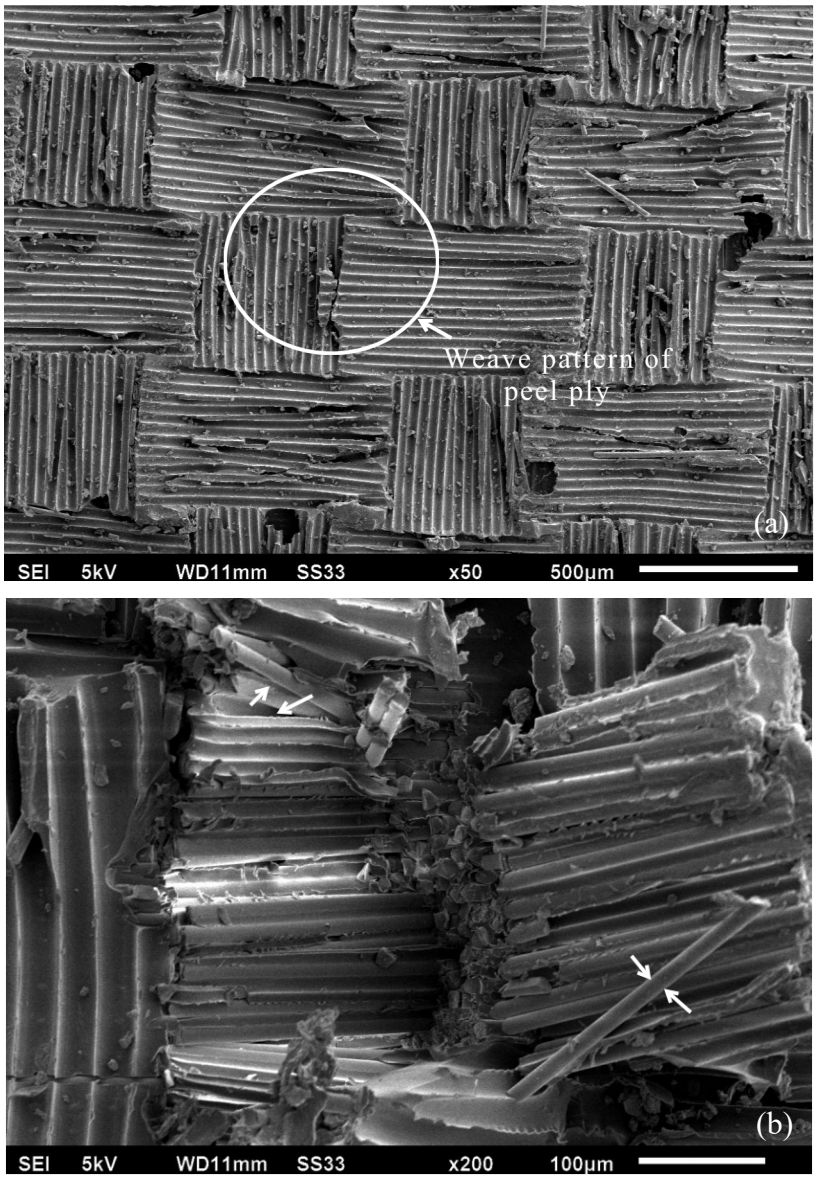

Figure 5.18 Scanning electron micrograph of (a) textured surface on neat epoxy GFRC (b) fractured surface

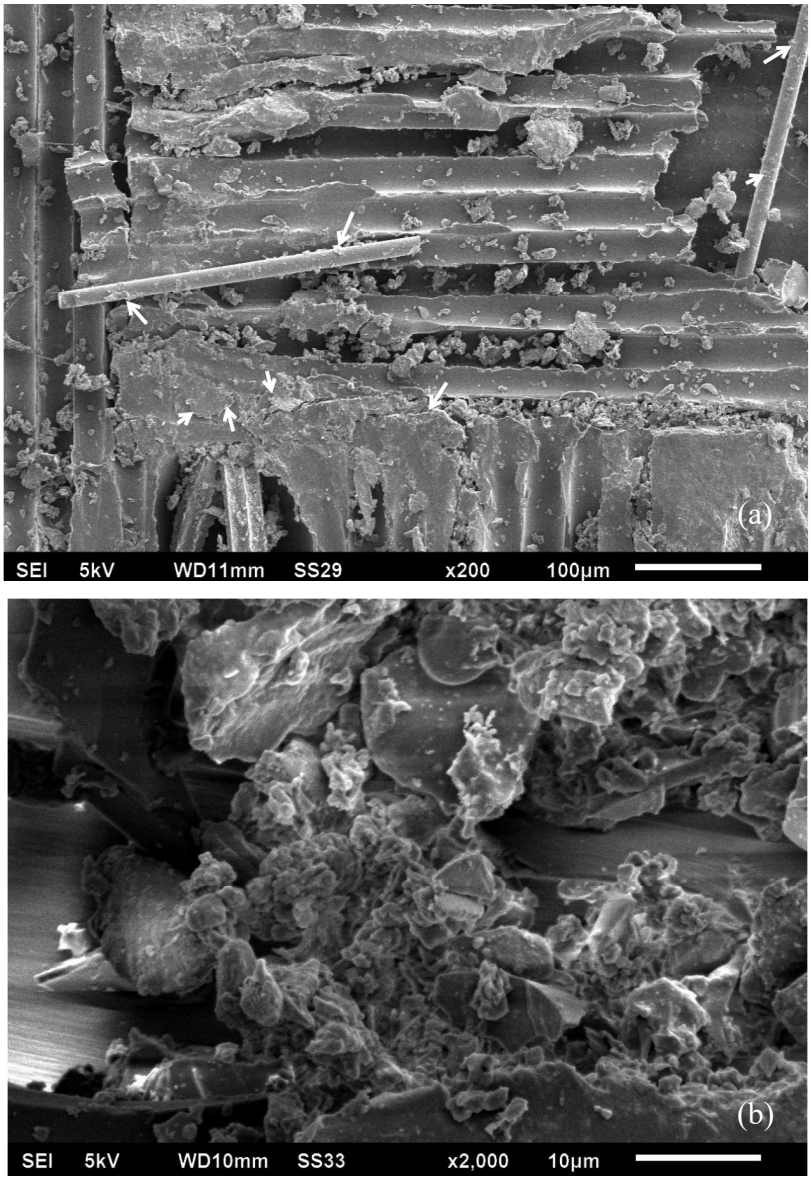

Figure 5.19 Scanning electron micrograph of C15GFRC showing (a) fibers (b) epoxy at fractured surface

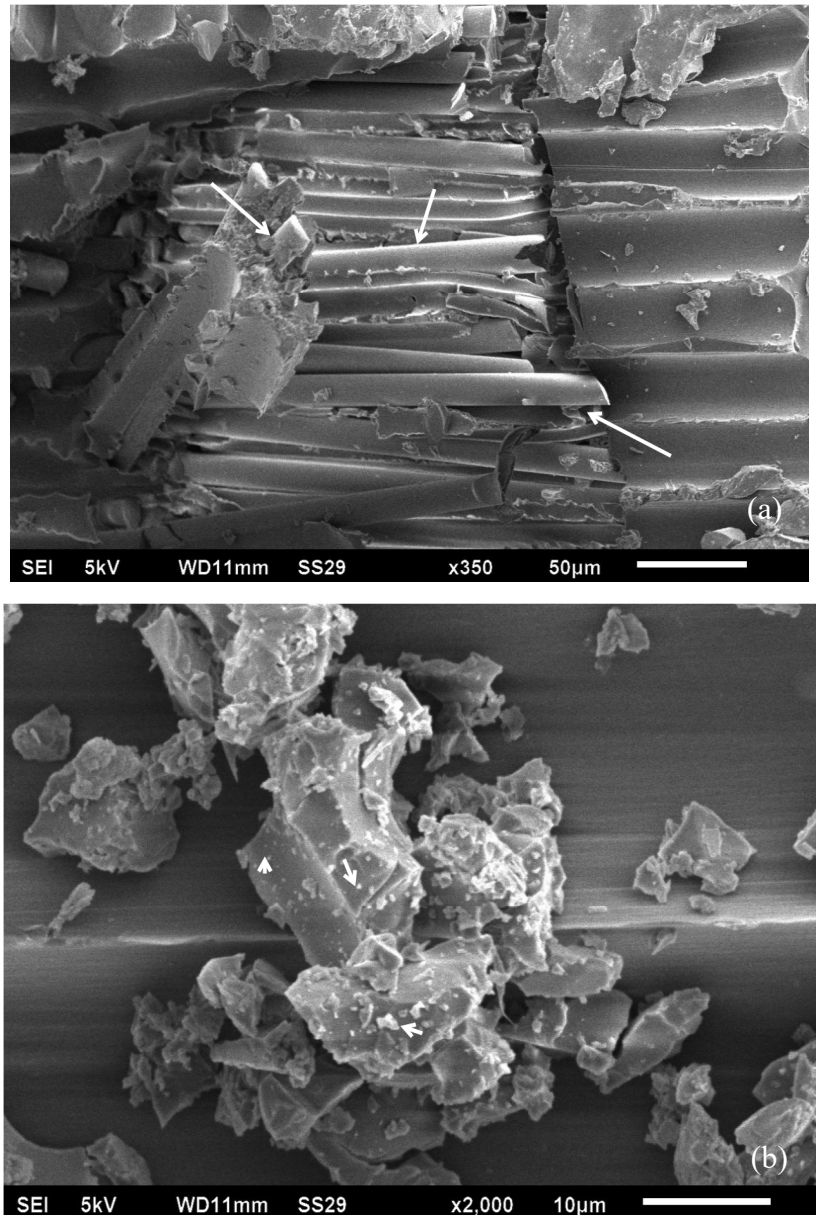

Figure 5.20 Scanning electron micrograph of AC15(2)GFRC showing (a) fiber matrix interface (b) dispersion of clay minerals in epoxy

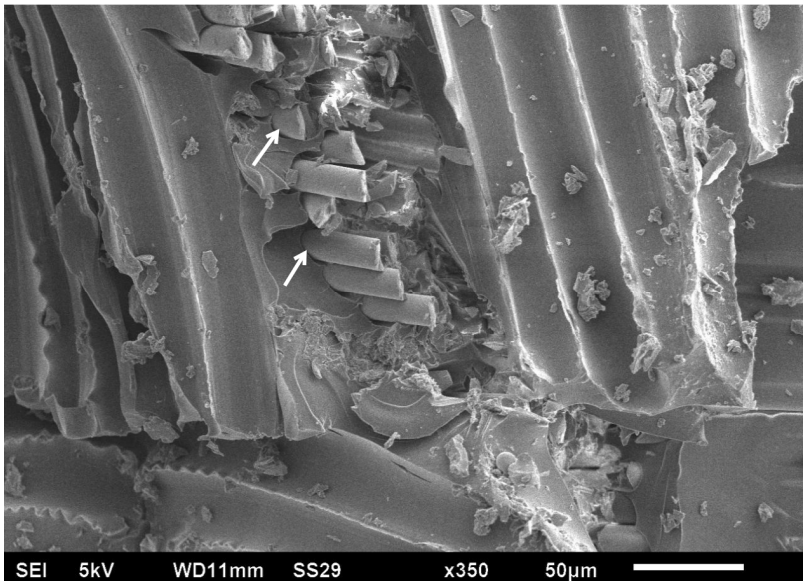

Figure 5.21 Scanning electron micrograph of GC15(2)GFRC

The fractured surface of the composite prepared using neat epoxy (GFRC) was smooth and the glass fiber surfaces were clean, which indicates poor adhesion between neat epoxy and glass fibers. Fiber breakage and fiber pullout were also evident from Figure 5.18(b). On the other hand, in the case of C15GFRC, the clay minerals and epoxy seem to be sticking with the glass fibers, as shown in Figure 5.19(a). The rough fracture surfaces with white fracture borders were also observed (Figure 5.19(b)). The scanning electron micrographs of fractured surfaces of AC15(2)GFRC and GC15(2)GFRC are shown in Figure 5.20 and Figure 5.21. In both cases, good interfacial adhesion between fiber and matrix was observed (Figure 5.20(a) and Figure 5.21), and the failure occurred because of fiber breakage and matrix cracking only, unlike in the case of GFRC or C15GFRC, where an additional failure mode of fiber pullout was also observed. The bright white spots on the epoxy surface (Figure 5.20(b)) were presumed to be clay mineral layers, having a lateral size in few microns, and these were well dispersed in the matrix. Good adhesion and well-dispersed clay mineral layers can clearly be the reason for the increase in mechanical properties of nanocomposites containing silane treated clay minerals.

5.4 Closing remarks

The mechanical properties of fiber reinforced epoxy-clay nanocomposites were influenced by a change in curing schedule. The highest mechanical properties were obtained by curing the epoxy at a temperature slightly below the temperature of the fully cured network ($T_{g\infty}$) obtained using differential scanning calorimetry. In this work, the silylation of clay minerals was

performed varying the ratio of the weight of the silane coupling agent to that of the weight of the clay minerals (X) from 0.1 to 6. Silane treatment was not performed on glass fibers. Small angle X-ray scattering and thermogravimetric analysis were performed on silane modified clay minerals to quantify the grafting of silanes as a function of the ratio of the weight of silane agent to that of the clay mineral. Thermogravimetric analysis results revealed that the grafting of silanes on clay minerals increased with an increase in silane concentration. The SAXS pattern of clay minerals modified using 3-aminopropyltriethoxysilane indicated that the silylated clay minerals had been exfoliated which can be attributed to the grafting of silane groups in interlayer space of clay minerals. The tensile modulus, tensile strength, flexural modulus and flexural strength increased by 30%, 37%, 139% and 146% respectively, in glass fiber reinforced containing clay minerals modified using 4X aminopropyltrietoxysilane. The Transmission electron microscopy of glass fiber reinforced-silylated clay nanocomposites indicated that clay mineral layers were exfoliated and observed to be spatially disordered and oriented in different directions. Exfoliation of clay mineral layers in matrix led to improvements in tensile and flexural properties of nanocomposites. The fractographic analysis of nanocomposites revealed a considerable difference in failure modes of fiber reinforced epoxy composites containing Cloisite® 15A and silane modified clay minerals. In case of glass fiber reinforced epoxy-silylated nanocomposites, a good interfacial adhesion between fiber and matrix was observed. The failure in these nanocomposites occurred because of fiber breakage and matrix cracking only, unlike in the case of GFRC or C15GFRC, where an additional failure mode of fiber pullout was also observed.

Chapter 6 Seawater ageing of glass fiber reinforced epoxy nanocomposites based on silylated clays

6.1 Introduction

The seawater durability of fiber reinforced epoxy composites in seawater is dependent on the resistance offered by matrix material to degradation due to hydrolytic attack and integrity of fiber-matrix interface after hygrothermal ageing. Therefore, modifying the matrix material with nanofillers to increase the service life of composites in marine conditions is a research area of great interest. In the field of nanocomposites, many studies are available which advocate excellent moisture barrier capacity of clay minerals (Abacha et al., 2007; Kim et al., 2005; Mittal et al., 2015; Tan and Thomas, 2016). The improvement in barrier properties of composites is achieved if the clay mineral layers are uniformly distributed in the polymeric matrix, has an intercalated or exfoliated morphology and forms strong interfacial bonds with matrix (Alamri and Low, 2012; Kim et al., 2005; Liu et al., 2005a; Tan and Thomas, 2016; Zainuddin et al., 2009).

Mittal et al. (Mittal et al., 2015) studied the effect of seawater absorption on properties of glass fiber reinforced vinyl ester composites based on montmorillonite and 3-aminopropyltriethoxysilane treated montmorillonite. The tensile and flexural properties of glass fiber reinforced composites increased with the incorporation of silyated montmorillonite, which had been attributed to exfoliation of clay mineral layers and improved adhesion between clay minerals and matrix. The nanocomposites containing silylated montmorillonite also showed better retention of mechanical properties after exposure to seawater as compared to composites containing untreated montmorillonite. The objective of this work was to determine the performance of fiber reinforced epoxy-clay nanocomposites incorporating silylated clay minerals exposed to seawater vis-à-vis the amount of silane grafted on clay minerals. The studies were carried out by exposing the fiber reinforced epoxy-clay nanocomposites to seawater at two different temperatures: 25°C and 55°C, and taking samples out from the water baths periodically and performing tensile and flexural tests. The temperature of seawater was maintained at 25°C, which is the average of temperatures of water in the Indian ocean throughout the year. The accelerated hygrothermal studies were carried out to predict the long-term durability of composites in seawater maintained at 55°C. The Fourier transform infrared (FTIR) spectroscopy was used to identify the nature of interactions of water molecules with epoxy matrix. Scanning electron microscopy (SEM) of fractured surfaces was carried out to

investigate the physical effects of seawater ageing on fibers, matrix and fiber-matrix interface in nanocomposites.

6.2 Materials and experimental work

A commercially available organically modified montmorillonite, Cloisite 15A ®, was surface modified using silane coupling agents: 3-Aminopropyltriethoxysilane (APTES; Purity >98%) and 3-Glycidyloxypropyltrimethoxysilane (GPTMS; Purity > 97%). Cloisite 15A® was purchased from Nanoshel limited, India. The silane coupling agents were purchased from Tokyo chemicals industry, Japan. Dow chemicals international limited, India supplied the Airstone epoxy system. The ECR glass woven roving, WR360 made of Advantex® glass fibers was purchased from Owens Corning, India. The silylation of clay minerals with different quantities of silane coupling agents (i.e. 0.1X, 0.5X, 2X, 4X and 6X, where X is the weight of clay minerals) was performed as per the method presented in our previous work (Sharma et al., 2017). 2 parts per hundred resin (phr) of clay was added to Airstone 780E resin and dispersed by stirring using a glass rod followed by high shear homogenization for 3 min at 20,000 rpm using Ultra-Turrax® T25 (IKA Inc., India). The ultrasonic mixing was done using a probe sonicator (Qsonica Q800, USA). The probe sonicator was operated for 5 min on pulse mode, 80-s on/ 30-s off with shutdown temperature of 40 °C. Subsequently, homogenization and sonication steps were repeated. A stoichiometric amount of Airstone 786 H hardener was added to homogeneous epoxy resin-clay mixture. Degassing of epoxy resin-clay mixture was done for 30 min under vacuum. Finally, the epoxy was infused into the fiber preforms using Vacuum assisted resin infusion molding (VARIM). The glass fiber reinforced nanocomposites were cured at 85°C for 7 h on the heated mould. It should be pointed out that it was not possible to infuse epoxy resin - silylated clay minerals (ratio of the weight of APTES to the weight of clay equal to 6) in glass fiber preforms using VARIM technique. This was because of the very high viscosity of epoxy resin-silylated clay mixture. The terminology used for nanocomposites containing silane modified clay minerals consists of a prefix A (for APTES) or G (for GPTMS) with the concentration of silane in parentheses and a suffix GFRC. The fiber reinforced epoxy composite and fiber reinforced epoxy composite containing organically modified montmorillonite Cloisite® 15A are symbolized as GFRC and C15GFRC, respectively. Transmission electron microscopy (TEM) was carried out using a transmission electron microscope (Tecnai G^2 20 S-Twin, FEI company, US) at an accelerating voltage of 100 kV. Fine particles were deposited on a copper grid for examination.

The specimens were cut and prepared as per the ASTM standards D3037/3039 and D790 for the tensile and flexural tests, respectively. The cut edges of the specimens were sealed by applying two coats of epoxy to inhibit absorption of water by capillary action from open edges. The seawater was prepared following the recommendations of ASTM D1141. The specimens were immersed in simulated seawater maintained at two different temperatures: 25°C ± 1°C and 55°C ± 1°C in stainless steel baths (Daihan WiseBath®, Korea). The pH of the simulated seawater was maintained in the range 8.0-8.2. Three samples of each composition were wiped to remove surface water and then tested immediately on a universal testing machine (Z010 TN Proline, Zwick/Roell, Germany) having a load cell of 10 kN. The tensile and flexural tests were conducted at a crosshead speed of 2 mm/ min and 1.34 mm/ min, respectively. The external surfaces exposed to seawater and fractured surfaces of the flexural test specimens were observed with Scanning electron microscope (JEOL, JSM-6510LV, Japan) equipped with an X-ray energy dispersive microanalyzer (INCA Xact, Oxford Instruments, UK). These surfaces were sputter coated with gold before SEM to avoid electric charging of specimens during the examination. Energy dispersive spectroscopy (EDS) was performed at the inner part of the hygrothermally aged fractured specimens and at the external surfaces exposed to seawater. FTIR spectroscopy of nanocomposites was performed using Perkin-Elmer spectrometer (Spectrum RX-I) in the range 4000 cm^{-1} to 450 cm^{-1} at a resolution of 4 cm^{-1} to detect the chemical modifications in epoxy as a result of seawater ageing.

The gravimetric measurements were performed using an analytical balance (XS104, Mettler Toledo, Switzerland) with a measurement precision of 0.1 mg. The samples were taken out of seawater, wiped with a cloth and dried for 5-7 min under ambient conditions, weighed and replaced in the bath after the measurements. The water uptake in samples was measured using the formula $M(\%) = \frac{M_t - M_0}{M_0} \times 100$

Where M_t is the weight at any time t and M_0 is the initial sample weight.

Fick's law was used to calculate diffusion coefficients because at the beginning the water uptake in all the nanocomposite was linearly proportional to square root of time. The diffusion coefficient (D) was determined by

$$D = \pi \left(\frac{h}{4M_\infty}\right)^2 \left(\frac{M_2 - M_1}{\sqrt{t_2} - \sqrt{t_1}}\right)^2 \left(1 + \frac{h}{L} + \frac{h}{w}\right)^{-2}$$

Where M_∞ is the equilibrium water uptake, M_1 and M_2 are water content at time t_1 and t_2, respectively. L is the length, w is width and h is the thickness of the specimen.

6.3 Results and Discussion

6.3.1 Water uptake

The water uptake curves of glass fiber reinforced epoxy composite (GFRC) samples immersed in seawater at 25°C and 55°C are shown in Figure 6.1(a). The water uptake curve of GFRC at 25°C initially show a linear increase, reaches a plateau and a further a slow increase until saturation is achieved. The two-stage diffusion is known to occur in polymer composites because of two distinct but interrelated phenomenon: swelling due to water absorption and time-dependent relaxation of polymeric chains (Kollia et al., 2015; Manfredi et al., 2008; Mourad et al., 2010; Weitsman, 2012a). However, this behavior has not been observed in fiber reinforced epoxy-clay nanocomposites. Epoxies have an inherent affinity for water because of a large amount of polar -OH groups, which facilitate attractive interaction with polar molecules. The water can transport in fiber reinforced polymer composites by diffusion via voids and microcracks in the matrix and voids along the fiber matrix interface. Further, the absorption of water also leads to swelling of epoxy that would cause debonding of fiber-matrix interfaces and micro cracks in epoxy and enhance the diffusion of water into the composite (Graham-Jones and Summerscales, 2015b; Weitsman, 2012a). A comparison of water uptake curves of glass fiber reinforced epoxy composite (GFRC) and glass fiber reinforced epoxy nanocomposite incorporating Cloisite 15A (C15GFRC) at 25°C indicates that the rate of water diffusion was not significantly altered by an addition of Cloisite 15A® in epoxy, but the maximum water uptake at equilibrium state had decreased slightly. C15GFRC had an intercalated clay structure, in which the clay particles had partially delaminated as shown in Figure 6.1(b). The intercalated epoxy-clay structure does not seem to reduce the diffusion of water in nanocomposites. The diffusion coefficient and equilibrium water uptake for all fiber reinforced clay-epoxy nanocomposites are shown in Table 6.1.

The nanocomposites containing silylated clay minerals had an exfoliated morphology with clay minerals mainly delaminated and randomly distributed in different directions as shown in Figure 6.2(b). The water uptake curves for specimens containing Cloisite® 15A modified using 0.1X, 0.5X, 2X of 3-aminopropyltriethoxysilane are shown in Figure 6.2(a). A noticeable decrease in water uptake by nanocomposites was observed that could be attributed to the improved water barrier properties of epoxy due to exfoliation of clay minerals. The exfoliated clay minerals decrease the rate of diffusion of water by increasing the effective diffusion path and hindering the water ingress (Alamri and Low, 2012; Ivanova et al., 2000; Kim et al., 2005; Saharudin et al., 2016). The water uptake curves for these compositions show no clear trend

of the influence of different quantities of silane coupling agent used during silanization. The water uptake curves of nanocomposites with GPTMS functionalized clay minerals are shown in Figure 6.3. The equilibrium water uptake in these nanocomposites was less than that in C15GFRC, AC15(0.1)GFRC and AC15(0.5)GFRC.

Table 6.1. Diffusion coefficients and equilibrium water uptake of fiber reinforced epoxy-clay nanocomposites immersed in seawater at 25°C and 55°C.

S.No.	Material	Seawater at 25 °C		Seawater at 55 °C	
		Diffusion coefficient, D (mm^2/s)	Equilibrium water uptake (%)	Diffusion coefficient, D (mm^2/s)	Equilibrium water uptake (%)
1.	GFRC	5.51×10^{-8}	2.41	1.01×10^{-8}	1.75
2.	C15GFRC	1.29×10^{-8}	1.68	3.33×10^{-8}	1.58
3.	AC15(0.1)GFRC	1.50×10^{-8}	1.29	5.62×10^{-8}	1.20
4.	AC15(0.5)GFRC	1.47×10^{-8}	1.68	3.41×10^{-8}	1.47
5.	AC15(2)GFRC	1.37×10^{-8}	1.05	5.85×10^{-8}	1.20
6.	AC15(4)GFRC	1.69×10^{-8}	2.54	6.17×10^{-8}	2.87
7.	GC15(0.1)GFRC	2.12×10^{-8}	0.88	3.02×10^{-8}	1.36
8.	GC15(0.5)GFRC	1.40×10^{-8}	1.26	1.00×10^{-8}	0.71
9.	GC15(2)GFRC	1.26×10^{-8}	1.07	3.03×10^{-8}	1.53
10.	GC15(4)GFRC	1.26×10^{-8}	1.44	1.36×10^{-9}	1.83
11.	GC15(6)GFRC	5.66×10^{-9}	1.16	1.17×10^{-9}	1.58

The water uptake curves of AC15(4)GFRC, GC15(4)GFRC and GC15(6)GFRC are shown in Figure 6.4(a). The effect of the polarity of amine groups in APTES treated clay minerals was seen on the water uptake behavior of these nanocomposites. The silylated clays in AC15(4)GFRC and GC15(4)GFRC had an exfoliated and encapsulating platelets morphology in nanocomposites as shown in Figures 6.4(b) and 6.4(c) owing to the formation of siloxane network layers. A significantly higher amount of silane was grafted onto clay mineral layer surfaces according to our previous work(Sharma et al., 2017). The encapsulated platelets have

a larger size than clay particles and impart dramatic improvement in mechanical properties to nanocomposites due to improved adhesion with polymers (Mballa et al., 2013; Mirzataheri et al., 2010; Rong et al., 2006). The rate of water uptake and maximum water uptake at equilibrium state were highest in AC15(4)GFRC. The equilibrium water uptake decreased in the following order GFRC > C15GFRC (Composite containing Cloisite® 15A) ~ AC15(0.5)GFRC (Composite containing Cloisite® 15A treated with 0.5X APTES) > GC15(4)GFRC (Composite containing Cloisite® 15A treated with 4X GPTMS)> AC15(0.1)GFRC (Composite containing Cloisite® 15A treated with 0.1X APTES) ~ GC15(0.5)GFRC (Composite containing Cloisite® 15A treated with 0.5X GPTMS) > GC15(6)GFRC (Composite containing Cloisite® 15A treated with 6X GPTMS) > GC15(2)GFRC (Composite containing Cloisite® 15A treated with 2X GPTMS) ~ AC15(2)GFRC (Composite containing Cloisite® 15A treated with 2X APTES) > GC15(0.1)GFRC (Composite containing Cloisite 15A® treated with 0.1X GPTMS).

It is well accepted that polarity of silanes and the polymer influence the diffusion of water in glass fiber reinforced composites. The results can be interpreted considering the compound effect of (i) hydrolytic reactivity of silanes (ii) extent of filler surface coverage by silane coupling agent or thickness of polysiloxane layer (iii) crosslink density of epoxy matrix. The detailed discussion is given in the following paragraph.

The silane coupling agents are effective for converting hydrophilic clay minerals to hydrophobic species and thus improve their compatibility with polymers (Kim et al., 2009; Mittal et al., 2015; Sharma et al., 2017). A successful hydrophobic silane coating must eliminate hydroxyl groups available on montmorillonite, which are the most common sites for interaction of water promoted via hydrogen bonding. Therefore, a higher amount of grafted silane should decrease the rate of water absorption. The highest water absorption in AC15(4)GFRC can be attributed to an excess of amine groups available at clay –polymer interface regions, which are more hydrophilic than GPTMS as well as onium ions present in Cloisite 15A. However, the equilibrium water uptake of AC15(2)GFRC was smaller than AC15(0.1)GFRC and AC15(0.5)GFRC, which may be attributed to a higher increased crosslink density of AC15(2)GFRC. The glass transition of epoxy reaches maximum temperature when it is completely cured. A higher crosslink density of epoxy in the case of AC15(2)GFRC was evident from the absence of residual cure peak in DSC studies, reported in previous work (Sharma et al., 2017). In this case, a completely cured network will have fewer unreacted polar groups (hydroxyl groups, amine groups), and absorbed water molecules will not tend to cluster together. A higher crosslink density also decreases the nanovoids in epoxy,

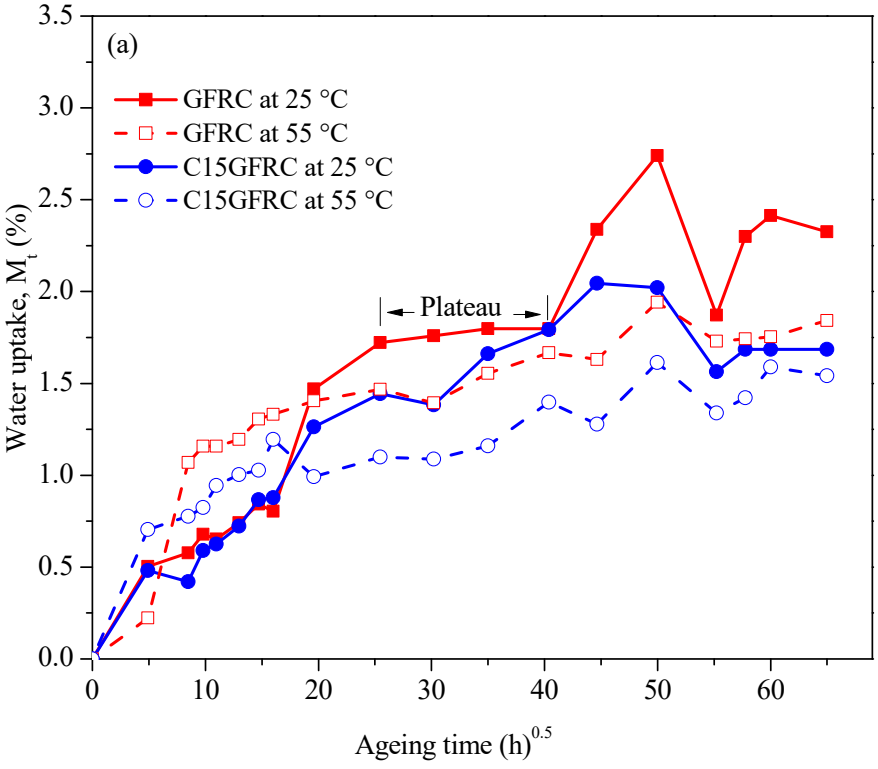

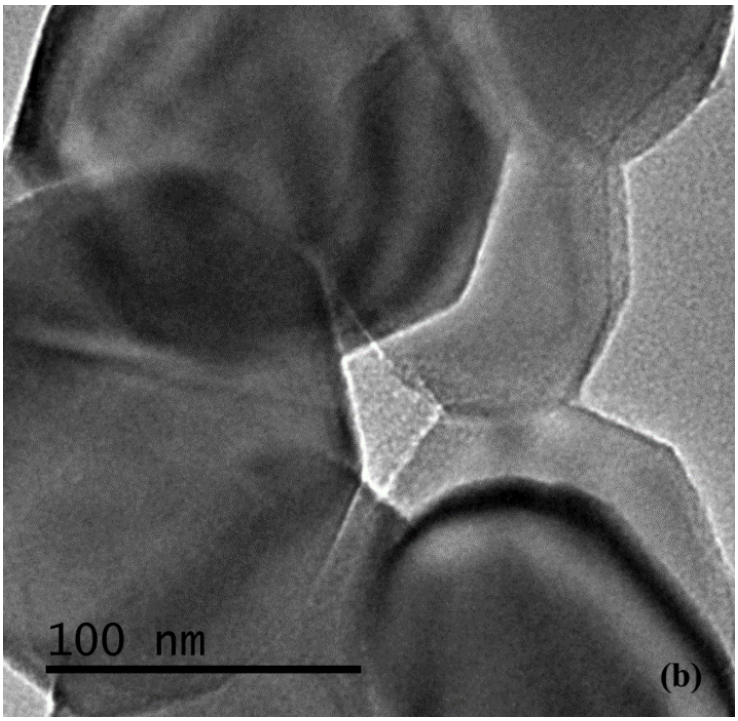

Figure 6.1 (a) Water uptake for GFRC and C15GFRC samples immersed in seawater at 25°C and 55°C (b) TEM micrograph of C15GFRC

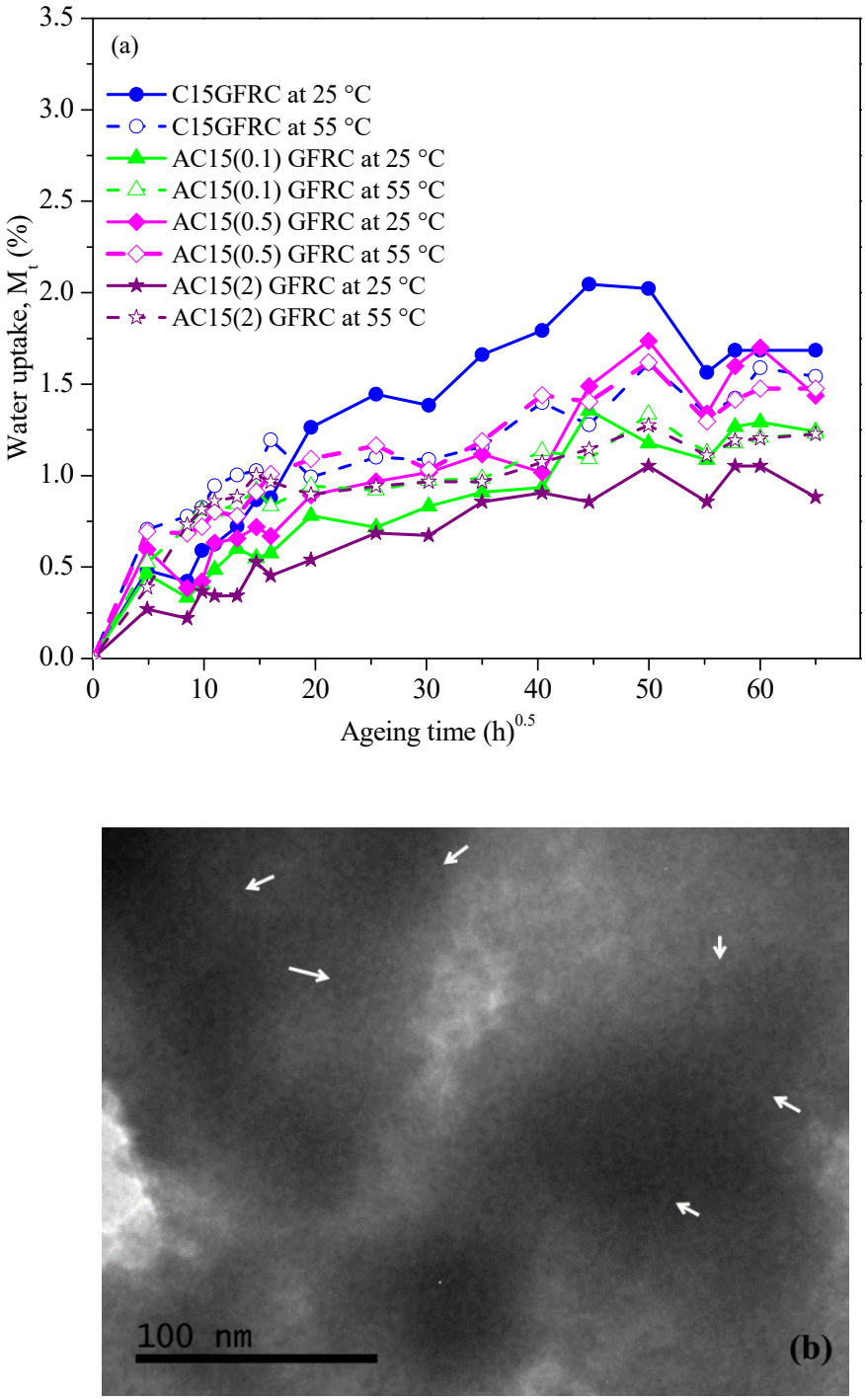

Figure 6.2 (a) Water uptake for AC15(0.1)GFRC, AC15(0.5)GFRC, AC15(2)GFRC samples immersed in seawater at 25°C and 55°C (b) TEM micrograph of AC15(2)GFRC.

which are occupied by water during absorption (Chatterjee and Gillespie, 2008; Sethi and Ray, 2015). The water uptake in epoxy would decrease with an increase in crosslink density of epoxy due to a decrease in sorption sites in epoxy. GC15(4)GFRC and GC15(6)GFRC had lower equilibrium water uptake as compared to other compositions. This can be attributed to lower reactivity of GPTMS as compared to APTES. The diffusion coefficients for GFRC samples were 5.51×10^{-8} mm^2/s and 1.01×10^{-8} mm^2/s in seawater at 25°C and 55°C, respectively. Generally, the rate of water uptake in fiber reinforced nanocomposites, characterized by diffusion coefficient, increased with an increase in temperature of seawater. The higher rates of diffusion with an increase in temperature of water have been also reported by other researchers also (Ellyin and Rohrbacher, 2000; Grammatikos et al., 2015; Mourad et al., 2010; Ray, 2006; Surathi and Karbhari, 2006).

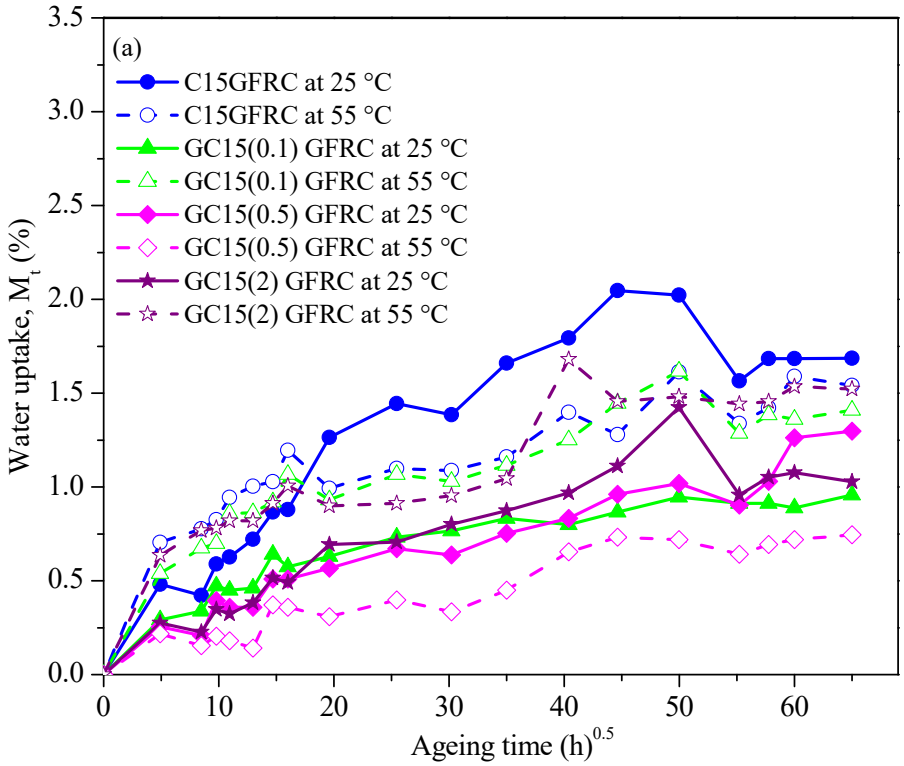

Figure 6.3 Water uptake for GC15(0.1)GFRC, GC15(0.5)GFRC, GC15(2)GFRC samples immersed in seawater at 25°C and 55°C

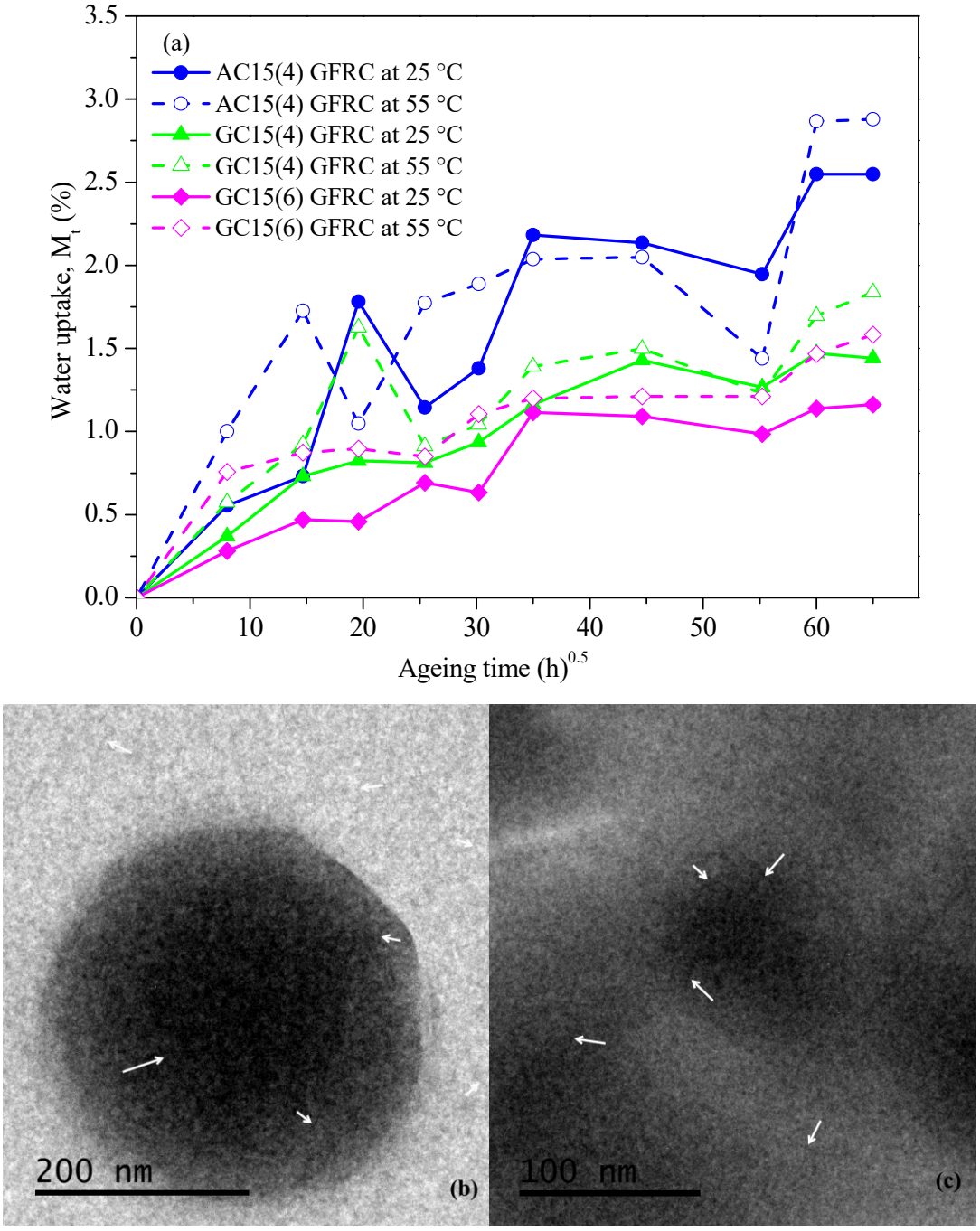

Figure 6.4 (a) Water uptake for AC15(4)GFRC, GC15(4)GFRC, GC15(6)GFRC samples immersed in seawater at 25°C and 55°C (b) TEM micrograph of AC15(4)GFRC and (c) TEM micrograph GC15(4)GFRC.

The equilibrium water uptake and the diffusion coefficient for C15GFRC immersed in seawater at 55°C were 1.58% and 3.33×10^{-8} mm^2/s, respectively. An anomaly in the equilibrium water uptake of nanocomposites immersed in seawater at 55°C was observed. The equilibrium water uptake in GFRC, C15GFRC, AC15(0.1)GFRC, AC15(0.5)GFRC, GC15(0.5)GFRC and GC15(4)GFRC after exposure to seawater at 55°C was less that at 25°C. This decrease in equilibrium water uptake can be explained by taking into account two competing effects: an increase in the rate of water uptake and loss of mass due to chemical degradation. The chemical degradation of epoxy cause roughening of the exposed surface and will not only lead to loss of weight because of leaching away of epoxy but also can help water uptake by facilitating diffusion of water by capillary action and also through direct transfer through the voids created in the composite. The roughening of the surface would also increase the surface area for water diffusion, and hence influence the water uptake rate and equilibrium moisture content. Another possible reason of a decreased water absorption may be restricted swelling of epoxy in water at 55 °C, which can decrease water uptake in the epoxy matrix because of hydrostatic pressure induced by swelling of epoxy (Derrien and Gilormini, 2009). The swelling of the epoxy matrix may be non-uniform and it is expected that the un-swollen part of epoxy and the glass fibers would exert a compressive force on the swollen region, causing the further swelling to be mainly along the direction of diffusion. Therefore it is not unreasonable to assume that the equilibrium water uptake is affected by the internal stresses due to restricted swelling of epoxy. Further studies are planned to ascertain the reasons for the higher final equilibrium uptake at 25°C vis a vis 55°C. The equilibrium water uptake for specimens immersed in seawater at 55°C decreased in an order AC15(4)GFRC > GC15(4)GFRC> C15GFRC ~ GC15(6)GFRC > GC15(2)GFRC > AC15(0.5)GFRC > GC15(0.1)GFRC > AC15(0.1)GFRC ~ AC15(2)GFRC > GC15(0.5)GFRC.

An elemental analysis carried out at the surface exposed to seawater using SEM-EDS revealed the presence of the elements Na, Cl, Ca, K, Mg, Sr as shown in Figure 6.5. The traces of other elements, which were dissolved in distilled water to prepare the simulated seawater were also observed. The accumulation of salts on the exposed surface increased after prolonged immersion in seawater. It was likely that the pores over the exposed surface get blocked due to the accumulation of ions, and this would inhibit water uptake of glass fiber reinforced epoxy composites after prolonged exposure to simulated seawater. The accumulation of salts during hygrothermal exposure can decrease the water reactivity at the exposed surface. To determine whether seawater ageing caused chemical and physical damage to the fiber reinforced epoxy-

clay nanocomposites after exposure to seawater at 55°C for 120 days, the samples were examined using Fourier transform infrared (FTIR) spectroscopy and Scanning electron microscopy (SEM).

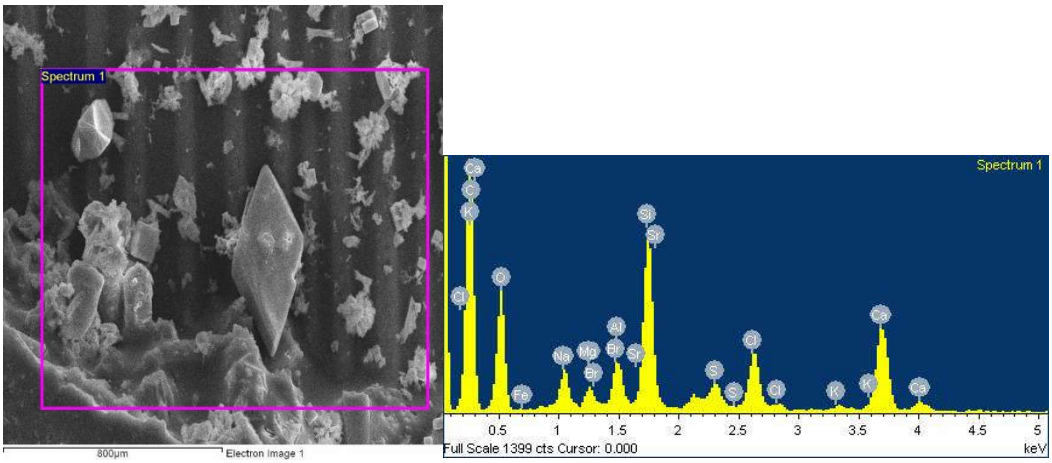

Figure 6.5 SEM-EDS results of fiber reinforced epoxy composites at surface exposed to seawater

6.3.2 Fourier transform infrared spectroscopy

The absorbed water exists in a polymer composite in different forms: highly mobile free water that fills the nanovoids in the matrix and fiber/matrix interface and, the water bonded to hydrophilic sites in epoxy. The water can interact with epoxy chains by vander Waals, hydrogen bonding and dipole-dipole interactions (Takeshita et al., 2014). The water-epoxy interactions can be studied by monitoring the changes in IR spectrum. The FTIR spectra of amine-cured epoxies in dry condition show a broad spectrum in the wavenumber range of 3100-3600 cm^{-1} which is attributed to the presence of alcohol, amine or carboxylic acid (González-González et al., 2012; Sugiman et al., 2016). The FTIR spectra of GFRC and C15GFRC after 120 days ageing in seawater at 55°C are shown in Figure 6.6. The increase in the intensity of bands associated with bonded –OH stretching vibrations indicate that water molecules were strongly bound with epoxy through hydrogen bonding (Cotugno et al., 2001; Musto et al., 2000). New hydroxyl groups formed as a result of hydrolysis increased the intensity of the corresponding infrared bands. The increase in the intensity of bands associated with alkyl stretching (2950 cm^{-1} – 2850 cm^{-1}), and carbonyl group (1605 cm^{-1}) further verify the contention that the epoxy was undergoing chemical hydrolysis. Hydrolysis can change the molecular weight of epoxy with a consequent drop in both stiffness and strength of polymer (Phua et al., 2011). Another possible effect of hydrolysis is swelling of epoxy, which can induce residual stresses and influence the mechanical behavior of composites (Garg et al.,

2016; Mourad et al., 2010; Ray, 2006). In FTIR spectra of C15GFRC, the increase in the intensity of band associated with hydrogen bonding of water was less than that in GFRC. This indicates better barrier properties of composites containing clay minerals. The FTIR spectra of the fiber reinforced nanocomposites containing silane treated clay minerals are shown in Figure 6.7. The polarity of silane coupling agents influenced the increase in the intensity of bands associated with bound water. A greater increase in the intensity of absorbance band in case of AC15(4)GFRC indicate a more significant number of bound water molecules than in GC15(4)GFRC. GC15(2)GFRC, AC15(0.1)GFRC and AC15(0.5)GFRC showed little change in intensity of this band. Moreover, the FTIR results were in good agreement with the results of water uptake studies discussed in the previous section.

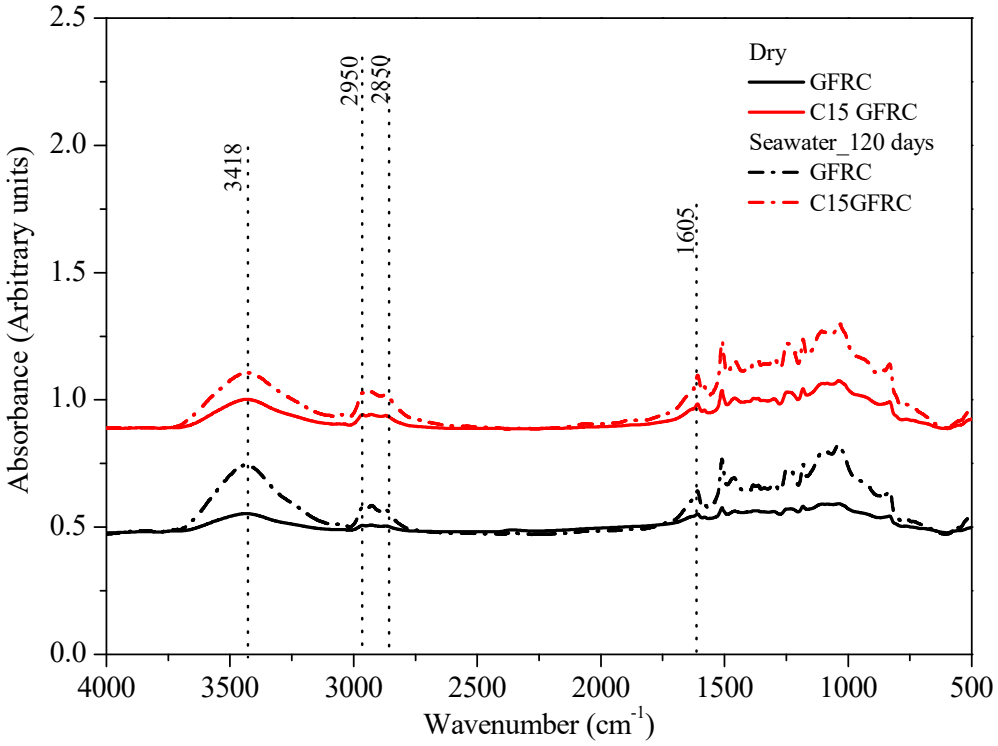

Figure 6.6 FTIR spectra of GFRC and C15GFRC

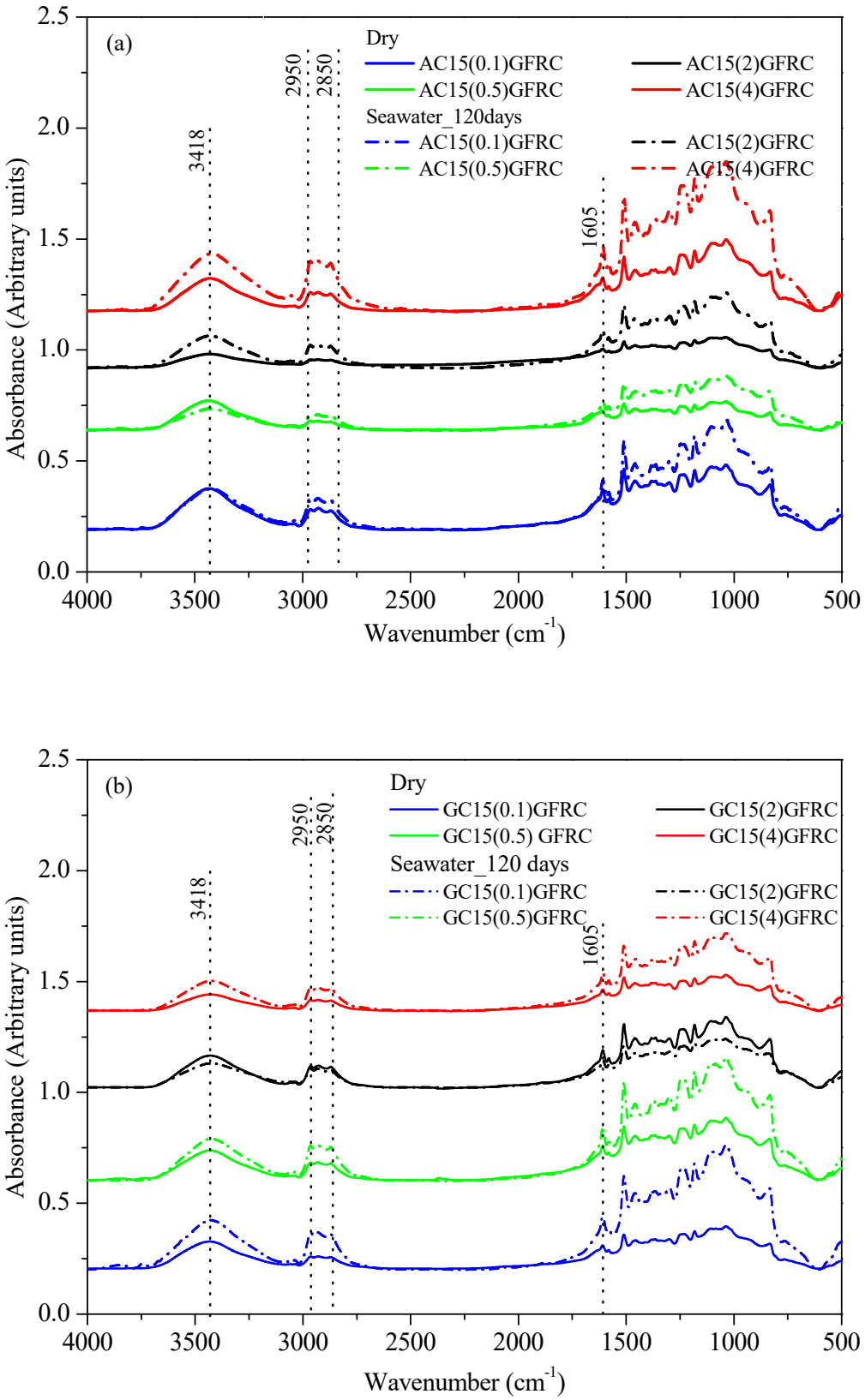

Figure 6.7 FTIR spectra of fiber reinforced epoxy- silylated clay nanocomposites

6.3.3 Scanning electron microscopy

The swelling of epoxy is often accompanied with (i) failure of matrix due to microcracks (ii) debonding of fibers from the matrix. After 120 days of immersion in seawater at 55 °C, GFRC showed significant swelling, fiber debonding and matrix cracking (Figure 6.8(a)). Figure 6.8(b) shows the fractured surfaces of C15GFRC after 120 days of ageing in seawater 55 °C. The nanophased matrix seem to be protect the fiber-matrix interface. The fractured surface of the fiber reinforced nanocomposites containing APTES treated clay minerals is shown in Figures 6.8(c) and 6.8(d). The failure in these composites was localized and less fiber breakage was observed in comparison to GFRC and C15GFRC. The matrix hydrolysis and debonding at the fiber-matrix interface region were the primary reasons for the reduction in strength of all nanocomposites. The cracks indicating embrittlement of epoxy matrix, pot holes, and river marks were also observed. In the case of AC15(4)GFRC, a lot of pot holes were formed on the matrix as shown in Figure 6.9. The salt ions (Na^+, Cl^-, K^+) would be able to penetrate through these microvoids and cracks, along with the channels. This can cause severe degradation of the matrix, fibers and fiber-matrix interfaces (Capiel et al., 2017; Hu et al., 2016; Wei et al., 2011). This would also accelerate the hydrolysis of epoxy by attacking the molecular chain. The accumulation of salt at the fiber-matrix interface as shown in Figure 6.10 can lead to embrittlement of E-CR glass fibers and damage the adhesion between glass fibers and epoxy. Also, the diffusion of chloride ions around the fiber matrix interface in the composite is the main reason for corrosive degradation of glass fibers (Kootsookos and Mouritz, 2004; Wei et al., 2011). It was observed that the surface of glass fibers had become rough, which can be due to the removal of sizing from the glass fiber and cleavage of chemical bonds with epoxy, but swelling in E-CR glass fibers was not observed. The size of the salt crystals increased after prolonged immersion in seawater as shown in Figure 6.11. The surface of the fiber reinforced epoxy-clay nanocomposites was analyzed using energy dispersive spectroscopy (EDS). The weight percentage of chemical elements present are shown in Table 6.2. It was clear from a comparison of the elemental changes (Al, Ca, Mg, Si) that glass fibers were affected by hygrothermal ageing. The variation of C shown in Table 6.2 can be attributed to the presence of residual matrix particles on the surface of the fibres. The swelling of matrix, and increase fiber debonding was clearly seen in composites exposed to seawater after 120 days.

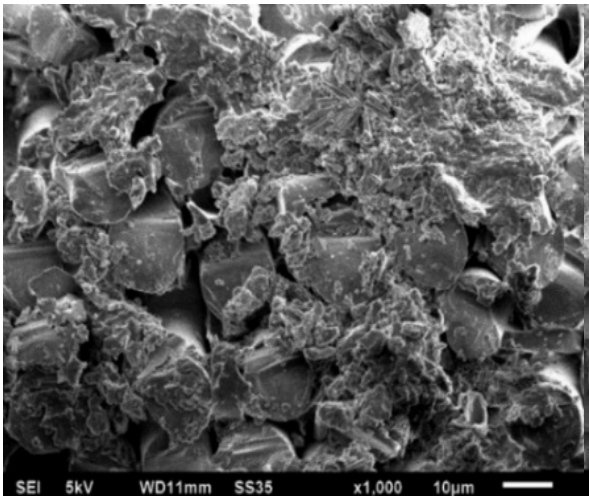

(a) GFRC after 120 days

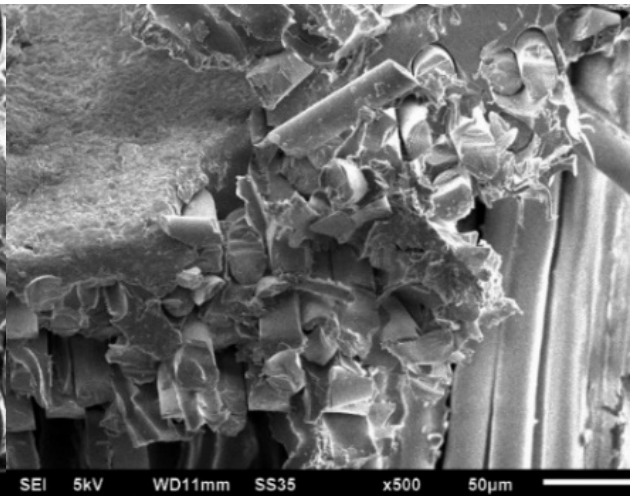

(b) C15GFRC after 120 days

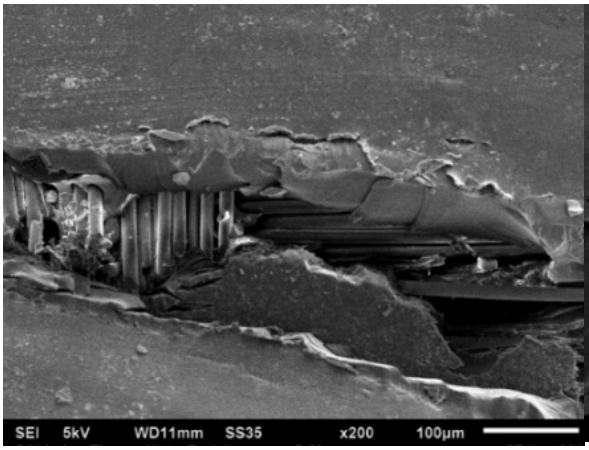

(c) AC15GFRC(0.1) after 120 days

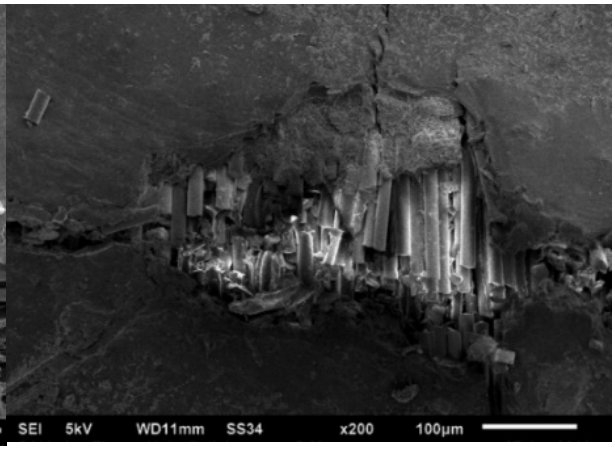

(d) AC15GFRC(2) after 120 days

Figure 6.8 SEM micrographs of nanocomposites showing fiber-matrix interfaces

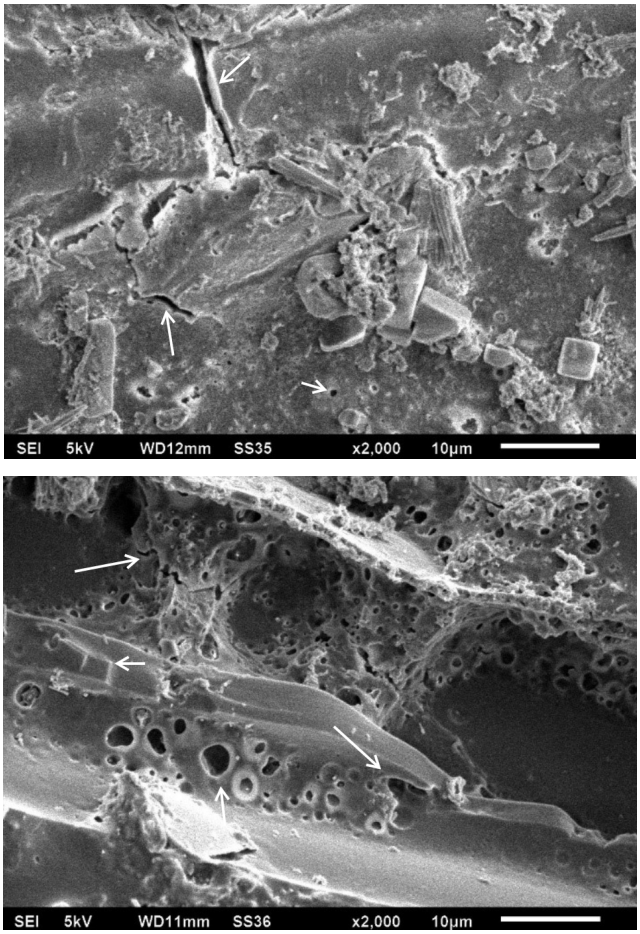

Figure 6.9 SEM micrographs showing pot holes on surface of epoxy matrix (a) GC15(0.1)GFRC, (b) AC15(4)GFRC after exposure to seawater at 55 °C

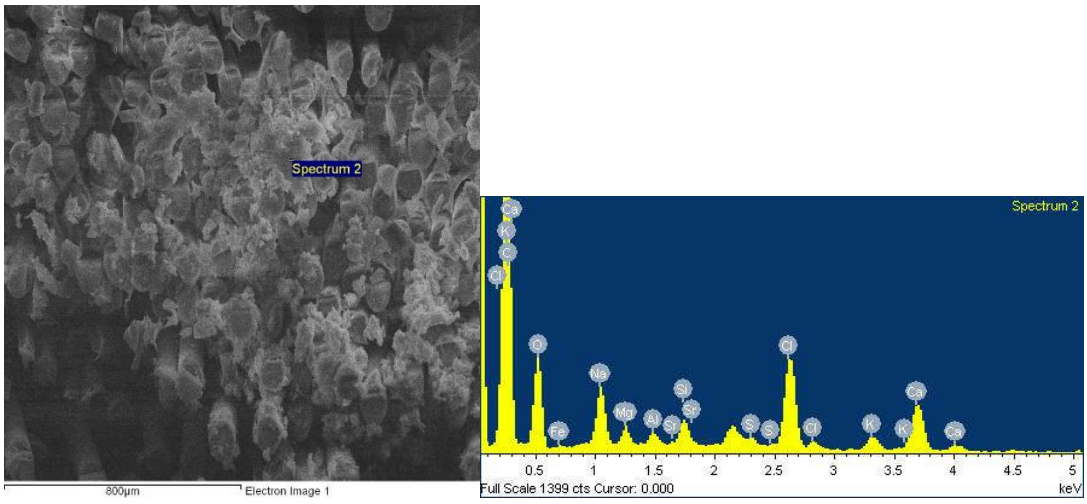

Figure 6.10 SEM-EDS results of flexural fracture surfaces after ageing in seawater at 55°C

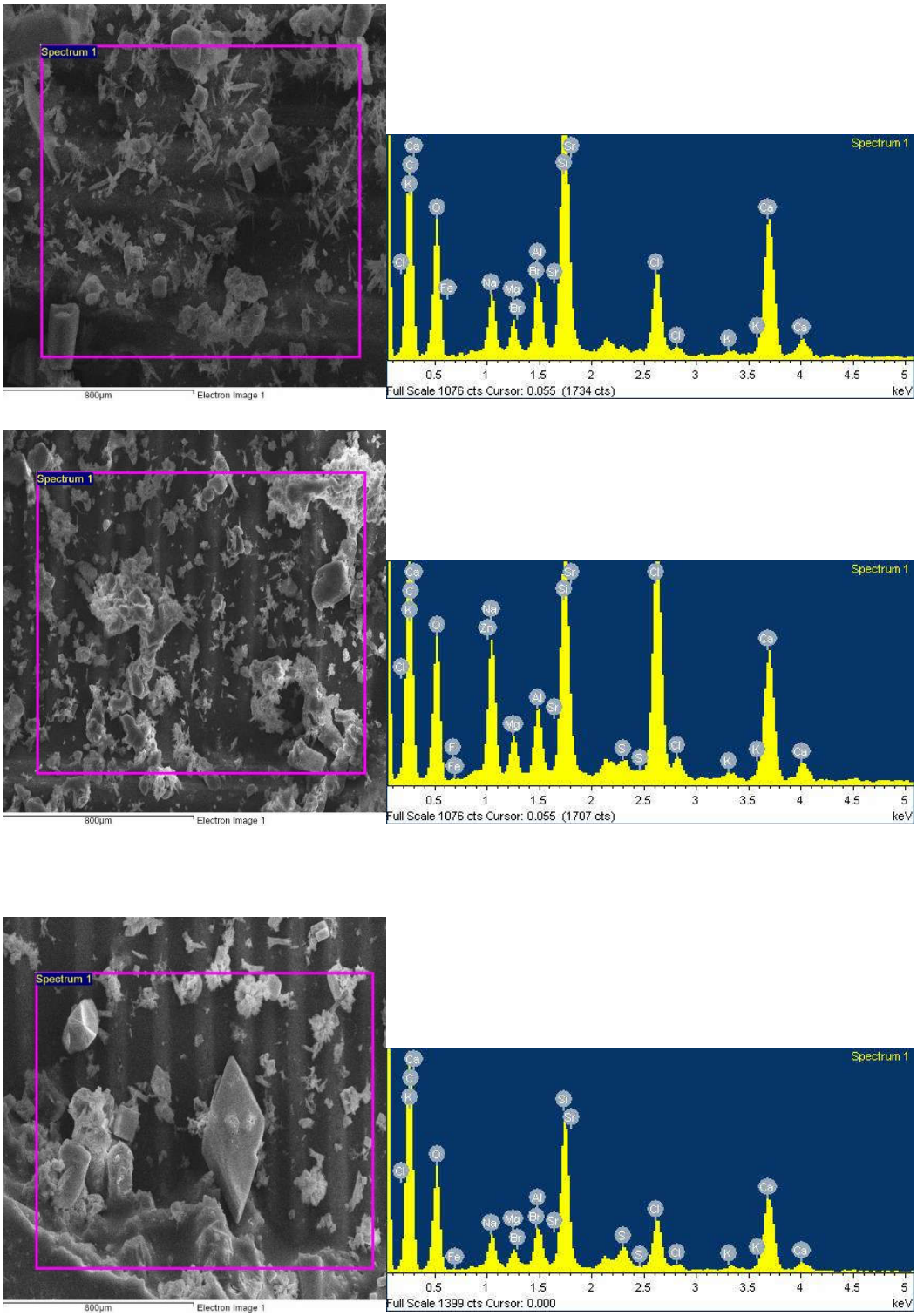

Figure 6.11 Seawater salt traces on surface of fiber reinforced epoxy-clay nanocomposites after 60 days and 120 days

Table 6.2 Percent composition of chemical elements at surface of fiber reinforced epoxy-clay nanocomposites

	C	O	Mg	Al	Si	Ca
Un-aged	42.76	33.23	0.99	1.94	8.06	6.73
60 days	44.77	27.93	1.06	1.48	5.55	4.96
120 days	51.17	31.59	0.66	0.86	5.28	4.37

6.3.4 Residual tensile and flexural properties

It is well known that a decrease in load carrying capacity of fiber reinforced polymer composites during hygrothermal ageing depends on temperature, immersion time and media. The hydrolytic damage in composites tends to increase with an increase in temperature and immersion time. The high pH of seawater and the presence of ions cause degradation of composite. The degradation of fiber reinforced composite in seawater can occur by a combination of mechanisms ranging from matrix-cracking, pitting, hydrolysis, matrix plasticization, fiber leaching, fiber fracture and fiber-matrix interface debonding. A high temperature of seawater can accelerate the damage caused by these mechanisms.

6.3.4.1 Effect of incorporation of Cloisite 15A®

The tensile modulus and tensile strength of GFRC and C15GFRC after immersion in seawater at two different temperatures, i.e. 25°C and 55°C, for 30 days, 60 days and 120 days are shown in Figures 6.13 and 6.14. The tensile modulus of GFRC and C15GFRC specimens immersed in seawater at 25°C after 30 days had increased by 21.5% and 12.5%, respectively. The tensile modulus of GFRC and C15GFRC specimens increased by 10% and 5.5% after immersion in seawater at 55 °C. The stress vs. percent elongation curves for representative samples are shown in Figure 6.12. A change in slope of stress vs elongation curves and a decrease in elongation at break of composites upon seawater ageing can be seen. The tensile modulus tends to increase with an increase in ageing time. It is possible that the presence of salts and continuous use of sodium hydroxide to maintain the pH of simulated seawater attack the E-CR glass fibers which led to embrittlement of glass fibers and fiber-matrix interphase (Bergeret et al., 2009). Exposure to seawater can cause plasticization and swelling of epoxy (Garg et al., 2016; Mourad et al., 2010; Ray, 2006; Thomason and Ali, 2009). The swelling of epoxy is

restricted due to weave architecture of glass fibers and therefore, the elastic deformation of glass fibers under external load may also be constrained. The other reason for an increase in tensile modulus of composites during initial stages of ageing can be additional cross-linking caused by the catalytic effect of Na^+ ions and water over post-curing reaction and interaction of water molecules with epoxy via multiple hydrogen bonds (Garg et al., 2016; Starkova et al., 2013; Sugiman et al., 2016; Wang et al., 2015; Zhou and Lucas, 1999).

The decrease in tensile strength of GFRC and C15GFRC was not significant in specimens immersed in seawater at 25°C even after a period of 120 days. The fiber reinforced epoxy-clay nanocomposites showed better resistance to deleterious effects of seawater ageing. The tensile strength of GFRC and C15GFRC decreased by 33.6% and 22%, respectively after 30 days of immersion in seawater at 55 °C. After ageing for 120 days in seawater at 55 °C, the tensile strength of both GFRC and C15GFRC specimens decreased by 48%.

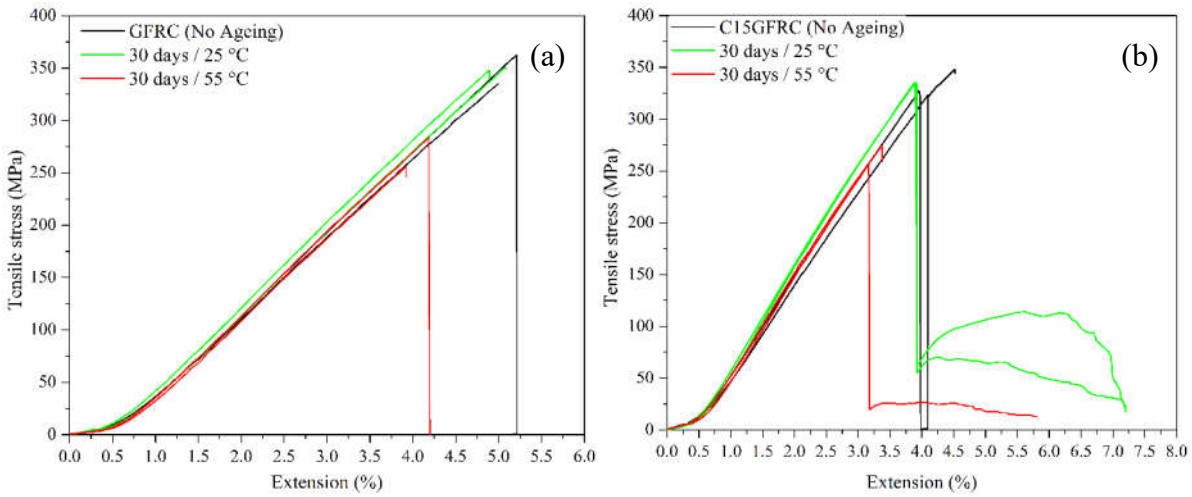

Figure 6.12 Tensile stress vs percentage extension in (a) GFRC (b) C15GFRC

The flexural properties of GFRC and C15GFRC as a function of immersion time and ageing temperature are shown in Figures 6.15 and 6.16. The flexural modulus and flexural strength of unaged GFRC specimens were 13 GPa and 253 MPa, respectively. The flexural modulus of GFRC immersed in seawater at 25°C for 120 days increased by 83%, whereas flexural strength increased by 43%. A similar increase in GFRC specimens was also observed after ageing in seawater at 55 °C, with flexural modulus increasing by 83% after ageing for 60 days only and stabilizing after that. The flexural strength had increased by 19% after ageing of 30 days and showed no significant change after 30 days. The C15GFRC specimen also showed an increase in both flexural modulus and flexural strength after hygrothermal ageing. The

increase in flexural properties can be attributed to the additional secondary cross-linking of epoxy and an increase in the modulus of elasticity of composite after seawater ageing. It is generally accepted that the absorption of water in polymer composites/ nanocomposites results in deterioration of mechanical properties (Saharudin et al., 2016; Weitsman, 2012b), but contrasting results have also been reported (Hossain et al., 2011; Zainuddin et al., 2010, 2009).

6.3.4.2 Effect of incorporation of silylated clay minerals

The effect of seawater ageing on tensile modulus and tensile strength of fiber reinforced composites containing silane treated clay minerals is shown in Figures 6.13 and 6.14. The tensile modulus of AC15(0.1)GFRC, AC15(0.5)GFRC, AC15(2)GFRC, GC15(0.1)GFRC, GC15(0.5)GFRC, GC15(2)GFRC increased with increase in ageing time. The tensile strength of the nanocomposites immersed in seawater at 25°C as well as at 55°C decreased with increase in ageing time. In case of fiber reinforced epoxy nanocomposites containing silane treated clay minerals, the tensile strength of AC15(0.1)GFRC and AC15(0.5)GFRC was unaffected after 30 days of immersion in seawater at 25 °C, but the tensile strength of AC15(2)GFRC and GC15(0.5)GFRC decreased by 6.5% and 11%, respectively. After 120 days of ageing, the decrease in tensile strength of AC15(0.1)GFRC, AC15(0.5)GFRC was not the significant but tensile strength of AC15(2)GFRC and AC15(4) GFRC decreased by 20% and 38%, respectively. Also, after 120 days, only AC15(0.1)GFRC and AC15(0.5)GFRC showed better strength retention in comparison to GFRC and C15GFRC. A higher water intake rate in case of AC15(4)GFRC resulted in higher degradation of tensile strength as compared to other nanocomposites containing APTES treated clay minerals. The tensile strength of GC15(0.5)GFRC, GC15(4)GFRC and GC15(6)GFRC also decreased significantly.

The tensile modulus and tensile strength of fiber reinforced epoxy nanocomposites incorporating clay minerals functionalized using 4X and 6X silanes concentrations decreased significantly irrespective of the type of silane. In fiber reinforced epoxy-silylated clay nanocomposites, the hydrolytic stability of the siloxane network is an important factor. The penetration of water into the interphase can hydrate the Si-O-Si and Si-O-C bonds, and a variety of oligomeric species are formed within the crosslinked siloxane layer (DiBenedetto, 2001). The oligomers would be desorbed by diffusion out of the crosslinked network due to long-term exposure to seawater at high temperature. The desorption of the siloxane network from both the clay surface and epoxy will create voids which will increase chemical degradation of the epoxy and fiber-matrix interfaces. A higher decrease in tensile strength of nanocomposites can be attributed increased hydrolytic damage to clay-siloxane linkages due to the presence of

unreacted polar groups at clay mineral surface. The size of voids created due to hydrolytic degradation of interface would also depend on the morphology of clay minerals in epoxy. The loss of encapsulated clay particles will lead to relatively bigger size voids as compared to those formed by loss of fully exfoliated clay mineral layers. This, in turn, will further increase the exposed surface area, where water molecules can cluster with each other. The clustering of water molecules in voids during hygrothermal ageing can cause plasticization and would lead to degradation of mechanical properties. Iglesias et al. (Iglesias et al., 2002) observed that the rate of hydrolytic degradation in glass fiber- siloxane linkages were highest in APTES treated glass fibers in comparison to fibers treated with other silane coupling agents. This led to a severe loss of the tensile strength of composites after exposure in water for 46 h. In another study, Salmon et al., 1997 had concluded that both APTES and GPTMS are reactive and cannot protect glass fiber reinforced composites from waterborne degradation.

The tensile strength of AC15(0.1)GFRC, AC15(0.5)GRFC and AC15(2)GFRC decreased by 52%, 41% and 57%, respectively after exposure to seawater at 55°C for 30 days. AC15(0.5)GFRC continued to perform better than other compositions. The tensile strength of fiber reinforced epoxy nanocomposites containing GPTMS treated clay minerals also decreased with an increase in ageing time. The tensile strength of GC15(0.1)GFRC and GC15(0.5)GFRC decreased by 12% and 24%, respectively after ageing in seawater at 55°C for 30 days. After 120 days, the tensile strength of all nanocomposites exposed to seawater at 55°C had decreased significantly. GC15(2)GFRC had notably, exhibited the lowest rate of water diffusion and had best retention of mechanical properties among other nanocomposites containing GPTMS treated clay minerals. In case of nanocomposites containing clay minerals modified using high quantities of APTES/GPTMS, the decrease in tensile strength after ageing in seawater at 25°C/ 55°C was significantly higher than other compositions (GFRC, C15GFRC, AC15(0.1)GFRC, AC15(0.5)GFRC, GC15(0.1)GFRC, GC15(0.5)GFRC, GC15(2)GFRC, GC15(6)GFRC).

The flexural strength of specimens increased with an increase in immersion time in seawater at 25 °C. At 55 °C, only the nanocomposites containing clay minerals modified using a higher concentration of APTES showed significant degradation in flexural strength, which can be attributed to plasticization of matrix and fiber-matrix debonding.

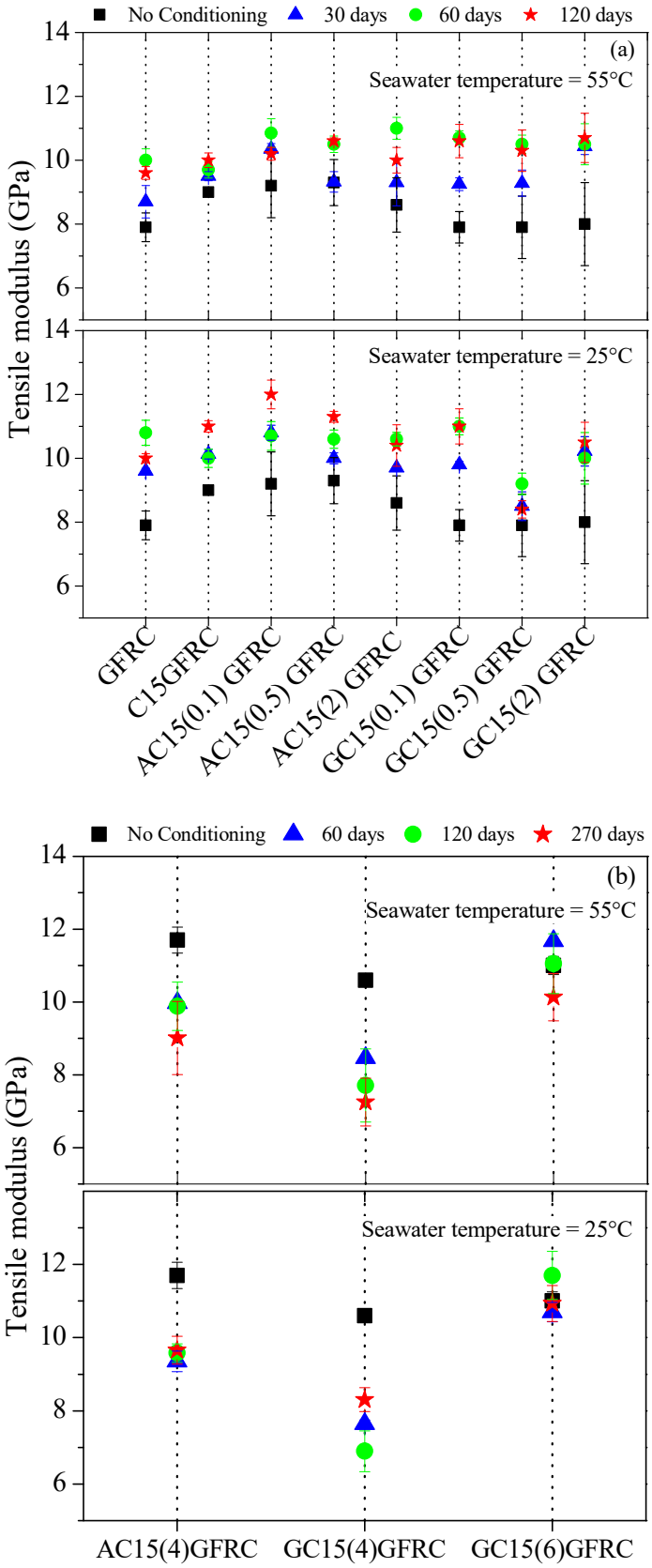

Figure 6.13 Tensile modulus of all compositions after ageing in seawater at different temperatures

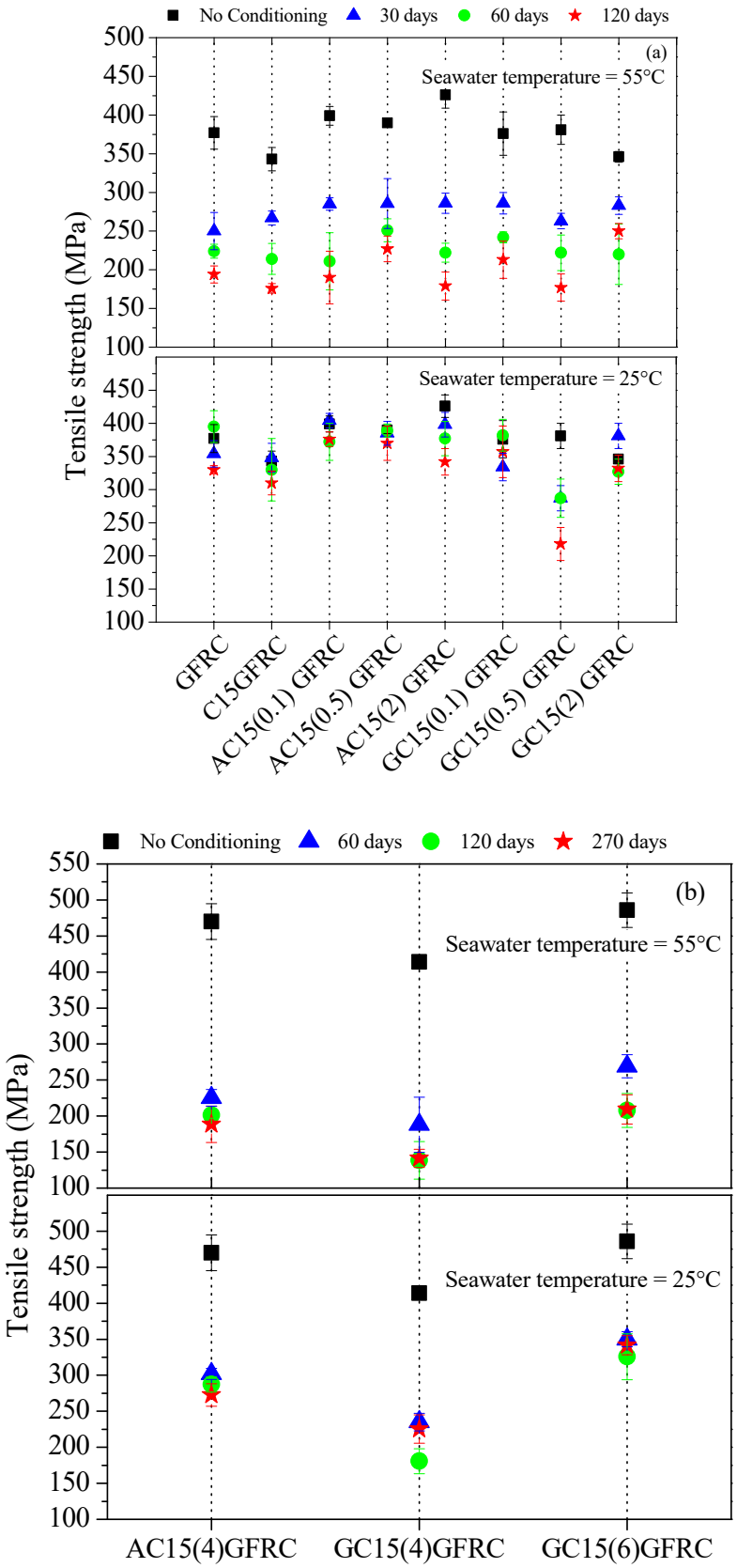

Figure 6.14 Tensile strength of all compositions after ageing in seawater at different temperatures

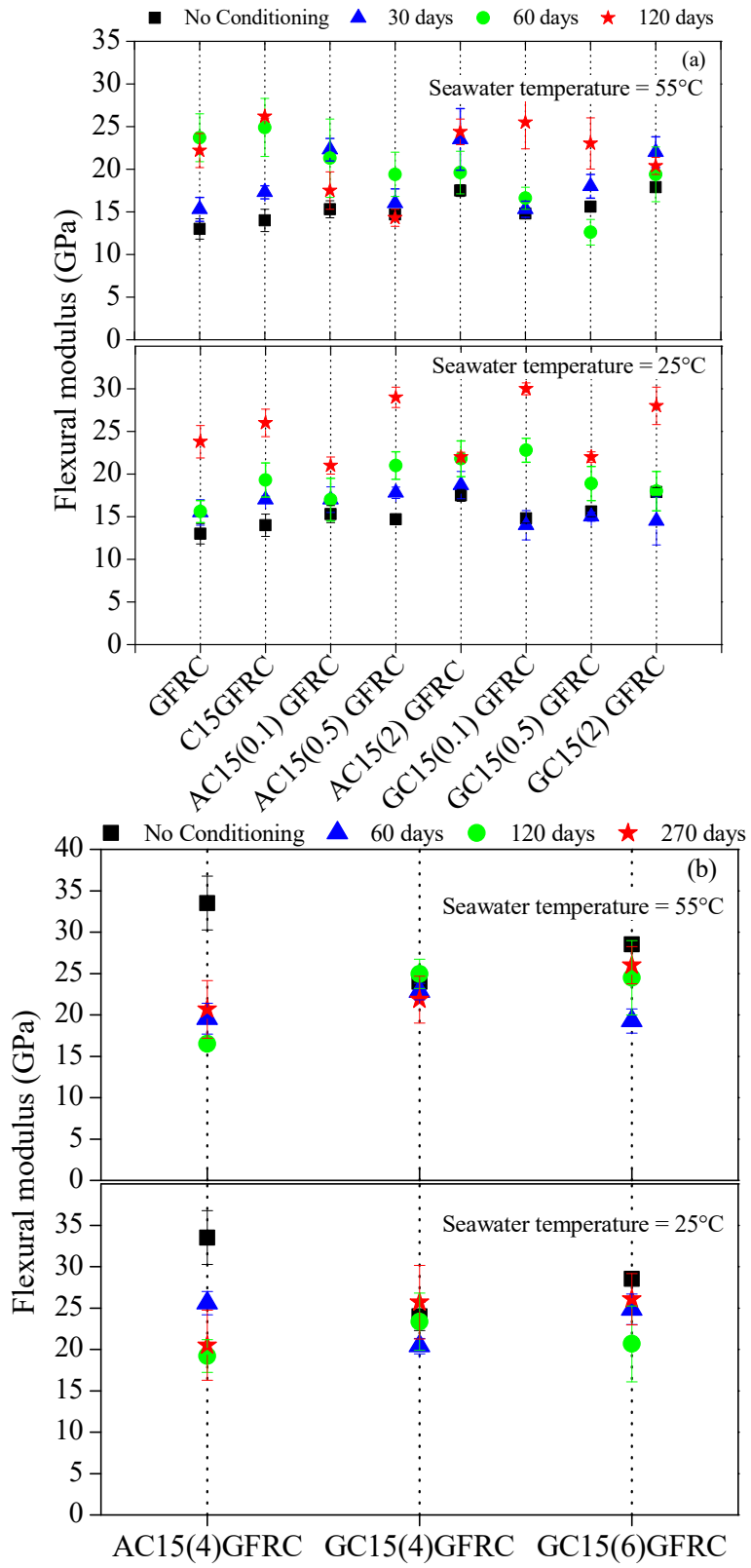

Figure 6.15 Flexural modulus of all compositions after ageing in seawater at different temperatures

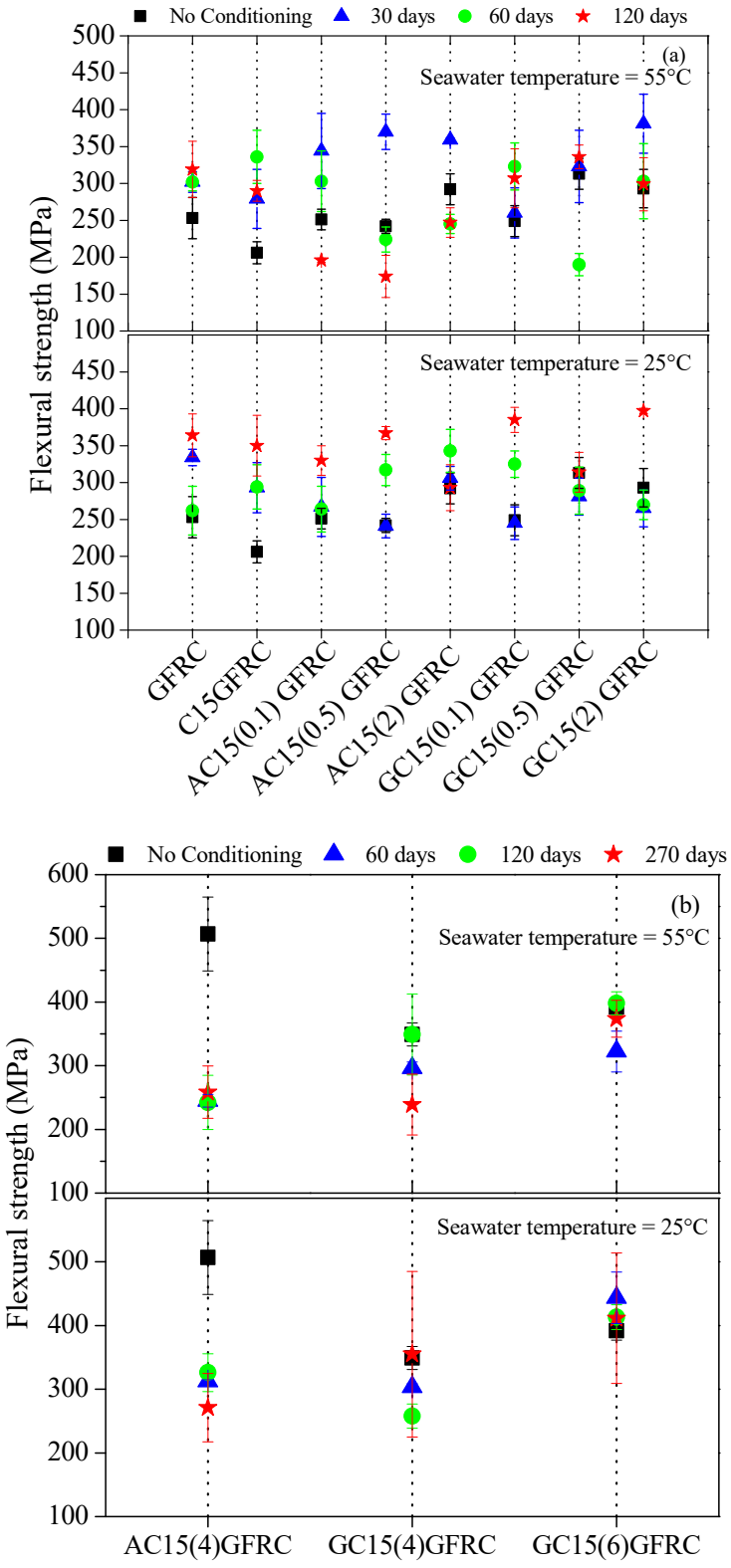

Figure 6.16 Flexural strength of all compositions after ageing in seawater at different temperature

6.4 Closing remarks

The rate of diffusion of water in fiber reinforced composites incorporating silylated clay minerals decreased as compared to glass fiber reinforced epoxy composites, as well as composites containing non-silane treated Cloisite® 15A. Various competing phenomena such as water wicking along glass fibers, hydrolysis, swelling induced by bound water, increase in effective diffusion path due to clay mineral layers, inhibition effect of ions in seawater, chemical degradation in epoxy and reactivity of silane can cause deviation from simple Fickian diffusion. The diffusion of seawater in all composites increased with an increase in exposure time and temperature. An assumption of neglecting hydrolytic degradation of epoxy, which would result in weight loss, was made while analyzing the diffusion data.

The polarity of silane groups and morphology of clay minerals in epoxy significantly influence the durability of the nanocomposite in seawater. The nanocomposites incorporating clay minerals modified using small quantities of silane coupling agents exhibited higher retention of tensile and flexural strength after hygrothermal exposure. The nanocomposites containing clay minerals surface modified with ratio of weight of 3-aminopropyltriethoxysilane (APTES) to that of weight of clay mineral equal to 0.1 and 0.5 showed excellent long-term durability after ageing in seawater at 25°C and 55°C because of strong covalent bonds at the interphase and an exfoliated structure, which improved the resistance to seawater penetration. The nanocomposites containing silylated clay minerals modified using 3-glycidyloxypropyltrimethoxysilane (GPTMS) showed good retention of tensile and flexural strength after exposure to seawater because of lower reactivity of glycidyl groups with water molecules.

The modification of clay minerals with a ratio of the weight of APTES to that of clay greater than 4 and the ratio of the weight of GPTMS to that of clay greater than 6 pose a big challenge in the processing of fiber reinforced epoxy-clay nanocomposites due to the high viscosity of epoxy resin – clay mixture. More importantly, use of higher concentration of APTES as well as GPTMS lead to decrease in barrier properties and poor long-term durability of fiber reinforced nanocomposites. An excess of silane coupling agents leache out from the composite. The relatively bigger size of voids left behind would lead to plasticization effect of accumulated water in the voids. Also, if the silane coated particles remain in the composite, they will act as stress concentration sites when mechanical load is applied. In general, irrespective of the concentration of reactive silane coupling agents and type, the coupling agents form linkages between organic and inorganic materials by an interpenetrating Si-O-Si

and Si-O-C network, which can desorb after long-term exposure to hygrothermal environment causing loss of strength in composites. Therefore care should be taken when choosing the type of silane coupling agent and more importantly the quantity of silane used for surface modification of clay minerals.

Chapter 7 Conclusion and recommendations for future work

In this work, properties of hybrid glass fiber reinforced epoxy-clay nanocomposites incorporating a small amount of organically modified montmorillonite Cloisite® 15A have been investigated. Some key aspects of hybrid nanocomposites are specifically studied, such as uniform dispersion of clay minerals in the matrix by selecting process parameters, surface treatment of clay minerals with silane coupling agents compatible with epoxy, effect of grafted silanes on morphology, mechanical and thermal properties of fiber reinforced epoxy-clay nanocomposites. The clay minerals have been surface treated with two different silane coupling agents viz. 3-Aminopropyltriethoxysilane (APTES) and 3-Glycidyloxypropyltrimethoxysilane (GPTMS) using a novel method, wherein clay minerals have been nano-dispersed in the silane solution. Table 7.1 summarizes all the tensile test and flexural test results for fiber reinforced epoxy-clay nanocomposites from the present study. Initially, exploratory studies on the effect of different processing parameters (premixing parameters, post-curing temperature, resin to hardener mix ratio) on the mechanical properties of fiber reinforced epoxy-clay nanocomposites containing 2 phr (parts per hundred resin) of Cloisite® 15A have been carried out. The glass fiber reinforced epoxy clay nanocomposites, C15GFRC(PC2) showed the highest improvement in tensile and flexural properties. However, the temperature of the epoxy and clay mixture was unsuitable for mass production of fiber reinforced epoxy-clay nanocomposites. It was decided to continue working with the speed of homogenization at 20000 rpm, ultrasonic probe amplitude 80% but the epoxy-clay mixture temperature during mixing was kept at 25°C. The small angle X-ray scattering (SAXS) and transmission electron microscopy (TEM) observations revealed that intercalated nanocomposites (C15GFRC(PC3)) was formed. Post-curing of fiber reinforced epoxy-clay nanocomposites at temperatures well above the glass transition temperature of the fully cured epoxy network ($T_{g\infty}$) led to a decrease in mechanical properties of nanocomposites C15GFRC(PC5) and C15GFRC(PC6).

Silane treatment of glass fibers showed a positive effect on the mechanical properties and in the case of C15 AGFRC tensile strength, flexural modulus and flexural strength increased by 18%, 66% and 96%, respectively. The initial work on fiber reinforced epoxy-clay nanocomposites containing silane treated clay minerals showed only small improvements in tensile properties and flexural properties. The quantity of silane coupling agents and silylation process parameters significantly influence the amount of silanes grafted on clay minerals. The silane coupling agents can form an interpenetrating network between clay minerals and epoxy,

which would lead to strong clay mineral-polymer interfacial interactions and a substantial increase in mechanical properties of nanocomposites. In the present work an optimum quantity of silane for successful modification of large surface area of clay minerals and curing schedule (7 h at 85 °C) which significantly increased the mechanical properties of fiber reinforced epoxy-clay nanocomposites have been arrived at. The tensile modulus, tensile strength, flexural modulus and bending strength increased by 30%, 37%, 139% and 146% respectively, in nanocomposites containing clay mineral modified using 4X aminopropyltrietoxysilane (AC15(4)GFRC).

Table 7.1 Summary of all the tensile test and flexural test results for fiber reinforced epoxy-clay nanocomposites

Material code	Tensile modulus, GPa	Tensile strength, MPa	Elongation at break, %	Flexural modulus, GPa	Flexural strength, MPa
Cured 7h at 70 °C					
GFRC	8.3 ± 0.16	313 ± 12	4.2 ± 0.3	10.2 ± 0.17	235 ± 18
C15GFRC(PC1)	7.2 ± 0.22	256 ± 22	3.9± 0.2	12.5 ± 0.61	304 ± 22
C15GFRC(PC2)	8.7 ± 0.15	368 ± 18	5.7 ± 0.1	15.3 ± 1.4	363 ± 20
C15GFRC(PC3)	9.2 ± 0.65	348 ± 7	5.6 ± 0.1	12.3 ± 1.05	262 ± 6
C15GFRC(PC4)	9.4 ± 0.01	378 ± 11	4.5 ± 0.1	13.8 ± 0.05	271 ± 19
C15GFRC(PC5)	8.4 ± 0.21	326 ± 12	4.7 ± 0.3	11.3 ± 0.70	229 ± 18
C15GFRC(PC6)	7.6 ± 0.09	270 ± 8	4.2 ± 0.3	11.4 ± 0.90	210 ± 25
C15GFRC(PC7)	7 ± 0.13	279 ± 23	4.4 ± 0.3	10.3 ± 0.35	178 ± 7
C15GFRC(PC8)	7.8 ± 0.53	279 ± 10	4.5± 0.5	9.6 ± 0.94	177 ± 21
Cured 7h at 70 °C					
C15 AGFRC	8.5 ± 0.15	369 ± 21	4.7 ± 0.1	17.0 ± 0.8	461 ± 13
C15 GGFRC	8.2 ± 0.15	329 ± 20	4.6 ± 0.2	14.6 ± 0.9	422 ± 32
AC15 AGFRC	7.8 ± 0.1	374 ± 45	5.5 ± 0.6	18.7 ± 0.9	386 ± 33
GC15 AGFRC	8.3 ± 0.1	356 ± 38	4.8 ± 0.4	17.0 ± 1.0	502 ± 37
AC15 GGFRC	6.9 ± 0.2	288 ± 5	4.5 ± 0.2	14.0 ± 0.4	325 ± 18
GC15 GGFRC	8.0 ± 0.2	290 ± 31	4.1 ± 0.4	15.5 ± 1.0	443 ± 22
AC15(0.1)GFRC	8.1 ± 0.67	322 ± 12	4.5 ± 0.1	11.5 ± 1.0	188 ± 15

GC15(0.1)GFRC	7.5 ± 0.14	289 ± 9	4.4 ± 0.2	8.96 ± 0.56	155 ± 6
AC15(0.5)GFRC	7.4 ± 0.35	295 ± 13	4.6 ± 0.1	10.5 ± 1.4	179 ± 22
GC15(0.5)GFRC	7.2 ± 0.05	261 ± 13	4.3 ± 0.3	9.6 ± 0.6	167 ± 14
AC15(2)GFRC	9.7 ± 0.07	390 ± 20	4.5 ± 0.3	14.10 ± 0.7	278 ± 15
GC15(2)GFRC	9.6 ± 0.1	378 ± 20	4.5 ± 0.3	15.9 ± 0.55	268 ± 16
AC15(4)GFRC	7.9 ± 0.23	290 ± 3	4.3 ± 0.2	8.2 ± 0.9	218 ± 25
GC15(4)GFRC	8.0 ± 0.11	343 ± 33	5 ± 0.4	8.2 ± 0.7	180 ± 15
Cured 7h at 85 °C					
C15 AGFRC	8.0 ± 0.45	377 ± 21	5.05 ± 0.2	13 ± 1.2	253 ± 22
AC15(0.1)GFRC	9.2 ± 1	399 ± 12	10.7 ± 0.5	15.3 ± 1	251 ± 14
AC15(0.5)GFRC	9.3 ± 0.72	390 ± 5	11 ± 0.7	14.7 ± 0.6	242 ± 10
AC15(2)GFRC	8.6 ± 0.85	426 ± 17	11.9 ± 0.6	17.5 ± 0.7	292 ± 21
AC15(4)GFRC	11.7 ± 0.36	470 ± 25	10.5 ± 1	33.5 ± 3.25	507 ± 27
GC15(0.1)GFRC	7.9 ± 0.49	376 ± 28	4.2 ± 0.4	14.8 ± 0.5	249 ± 21
GC15(0.5)GFRC	7.9 ± 0.98	381 ± 19	10.3 ± 0.9	15.6 ± 0.6	313 ± 21
GC15(2)GFRC	8.0 ± 1.3	346± 7	10 ± 0.3	17.9 ± 0.6	293 ± 26
GC15(4)GFRC	10.6 ± 0.1	414 ± 7	5.8 ± 2	24 ± 1.7	349 ± 18
GC15(6)GFRC	11 ± 0.25	486 ± 24	7.6 ± 2	28.5 ± 0.6	392± 15

A comprehensive understanding of silanization of clay minerals and processing-structure-property of fiber reinforced silylated epoxy-clay nanocomposites has been achieved. A uniform dispersion, exfoliation, improved adhesion of clay minerals in epoxy also arrested deleterious effects of water infusion on mechanical properties of composites, during ageing in simulated seawater. Some important conclusion from studies of fiber reinforced epoxy-clay nanocomposites are:

7.1 Fiber reinforced epoxy-clay nanocomposites

1. A combination of high shear homogenization and ultrasonication during premixing of Cloisite® 15A in epoxy resin proved to be a promising method to delaminate the clay particles to individual layers. TEM images indicated ordered intercalated clay mineral layers along with some exfoliated regions in epoxy matrix. Better dispersion of clay minerals obtained using high speed of homogenization and high ultrasonic probe amplitude

has been manifested by an increase in tensile modulus, tensile strength, and elongation at break of fiber reinforced epoxy-clay nanocomposites.

2. The improvement in tensile strength, flexural modulus and flexural strength of glass fiber reinforced composites incorporating clay minerals were dependent on the dispersion state of clay minerals in epoxy. A high temperature of epoxy-clay mixture (80°C), the speed of homogenization (20000 rpm) and ultrasonic probe amplitude (80%) during premixing step resulted in the highest improvement in mechanical properties of fiber reinforced epoxy-clay nanocomposites. The tensile strength, flexural modulus, flexural strength and interlaminar shear strength increased by 17%, 50%, 54% and 58%, respectively in these nanocomposites as compared to glass fiber reinforced neat epoxy composites.
3. The glass transition temperature (T_g) of fiber reinforced epoxy composites increased on the incorporation of organically modified clay minerals due to clay - polymer interactions, which restrict the mobility of chains.
4. Post-curing of fiber reinforced epoxy-clay nanocomposites at 100°C showed no significant change in mechanical properties in comparison to samples which have not been post-cured. The mechanical properties of fiber reinforced epoxy-clay nanocomposites reduced after post-cure at higher temperatures viz. 130°C and 150°C, and this could be attributed to the generation of voids and internal stresses due to 1. boiling of free or bound water and low molecular weight impurities present in the nanocomposites 2. residual stresses due to thermal cooling. Therefore, the post-curing of these composites above 100°C leads to the deterioration of mechanical properties.
5. The non-stoichiometric ratio of epoxy resin and hardener e.g. 100: 29.5 and 100:28 as compared to stoichiometric ratio 100:31 resulted in a decrease in both the extent of cure of epoxy and mechanical properties of fiber reinforced epoxy-clay nanocomposites. The Fourier transform infrared (FTIR) spectra revealed that the curing reaction was not complete due to the scarcity of amino groups, which resulted in a significant decrease in the mechanical properties of fiber reinforced epoxy-clay nanocomposite.

7.2 Effect of surface treatment of glass fibers and clay minerals

1. The functionalization of glass fibers with 3-aminopropyltriethoxysilane (APTES) and 3-glycidyloxypropyltrimethoxysilane (GPTMS) resulted in a significant increase in flexural modulus, flexural strength and interlaminar shear strength due to improved fiber-matrix adhesion.

2. The grafting of silanes on Cloisite® 15A has been confirmed by FTIR. A new band appeared at 1047 cm^{-1} which was assigned to the Si–O –Si stretching in silylated clay minerals.
3. The functionalization of clay minerals with APTES and GPTMS aided exfoliation in epoxy as evident from TEM and SAXS results. This promoted adhesion between inorganic clay mineral layers and epoxy as revealed by tensile tests, which indicated an increase in the tensile strength and elongation at failure of fiber reinforced epoxy-clay nanocomposites.
4. The differential scanning calorimetry was used to gauge the extent of curing of different compositions. The incorporation of silylated clays in epoxy led to an increase in glass transition temperature (T_g) of fiber reinforced nanocomposites, which can be attributed to increased matrix cross-linking, improved interactions and exfoliation of clay minerals in epoxy.

7.3 Curing studies and mechanical properties of fiber reinforced epoxy-clay nanocomposites

1. The results of the thermogravimetric analysis showed that the amount of grafted silane increased with an increase in the concentration of APTES/ GPTMS in the solvent during silanization reaction. The grafting of APTES in interlayer space was confirmed by exfoliation of clay minerals as indicated by eventual disappearance of the characteristic peak of Cloisite® 15A at $2\theta = 2.71°$.
2. The highest mechanical properties of fiber reinforced epoxy-clay nanocomposites were obtained by curing the epoxy at a temperature slightly below the temperature of the fully cured network ($T_{g\infty}$), 87°C obtained using differential scanning calorimetry. Also, a remarkable increase in tensile and flexural properties was achieved with the incorporation of silane modified clays prepared using chosen curing schedule. The tensile modulus, tensile strength, flexural modulus and flexural strength increased by 30%, 37%, 139% and 146%, respectively in nanocomposites containing clay minerals modified using 4X aminopropyltrietoxysilane, i.e. the quantity of silane = 4 times the weight of clay.
3. The fractographic analysis of nanocomposites revealed a considerable difference in failure modes of fiber reinforced epoxy composites containing Cloisite® 15A and silane modified clay minerals. A good interfacial adhesion between fiber and matrix was observed, and failure occurred because of fiber breakage and matrix cracking only, unlike in the case of glass fiber reinforced neat epoxy composite, where an additional failure mode of fiber pullout was also observed.

7.4 Seawater ageing of glass fiber reinforced epoxy-clay nanocomposites

1. The ageing in seawater at 25°C and 55°C resulted in a decrease in load-carrying capacity of specimens. A high temperature of seawater accelerated the water diffusion rate of seawater and hydrolytic degradation in all composites.
2. The rate of diffusion of water in fiber reinforced composites incorporating silylated clay minerals decreased as compared to glass fiber reinforced epoxy composites, as well as composites containing non-silane treated Cloisite® 15A
3. The use of a high concentration of APTES as well as GPTMS in silylation of clay minerals leads to a decrease in barrier properties and poor long-term durability of fiber reinforced nanocomposites. An excess of silane coupling agents leache out from the composite during seawater ageing. The relatively bigger size of voids left behind would lead to plasticization effect of accumulated water in the voids.
4. The flexural modulus and tensile modulus of composites increased after exposure in seawater. This can be attributed to (i) embrittlement of glass fibers and fiber-matrix interphase due to presence of salts in seawater and continuous use of sodium hydroxide, (ii) restricted swelling of epoxy, the free expansion of epoxy due to swelling can be restricted by the glass fibers reinforcement, which changed the stress - strain behavior of composites, (iii) additional cross-linking caused by the catalytic effect of Na^+ ions and water over post-curing reaction and interaction of water molecules with epoxy via multiple hydrogen bonds.
5. FTIR spectra of nanocomposites after exposure to seawater confirmed hydrogen bonding between water molecules and epoxy matrix. New hydroxyl groups formed as a result of hydrolysis increase the intensity of the corresponding infrared bands. The increase in the intensity of bands associated with alkyl stretching (2950 cm^{-1} – 2850 cm^{-1}), and carbonyl group (1605 cm^{-1}) indicated that the epoxy was undergoing chemical hydrolysis.
6. The fiber-matrix interface was severely affected due to swelling of the epoxy matrix and loss of adhesion between glass fibers and epoxy due to the accumulation of salt crystals. The cracks indicating embrittlement of epoxy matrix, potholes, and river marks were also observed.

7.5 Future scope of work

1. Study of other nanofillers like Graphene and Halloysite clay can be incorporated in fiber reinforced polymer nanocomposites.
2. The effect of incorporation of silylated clay minerals in epoxy on the extent of curing and curing kinetics would be very interesting.
3. The hygrothermal study can be done for the longer duration of immersion time both at room temperature and elevated temperature.
4. The behavior of fiber reinforced silylated clay nanocomposites under fatigue, creep and compressive and impact loads can be studied.
5. Compatibilization of nanofillers can be further studied. For example, modification of clay minerals using other silane agents can be studied.
6. Nondestructive techniques to detect manufacturing, as well as usage flaws, can be investigated.
7. Modeling and simulation of the mechanical response of fiber reinforced epoxy-clay nanocomposites under different loads and their hygrothermal behavior would be very useful.

References

Abacha, N., Kubouchi, M., Tsuda, K., Sakai, T., 2007. Performance of epoxy-nanocomposite under corrosive environment. Express Polym. Lett. 1, 364–369. doi:10.3144/expresspolymlett.2007.51

Agubra, V., Owuor, P., Hosur, M., 2013. Influence of nanoclay dispersion methods on the mechanical behavior of E-glass/epoxy nanocomposites. Nanomaterials 3, 550–563. doi:10.3390/nano3030550

Al-Qadhi, M., Merah, N., Gasem, Z.M., 2013. Mechanical properties and water uptake of epoxy-clay nanocomposites containing different clay loadings. J. Mater. Sci. 48, 3798–3804. doi:10.1007/s10853-013-7180-5

Alamri, H., Low, I.M., 2012. Effect of water absorption on the mechanical properties of nano-filler reinforced epoxy nanocomposites. Mater. Des. 42, 214–222. doi:10.1016/j.matdes.2012.05.060

Alamri, H., Low, I.M., Alothman, Z., 2012. Mechanical, thermal and microstructural characteristics of cellulose fibre reinforced epoxy/organoclay nanocomposites. Compos. Part B Eng. 43, 2762–2771. doi:10.1016/j.compositesb.2012.04.037

Albdiry, M., Yousif, B., Ku, H., Lau, K., 2012. A critical review on the manufacturing processes in relation to the properties of nanoclay/polymer composites. J. Compos. Mater. 47, 1093–1115. doi:10.1177/0021998312445592

Arkles, B., Kim, Y.M., Pan, Y., 2009. The role of polarity in the structure of silanes employed in surface modification, in: Silanes and Other Coupling Agents, Volume 5. pp. 51–64. doi:10.1163/ej.9789004165915.i-348.37

Armstrong, G., Thornton, R., Ryan, M.P., Laffir, F., Russell, R.J., Bala, T., Keely, C., Babu, R., 2012. Formulation of epoxy–polyester powder coatings containing silver-modified nanoclays and evaluation of their antimicrobial properties. Polym. Bull. 68, 1951–1963. doi:10.1007/s00289-011-0695-5

Avila, A., Duarte, H. V., Soares, M.I., 2006. The nanoclay influence on impact response of laminated plates. Lat. Am. J. Solids Struct. 3, 3–20.

Azeez, A.A., Rhee, K.Y., Park, S.J., Hui, D., 2013. Epoxy clay nanocomposites - Processing, properties and applications: A review. Compos. Part B Eng. 45, 308–320. doi:10.1016/j.compositesb.2012.04.012

Bakar, M., Kostrzewa, M., Białkowska, A., Pawelec, Z., 2014. Effect of mixing parameters on the mechanical and thermal properties of a nanoclay-modified epoxy resin. High

Perform. Polym. 26, 298–306. doi:10.1177/0954008313512141

Banerjee, S., Joshi, M., Ghosh, A.K., 2013. Investigations on clay dispersion in polypropylene/clay nanocomposites using rheological and microscopic analysis. J. Appl. Polym. Sci. 130, 4464–4473. doi:10.1002/app.39590

Becker, O., Cheng, Y.B., Varley, R.J., Simon, G.P., 2003. Layered silicate nanocomposites based on various high-functionality epoxy resins: The influence of cure temperature on morphology, mechanical properties, and free volume. Macromolecules 36, 1616–1625. doi:10.1021/MA0213448

Becker, O., Simon, G.P., Dusek, K., 2005. Epoxy layered silicate nanocomposites, in: Inorganic Polymeric Nanocomposites and Membranes. Springer Berlin Heidelberg, pp. 29–82. doi:10.1007/b107204

Bergaya, F., Lagaly, G., 2006. General introduction: Clays, clay minerals, and clay science, in: Handbook of Clay Science. Elsevier, Amsterdam, pp. 1–18. doi:10.1016/S1572-4352(05)01001-9

Bergeret, A., Ferry, L., Ienny, P., 2009. Influence of the fibre/matrix interface on ageing mechanisms of glass fibre reinforced thermoplastic composites (PA-6,6, PET, PBT) in a hygrothermal environment. Polym. Degrad. Stab. 94, 1315–1324. doi:10.1016/j.polymdegradstab.2009.04.009

Bertuoli, P.T., Piazza, D., Scienza, L.C., Zattera, A.J., 2014. Preparation and characterization of montmorillonite modified with 3-aminopropyltriethoxysilane. Appl. Clay Sci. 87, 46–51. doi:10.1016/j.clay.2013.11.020

Beyer, G., 2002. Nanocomposites: A new class of flame retardants for polymers. Plast. Addit. Compd. 4, 22–28. doi:10.1016/S1464-391X(02)80151-9

Blum, F.D., 2016. Silane coupling agents, in: Encyclopedia of Polymer Science and Technology. John Wiley & Sons, Inc., Hoboken, NJ, USA, pp. 1–15. doi:10.1002/0471440264.pst481.pub2

Borsig, E., Ujhelyiová, A., Mlynarčíková, Z., Kaemfer, D., Mülhaupt, R., Marcinčin, A., Berek, D., 2007. DSC study of syndiotactic polypropylene/organoclay nanocomposite fibers: Crystallization and melting behavior. Int. J. Polym. Mater. 56, 771–788. doi:10.1080/00914030601163399

Bozkurt, E., Kaya, E., Tanoğlu, M., 2007. Mechanical and thermal behavior of non-crimp glass fiber reinforced layered clay/epoxy nanocomposites. Compos. Sci. Technol. 67, 3394–3403. doi:10.1016/j.compscitech.2007.03.021

Bruce, A.N., Lieber, D., Hua, I., Howarter, J.A., 2014. Rational interface design of epoxy-

organoclay nanocomposites: Role of structure-property relationship for silane modifiers. J. Colloid Interface Sci. 419, 73–78. doi:10.1016/j.jcis.2013.12.051

Camargo, P.H.C., Satyanarayana, K.G., Wypych, F., 2009. Nanocomposites : Synthesis , structure , properties and new application opportunities. Mater. Res. 12, 1–39. doi:10.1590/S1516-14392009000100002

Capiel, G., Miccio, L.A., Montemartini, P.E., Schwartz, G.A., 2017. Water diffusion and hydrolysis effect on the structure and dynamics of epoxy-anhydride networks. Polym. Degrad. Stab. 143, 57–63. doi:10.1016/j.polymdegradstab.2017.06.010

Carbas, R.J.C., da Silva, L.F.M., Marques, E.A.S., Lopes, A.M., 2013. Effect of post-cure on the glass transition temperature and mechanical properties of epoxy adhesives. J. Adhes. Sci. Technol. 27, 2542–2557. doi:10.1080/01694243.2013.790294

Carbas, R.J.C., Marques, E.A.S., da Silva, L.F.M., Lopes, A.M., 2014. Effect of cure temperature on the glass transition temperature and mechanical properties of epoxy adhesives. J. Adhes. 90, 104–119. doi:10.1080/00218464.2013.779559

Carli, L.N., Daitx, T.S., Soares, G. V., Crespo, J.S., Mauler, R.S., 2014. The effects of silane coupling agents on the properties of PHBV/halloysite nanocomposites. Appl. Clay Sci. 87, 311–319. doi:10.1016/j.clay.2013.11.032

Cervantes-Uc, J.M., Cauich-Rodríguez J.V., Vázquez-Torres H., Garfias-Mesías, L.F., Paul, D.R., 2007. Thermal degradation of commercially available organoclays studied by TGA-FTIR. Thermochim. Acta 457, 92–102. doi:10.1016/j.tca.2007.03.008

Chatterjee, A., Gillespie, J.W., 2008. Moisture absorption behavior of epoxies and their S2 glass composites. J. Appl. Polym. Sci. 108, 3942–3951. doi:10.1002/app.28076

Chen, C., Tolle, T.B., 2004. Fully exfoliated layered silicate epoxy nanocomposites. J. Polym. Sci. Part B Polym. Phys. 42, 3981–3986. doi:10.1002/polb.20259

Chen, G., Yoon, J.S., 2005a. Clay functionalization and organization for delamination of the silicate tactoids in poly(L-lactide) matrix. Macromol. Rapid Commun. 26, 899–904. doi:10.1002/marc.200500046

Chen, G., Yoon, J.S., 2005b. Nanocomposites of poly[(butylene succinate)-co-(butylene adipate)] (PBSA) and twice-functionalized organoclay. Polym. Int. 54, 939–945. doi:10.1002/pi.1793

Chen, G.X., Choi, J.B., Yoon, J.S., 2005a. The role of functional group on the exfoliation of clay in poly(L-lactide). Macromol. Rapid Commun. 26, 183–187. doi:10.1002/marc.200400452

Chen, G.X., Kim, H.S., Shim, J.H., Yoon, J.S., 2005b. Role of epoxy groups on clay surface

in the improvement of morphology of poly(L-lactide)/clay composites. Macromolecules 38, 3738–3744. doi:10.1021/ma0488515

Chin, I.J., Thurn-Albrecht, T., Kim, H.C., Russell, T.P., Wang, J., 2001. On exfoliation of montmorillonite in epoxy. Polymer (Guildf). 42, 5947–5952. doi:10.1016/S0032-3861(00)00898-3

Choi, Y.Y., Lee, S.H., Ryu, S.H., 2009. Effect of silane functionalization of montmorillonite on epoxy/montmorillonite nanocomposite. Polym. Bull. 63, 47–55. doi:10.1007/s00289-009-0068-5

Cholake, S.T., Mada, M.R., Singh Raman, R.K., Bai, Y., Zhao, X.L., Rizkalla, S., Bandyopadhyay, S., 2014. Quantitative analysis of curing mechanisms of epoxy resin by mid- and near-fourier transform infra red spectroscopy. Def. Sci. J. 64, 314–321. doi:10.14429/dsj.64.7326

Chow, W.S., 2007. Water absorption of epoxy/glass fiber/organo-montmorillonite nanocomposites. Express Polym. Lett. 1, 104–108. doi:10.3144/expresspolymlett.2007.18

Chow, W.S., Yap, Y.P., 2008. Optimization of process variables on flexural properties of epoxy/organo-montmorillonite nanocomposite by response surface methodology. Express Polym. Lett. 2, 2–11. doi:10.3144/expresspolymlett.2008.2

Chowdhury, F.H., Hosur, M. V., Jeelani, S., 2006. Studies on the flexural and thermomechanical properties of woven carbon/nanoclay-epoxy laminates. Mater. Sci. Eng. A 421, 298–306. doi:10.1016/j.msea.2006.01.074

Coates, J., 2000. Interpretation of infrared spectra, a practical approach, in: Encyclopedia of Analytical Chemistry. John Wiley & Sons Ltd, pp. 10815–10837.

Corning, O., 2006. Customer acceptance standards. doi:ECM23

Cotugno, S., Larobina, D., Mensitieri, G., Musto, P., Ragosta, G., 2001. A novel spectroscopic approach to investigate transport processes in polymers: the case of water-epoxy system. Polymer (Guildf). 42, 6431–6438. doi:10.1016/S0032-3861(01)00096-9

Daitx, T.S., Carli, L.N., Crespo, J.S., Mauler, R.S., 2015. Effects of the organic modification of different clay minerals and their application in biodegradable polymer nanocomposites of PHBV. Appl. Clay Sci. 115, 157–164. doi:10.1016/j.clay.2015.07.038

Daud, W., Bersee, H.E.N., Picken, S.J., Beukers, A., 2009. Layered silicates nanocomposite matrix for improved fiber reinforced composites properties. Compos. Sci. Technol. 69, 2285–2292. doi:10.1016/j.compscitech.2009.01.009

Davies, L.W., Day, R.J., Bond, D., Nesbitt, A., Ellis, J., Gardon, E., 2007. Effect of cure cycle heat transfer rates on the physical and mechanical properties of an epoxy matrix composite. Compos. Sci. Technol. 67, 1892–1899. doi:10.1016/j.compscitech.2006.10.014

de Azeredo, H.M.C., 2012. Antimicrobial activity of nanomaterials for food packaging applications, in: Nano-Antimicrobials. Springer Berlin Heidelberg, pp. 375–394. doi:10.1007/978-3-642-24428-5_13

De Maria, A., Aurora, A., Montone, A., Tapfer, L., Pesce, E., Balboni, R., Schwarz, M., Borriello, C., 2011. Synthesis and characterization of PMMA/silylated MMTs. J. Nanoparticle Res. 13, 6049–6058. doi:10.1007/s11051-011-0496-7

de Paiva, L.B., Morales, A.R., Valenzuela Diaz, F.R., 2008. Organoclays: Properties, preparation and applications. Appl. Clay Sci. 42, 8–24. doi:10.1016/j.clay.2008.02.006

Dean, D., Obore, A.M., Richmond, S., Nyairo, E., 2006. Multiscale fiber-reinforced nanocomposites: Synthesis, processing and properties. Compos. Sci. Technol. 66, 2135–2142. doi:10.1016/j.compscitech.2005.12.015

Dean, K., Krstina, J., Tian, W., Varley, R.J., 2007. Effect of ultrasonic dispersion methods on thermal and mechanical properties of organoclay epoxy nanocomposites. Macromol. Mater. Eng. 292, 415–427. doi:10.1002/mame.200600435

Demjen, Z., Pukanszky, B., Foldes, E., Nagy, J., 1997. Interaction of silane coupling agents with CaCO3. J. Colloid Interface Sci. 190, 427–436. doi:papers://590F92D9-0B76-4B88-8729-9AF064BE5AC8/Paper/p5242

Derrien, K., Gilormini, P., 2009. The effect of moisture-induced swelling on the absorption capacity of transversely isotropic elastic polymer-matrix composites. Int. J. Solids Struct. 46, 1547–1553. doi:10.1016/j.ijsolstr.2008.11.014

DiBenedetto, A.T., 2001. Tailoring of interfaces in glass fiber reinforced polymer composites: A review. Mater. Sci. Eng. A 302, 74–82. doi:10.1016/S0921-5093(00)01357-5

Dong, H., Wu, L., Zhang, L., Chen, H., Gao, C., 2015. Clay nanosheets as charged filler materials for high-performance and fouling-resistant thin film nanocomposite membranes. J. Memb. Sci. 494, 92–103. doi:10.1016/j.memsci.2015.07.049

Dorigato, A., Morandi, S., Pegoretti, A., 2012. Effect of nanoclay addition on the fiber/matrix adhesion in epoxy/glass composites. J. Compos. Mater. 46, 1439–1451. doi:10.1177/0021998311420311

Drzal, L.T., 1990. The role of the fiber-matrix interphase on composite properties. Vacuum

41, 1615–1618. doi:10.1016/0042-207X(90)94034-N

Edwards, G., Halley, P., Kerven, G., Martin, D., 2005. Thermal stability analysis of organo-silicates, using solid phase microextraction techniques. Thermochim. Acta 429, 13–18. doi:10.1016/j.tca.2004.11.020

Ellyin, F., Rohrbacher, C., 2000. Effect of aqueous environment and temperature on glass-fibre epoxy resin composites. J. Reinf. Plast. Compos. 19, 1405–1427. doi:10.1177/073168400772678518

Firdosh, S., Murthy, H.N., Pal, R., Angadi, G., Raghavendra, N., Krishna, M., 2015. Durability of GFRP nanocomposites subjected to hygrothermal ageing. Compos. Part B Eng. 69, 443–451. doi:10.1016/j.compositesb.2014.09.028

Gabr, M.H., Okumura, W., Ueda, H., Kuriyama, W., Uzawa, K., Kimpara, I., 2015. Mechanical and thermal properties of carbon fiber/polypropylene composite filled with nano-clay. Compos. Part B Eng. 69, 94–100. doi:10.1016/j.compositesb.2014.09.033

Gao, L., Zhang, Q., Guo, J., Li, H., Wu, J., Yang, X., Sui, G., 2016. Effects of the amine/epoxy stoichiometry on the curing behavior and glass transition temperature of MWCNTs-NH2/epoxy nanocomposites. Thermochim. Acta 639, 98–107. doi:10.1016/j.tca.2016.07.017

García del Cid, M.A., Prolongo, M.G., Salom, C., Arribas, C., Sánchez-Cabezudo, M., Masegosa, R.M., 2012. The effect of stoichiometry on curing and properties of epoxy-clay nanocomposites. J. Therm. Anal. Calorim. 108, 741–749. doi:10.1007/s10973-012-2215-8

Garg, M., Sharma, S., Mehta, R., 2016. Carbon nanotube-reinforced glass fiber epoxy composite laminates exposed to hygrothermal conditioning. J. Mater. Sci. 51, 8562–8578. doi:10.1007/s10853-016-0117-z

Gelsest, C., 1967. Reactive silicones: forging new polymer links, Gelest Inc, Morrisville, Pennsylvania.

González-González, M., Cabanelas, J.C., Baselga, J., 2012. Applications of FTIR on Epoxy Resins - Identification, Monitoring the Curing Process, Phase Separation and Water Uptake. Univ. Carlos III Madrid 2, 261–284. doi:10.5772/2055

Goodman, S.H., Hanna, D., 2014. Handbook of thermoset plastics. William Andrew.

Graham-Jones, J., Summerscales, J., 2015a. Introduction, Marine Applications of Advanced Fibre-Reinforced Composites. Woodhead Publishing Limited. doi:10.1016/B978-1-78242-250-1.00001-6

Graham-Jones, J., Summerscales, J., 2015b. Marine applications of advanced fibre-reinforced

composites.

Grammatikos, S.A., Zafari, B., Evernden, M.C., Mottram, J.T., Mitchels, J.M., 2015. Moisture uptake characteristics of a pultruded fibre reinforced polymer flat sheet subjected to hot/wet aging. Polym. Degrad. Stab. 121, 407–419. doi:10.1016/j.polymdegradstab.2015.10.001

Grave, C., McEwan, I., Pethrick, R.A., 1998. Influence of stoichiometric ratio on water absorption in epoxy resins. J. Appl. Polym. Sci. 69, 2369–2376. doi:10.1002/(SICI)1097-4628(19980919)69:12<2369::AID-APP8>3.0.CO;2-6

Gude, M.R., Prolongo, S.G., Ureña, A., 2012. Effect of the epoxy/amine stoichiometry on the properties of carbon nanotube/epoxy composites. J. Therm. Anal. Calorim. 108, 717–723. doi:10.1007/s10973-011-2056-x

Guermazi, N., Ben Tarjem, A., Ksouri, I., Ayedi, H.F., 2013. On the durability of FRP composites for aircraft structures in hygrothermal conditioning. Compos. Part B Eng. 85, 294–304. doi:10.1016/j.compositesb.2015.09.035

Guo, Y., Wang, M., Zhang, H., Liu, G., Zhang, L., Qu, X., 2008. The surface modification of nanosilica, preparation of nanosilica/acrylic core-shell composite latex, and its application in toughening PVC matrix. J. Appl. Polym. Sci. 107, 2671–2680. doi:10.1002/app.27310

Gurusideswar, S., Velmurugan, R., 2014. Strain rate sensitivity of glass/epoxy composites with nanofillers, Materials & Design. doi:10.1016/j.matdes.2014.03.065

Ha, S.R., Rhee, K.Y., 2008. Effect of surface-modification of clay using 3-aminopropyltriethoxysilane on the wear behavior of clay/epoxy nanocomposites. Colloids Surfaces A Physicochem. Eng. Asp. 322, 1–5. doi:10.1016/j.colsurfa.2008.03.007

Ha, S.R., Rhee, K.Y., Kim, H.C., Kim, J.T., 2008. Fracture performance of clay/epoxy nanocomposites with clay surface-modified using 3-aminopropyltriethoxysilane. Colloids Surfaces A Physicochem. Eng. Asp. 313–314, 112–115. doi:10.1016/j.colsurfa.2007.04.082

Ha, S.R., Rhee, K.Y., Park, S.J., Lee, J.H., 2010. Temperature effects on the fracture behavior and tensile properties of silane-treated clay/epoxy nanocomposites. Compos. Part B Eng. 41, 602–607. doi:10.1016/j.compositesb.2010.09.015

Ha, S.R., Ryu, S.H., Park, S.J., Rhee, K.Y., 2007. Effect of clay surface modification and concentration on the tensile performance of clay/epoxy nanocomposites. Mater. Sci. Eng. A 448, 264–268. doi:10.1016/j.msea.2006.10.052

Hamidah, N., Zulfli, M., Shyang, C.W., 2010. Flexural and morphological properties of epoxy / glass fibre / silane- treated organo-montmorillonite composites. J. Phys. Sci. 21, 41–50.

Hamidi, Y.K., Aktas, L., Altan, M.C., 2008. Effect of nanoclay content on void morphology in resin transfer molded composites. J. Thermoplast. Compos. Mater. 21, 141–163. doi:10.1177/0892705707083635

Haque, A., Shamsuzzoha, M., Hussain, F., Dean, D., 2003. S2-glass/epoxy polymer nanocomposites: manufacturing, structures, thermal and mechanical properties. J. Compos. Mater. 37, 1821–1837. doi:10.1177/002199803035186

He, H., Duchet, J., Galy, J., Gerard, J.F., 2005. Grafting of swelling clay materials with 3-aminopropyltriethoxysilane. J. Colloid Interface Sci. 288, 171–176. doi:10.1016/j.jcis.2005.02.092

He, H., Tao, Q., Zhu, J., Yuan, P., Shen, W., Yang, S., 2013. Silylation of clay mineral surfaces. Appl. Clay Sci. 71, 15–20. doi:10.1016/j.clay.2012.09.028

Helmy, S., Hoa, S.V., 2014. Tensile fatigue behavior of tapered glass fiber reinforced epoxy composites containing nanoclay. Compos. Sci. Technol. 102, 10–19. doi:10.1016/j.compscitech.2014.05.038

Herrera, N.N., Letoffe, J., Putaux, J., David, L., Bourgeat-lami, E., Lyon, C.B., Cedex, V., 2004. Aqueous dispersions of silane-functionalized laponite clay platelets. A first step toward the elaboration of water-based polymer/clay nanocomposites. Langmuir 20, 1564–1571.

Hiremath, V., Singh, M., Shukla, D.K., 2014. Effect of post curing temperature on viscoelastic and flexural properties of epoxy/alumina polymer nanocomposites. Procedia Eng. 97, 479–487. doi:10.1016/j.proeng.2014.12.272

Ho, M.W., Lam, C.K., Lau, K. tak, Ng, D.H.L., Hui, D., 2006. Mechanical properties of epoxy-based composites using nanoclays. Compos. Struct. 75, 415–421. doi:10.1016/j.compstruct.2006.04.051

Hossain, M.K., Chowdhury, M.M.R., Imran, K.A., Salam, M.B., Tauhid, A., Hosur, M., Jeelani, S., 2014. Effect of low velocity impact responses on durability of conventional and nanophased CFRP composites exposed to seawater. Polym. Degrad. Stab. 99, 180–189. doi:10.1016/j.polymdegradstab.2013.11.008

Hossain, M.K., Imran, K.A., Hosur, M. V., Jeelani, S., 2011. Degradation of mechanical properties of conventional and nanophased carbon/epoxy composites in seawater. J. Eng. Mater. Technol. 133, 041004. doi:10.1115/1.4004691

Hu, Y., Li, X., Lang, A.W., Zhang, Y., Nutt, S.R., 2016. Water immersion aging of polydicyclopentadiene resin and glass fiber composites. Polym. Degrad. Stab. 124, 35–42. doi:10.1016/j.polymdegradstab.2015.12.008

Huskić, M., Žigon, M., Ivanković, M., 2013. Comparison of the properties of clay polymer nanocomposites prepared by montmorillonite modified by silane and by quaternary ammonium salts. Appl. Clay Sci. 85, 109–115. doi:10.1016/j.clay.2013.09.004

Hutchinson, J.M., McCarthy, D., Montserrat, S., Cortés, P., 1996. Enthalpy relaxation in a partially cured epoxy resin. J. Polym. Sci. Part B Polym. Phys. 34, 229–239.

Ianchis, R., Cinteza, L.O., Donescu, D., Petcu, C., Corobea, M.C., Somoghi, R., Ghiurea, M., Spataru, C., 2011. Implications of silylated montmorillonite on montmorillonite-polyacrylate nanocomposites. Appl. Clay Sci. 52, 96–103. doi:10.1016/j.clay.2011.02.004

Ianchis, R., Corobea, M.C., Donescu, D., Rosca, I.D., Cinteza, L.O., Nistor, L.C., Vasile, E., Marin, A., Preda, S., 2012. Advanced functionalization of organoclay nanoparticles by silylation and their polystyrene nanocomposites obtained by miniemulsion polymerization. J. Nanoparticle Res. 14, 1233–1244. doi:10.1007/s11051-012-1233-6

Ianchis, R., Rosca, I.D., Ghiurea, M., Spataru, C.I., Nicolae, C.A., Gabor, R., Raditoiu, V., Preda, S., Fierascu, R.C., Donescu, D., 2015. Synthesis and properties of new epoxy-organolayered silicate nanocomposites. Appl. Clay Sci. 103, 28–33. doi:10.1016/j.clay.2014.10.020

Iglesias, J.G., González-Benito, J., Aznar, A.J., Bravo, J., Baselga, J., 2002. Effect of glass fiber surface treatments on mechanical strength of epoxy based composite materials. J. Colloid Interface Sci. 250, 251–260. doi:10.1006/jcis.2002.8332

Ingram, S., Rhoney, I., Liggat, J.J., Hudson, N.E., Pethrick, R.A., 2007. Some factors influencing exfoliation and physical property enhancement in nanoclay epoxy resins based on diglycidyl ethers of bisphenol A and F. J. Appl. Polym. Sci. 106, 5–19. doi:10.1002/app.25474

Iqbal, K., Khan, S.-U., Munir, A., Kim, J.-K., 2009. Impact damage resistance of CFRP with nanoclay-filled epoxy matrix. Compos. Sci. Technol. 69, 1949–1957. doi:10.1016/j.compscitech.2009.04.016

Ishida, H., 1984. A review of recent progress in the studies of molecular and microstructure of coupling agents and their functions in composites, coatings and adhesive joints. Polym. Compos. 5, 101–123. doi:10.1002/pc.750050202

Ivanova, K.I., Pethrick, R.A., Affrossman, S., 2000. Investigation of hydrothermal ageing of

a filled rubber toughened epoxy resin using dynamic mechanical thermal analysis and dielectric spectroscopy. Polymer (Guildf). 41, 6787–6796. doi:10.1016/S0032-3861(00)00042-2

Kango, S., Kalia, S., Celli, A., Njuguna, J., Habibi, Y., Kumar, R., 2013. Surface modification of inorganic nanoparticles for development of organic-inorganic nanocomposites - A review. Prog. Polym. Sci. 38, 1232–1261. doi:10.1016/j.progpolymsci.2013.02.003

Kanny, K., Mohan, T.P., 2014. Resin infusion analysis of nanoclay filled glass fiber laminates. Compos. Part B Eng. 58, 328–334. doi:10.1016/j.compositesb.2013.10.025

Kaushik, A., Singh, P., Bhagat, S., 2009. Preparation and characterization of graphite flakes–filled polyester composites. Polym. Plast. Technol. Eng. 48, 802–807. doi:10.1080/03602550902827286

Khan, S.U., Iqbal, K., Munir, A., Kim, J.-K., 2011. Quasi-static and impact fracture behaviors of CFRPs with nanoclay-filled epoxy matrix. Compos. Part A Appl. Sci. Manuf. 42, 253–264. doi:10.1016/j.compositesa.2010.11.011

Khan, S.U., Munir, A., Hussain, R., Kim, J.-K., 2010. Fatigue damage behaviors of carbon fiber-reinforced epoxy composites containing nanoclay. Compos. Sci. Technol. 70, 2077–2085. doi:10.1016/j.compscitech.2010.08.004

Kim, B.C., Park, S.W., Lee, D.G., 2008. Fracture toughness of the nano-particle reinforced epoxy composite. Compos. Struct. 86, 69–77. doi:10.1016/j.compstruct.2008.03.005

Kim, E.S., Shim, J.H., Woo, J.Y., Yoo, K.S., Yoon, J.S., 2010. Effect of the silane modification of clay on the tensile properties of nylon 6/clay nanocomposites. J. Appl. Polym. Sci. 117, 809–816. doi:10.1002/app.31077

Kim, J.-K., Mai, Y.W., 1998. Engineered interfaces in fiber reinforced composites. Elsevier Sciences.

Kim, J.K., Hu, C., Woo, R.S.C., Sham, M.L., 2005. Moisture barrier characteristics of organoclay-epoxy nanocomposites. Compos. Sci. Technol. 65, 805–813. doi:10.1016/j.compscitech.2004.10.014

Kim, M., Park, Y.-B., Okoli, O.I., Zhang, C., 2009. Processing, characterization, and modeling of carbon nanotube-reinforced multiscale composites. Compos. Sci. Technol. 69, 335–342. doi:10.1016/j.compscitech.2008.10.019

Kojima, Y., Usuki, A., Kawasumi, M., Okada, A., Kurauchi, T., Kamigaito, O., 1993. Synthesis of nylon 6–clay hybrid by montmorillonite intercalated with ε-caprolactam. J. Polym. Sci. Part A Polym. Chem. 31, 983–986. doi:10.1002/pola.1993.080310418

Kollia, E., Loutas, T., Fiamegkou, E., Vavouliotis, A., Kostopoulos, V., 2015. Degradation behavior of glass fiber reinforced cyanate ester composites under hydrothermal ageing. Polym. Degrad. Stab. 121, 200–207. doi:10.1016/j.polymdegradstab.2015.08.015

Kootsookos, A., Mouritz, A.P., 2004. Seawater durability of glass- and carbon-polymer composites. Compos. Sci. Technol. 64, 1503–1511. doi:10.1016/j.compscitech.2003.10.019

Kornmann, X., Lindberg, H., Berglund, L.A., 2001. Synthesis of epoxy–clay nanocomposites. Influence of the nature of the curing agent on structure. Polymer (Guildf). 42, 4493–4499. doi:10.1016/S0032-3861(00)00801-6

Kornmann, X., Rees, M., Thomann, Y., Necola, A., Barbezat, M., Thomann, R., 2005. Epoxy-layered silicate nanocomposites as matrix in glass fibre-reinforced composites. Compos. Sci. Technol. 65, 2259–2268. doi:10.1016/j.compscitech.2005.02.006

Kotal, M., Bhowmick, A.K., 2015. Polymer nanocomposites from modified clays: Recent advances and challenges. Prog. Polym. Sci. 51, 127–187. doi:10.1016/j.progpolymsci.2015.10.001

Kráčalík, M., Studenovský, M., Mikešová, J., Sikora, A., Thomann, R., Friedrich, C., Fortelný, I., Šimoník, J., 2007. Recycled PET nanocomposites improved by silanization of organoclays. J. Appl. Polym. Sci. 106, 926–937. doi:10.1002/app.26690

Kumar, D.S., Shukla, M.J., Mahato, K.K., Rathore, D.K., Prusty, R.K., Ray, B.C., 2015. Effect of post-curing on thermal and mechanical behavior of GFRP composites, in: IOP Conference Series: Materials Science and Engineering. p. 012012. doi:10.1088/1757-899X/75/1/012012

Kumar, M.A., Reddy, K.H., Reddy, Y.V.M., Reddy, G.R., Naidu, S.V., 2010. Improvement of tensile and flexural properties in epoxy/clay nanocomposites reinforced with weave glass fiber reel. Int. J. Polym. Mater. 59, 854–862. doi:10.1080/00914037.2010.504144

Lam, C.K., Cheung, H.Y., Lau, K.T., Zhou, L.M., Ho, M.W., Hui, D., 2005a. Cluster size effect in hardness of nanoclay/epoxy composites. Compos. Part B Eng. 36, 263–269. doi:10.1016/j.compositesb.2004.09.006

Lam, C.K., Lau, K.T., Cheung, H.Y., Ling, H.Y., 2005b. Effect of ultrasound sonication in nanoclay clusters of nanoclay/epoxy composites. Mater. Lett. 59, 1369–1372. doi:10.1016/j.matlet.2004.12.048

Lan, T., Kaviratna, P.D., Pinnavaia, T.J., 1996. Epoxy self-polymerization in smectite clays. J. Phys. Chem. Solids 57, 1005–1010. doi:10.1016/0022-3697(95)00388-6

Le Pluart, L., Duchet, J., Sautereau, H., 2005. Epoxy/montmorillonite nanocomposites:

influence of organophilic treatment on reactivity, morphology and fracture properties. Polymer (Guildf). 46, 12267–12278. doi:10.1016/j.polymer.2005.10.089

Li, H., Richards, C., Watson, J., 2014. High-performance glass fiber development for composite applications. Int. J. Appl. Glas. Sci. 5, 65–81. doi:10.1111/ijag.12053

Lin, L.Y., Lee, J.H., Hong, C.E., Yoo, G.H., Advani, S.G., 2006. Preparation and characterization of layered silicate/glass fiber/epoxy hybrid nanocomposites via vacuum-assisted resin transfer molding (VARTM). Compos. Sci. Technol. 66, 2116–2125. doi:10.1016/j.compscitech.2005.12.025

Liu, W., Hoa, S. V., Pugh, M., 2005a. Fracture toughness and water uptake of high-performance epoxy/nanoclay nanocomposites. Compos. Sci. Technol. 65, 2364–2373. doi:10.1016/j.compscitech.2005.06.007

Liu, W., Hoa, S. V., Pugh, M., 2005b. Organoclay-modified high performance epoxy nanocomposites. Compos. Sci. Technol. 65, 307–316. doi:10.1016/j.compscitech.2004.07.012

Lu, H., Nutt, S., 2003a. Enthalpy relaxation of layered silicate-epoxy nanocomposites. Macromol. Chem. Phys. 204, 1832–1841. doi:10.1002/macp.200350046

Lu, H., Nutt, S., 2003b. Restricted relaxation in polymer nanocomposites near the glass transition. Macromolecules 36, 4010–4016. doi:10.1021/ma034049b

Manfredi, L.B., De Santis, H., Vázquez, A., 2008. Influence of the addition of montmorillonite to the matrix of unidirectional glass fibre/epoxy composites on their mechanical and water absorption properties. Compos. Part A Appl. Sci. Manuf. 39, 1726–1731. doi:10.1016/j.compositesa.2008.07.016

Marquis, D.M., Guillaume, É., Chivas-joly, C., 2011. Properties of Nanofillers in Polymer, in: Nanocomposites and Polymers with Analytical Methods. pp. 261–284. doi:10.5772/21694

Maxwell, A.S., Broughton, W.R., Dean, G., Sims, G.D., 2005. Review of accelerated ageing methods, National Physical Laboratory. Middlesex. doi:ISSN 1744-0270

Mballa, M.A.M., Heuts, J.P.A., Van Herk, A.M., 2013. Encapsulation of non-chemically modified montmorillonite clay platelets via emulsion polymerization. Colloid Polym. Sci. 291, 501–513. doi:10.1007/s00396-012-2732-9

McIntyre, S., Kaltzakorta, I., Liggat, J.J., Pethrick, R. a., Rhoney, I., 2005. Influence of the epoxy structure on the physical properties of epoxy resin nanocomposites. Ind. Eng. Chem. Res. 44, 8573–8579. doi:10.1021/ie048835w

Minty, R.F., Thomason, J.L., Yang, L., 2016. The role of the epoxy resin: curing agent ratio

on composite interfacial strength and thermal performance, in: 17th European Conference on Composite Materials. Munich, Germany, pp. 1–8.

Mirzataheri, M., Atai, M., Mahdavian, A.R., 2010. Physical and mechanical properties of nanocomposite barrier film containing encapsulated nanoclay. J. Appl. Polym. Sci. 118, 3284–3291. doi:10.1002/app.32711

Mittal, G., Dhand, V., Rhee, K.Y., Park, S.J., Kim, H.J., Jung, D.H., 2015. Investigation of seawater effects on the mechanical properties of untreated and treated MMT-based glass fiber/vinylester composites. Ocean Eng. 108, 393–401. doi:10.1016/j.oceaneng.2015.08.019

Mohan, T.P., Velmurugan, R., Kanny, K., 2015. Damping characteristics of nanoclay filled hybrid laminates during medium velocity impact. Compos. Part B Eng. 82, 178–189. doi:10.1016/j.compositesb.2015.08.016

Morancho, J.M., Salla, J.M., 1999. Relaxation in partially cured samples of an epoxy resin and of the same resin modified with a carboxyl-terminated rubber. Polymer (Guildf). 40, 2821–2828. doi:10.1016/S0032-3861(98)00467-4

Mourad, A.H.I., Beckry Mohamed, A.M., El-Maaddawy, T., 2010. Effect of seawater and warm environment on glass/epoxy and glass/polyurethane composites. Appl. Compos. Mater. 17, 557–573. doi:10.1007/s10443-010-9143-1

Mouritz, A.., Gellert, E., Burchill, P., Challis, K., 2001. Review of advanced composite structures for naval ships and submarines. Compos. Struct. 53, 21–42. doi:10.1016/S0263-8223(00)00175-6

Moy, S., 2013. Advance fiber-reinforced polymer (FRP) composites for civil engineering applications, in: Developments in Fiber-Reinforced Polymer (FRP) Composites for Civil Engineering. Cambridge: Woohead Publishing Limited, pp. 177–204. doi:10.1533/9780857098955.2.177

Mravljak, M., Šernek, M., 2011. The influence of curing temperature on rheological properties of epoxy adhesives. Drv. Ind. 62, 19–25. doi:10.5552/drind.2011.1042

Musto, P., Ragosta, G., Mascia, L., 2000. Vibrational spectroscopy evidence for the dual nature of water sorbed into epoxy resins. Chem. Mater. 12, 1331–1341. doi:10.1021/cm9906809

Nazir, M.S., Mohamad Kassim, M.H., Mohapatra, L., Gilani, M.A., Raza, M.R., and Majeed, K., 2016. Characteristic properties of nanoclays and characterization of nanoparticulates and nanocomposites, in: Springer (Ed.), Nanoclay Reinforced Polymer Composites. pp. 35–56. doi:10.1007/978-981-10-1953-1

Ngo, T.-D., Ton-That, M.-T., Hoa, S.V., Cole, K.C., 2012. Preparation and properties of epoxy nanocomposites. Part 2: The effect of dispersion and intercalation/exfoliation of organoclay on mechanical properties. Polym. Eng. Sci. 52, 607–614. doi:10.1002/pen.22123

Ngo, T.-D., Ton-That, M.-T., Hoa, S.V., Cole, K.C., 2007. Curing kinetics and mechanical properties of epoxy nanocomposites based on different organoclays. Polym. Eng. Sci. 47, 649–661. doi:10.1002/pen.20737

Ngo, T.D., Ton-That, M.T., Hoa, S. V., Cole, K.C., 2009. Effect of temperature, duration and speed of pre-mixing on the dispersion of clay/epoxy nanocomposites. Compos. Sci. Technol. 69, 1831–1840. doi:10.1016/j.compscitech.2009.03.024

Njuguna, J., Pielichowski, K., Alcock, J.R., 2007. Epoxy-based fibre reinforced nanocomposites. Adv. Eng. Mater. 9, 835–847. doi:10.1002/adem.200700118

Nuhiji, B., Attard, D., Deveth, A., Bungur, J., Fox, B., 2016. The influence of processing techniques on the matrix distribution and filtration of clay in a fibre reinforced nanocomposite. Compos. Part B Eng. 84, 1–8. doi:10.1016/j.compositesb.2015.08.067

Nuhiji, B., Attard, D., Thorogood, G., Hanley, T., Magniez, K., Bungur, J., Fox, B., 2013. The effect of a rapid heating rate, mechanical vibration and surfactant chemistry on the structure-property relationships of epoxy/clay nanocomposites. Materials (Basel). 6, 3624–3640. doi:10.3390/ma6083624

Odegard, G.M., Bandyopadhyay, A., 2011. Physical aging of epoxy polymers and their composites. J. Polym. Sci. Part B Polym. Phys. 49, 1695–1716. doi:10.1002/polb.22384

Okada, A., Usuki, A., 1995. The chemistry of polymer-clay hybrids. Mater. Sci. Eng. C 3, 109–115. doi:10.1016/0928-4931(95)00110-7

Olad, A., 2011. Polymer/clay nanocomposites, in: Advances in Diverse Industrial Applications of Nanocomposites. InTech., pp. 113–138. doi:10.5772/1931

Palmese, G.R., McCullough, R.L., 1992. Effect of epoxy-amine stoichiometry on cured resin material properties. J. Appl. Polym. Sci. 46, 1863–1873. doi:10.1002/app.1992.070461018

Paluvai, N.R., Mohanty, S., Nayak, S.K., 2014. Synthesis and modifications of epoxy resins and their composites: A review. Polym. Plast. Technol. Eng. 53, 1723–1758. doi:10.1080/03602559.2014.919658

Park, J., Jana, S.C., 2004. Adverse effects of thermal dissociation of alkyl ammonium ions on nanoclay exfoliation in epoxy-clay systems. Polymer (Guildf). 45, 7673–7679. doi:10.1016/j.polymer.2004.08.075

Park, R., Jang, J., 2004. Effect of surface treatment on the mechanical properties of glass fiber / vinylester composites. J. Appl. Polym. Sci. 91, 3730–3736.

Park, S.J., Kim, B.J., Seo, D. Il, Rhee, K.Y., Lyu, Y.Y., 2009. Effects of a silane treatment on the mechanical interfacial properties of montmorillonite/epoxy nanocomposites. Mater. Sci. Eng. A 526, 74–78. doi:10.1016/j.msea.2009.07.023

Paul, D.R., Robeson, L.M., 2008. Polymer nanotechnology: Nanocomposites. Polymer (Guildf). 49, 3187–3204. doi:10.1016/j.polymer.2008.04.017

Pavlidou, S., Papaspyrides, C.D., 2008. A review on polymer-layered silicate nanocomposites. Prog. Polym. Sci. 33, 1119–1198. doi:10.1016/j.progpolymsci.2008.07.008

Peponi, L., Puglia, D., Torre, L., Valentini, L., Kenny, J.M., 2014. Processing of nanostructured polymers and advanced polymeric based nanocomposites. Mater. Sci. Eng. R Reports 85, 1–46. doi:10.1016/j.mser.2014.08.002

Phua, Y.J., Chow, W.S., Mohd Ishak, Z.A., 2011. The hydrolytic effect of moisture and hygrothermal aging on poly(butylene succinate)/organo-montmorillonite nanocomposites. Polym. Degrad. Stab. 96, 1194–1203. doi:10.1016/j.polymdegradstab.2011.04.017

Piscitelli, F., Posocco, P., Toth, R., Fermeglia, M., Pricl, S., Mensitieri, G., Lavorgna, M., 2010. Sodium montmorillonite silylation: Unexpected effect of the aminosilane chain length. J. Colloid Interface Sci. 351, 108–115. doi:10.1016/j.jcis.2010.07.059

Piscitelli, F., Scamardella, A.M., Romeo, V., Lavorgna, M., Barra, G., Amendola, E., 2012. Epoxy composites based on amino-silylated MMT: The role of interfaces and clay morphology. J. Appl. Polym. Sci. 124, 616–628. doi:10.1002/app.35015

Plueddemann, E.P., 1982. Silane coupling agents, Shin-Etsu Silicone.

Poisson, N., Lachenal, G., Sautereau, H., 1996. Near-and mid-infrared spectroscopy studies of an epoxy reactive system. Vib. Spectrosc. 12, 237–247.

Polymer, INC., A., 2011. Silane coupling agents [WWW Document]. Adv. Polym. Inc. doi:63

Qi, B., Zhang, Q.X., Bannister, M., Mai, Y.W., 2006. Investigation of the mechanical properties of DGEBA-based epoxy resin with nanoclay additives. Compos. Struct. 75, 514–519. doi:10.1016/j.compstruct.2006.04.032

Qian, Z., Zhou, H., Xu, X., Ding, Y., Zhang, S., Yang, M., 2009. Effect of the grafted silane on the dispersion and orientation of clay in polyethylene nanocomposites. Polym. Compos. 30, 1234–1242. doi:10.1002/pc.20683

Quaresimin, M., Varley, R.J., 2008. Understanding the effect of nano-modifier addition upon the properties of fibre reinforced laminates. Compos. Sci. Technol. 68, 718–726. doi:10.1016/j.compscitech.2007.09.005

Rafiq, A., Merah, N., Boukhili, R., Al-Qadhi, M., 2017. Impact resistance of hybrid glass fiber reinforced epoxy/nanoclay composite. Polym. Test. 57, 1–11. doi:10.1016/j.polymertesting.2016.11.005

Raji, M., Mekhzoum, M., el Kacem Qaiss, A., Bouhfid, R., 2016. Nanoclay modification and functionalization for nanocomposites development: Effect on the structural, morphological, mechanical and rheological properties, in: Nanoclay Reinforced Polymer Composites. Springer Singapore, pp. 1–34. doi:10.1007/978-981-10-0950-1

Ratna, D., 2009. Epoxy Resins, in: Handbook of Thermoset Resins. Shawbury, UK: ISmithers, pp. 155–181. doi:10.1002/0471743984.vse3011.pub2

Ray, B.C., 2006. Temperature effect during humid ageing on interfaces of glass and carbon fibers reinforced epoxy composites. J. Colloid Interface Sci. 298, 111–117. doi:10.1016/j.jcis.2005.12.023

Ray, B.C., Rathore, D., 2014. Durability and integrity studies of environmentally conditioned interfaces in fibrous polymeric composites: Critical concepts and comments. Adv. Colloid Interface Sci. 209, 68–83. doi:10.1016/j.cis.2013.12.014

Romanzini, D., Frache, A., Zattera, A.J., Amico, S.C., 2015a. Effect of clay silylation on curing and mechanical and thermal properties of unsaturated polyester/montmorillonite nanocomposites. J. Phys. Chem. Solids 87, 9–15. doi:10.1016/j.jpcs.2015.07.019

Romanzini, D., Piroli, V., Frache, A., Zattera, A.J., Amico, S.C., 2015b. Sodium montmorillonite modified with methacryloxy and vinylsilanes: Influence of silylation on the morphology of clay/unsaturated polyester nanocomposites. Appl. Clay Sci. 114, 550–557. doi:10.1016/j.clay.2015.07.003

Rong, M.Z., Zhang, M.Q., Ruan, W.H., 2006. Surface modification of nanoscale fillers for improving properties of polymer nanocomposites: a review. Mater. Sci. Technol. 22, 787–796. doi:10.1179/174328406X101247

Ryu, S.H., Reddy, M.J.K., Shanmugharaj, A., 2016. Role of silane concentration on the structural characteristics and properties of epoxy-/silane-modified montmorillonite clay nanocomposites. J. elastomers Plast. 1–19. doi:10.1177/0095244316683546

Saba, N., Jawaid, M., Asim, M., 2016. Recent Advances in Nanoclay/Natural Fibers Hybrid Composites BT - Nanoclay Reinforced Polymer Composites: Natural Fibre/Nanoclay Hybrid Composites, in: Jawaid, M., Kacem, A. el, Bouhfid, Q. (Eds.), Nanoclay

Reinforced Polymer Composites. Springer Singapore, pp. 1–28. doi:10.1007/978-981-10-0950-1_1

Safarabadi, M., Shokrieh, M.M., 2014. Understanding residual stresses in polymer matrix composites, in: Residual Stresses in Composite Materials. Woodhead Publishing Limited, pp. 197–232. doi:10.1533/9780857098597.2.197

Saharudin, M.S., Atif, R., Shyha, I., Inam, F., 2016. The degradation of mechanical properties in polymer nano-composites exposed to liquid media – a review. RSC Adv. 6, 1076–1089. doi:10.1039/C5RA22620A

Salmon, L., Thominette, F., Pays, M.F., Verdu, J., 1997. Hydrolytic degradation of model networks simulating the interfacial layers in silanecoupled epoxy/glass composites. Compos. Sci. Technol. 57, 1119–1127. doi:10.1016/S0266-3538(97)00038-9

Santhosh, K., Muniraju, M., Shivakumar, N., Raguraman, M., 2011. Hygrothermal durability and failure modes of FRP for marine applications. J. Compos. Mater. 46, 1889–1896. doi:10.1177/0021998311427776

Sathishkumar, T.P. Satheeshkumar, S., Naveen, J., 2014. Glass fiber-reinforced polymer composites - A review. J. Reinf. Plast. Compos. 33, 1258–1275. doi:10.1177/0731684414530790

Senthil Kumar, M.S., Mohana Sundara Raju, N., Sampath, P.S., Vivek, U., 2015. Tribological analysis of nano clay/epoxy/glass fiber by using Taguchi's technique. Mater. Des. 70, 1–9. doi:10.1016/j.matdes.2014.12.033

Sethi, S., Ray, B.C., 2015. Environmental effects on fibre reinforced polymeric composites: Evolving reasons and remarks on interfacial strength and stability. Adv. Colloid Interface Sci. 217, 43–67. doi:10.1016/J.CIS.2014.12.005

Sever, K., Sarikanat, M., Seki, Y., Cecen, V., Tavman, I.H., 2008. Effects of fiber surface treatments on mechanical properties of epoxy composites reinforced with glass fabric. J. Mater. Sci. 43, 4666–4672. doi:10.1007/s10853-008-2679-x

Shanmugharaj, A.M., Rhee, K.Y., Ryu, S.H., 2006. Influence of dispersing medium on grafting of aminopropyltriethoxysilane in swelling clay materials. J. Colloid Interface Sci. 298, 854–859. doi:10.1016/j.jcis.2005.12.049

Shanmugharaj, A.M., Ryu, S.H., 2012. Study on the effect of aminosilane functionalized nanoclay on the curing kinetics of epoxy nanocomposites. Thermochim. Acta 546, 16–23. doi:10.1016/j.tca.2012.07.026

Sharma, B., Chhibber, R., Mehta, R., 2017. Curing studies and mechanical properties of glass fi ber reinforced composites based on silanized clay minerals. Appl. Clay Sci. 138, 89–

99. doi:10.1016/j.clay.2016.12.038

Sharma, B., Chhibber, R., Mehta, R., 2016. Effect of surface treatment of nanoclay on the mechanical properties of epoxy/glass fiber/clay nanocomposites. Compos. Interfaces 23, 623–640. doi:10.1080/09276440.2016.1165522

Sharma, B., Mahajan, S., Chhibber, R., Mehta, R., 2012. Glass fiber reinforced polymer-clay nanocomposites : Processing , structure and hygrothermal effects on mechanical properties. Procedia Chem. 4, 39–46. doi:10.1016/j.proche.2012.06.006

Shen, W., He, H.P., Zhu, J., Yuan, P., Frost, R.L., 2007. Grafting of montmorillonite with different functional silanes via two different reaction systems. J. Colloid Interface Sci. 313, 268–273. doi:10.1016/j.jcis.2007.04.029

Shokoohi, S., Arefazar, A., Khosrokhavar, R., 2008. Silane coupling agents in polymer-based reinforced composites: A Review. J. Reinf. Plast. Compos. 27, 473–485. doi:10.1177/0731684407081391

Silva, A.A., Dahmouche, K., Soares, B.G., 2011. Nanostructure and dynamic mechanical properties of silane-functionalized montmorillonite/epoxy nanocomposites. Appl. Clay Sci. 54, 151–158. doi:10.1016/j.clay.2011.08.002

Singla, P., Mehta, R., Upadhyay, S.N., 2014. Microwave assisted in situ ring-opening polymerization of polylactide/clay nanocomposites: Effect of clay loading. Appl. Clay Sci. 95, 67–73. doi:10.1016/j.clay.2014.03.012

Sinha Ray, S., 2013. An Overview of Pure and Organically Modified Clays. Clay-containing Polym. Nanocomposites 1–24. doi:http://dx.doi.org/10.1016/B978-0-444-59437-2.00001-6

Sinha Ray, S., Okamoto, M., 2003. Polymer/layered silicate nanocomposites: A review from preparation to processing. Prog. Polym. Sci. 28, 1539–1641. doi:10.1016/j.progpolymsci.2003.08.002

Starkova, O., Buschhorn, S.T., Mannov, E., Schulte, K., Aniskevich, A., 2013. Water transport in epoxy/MWCNT composites. Eur. Polym. J. 49, 2138–2148. doi:10.1016/j.eurpolymj.2013.05.010

Stickel, J.M., Nagarajan, M., 2012. Glass fiber-reinforced composites: from formulation to application. Int. J. Appl. Glas. Sci. 3, 122–136. doi:10.1111/j.2041-1294.2012.00090.x

Su, L., Tao, Q., He, H., Zhu, J., Yuan, P., 2012. Locking effect : A novel insight in the silylation of montmorillonite surfaces. Mater. Chem. Phys. 136, 292–295. doi:10.1016/j.matchemphys.2012.07.010

Su, L., Tao, Q., He, H., Zhu, J., Yuan, P., Zhu, R., 2013. Silylation of montmorillonite

surfaces: Dependence on solvent nature. J. Colloid Interface Sci. 391, 16–20. doi:10.1016/j.jcis.2012.08.077

Subramaniyan, A.K., Sun, C.T., 2006. Enhancing compressive strength of unidirectional polymeric composites using nanoclay. Compos. Part A Appl. Sci. Manuf. 37, 2257–2268. doi:10.1016/j.compositesa.2005.12.027

Sugiman, S., Putra, I.K.P., Setyawan, P.D., 2016. Effects of the media and ageing condition on the tensile properties and fracture toughness of epoxy resin. Polym. Degrad. Stab. 134, 311–321. doi:10.1016/j.polymdegradstab.2016.11.006

Summerscales, J., 2015. Composites manufacturing for marine structures, in: Marine Applications of Advanced Fibre-Reinforced Composites. Cambridge: Woodhead Publishing, pp. 19–55. doi:10.1016/B978-1-78242-250-1.00002-8

Šupová, M., Martynková, G.S., Barabaszová, K., 2011. Effect of nanofillers dispersion in polymer matrices: A review. Sci. Adv. Mater. 3, 1–25. doi:10.1166/sam.2011.1136

Surathi, P., Karbhari, V.M., 2006. Hygrothermal effects on durability and moisture kinetics of fiber-reinforced polymer composites. Composites 1–9.

Takeshita, Y., Becker, E., Sakata, S., Miwa, T., Sawada, T., 2014. States of water absorbed in water-borne urethane/epoxy coatings. Polym. (United Kingdom) 55, 2505–2513. doi:10.1016/j.polymer.2014.03.027

Tan, B., Thomas, N.L., 2016. A review of the water barrier properties of polymer/clay and polymer/graphene nanocomposites. J. Memb. Sci. 514, 595–612. doi:10.1016/j.memsci.2016.05.026

Thelakkadan, A.S., Coletti, G., Guastavino, F., Fina, A., 2013. Effect of clay dispersion methods on the mechano-dynamical and electrical properties of epoxy-organoclay nanocomposites. Polym. Bull. 70, 489–506. doi:10.1007/s00289-012-0815-x

Thomason, J.L., Ali, J.Z., 2009. The dimensional stability of glass–fibre reinforced polyamide 66 during hydrolysis conditioning. Compos. Part A Appl. Sci. Manuf. 40, 625–634. doi:10.1016/j.compositesa.2009.02.017

Timmerman, J.F., Hayes, B.S., Seferis, J.C., 2002. Nanoclay reinforcement effects on the cryogenic microcracking of carbon fiber / epoxy composites. Compos. Sci. Technol. 62, 1249–1258. doi:10.1016/S0266-3538(02)00063-5

Traynor, D.H., Xu, H., Traynor, H.G., Carson, J., Flacks, M.S., and Sullivan, R., 2015. Ceramic encapsulation with controlled layering by use of prehydrolyzed functionalized silanes.

Tsai, J.L., Kuo, J.C., Hsu, S.M., 2006. Organoclay effect on transverse compressive strength

of glass/epoxy nanocomposites. J. Mater. Sci. 41, 7406–7412. doi:10.1007/s10853-006-0800-6

Varadwaj, G.B.B., Parida, K., Nyamori, V.O., 2016. Transforming inorganic layered montmorillonite into inorganic–organic hybrid materials for various applications: a brief overview. Inorg. Chem. Front. 3, 1100–1111. doi:10.1039/C6QI00179C

Vejayakumaran, P., Rahman, I.A., Sipaut, C.S., Ismail, J., Chee, C.K., 2008. Structural and thermal characterizations of silica nanoparticles grafted with pendant maleimide and epoxide groups. J. Colloid Interface Sci. 328, 81–91. doi:10.1016/j.jcis.2008.08.054

Velmurugan, R., Mohan, T.P., 2004. Room temperature processing of epoxy-clay nanocomposites. J. Mater. Sci. 39, 7333–7339. doi:10.1023/B:JMSC.0000048748.35490.9f

Venkatram, B., Kailasanathan, C., Seenikannan, P., Paramasamy, S., 2016. Study on the evaluation of mechanical and thermal properties of natural sisal fiber/general polymer composites reinforced with nanoclay. Int. J. Polym. Anal. Charact. 5341, 1–10. doi:10.1080/1023666X.2016.1194616

Vennerberg, D., Rueger, Z., Kessler, M.R., 2014. Effect of silane structure on the properties of silanized multiwalled carbon nanotube-epoxy nanocomposites. Polym. (United Kingdom) 55, 1854–1865. doi:10.1016/j.polymer.2014.02.018

Verma, D., 2016. Processing techniques of nanoclay based natural fibre reinforced polymer composites, in: Nanoclay Reinforced Polymer Composites. Springer Singapore, pp. 209–237. doi:10.1007/978-981-10-0950-1_9

Vlasveld, D.P.N., Bersee, H.E.N., Picken, S.J., 2005. Nanocomposite matrix for increased fibre composite strength. Polymer (Guildf). 46, 10269–10278. doi:10.1016/j.polymer.2005.08.003

Vlasveld, D.P.N., Daud, W., Bersee, H.E.N., Picken, S.J., 2007. Continuous fibre composites with a nanocomposite matrix: Improvement of flexural and compressive strength at elevated temperatures. Compos. Part A Appl. Sci. Manuf. 38, 730–738. doi:10.1016/j.compositesa.2006.09.010

Voorn, D.J., Ming, W., Van Herk, A.M., 2006. Clay platelets encapsulated inside latex particles. Macromolecules 39, 4654–4656. doi:10.1021/MA060900L

Wan, C., Bao, X., Zhao, F., Kandasubramanian, B., Duggan, M.P., 2008. Morphology and properties of silane-modified montmorillonite clays and clay/PBT composites. J. Appl. Polym. Sci. 110, 550–557. doi:10.1002/app.28672

Wang, J., GangaRao, H., Liang, R., Zhou, D., Liu, W., Fang, Y., 2015. Durability of glass

fiber-reinforced polymer composites under the combined effects of moisture and sustained loads. J. Reinf. Plast. Compos. 34, 1739–1754. doi:10.1177/0731684415596846

Wang, K., Chen, L., Wu, J., Toh, M.L., He, C., Yee, A.F., 2005. Epoxy nanocomposites with highly exfoliated clay: Mechanical properties and fracture mechanisms. Macromolecules 38, 788–800. doi:10.1021/ma048465n

Wang, L., Wang, K., Chen, L., He, C., Zhang, Y., 2006a. Hydrothermal effects on the thermomechanical properties of high performance epoxy/clay nanocomposites. Polym. Eng. Sci. 46, 215–221. doi:10.1002/pen.20453

Wang, L., Wang, K., Chen, L., Zhang, Y., He, C., 2006b. Preparation, morphology and thermal/mechanical properties of epoxy/nanoclay composite. Compos. Part A Appl. Sci. Manuf. 37, 1890–1896. doi:10.1016/j.compositesa.2005.12.020

Wang, R.-M., Zheng, S.-R., Zheng, Y.-P., 2011. Introduction to polymer matrix composites. Polym. matrix Compos. Technol. 1–548. doi:10.1533/9780857092229.1

Wei, B., Cao, H., Song, S., 2011. Degradation of basalt fibre and glass fibre / epoxy resin composites in seawater. Corros. Sci. 53, 426–431. doi:10.1016/j.corsci.2010.09.053

Weitsman, Y.J., 2012a. Fluid effects in polymers and polymeric composites, Mechanical Engineering Series. Springer US, Boston, MA. doi:10.1007/978-1-4614-1059-1

Weitsman, Y.J., 2012b. Effects of fluids on mechanical properties and performance, in: Fluid Effects in Polymers and Polymeric Composites. Springer US. doi:10.1007/978-1-4614-1059-1_7

Weitsman, Y.J., Elahi, M., 2000. Effects of fluids on the deformation, strength and durability of polymeric composites - an overview. Mech. Time-Dependent Mater. 4, 107–126. doi:10.1023/A:1009838128526

Withers, G.J., Yu, Y., Khabashesku, V.N., Cercone, L., Hadjiev, V.G., Souza, J.M., Davis, D.C., 2015. Improved mechanical properties of an epoxy glass–fiber composite reinforced with surface organomodified nanoclays. Compos. Part B Eng. 72, 175–182. doi:10.1016/j.compositesb.2014.12.008

Woo, R.S.C., Chen, Y., Zhu, H., Li, J., Kim, J.K., Leung, C.K.Y., 2007. Environmental degradation of epoxy-organoclay nanocomposites due to UV exposure. Part I: Photo-degradation. Compos. Sci. Technol. 67, 3448–3456. doi:10.1016/j.compscitech.2007.03.004

Xia, H., Wang, Q., Qiu, G., 2003. Polymer-encapsulated carbon nanotubes prepared through ultrasonically initiated in situ emulsion polymerization. Chem. Mater. 15, 3879–3886.

doi:10.1021/cm0341890

Xie, W., Gao, Z., Liu, K., Pan, W.-P., Vaia, R., Hunter, D., Singh, A., 2001. Thermal characterization of organically modified montmorillonite. Thermochim. Acta 367–368, 339–350. doi:10.1016/S0040-6031(00)00690-0

Xie, Y., Hill, C.A.S., Xiao, Z., Militz, H., Mai, C., 2010. Silane coupling agents used for natural fiber/polymer composites: A review. Compos. Part A Appl. Sci. Manuf. 41, 806–819. doi:10.1016/j.compositesa.2010.03.005

Xu, X., Ding, Y., Qian, Z., Wang, F., Wen, B., Zhou, H., Zhang, S., Yang, M., 2009. Degradation of poly(ethylene terephthalate)/clay nanocomposites during melt extrusion: Effect of clay catalysis and chain extension. Polym. Degrad. Stab. 94, 113–123. doi:10.1016/j.polymdegradstab.2008.09.009

Xu, Y., Hoa, S. Van, 2008. Mechanical properties of carbon fiber reinforced epoxy/clay nanocomposites. Compos. Sci. Technol. 68, 854–861. doi:10.1016/j.compscitech.2007.08.013

Yang, J.P., Yang, G., Xu, G., Fu, S.Y., 2007. Cryogenic mechanical behaviors of MMT/epoxy nanocomposites. Compos. Sci. Technol. 67, 2934–2940. doi:10.1016/j.compscitech.2007.05.012

Yang, S. qin, Yuan, P., He, H. ping, Qin, Z. hua, Zhou, Q., Zhu, J. xi, Liu, D., 2012. Effect of reaction temperature on grafting of γ-aminopropyl triethoxysilane (APTES) onto kaolinite. Appl. Clay Sci. 62–63, 8–14. doi:10.1016/j.clay.2012.04.006

Yasmin, A., Luo, J.J., Abot, J.L., Daniel, I.M., 2006. Mechanical and thermal behavior of clay/epoxy nanocomposites. Compos. Sci. Technol. 66, 2415–2422. doi:10.1016/j.compscitech.2006.03.011

Yuhana, N.Y., Ahmad, S., Bahri, A.R.S., 2012. The effect of ultrasonic treatment on thermal stability of the cured epoxy/layered silicate nanocomposite. Adv. Mater. Sci. Eng. 2012. doi:10.1155/2012/789815

Zabihi, O., Ahmadi, M., Nikafshar, S., Chandrakumar Preyeswary, K., Naebe, M., 2018. A technical review on epoxy-clay nanocomposites: Structure, properties, and their applications in fiber reinforced composites. Compos. Part B Eng. 135, 1–24. doi:10.1016/j.compositesb.2017.09.066

Zainuddin, S., Hosur, M. V., Zhou, Y., Kumar, A., Jeelani, S., 2010. Durability study of neat/nanophased GFRP composites subjected to different environmental conditioning. Mater. Sci. Eng. A 527, 3091–3099. doi:10.1016/j.msea.2010.02.022

Zainuddin, S., Hosur, M. V., Zhou, Y., Kumar, A., Jeelani, S., 2009. Durability studies of

montmorillonite clay filled epoxy composites under different environmental conditions. Mater. Sci. Eng. A 507, 117–123. doi:10.1016/j.msea.2008.11.058

Zerda, A.S., Lesser, A.J., 2001. Intercalated clay nanocomposites: Morphology, mechanics, and fracture behavior. J. Polym. Sci. Part B Polym. Phys. 39, 1137–1146. doi:10.1002/polb.1090

Zhang, J., Fox, B.L., 2005. Characterization and analysis of delamination fracture and nanocreep properties in carbon epoxy composites manufactured by different processes. J. Compos. Mater. 40, 1287–1299. doi:10.1177/0021998305057438

Zhang, J., Gupta, R.K., Wilkie, C.A., 2006. Controlled silylation of montmorillonite and its polyethylene nanocomposites. Polymer (Guildf). 47, 4537–4543. doi:10.1016/j.polymer.2006.04.057

Zhang, Y., Xia, Z., Ellyin, F., 2004. Evolution and influence of residual stresses/strains of fiber reinforced laminates. Compos. Sci. Technol. 64, 1613–1621. doi:10.1016/j.compscitech.2003.11.012

Zhao, L.G., Warrior, N.A., Long, A.C., 2006. A micromechanical study of residual stress and its effect on transverse failure in polymer – matrix composites 43, 5449–5467. doi:10.1016/j.ijsolstr.2005.08.012

Zhou, G., Movva, S., Lee, L.J., 2008. Nanoclay and long-fiber-reinforced composites based on epoxy and phenolic resins. J. Appl. Polym. Sci. 108, 3720–3726. doi:10.1002/app.27886

Zhou, J., Lucas, J.P., 1999. Hygrothermal effects of epoxy resin. Part II: Variations of glass transition temperature. Polymer (Guildf). 40, 5513–5522. doi:10.1016/S0032-3861(98)00791-5

Zhou, Y., Hosur, M., Jeelani, S., Mallick, P.K., 2012. Fabrication and characterization of carbon fiber reinforced clay/epoxy composite. J. Mater. Sci. 47, 5002–5012. doi:10.1007/s10853-012-6376-4

Zulfli, M., Chow, W., 2012. Mechanical and thermal behaviours of glass fiber reinforced epoxy hybrid composites containing organo-montmorillonite. Malaysian Polym. J. 7, 1–8.

Zunjarrao, S.C., Sriraman, R., Singh, R.P., 2006. Effect of processing parameters and clay volume fraction on the mechanical properties of epoxy-clay nanocomposites. J. Mater. Sci. 41, 2219–2228. doi:10.1007/s10853-006-7179-2